The role of E-cadherin loss in transgenic mouse skin carcinogenesis

Rema Zaweia

Thesis submitted in fulfilment of the requirements for the
Degree of
Doctor of Philosophy

School of Medicine, Dentistry and Nursing
College of Medical, Veterinary and Life Sciences
University of Glasgow

November 2024

Summary

The purpose of this study is to examine the role of E-cadherin in cell-cell adhesion failure and altered signalling within a transgenic mouse skin carcinogenesis model that models human carcinogenesis. The main aim is to understand how the loss of E-cadherin collaborates with the activation of ras and fos oncogenes, along with PTEN loss, in driving the transformation of benign tumours into malignancies and their subsequent progression to aggressive squamous cell carcinomas (SCC). These are considered the most critical events in the progression of carcinogenesis from a patient's perspective.

E-cadherin is a highly conserved adhesion molecule essential for maintaining epithelial integrity through its interaction with ß-catenin. Loss of E-cadherin disrupts adhesion, promoting invasion and progression. Although many studies support this view, emerging evidence, such as that from Padmanaban et al. (2019), suggests that E-cadherin may also be necessary for certain types of invasion, emphasising the complexity of its role and the importance of tissue context in carcinogenesis.

To address these challenges, the approach involved a well-characterised transgenic mouse skin carcinogenesis model that expresses a combination of ras and fos activation, via a modified human keratin 1 vector (*HK1.ras*; *HK1.fos*), ensuring that ras and fos oncogenes are exclusively expressed in the proliferative basal layers of the epidermis and in malignant tumours. This results in hyperplasia and papillomatogenesis but shows no evidence of spontaneous malignant conversion. The stability of this phenotype makes it ideal for investigating the roles of oncogene cooperation in the development of benign tumours and their progression to malignancy. To explore the specific roles of E-cadherin in skin carcinogenesis models, the RU486-inducible cre/lox method was utilised to exclusively knock out E-cadherin via exon 6-10 ablation (*K14creP/Δ-6-10Ecad*^{flx}).

These transgenic mice expressed activated ras and/or fos oncogenes (*HK1.ras*, *HK1.fos*). Inducible mutation of PTEN-regulated AKT activation via exon 5 ablation (*K14creP/Δ5PTEN*^{flx}) was also incorporated into this model by using the RU486-inducible cre/loxP method. Previous analysis of endogenous E-cadherin expression in the *HK1.ras.fos-K14creP/Δ5PTEN*$^{flx/flx}$

transgenic skin mouse model showed a reduction in membranous E-cadherin expression at the invasive front of well-differentiated SCC (wdSCC) following p53 loss.

In bi-genic *HK1.ras-K14creP/Δ6-10Ecad^{flx}* mice, the synergistic effect between E-cadherin loss and wound-promotion sensitive (ear tagging) HK1.ras1205 line was observed to induce malignant conversion. The results showed that reduced functional E-cadherin in *HK1.ras-K14creP/Δ6-10Ecad$^{flx/het}$* mice led to hyperplasia and papillomas similar to HK1.ras mice, but with intercellular gaps in the basal keratinocytes and carcinoma in situ. Functional E-cadherin ablation in *HK1.ras-K14creP/Δ6-10Ecad$^{flx/flx}$* initially caused malignant transformation into well-differentiated squamous cell carcinoma (wdSCC) that invaded in a grouped, collective manner but rapidly progressed into poorly differentiated squamous cell carcinoma (pdSCC), consistent with cell-cell adhesion failures and invasion by the more aggressive individual mode. These tumours correlated with cell-cell adhesion failure associated with p53 loss and nuclear ß-catenin expression.

The heterozygous *HK1.fos-K14creP/Δ5PTEN$^{flx/flx}$/Δ6-10Ecad$^{flx/het}$* mice develop keratoacanthomas (KAs) similar to *HK1.fos-K14creP/Δ5PTEN$^{flx/flx}$* mice, exhibiting characteristic micro-cysts that indicate accelerated and premature differentiation. No malignant transformation was observed because of strong membranous basal E-cadherin and basal membranous ß-catenin expression, which triggers nuclear p53 expression. However, functional ablation of E-cadherin in *HK1.fos-K14creP/Δ5PTEN$^{flx/flx}$/Δ6-10Ecad$^{flx/flx}$* KAs led to malignant conversion into invasive wdSCC. The *HK1.fos-K14creP/Δ5PTEN$^{flx/flx}$/Δ6-10Ecad$^{flx/flx}$* mice initially develop KA-like tumours, with minimal effects on early pre-KA hyperplasia stages, similar to observations in *HK1.ras* mice. Over time, these tumours progress to invasive wdSCC with scattered areas of SCC. This progression ultimately results in the development of aggressive SCC. The gradual loss of p53, combined with a decrease in membranous and an increase in nuclear ß-catenin expression, along with the progressive loss of Δ6-10E-cadherin, indicates a shift towards a more advanced SCC phenotype. These molecular changes suggest an increased potential for invasion and highlight the crucial role of these factors in driving malignant transformation and progression.

The *HK1.ras1276.fos-K14creP/Δ5PTEN$^{flx/flx}$/Δ6-10Ecad^{flx}* model was also utilised, and in this model, the tumours were independent of wound promotion. This was evident as tumours developed in both TGE and NTGE of RU486-treated *HK1.ras1276.fos-K14creP/Δ5PTEN$^{flx/flx}$/Δ6-10Ecad^{flx}* mice. The emergence of these tumours demonstrated a synergic interaction, resulting in a rapid malignant conversion and progression to SCC/pdSCC soon after p53 loss, consistent with cell-cell adhesion failure and deregulated signalling to ß-catenin. Interestingly, these tumours were associated with loss of ß-catenin, suggesting a critical link between E-cadherin loss and the dysregulation of ß-catenin signalling. The loss of E-cadherin, a key component of adherens junctions, might disrupt the normal Wnt/ß-catenin signalling dynamics, particularly affecting its nuclear translocation. This disruption may lead to inadequate accumulation of nuclear ß-catenin, promoting its degradation rather than facilitating its role in gene transcription regulation. The consequent reduction in ß-catenin expression could further exacerbate the loss of cell-cell adhesion, thereby accelerating the malignant progression of these tumour models.

In summary, this study demonstrates that E-cadherin loss has a minimal impact on papillomatogenesis but promotes hyperplasia and, in cooperation with Ras activation and endogenous p53 loss, facilitates malignant conversion. Furthermore, in the context of ras and fos activation with PTEN loss, E-cadherin loss accelerated malignant progression, consistent with disruption of cell-cell adhesion. Altogether, these models recapitulate key features of human SCC progression and provide insight into the molecular mechanisms linking E-cadherin loss, ß-catenin dysregulation, and tumour invasiveness. Understanding these interactions not only deepens the comprehension of SCC pathogenesis but also highlights potential therapeutic targets aimed at restoring adhesion or modulating Wnt/ß-catenin signalling to delay or prevent malignant progression.

Table of Contents

List of Tables

List of Figures

Acknowledgement

I am deeply grateful to my primary supervisor, Dr. David A. Greenhalgh, for his exceptional support, insightful feedback, enthusiasm, and constructive criticism throughout my research. I would also like to express my sincere appreciation to my second supervisor, Dr. Jean Quinn, for her invaluable help during my writing, her scientific advice, and her constant encouragement. I feel fortunate to have learned from such accomplished scientists.

My heartfelt thanks go to my family for their unwavering support, especially to my husband, Almoatz Keshik, and my children, including my baby girl. I would also like to honour my late father, Mahmoud Zawia, whose encouragement inspired me to pursue this PhD journey.

Lastly, I would like to acknowledge the Libyan Embassy and the Minister of Education for their generous financial support for this research.

Author's Declaration

I declare that, unless explicitly stated otherwise, this PhD thesis represents my own research and work. It has not been submitted for consideration for any other degree at the University of Glasgow or any other institution.

Rema Mahmoud Zaweia

November 2024

Definitions/Abbreviations

List of abbreviation	
µg	microgram
µl	microliter
AJs	Adherens junctions
AP-1	Activated protein 1
APC	Adenomatous Polyposis Coli
BCC	Basal cell carcinoma
BSA	Bovine serum albumin
creP	Cyclisation recombination gene of bacteriophage P1
cSCC	Cutaneous squamous cell carcinoma
DAB	3,3'-Diaminobenzidine
DCIS	Ductal Carcinoma *in situ*
DMBA	7-12-Dimethylbenzanthracene
DNA	Deoxyribonucleic acid
dNTPs	Deoxynucleotide triphosphatase
E-cadherin	Epithelial cadherin
EDTA	Ethylenediaminetetra-acetate
EGFR	Epidermal growth factor receptor
EMT	Epithelial-to-mesenchymal transition
EPLIN	Epithelial protein lost in neoplasm
ERK	Extracellular signal-regulated kinase
g	Gram
GAP	GTPas-activating proteins
GDP	Guanosine diphosphate
GEF	Guanine nucleotide exchange factors
GSK3ß	Glycogen Synthase Kinase 3-ß
GTP	Guanosine triphosphate
H&E	Hematoxylin and eosin
HCl	Hydrochloride acid
HF	Hair follicle
HK1.fos	Transgenic mice expressing *v-FOS* from a modified K1 vector
HK1.ras	Transgenic mice expressing *v-HRAS* from a modified K1 vector

IDC	Invasive ductal carcinoma
IF	Immunofluorescence
IHC	Immunohistochemistry
KA	Keratoacanthoma
LEF	lymphoid enhancer factor
LRP	LHR-related protein
MAPK	Mitogen activated protein kinase
MEK	Mitogen-activated protein kinase/Extracellular signal-regulated kinase
mg	milligram
MMPs	Matrix metalloproteinases
NMSK	Non melanoma skin cancer
p53	Tumour suppressor protein 53
PBS	Phosphate buffered saline
P-cadherin	Placenta cadherin
PCR	Polymerase chain reaction
pdSCC	Poorly-differentiate squamous cell carcinoma
P-EMT	Partial epithelial-to-mesenchymal transition
PI3K	Phosphatidylinositol-3-kinase
PIP2	Phosphoinositide bisphosphate
PIP3	Phosphoinositide triphosphate
PLBD	Progesterone Ligand Binding Domain
PTEN	Phosphatase and Tensin Homolog
RTKs	Receptor tyrosine kinases
SCC	Squamous cell carcinoma
SDS	Sodium dodecyl sulphate
TCF	T-transduced cell factor
TGFβ	Transforming Growth Factor-β
TPA	12-O-Tetradecanoylphorbol-13-acetate
TSGs	Tumour suppressor genes
wdSCC	Well-differentiated squamous cell carcinoma
β-cat	β-catenin

Chapter 1 Introduction

1.1 Cancer

Cancer, as a disease, has become more complex in recent decades due to the rapid progress in understanding underlying carcinogenic factors, ranging from UVB exposure and smoking to familial genomic instability syndromes. Studies have shown that cancers share several common hallmarks, including sustained proliferative signalling, evasion of growth suppressors, resistance to programmed cell death (apoptosis), and impaired terminal differentiation, ultimately disrupting normal homeostasis and enabling cellular immortality.

From both a patient and clinical perspective, understanding the mechanism(s) that drive the progression of benign tumours to become malignant and ultimately invasive is of great importance. One major part of this process is likely to focus on failures of cell-cell adhesion and cellular matrix interactions that coordinate cell-cell signalling (Fessler et al., 2009; Morin, 1999). Furthermore, such failures or changes may affect the early development of neoplasia (Hanahan & Weinberg, 2000; Hanahan & Weinberg, 2011; Tinkle et al., 2004), or aid progression through the benign stages to malignancy and, more importantly, invasion and metastasis.

In skin cancer, one of the earliest and most crucial characteristics acquired by cancer cells is sustained proliferation, resulting from either congenital genetic mutation, such as those in Cowden's disease (Liaw et al., 1997), or acquired mutations due to factors such as sun exposure (Leiter, 2021; Sharma et al., 2023; Ziegler et al., 1994). These mutations may result in the disruption of normal cell signalling and can equally lead to a dysregulation of cell growth, allowing cancer cells to maintain their vitality and continue proliferating (Janus et al., 2017). This abnormally excessive state of cell proliferation is a fundamental aspect in the development and progression of cancer. The acquisition of specific functions and capabilities in different types of tumours through diverse mechanisms acts as a driver or inhibitor at various stages of tumorigenesis. The outcome of a tumour, whether it remains benign, regresses, or progresses to malignancy, depends on the stage-specific responses of the transformed cells during tumour development, including initiation, promotion, and progression. This

emphasises the complex and context-dependent nature of tumour development and progression.

In the context of various carcinogenic signalling pathways across tumour types, a specific example is mutations in the *ras* oncogene, which encodes a small GTPase. Primarily, these are point mutations at codons 12, 13, or 61, which alter the protein configuration and impair the intrinsic GTPase activity of ras, disrupting the negative feedback mechanisms that normally regulate ras signalling, leading to persistent activation of ras pathways (Der et al., 1986). This continuous activation can drive aberrant cell proliferation and survival. Furthermore, the deregulation of nuclear transcription factors, exemplified by fos, can lead to altered gene expression profiles that contribute to tumour development. Additionally, mutations or loss of function in membrane-associated signalling components such as PTEN can disrupt the AKT signalling pathway, promoting unchecked cell growth and survival. These molecular alterations collectively contribute to tumorigenesis by enhancing oncogenic signalling and evading cellular growth controls (Calautti et al., 2005). This dysregulation affects various downstream signalling pathways involved in promoting cell proliferation, migration, and cell progression.

The cooperation between these signalling pathways, such as the mitogen-activated protein kinase/extracellular signal-regulated kinase (MAPK/ERK) pathway and the phosphatidylinositol-3-kinase/protein kinase B (PI3K/AKT) pathway, regulates cell-cell adhesion by controlling the expression of adhesion molecules, including E-cadherin. These pathways can also modulate essential cellular behaviours, including migration, proliferation, apoptosis and cell differentiation, all of which are relevant to epithelial tissue homeostasis and tumour development (Hülsken et al., 1994; Morin, 1999; Pećina-Slaus, 2003). These effects occur via interactions with regulatory proteins and tumour suppressor genes (TSGs). For example, Glycogen Synthase Kinase 3-β (GSK3β) regulates β-catenin, thereby controlling transcriptional programs involved in cell adhesion and proliferation pathways, influencing TSGs, such as p53 and p21, which modulate cell cycle progression and apoptosis.

Furthermore, it is crucial to maintain both negative and positive feedback signalling during normal conditions, thereby ensuring the

homeostatic regulation of intracellular pathways. Defects in these feedback mechanisms can lead to continuous proliferative growth or differentiation, thus enabling some cells to adapt to high levels of oncogenic signalling, preventing senescence and/or apoptosis (Collado & Serrano, 2010; Evan & d'Adda di Fagagna, 2009).

In addition to the many genes that are responsible for cell proliferation and differentiation, extensive research has been conducted into the contributions of the microenvironment to tumorigenesis (Li et al., 2019). The structure and signalling interactions of the microenvironment are vital to cancer phenotypes, especially in the process of invasion (Quail & Joyce, 2013). The ability to initiate and enhance growth by these stimulatory signals, a hallmark of cancer, allows cancer cells to exploit mechanisms that regulate cell proliferation by stimulatory signals and enhance growth (Hanahan & Weinberg, 2011). In addition, cancer cells must evade the growth-inhibitory mechanisms that normally regulate cell proliferation, many of the TSGs (Muller & Vousden, 2013).

Several TSGs play vital roles in controlling cell growth and restricting proliferation through their specific mechanisms of action (Hanahan & Weinberg, 2000). Failures or inappropriate responses of these genes are linked to various pathological conditions, including cancer. Therefore, it is vital for cancer cells not only to sustain proliferation but also to develop mechanisms to evade or counteract the regulatory functions of TSGs, such as p53. The p53 protein plays a crucial role in maintaining genomic integrity by regulating cell cycle progression and inducing apoptosis (programmed cell death) in response to DNA damage (Mollereau & Ma, 2014; Vousden & Prives, 2009). Therefore, the ability of cancer cells to bypass p53-mediated tumour suppression is a crucial factor in tumour progression and malignancy (Mollereau & Ma, 2014). Mutations in p53 are among the most common genetic alterations found in human cancer, significantly impacting tumour progression and resistance to therapy (Hollstein et al., 1997).

In the context of human skin squamous cell carcinoma (SCC), p53 mutations are particularly prevalent due to the high mutagenic potential of ultraviolet (UV) radiation, which induces specific mutations in the p53 gene, often resulting in a loss of its tumour suppressor functions (Brash et al., 1996). These UV-induced mutations typically involve C-to-T transitions at

dipyrimidine sites, leading to amino acid substitutions that impair the protein's ability to bind DNA and activate target genes crucial for cell cycle arrest and apoptosis (Brash et al., 1996). Consequently, the accumulation of such mutations contributes to the malignant transformation of skin cells and the progression of SCC (Brash et al., 1996).

The failure of cellular protective mechanisms or the inadequacy of DNA repair processes to rectify irreversible DNA damage can promote malignant transformation (Reed, 2000). This results in the acquisition of resistance to apoptosis, facilitating neoplastic cell survival (Vaseva et al., 2009). E-cadherin, a critical tumour suppressor gene encoding an epithelial cell adhesion molecule, is frequently downregulated or mutated in various cancers (Christofori et al., 1998). The loss of E-cadherin function disrupts cell-cell adhesion and tissue integrity, thereby contributing to increased cellular motility and invasion of carcinoma cells (Berx et al., 1995).

Non-melanoma skin cancer (NMSC) is one of the most common cancers in the world, and the incidence of cutaneous squamous cell carcinoma (cSCC) is increasing annually in many countries due to UV-B exposure (Rogers et al 2015; Berger, 2018). Two main forms exist: basal cell carcinoma (BCC) and squamous cell carcinoma (SCC). BCC is primarily a disease of the elderly, and the observed incidence of BCC in the UK over the last few decades has increased (Migden et al., 2020); (Briefing, 2013). It is estimated that 110,000 adults developed BCC in 2011 alone (Venables et al., 2019). It poses a significant health burden due to tissue destruction and the associated treatment requirements (Berger, 2018). In contrast, SCC has a well-recognised propensity to metastasise. Metastatic cases have significantly poorer outcomes, with 3-year survival rates ranging from 29% to 46% (Venables et al., 2019), and approximately 76% of SCC-related deaths in the UK occur in individuals aged 75 and older (Migden et al., 2020; Rischin et al., 2022), highlighting the influence of age on prognosis. Globally, five-year survival rates for SCC have improved over time, though outcomes remain poorer for older adults and males (Migden et al., 2020; Rischin et al., 2022). These disparities may relate to delayed diagnosis, comorbidities, or greater cumulative exposure to ultraviolet (UV) radiation (Li et al., 2024). Major risk factors include UV radiation, fair skin, age, male sex, and

immunosuppression (Li et al., 2024). Recognising these factors is crucial for early detection and improved outcomes.

SCC is a cancer of the keratinocytes in the basal layer of the epidermis and the stem cell niche of the hair follicle (Jensen et al., 2008) and represents up to 35% of all skin cancers, resulting in around 10,000 cases per year in England and Wales. Although the mortality rate of cutaneous SCC metastasis is low (<5%) and the majority of cSCCs are successfully treated by surgical excision, the risk of recurrent disease and future metastasis is still high (Que et al., 2018).

The increased incidence of cSCC has been largely attributed to the growing popularity of artificial UV tanning beds and travelling to regions with high UV exposure. This increase is particularly observed in individuals with type I-III Fitzgerald phototype skin, which refers to fair to light skin, who are more susceptible to UV damage (Olsen & Green, 2012; Zhang et al., 2012). Mutations induced by UV radiation, specifically the formation of pyrimidine dimers, are strongly associated with the development of SCCs (Kim & He, 2014). The mutational landscape of SCCs is characterised by a high number of mutations, with an average of 50 mutations per megabase pair of DNA (South et al., 2014). This can also obscure which genes are the driver mutations. A significant aspect of these mutations is the involvement of key TSGs, such as *p53* and *ras* mutations.

Thus, the main objective of this study is to investigate the mechanisms of skin carcinogenesis using transgenic mouse multistage skin carcinogenesis models. The study aims to elucidate how disruptions in adhesion signalling pathways contribute to oncogenesis by examining the effects of E-cadherin loss at different stages of skin carcinogenesis, given its involvement in cell-cell adhesion and interaction with *ras*/*fos* oncogenes and PTEN loss. Also, the study aims to assess the role of E-cadherin-mediated ß-catenin signalling and p53 status within these models (Tan et al., 2012; Yao et al., 2008).

1.2 Skin layers

The outer layer of the skin, the epidermis, and its appendages, is a dynamic structure that continually regenerates itself in a controlled manner (Fuchs, 2007). To maintain the protective function of the skin against damage, the tissue undergoes continuous renewal and repair. This involves proliferative cells in the basal layer transitioning through different layers of the epidermis (spinosum, granulosum, and corneum) before being shed and replaced (Figure 1-1). This process includes the loss of hemidesmosomes that anchor the cells to the basement membrane and is facilitated by specific protein expression and the differentiation of keratinocyte cell types across the epidermal layers (Fuchs & Green, 1980).

Keratinocytes play an active role in epidermal morphogenesis, as well as in regulating epidermal polarisation, signalling and skin barrier formation (Fuchs & Green, 1980; Green et al., 2011). The skin is composed of several cell types, including keratinocytes, melanocytes and immune cells, with stem cell populations located in the hair follicles. Most epidermal stem cells are in the hair follicles; however, interfollicular stem cell populations have been identified, which can be used to study the interaction between different stem cell populations and their niches during cancer formation (Fuchs, 2007; Watt & Jensen, 2009).

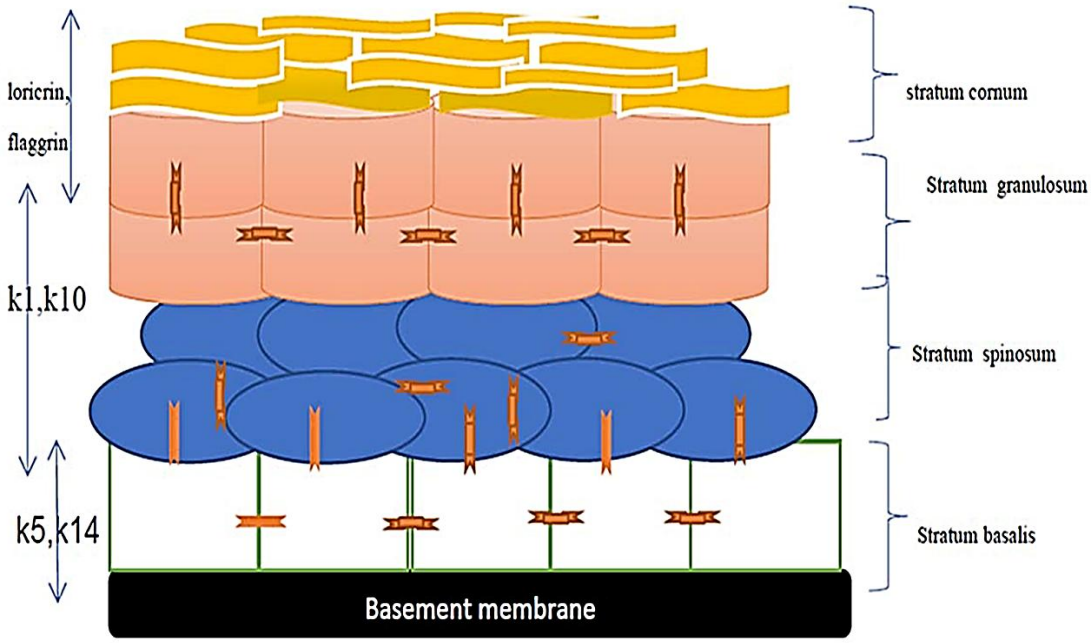

Figure 1-1 Diagram of a typical stratified epidermis with typical markers The epidermis consists of stratified epithelia of basal, suprabasal, and granular layer keratinocytes. Typical markers associated with terminal differentiation through each layer include Keratins K5 and K14, which indicate the proliferative basal compartment. Keratins K1 and K10 are early differentiation markers that are expressed as keratinocytes commit to differentiation and leave the basal layer, whereas loricrin and filaggrin are late-stage markers. Other keratins, such as K6, which is normally expressed in hair follicles, can be exploited as markers of proliferative disease when expressed in all layers, indicating anomalous, pre-neoplastic, hyperplasia, or epidermal stress (original diagram).

The stratum basalis, (Figure 1-1) known as the basal layer, is the deepest layer of the epidermis that is directly attached to the basement membrane separating the epidermis from the dermis. This layer consists of actively dividing keratinocytes known as proliferative transient amplifying cells, as well as occasional interfollicular epidermal stem cells; however, most pluripotent stem cells are in the bulge region of hair follicles (Fuchs, 2007; Watt & Collins, 2008).

These cells, working together, are essential for maintaining the epidermis. Simple transient amplifying keratinocytes divide into a transient amplifying cell and a daughter cell that undergoes terminal differentiation, contributing to the development of mature skin (Rangel-Huerta & Maldonado, 2017). As the epidermis undergoes continuous renewal to maintain its integrity, cells with mutations or those infected with viruses are eventually eliminated. The regulation of this process is controlled by a complex signalling pathway called Wnt signalling, which plays a crucial role in hair follicles, sebaceous glands, and the differentiation of keratinocytes in the maintenance of the epidermis (Alonso & Fuchs, 2003; Watt & Collins, 2008).

The proliferative basal layer of the skin expresses two types of keratins, keratin14 (K14) and keratin5 (K5) (Figure 1-1) that play a role in maintaining the structural integrity of the skin (Fuchs & Raghavan, 2002; Weinberg, 2007). Additionally, the hair follicles express other keratins, such as K15 and K6, which are markers for skin damage or epidermal hyperproliferation (Rothnagel et al., 1999).

As proliferative cells in the basal layer move upward, they undergo differentiation into either the spinous layer or the suprabasal layer. These differentiated layers express the early differentiated markers K1 and K10. K1 and K10 are stable (mRNA production is turned off, but the proteins remain stable, so they persist despite the cessation of transcription) (Rothnagel et al., 1999). This suggests that their sustained presence in the epidermis does not rely on continuous transcription. However, the initial activation of their expression still depends on the formation of a specific transcription complex. In differentiating keratinocytes, this complex includes Activation Protein 1 (AP-1), which is composed of specific members of fos and jun families of transcription factors. AP-1 ensures that the K5,

K14, K1, and K10 genes are turned on at the correct stage of keratinocyte differentiation, to maintain epidermal structure and function (Greenhalgh et al., 1993b; Greenhalgh et al., 1990; Greenhalgh & Yuspa, 1988). These keratins are linked together through intermediate filaments (Fuchs & Green, 1980), which in turn connect the basal cells to the basement membrane via hemidesmosomes.

During the process of keratinocyte differentiation, cells from the suprabasal layer migrate into the granular layer. This layer contains keratohyalin granules, which contribute to the production of late-stage differentiation markers such as filaggrin. Additionally, structural proteins like loricrin and keratinocyte transglutaminase are also present in this layer (Candi et al., 2002; Yuspa, 1994; Yuspa et al., 1989).

The outermost layer of skin, the cornified layer, is formed through the process of filaggrin collapsing and flattening the shape of cells (Figure 1-1). This process gives the layer its characteristic cornified appearance and strengthens it by cross-linking various proteins, including loricrin, which is regulated by transglutaminase (Candi et al., 2002).

1.2.1 Cell-cell junctions in the epidermis

The epidermis relies on several distinct types of cell-cell junctions to maintain tissue cohesion, barrier integrity, and intercellular communication.

1.2.1.1 Adherens Junctions

In the epidermis, adherens junctions (AJs) are essential, as they provide tensile strength in the epidermal spinous layers and facilitate communication between proliferative and differentiated cells, thereby maintaining barrier functions and inhibiting the cellular transformation of damaged cells (Gall & Frampton, 2013; Tinkle et al., 2004; Zhao et al., 2008). To maintain proper adhesion and communication between epidermal cells, the attachment of cytoplasmic intermediate filaments, which are formed by the correct expression of specific keratins, is necessary for anchorage of desmosomes and hemidesmosomes (Green & Jones, 1996; Jones et al., 2017; Stappenbeck et al., 1993). This provides structural support and integrity to the epidermal cells, allowing them to withstand mechanical stress while ensuring cellular adhesion and signalling through binding to cadherin-mediated desmosomal

arrangements at the cell membrane (Goldenberg & Harris, 2013; Hartsock & Nelson, 2008).

1.2.1.2 Desmosomes

Desmosomes are specialised intercellular junctions that provide mechanical integrity to the epidermis by anchoring intermediate filaments between adjacent keratinocytes. These junctions are primarily composed of cadherin family proteins, specifically desmogleins and desmocollins, which are linked to cytoplasmic proteins such as plakoglobin and desmoplakin, which in turn connect to the keratin intermediate filament network (Green et al., 1987; Green & Jones, 1996). This cytoskeletal linkage allows the epidermis to withstand mechanical stress and maintain tissue cohesion (Moch et al., 2020; Yeruva & Waschke, 2023). While desmosomes provide structural stability to the suprabasal layers, the basal layer relies on dynamic cell-cell adherens junctions, mediated by E-cadherin and ß-catenin proteins (Young et al., 2003). The involvement of E-cadherin in maintaining cellular adhesion has prompted investigations into its role in the development, progression, and invasion of skin cancer. This highlights the importance of these proteins in cell adhesion and their potential role in the invasive behaviour of skin cancer. Reduced desmosomal expression, including desmogleins and desmocollins, has been implicated in various cancers, potentially compromising cell adhesion and promoting invasion and metastasis. Notably, desmoglein 2 (DSG2) overexpression has been associated with poorer prognosis and higher recurrence risk in breast cancer patients (Moch et al., 2020; Yeruva & Waschke, 2023).

1.2.1.3 Tight Junctions

In addition to desmosomes and AJs, other cell-cell junctions play vital roles in maintaining epidermal structure and function. Tight junctions, primarily composed of claudins, occludins, and junctional adhesion molecules (JAMs), are located in the granular layer of the epidermis and are crucial for establishing the epidermal barrier (Katsarou et al., 2023). They prevent uncontrolled water loss and block the entry of pathogens or toxins by regulating paracellular permeability. Disruption of tight junction integrity has been associated with skin disorders and may also contribute to tumour

invasion by weakening the barrier function. Alterations in tight junction proteins, such as claudin-1 overexpression, have been observed in skin cancer, like Merkel cell carcinoma, indicating their potential role in tumour progression (Werling et al., 2011).

1.2.1.4 Gap Junctions

Gap junctions are specialised intercellular connections formed by connexin (Cx) proteins, such as Cx 26 and Cx 43, which allow the direct passage of ions, metabolites, and small signalling molecules between neighbouring cells (Djalilian, 2006; Wang et al., 2010). These junctions facilitate coordinated cellular activity, such as synchronised keratinocyte proliferation, differentiation, and response to injury, which is essential for maintaining epidermal homeostasis and tissue integrity (Sun et al., 2021; Yasarbas et al., 2024). Alternations in connexin expression, such as overexpression of Cx43, have been linked to abnormal keratinocyte behaviour and skin tumorigenesis (Sun et al., 2021; Tittarelli et al., 2015). Increased Cx26 expression is associated with lymphatic vessel invasion and poor prognosis in human breast cancer (Naoi et al., 2007). While multiple junctional complexes cooperate to maintain epidermal architecture and function, E-cadherin remains central to the integrity of AJs, and its dysregulation plays a pivotal role in skin tumour progression.

1.3 E-cadherin structure and overview

Cadherins are a large family of transmembrane calcium-dependent cell adhesion proteins (Dalle Vedove et al., 2019). They have a key role in tissue morphogenesis and maintaining architecture. Due to their involvement in processes such as cell proliferation, migration, and signalling, cadherins are increasingly recognised as potential targets for drug discovery in cancer treatment. E-cadherin mediates cell-cell adhesion through homophilic interactions that involve calcium-dependent dimerisation and oligomerisation of extracellular cadherin domains on adjacent cells. This interaction forms a stable and extensive adhesive interface that is critical for epithelial tissue integrity (Nelson, 2008).

Typical types of cadherins, which are necessary for skin morphogenesis, are epithelial cadherin (E-cadherin) and placental cadherin (P-cadherin)

(Lourenço et al., 2008). The prototype E-cadherin forms homophilic clusters between epithelial cells and is the fundamental source of epithelial adherent junctions. These junctions are vital for tissue development, differentiation, maintenance of epithelial barrier function and tissue homeostasis (Margulis, et al., 2005). In normal epidermis, E-cadherin is expressed in the differentiated suprabasal layer and is a vital component of the spinous layer due to its role in maintaining tissue integrity and intercellular adhesion. Thus, any defect in E-cadherin may lead to hyperproliferation, defective differentiation and impaired barrier formation with loss of adherent junctions (Tinkle et al., 2004; Zhang et al., 2009). E-cadherins are linked to the actin cytoskeleton through ß-catenin (Drees et al., 2005), which also binds to the cytoskeletal complex involving the Adenomatous Polyposis Coli (APC) gene. This complex interacts with multiple signalling pathways (Figure 1-2), including MAPK tyrosine kinases via α-catenin (Conacci-sorrell et al., 2002), Phosphatase and Tensin Homolog (PTEN) (Subauste et al., 2005), and canonical Wnt signalling (Grigoryan et al., 2008).

E-cadherin is a calcium-dependent transmembrane glycoprotein composed of five extracellular cadherin (EC) repeats, a single transmembrane domain, and a cytoplasmic tail that binds to catenins. The extracellular repeats (EC1-EC5) mediate homophilic adhesion by binding to identical E-cadherin molecules on adjacent cells in a calcium-dependent manner, stabilising cell-cell adhesion. Calcium ions are essential for rigidifying the extracellular domain and enabling adhesive interactions (Huber & Weis, 2001). On the cytoplasmic side, E-cadherin connects to the actin cytoskeleton via ß-catenin and α-catenin (Figure 1-2), forming part of the junction complex (Huber & Weis, 2001). Loss or downregulation of E-cadherin expression, or a switch to N-cadherin, is a hallmark of epithelial to mesenchymal transition (EMT) (Martins-Lima et al., 2022), a process critical in cancer invasion and metastasis during which epithelial cells lose polarity and intercellular junctions and gain mesenchymal traits, including increased motility and invasiveness (Martins-Lima et al., 2022) (see below). The switch from E-cadherin to N-cadherin reduces epithelial cohesion and enhances the interaction with stromal components, facilitating tumour cell dissemination and metastasis (Gravdal et al., 2007). This switch is not merely a structural change; it has profound effects on signalling pathways and transcriptional

regulation associated with tumour progression. As a result, downstream signalling dynamics are also altered, particularly those involving ß-catenin.

There are two distinct pools of ß-catenin: membrane-associated ß-catenin, which binds to E-cadherin, and cytoplasmic/nuclear ß-catenin. The loss of E-cadherin can have significant implications for carcinogenesis by altering ß-catenin signalling (Figure 1-3). Specifically, the disruption in E-cadherin-mediated signalling can lead to the accumulation of ß-catenin in the cytoplasm and its subsequent translocation to the nucleus, where ß-catenin forms a complex with T-transduced cell factor and lymphoid enhancer factor (TCF/LEF), which drives the transcription of target genes associated with oncogenesis (Morin, 1999).

The increased nuclear localisation of ß-catenin in carcinoma indicates its important role in regulating the canonical Wnt signalling pathway (Figure 1-3). This pathway is activated when Wnt ligands bind to Frizzled and LHR-related protein (LRP) receptors, leading to inhibition of GSK3ß, and stabilisation of ß-catenin in the cytoplasm (Figure 1-3). Following its accumulation in the cytoplasm, ß-catenin translocates to the nucleus, where it forms complexes with TCF and LEF, which are integral to the Wnt signalling pathway (Behrens et al., 1998; Behrens et al., 1996; Grigoryan et al., 2008).

Activation of the Wnt/ß-catenin signalling pathway can subsequently induce the activation of additional signalling pathways, including Notch and Sonic Hedghog (Watt & Collins, 2008).

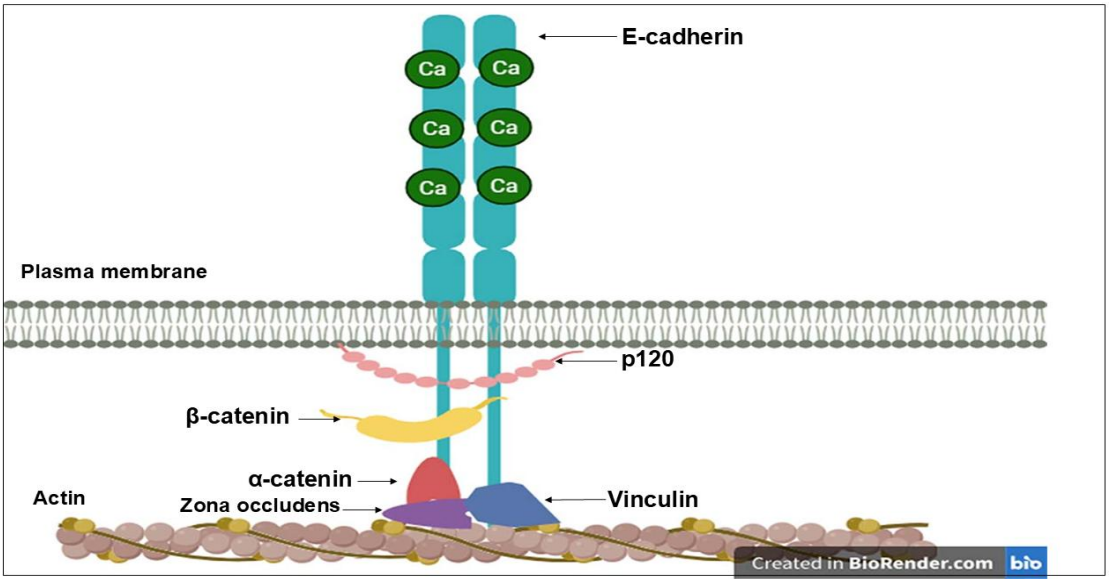

Figure 1-2 The E-cadherin interface mediating cell–cell adhesion. The extracellular domain connects to the extracellular domain of E-cadherin on the adjacent junction to create an Adherens Junction. The intracellular domain binds to p120 catenin, α-catenin and β-catenin. The complex with β-catenin allows α-catenin to link this complex to the cellular actin cytoskeleton. (Original).

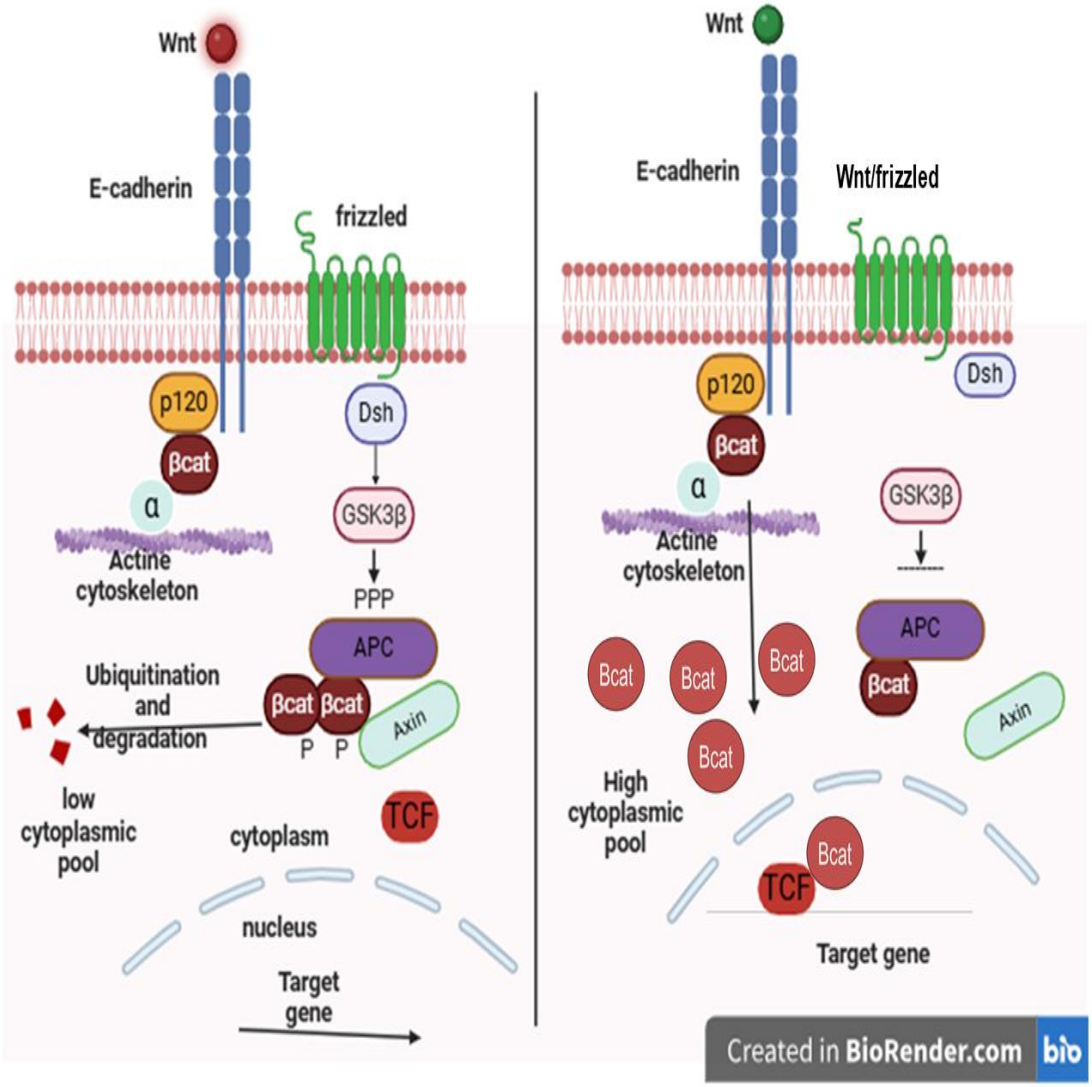

Figure 1-3 Interaction of E-cadherin/β-catenin complex and Wnt signalling pathway in Epithelial cell-cell adhesion. E-cadherin is essential for maintaining epithelial tissue integrity by forming adherens junctions between cells, where β-catenin also plays a key role in Wnt signalling. In the OFF state of Wnt signalling, β-catenin is associated with E-cadherin at the membrane, while the destruction complex, which includes APC and GSK3β, promotes the degradation of free β-catenin, preventing its nuclear entry. When Wnt signalling is ON, the receptor FRIZZLED is activated, inhibiting the destruction complex. This allows β-catenin to accumulate in the cytoplasm and translocate into the nucleus, where it activates transcription of genes that regulate cell proliferation and migration. This shift reduces β-catenin availability for adhesion, weakening cell-cell adhesions.

To inhibit this ß-catenin signalling process, GSK3ß binds to APC and forms a complex with ß-catenin for ubiquitination (Figure 1-3), Wnt signalling is halted (Grigoryan et al., 2008). ß-catenin appears essential for E-cadherin to express its normal adherent role, as a previous study indicated that an E-cadherin deletion mutant lacking its ß-catenin binding region was not functional in cell-cell adhesion (Margulis et al., 2005).

1.3.1 E-cadherin and cancer:

E-cadherin is a highly conserved gene that plays a crucial role in carcinogenesis, particularly in tumour progression. The suppression of E-cadherin expression is considered one of the primary molecular events responsible for dysfunctional cell-cell adhesion. Thus, suppression or loss of E-cadherin function is associated with a higher chance of invasion and metastasis, so it is named the "suppressor of invasion" gene (Pećina-Slaus, 2003). A previous study investigated E-cadherin expression *in vitro*, revealing decreased levels of E-cadherin accompanied by a compensatory redistribution of ß-catenin to the cytoplasm, associated with loss of intercellular adhesion (Margulis et al. 2005), decreased ß-catenin-mediated transcription and increased cell invasion in 3D models. Therefore, the suppression of E-cadherin expression and the subsequent loss of its function fundamentally promote the progression of SCC by weakening cell-cell adhesion, activating oncogenic Wnt signalling, and enhancing cellular invasion and metastasis (Margulis et al. 2005). However, it has not been confirmed whether the loss of E-cadherin plays a critical role earlier in SCC development, if it occurs gradually during the conversion process, or if it is merely a consequence of other molecular changes, such as ß-catenin overexpression. Moreover, studies have suggested that the loss of E-cadherin may lead to ß-catenin activity. However, it remains unconfirmed whether this increase is due to the Wnt signalling pathway or potential regulatory mechanisms involving E-cadherin signalling, which ultimately enhance expression of ß-catenin (Margulis et al. 2005).

The underlying carcinogenesis mechanism depends on the failure of cell-cell adhesion signalling systems, which normally regulate the proliferation, differentiation, and polarity of cells (Margulis et al., 2005). Evidence suggests that progression is mediated via failures in gene function

at the primary level of direct physical cell-cell contact, such as E-cadherin, which signals to the APC/GSK3β axis via β-catenin (Conacci-Sorrell et al., 2002), which is also regulated by PTEN/AKT signalling and the MAPK pathway (See Figure 1-6) (Perez-Moreno et al., 2003). The downregulation or loss of E-cadherin expression, whether through mutations in the E-cadherin gene or other mechanisms that disrupt E-cadherin signalling and compromise the integrity of AJs, is a phenomenon observed in various carcinomas, contributing to the loss of cell-cell adhesion (Conacci-Sorrell et al., 2002).

A recent study has challenged the dogma that E-cadherin loss is a marker or driver of malignant conversion. Interestingly, the results demonstrated that E-cadherin expression was essential for tumour invasion (Padmanaban et al., 2019). Paradoxically, the study also demonstrated that cell proliferation and metastasis were reduced in transgenic models with conditional loss of E-cadherin. E-cadherin functions were essential regulators of cancer cell survival, as E-cadherin loss was accompanied by upregulation of genes such as Transforming Growth Factor-β (TGFβ), which, at the early stages of Ductal Carcinoma *in situ* (DCIS) and in skin papilloma formation, acts as a repressor of proliferation, becoming oncogenic at later stages (Glick et al., 1991), and also increased the apoptosis signalling pathways (Padmanaban et al., 2019). These findings suggest a more complex role for E-cadherin in carcinoma progression and highlight the necessity for further investigation using *in vivo* models, such as the multistage skin carcinogenesis transgenic mouse model, as this project aims to explore.

Therefore, this project investigated the stage-specific loss of E-cadherin function during papilloma formation and determined the cooperation of E-cadherin with epidermal *HRAS* and/or *fos* oncogene activation and PTEN loss, as well as the signalling pathways associated with E-cadherin-mediated carcinogenesis.

1.3.2 E-cadherin loss and Epithelial-Mesenchymal Transition (EMT)

Epithelial to mesenchymal transition (EMT) is a fundamental biological process through which epithelial cells lose their cell-cell adhesion and polarity, acquiring migratory and invasive mesenchymal properties. EMT is orchestrated by transcription factors such as Snail, Slug, Twist, and ZEB1/2, which suppress epithelial markers, including E-cadherin, and upregulate

markers like N-cadherin and vimentin (Haslehurst et al., 2012). In the context of cSCC, EMT contributes to tumour progression, invasion, and metastasis (Sunkara et al., 2020; Tian et al., 2011).

Loss of E-cadherin is a hallmark of EMT and is frequently observed at the invasive front in cSCC (Pulford et al., 2022). This downregulation destabilises the E-cadherin-catenin complex, allowing ß-catenin to translocate to the nucleus and activate Wnt-driven transcriptional programs involved in tumour progression. EMT markers, including reduced membranous E-cadherin and increased nuclear ß-catenin, have been well characterised in several cSCC studies (Pulford et al., 2022), suggesting that partial EMT may support both local invasion and the maintenance of proliferative capacity.

1.4 The classical skin mouse models of two-stage chemical carcinogenesis

The use of animal models, particularly mice, has been a crucial tool in studying and understanding human cancer for the past century (Tuveson, 2021). The similarities in mutated genes between humans and mice, estimated to be around 80%, have facilitated the development of transgenic mouse models that allow for the induction of mutations in the mouse genome, enabling a better understanding of cancer biology (Zhang et al., 2022). Various methods, such as retroviral infection, microinjection of DNA constructs, or gene-targeted transgene approaches, have been employed to create transgenic mice with specific gene mutations associated with the development of cancer types that mimic human cancer (Ogilvie et al., 2017; Tuveson, 2021).

The complex multi-stage nature of the carcinogenic process can be explored via the development of different models *in vivo* and *in vitro*, providing an ideal opportunity to study the underlying molecular mechanisms of progression. Also, these models may help to define the common mutations that cooperate within carcinogenesis and verify their causal roles (Balmain, 2020; Kim et al., 2021). In addition, analysis allows for the exploration of progression mechanisms and how they unfold *in vivo*, potentially revealing systems that have developed to inhibit carcinogenesis at each specific stage.

For over 100 years, the nature of multistage carcinogenesis has been defined by applying topical chemical carcinogenesis onto mouse skin that initiates mutation and establishes a pool of cancerous cells (Balmain and Yuspa, 2014; Yuspa, 1998). Since then, mouse skin has been the classical model for multi-stage carcinogenesis, defining the stages of initiation, promotion, malignant conversion and malignant progression (Balmain and Yuspa, 2014; Yuspa, 1998). This regime is characterised by the stage of initiation, the promotion stage, and then either benign conversion, regression, or malignant conversion (Figure 1-4).

Under normal conditions, basal layer keratinocytes divide in a regulated manner in response to environmental signals (Oh et al., 2016). However, genetic mutations can disrupt this regulation, leading to rapid and uncontrolled cell division (Oh et al., 2016). This accelerated proliferation in the epidermis results in thickening and a predisposition to develop papillomas, which may persist, regress, or progress into SCC. With additional mutations, SCC can evolve into more aggressive forms, ultimately leading to invasive poorly differentiated squamous cell carcinoma (pdSCC) (Oh et al., 2016).

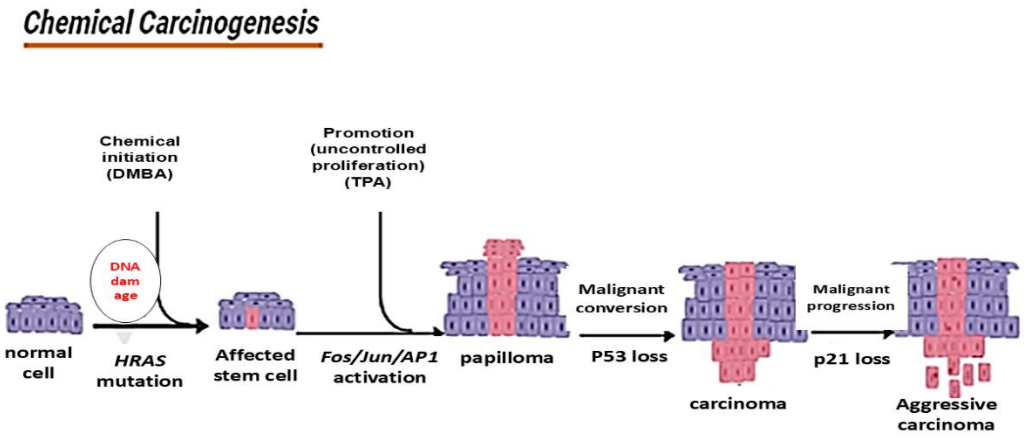

Figure 1-4 The classic mouse skin model of chemical carcinogenesis

Initial *HRAS* mutations are induced by applying 7-12-dimethylbenzanthracene (DMBA) to the skin. This initial mutation does not cause any visible changes. Tumorigenesis is then promoted by repeatedly applying 12-O-tetradecanoylphorbol-13-acetate (TPA) for several weeks to one year. During the first 2-20 weeks, visible papilloma (benign tumours) develops, which can persist, regress, or convert to well-differentiated squamous cell carcinoma (wdSCC) and onto aggressive SCC. The model highlights the importance of multiple genetic changes in the development of malignant tumours (Original, created by BioRender).

The most common protocol used was topical application of 7, 12-dimethyl-benzanthracene (DMBA), followed by weekly applications of 12-O-Tetradecanoylphorbol-13-acetate (TPA) promotion and this treatment regime can continue for up to 60 weeks (Balmain et al., 1984; DiGiovanni et al., 2009; Tremmel et al., 2019). This classical agent activates several pathways, including the c-FOS oncogene in the AP-1 transcription factor complex (Curran & Teich, 1982; Greenhalgh et al., 1990). DMBA is a mutagen used at low levels that does not elicit tumours unless promoted, and yet induces several mutations, including a specific *HRAS* mutation at codon 61 (Balmain et al, 1985; Roop et al., 1986). This mutation is considered the main initiating mutation in the two-stage chemical carcinogenesis model and is the most common ras mutation in human SCCs (Huang and Balmain, 2014). These mutations lead to irreversible DNA damage and contribute to the development of cancer. Mice can be promoted up to a year post-initial treatment, suggesting that epidermal stem cells from the HF are mutated. Therefore, *HRAS* is one of the most frequently mutated genes (Figure 1-4), being activated in 85% of papillomas (Balmain et al., 1984).

Many human SCCs also have activating mutations in the ras oncogene, which participates in cell signalling pathways, resulting in cell growth, differentiation and apoptosis (Pierceall et al., 1991). Previous studies have indicated that in human skin cancer due to prolonged UV exposure, an activated form of the *HRAS* gene is found in up to 50% of SCCs, depending upon latitude and the intensity of UV exposure, as the sequence of GGCC at codon 12 GGA gly arg is susceptible to UV-B induced pyrimidine dimers (Pierceall et al., 1991). Whereas, in mouse tumours initiated by DMBA, most exhibit a specific A-T transversion at the second nucleotide of codon 61 of the *HRAS* gene (Balmain et al., 1984), which also activates the gene.

To further explore this model system, keratinocytes were transformed *in vitro* by infection with v-HRAS and then grafted onto nude mice to investigate carcinogenesis (Roop et al., 1986 ; Strickland et al., 1988). This resulted in the production of benign papillomas due to ras activation. However, conversion to malignant SCC was shown to require extra mutations such as activated fos (Greenhalgh et al., 1988,1990). Thus, this model still requires a promotion step for papilloma formation (see below) (Balmain et al., 1984). This is achieved by application of the TPA promoter, which

activates c-FOS signalling within the AP-1 transcription complex (Greenhalgh 1988; 1990; Yuspa, 1998). As a result, a benign squamous cell papilloma develops. These papillomas may either regress if they remain TPA-dependent or progress to malignancy if they become TPA-independent, evolving first into wdSCC and, over time, into pdSCC (Briefing, 2013).

These two-stage chemical carcinogenesis and graft models, although valuable for studying cancer development (Balmain et al., 1984; Hennings et al., 1993), have a limitation in that they involve the use of mutagens that can induce irrelevant mutations of cells cultured *in vitro*. Thus, the development of transgenic mice that replicate the two-stage process of carcinogenesis was employed, leading to the formation of papillomas and carcinomas, without the need for mutagens. This alternative model enables a more focused investigation of the relevant mechanisms involved in cancer progression (see below). However, it was the cooperation between *ras* and *fos in vitro,* leading to papilloma and carcinoma (Greenhalgh & Yuspa, 1988). This led them to be chosen for targeting the skin and development of transgenic mouse models to study carcinogenesis *in vivo* and replace classic chemical carcinogenesis models, which have many irrelevant mutations.

1.4.1 The HK1 and K14/cre/lox transgenic mouse models

As outlined above, from the patient's viewpoint, the most significant events are those that drive the malignant conversion of benign tumours to carcinomas and subsequent progression with increasing metastatic potential. Therefore, the development of transgenic mice that precisely mimic the multistage nature of carcinogenesis offers an excellent opportunity to investigate the molecular mechanisms driving disease progression. Genetic modifications targeting cutaneous keratinocytes can be achieved through a specific targeting vector or via topical application of RU486 (see Figure 1-7), which activates Cre recombinase in a ligand-inducible system to trigger gene recombination specifically in keratinocytes, both methods effectively prevent unnecessary disease in internal tissues during embryogenesis.

This allows for observation of skin lesion development, thereby reducing the need for invasive surgical procedures. Tissue phenotypes can be confined to locations or specific tumour stages/times (Ogilvie et al., 2017).

To begin to model carcinogenesis *in vivo*, a transgenic mouse model requires targeting vector(s) that are exclusively expressed in the epidermis (Greenhalgh & Roop, 1994). For this, the Human keratin K1 (HK1) gene is considered an ideal targeting vector, whilst mouse K1 (mK1) is expressed only in the differentiated layers; the HK1 targeting vector is a mutated and truncated form missing many regulatory elements and is expressed in the proliferative basal layers (Figure 1-5). The truncated keratin K1 gene remains expressed at the late developmental stage (dE19), so it prevents lethality *in utero*, and it is expressed efficiently in up to 30% of proliferative basal cells but is only expressed in the epidermis (See Figure 1-5), particularly in the ears, and this avoids any tumours in the internal organs.

HK1 differs from the endogenous mouse K1 gene as it possesses efficient expression in malignant keratinocytes transformed by infection *in vitro* with *HRAS* murine sarcoma virus (Rosenthal et al., 1991) and thus remains expressed in HK1 transgenic SCC *in vivo* (Greenhalgh et al., 1993c; Greenhalgh et al., 1993a; Greenhalgh et al., 1993b; Greenhalgh et al., 1995). The expression of the truncated HK1 clone in the basal layer of the skin makes it a suitable tool for achieving exclusive expression in the epidermis and specifically targeting the proliferating basal layer keratinocytes. This targeted expression is achieved by introducing activated *ras* and *fos* oncogenes into the basal layer keratinocytes using the HK1 clone as a vector, allowing for the study of the role of these oncogenes in tumour progression and conversion to carcinoma (Figure 1-5).

As shown in Figure 1-5 PCR/subcloning techniques were employed to design the HK1 targeting vector. The coding regions of HK1 were deleted, leaving the first intron and a poly linker sequence to enable the transgene to be inserted (Figure 1-5), using the ß-galactosidase (ß-gal) gene as a reporter to confirm that expression occurred exclusively in both the proliferative and the differentiated layers of the epidermis, but not in any other squamous epithelia (Greenhalgh et al., 1993c; Greenhalgh et al., 1993a; Greenhalgh et al., 1993b).

Thus, this HK1 model was employed to establish transgenic mice with the potential to produce preneoplastic and benign tumours, which can progress to malignancy through additional genetic alterations or promoter

treatment such as TPA (Greenhalgh et al., 1993c; Greenhalgh & Roop, 1994; Greenhalgh et al., 1993a; Greenhalgh et al., 1993b; Greenhalgh et al., 1995).

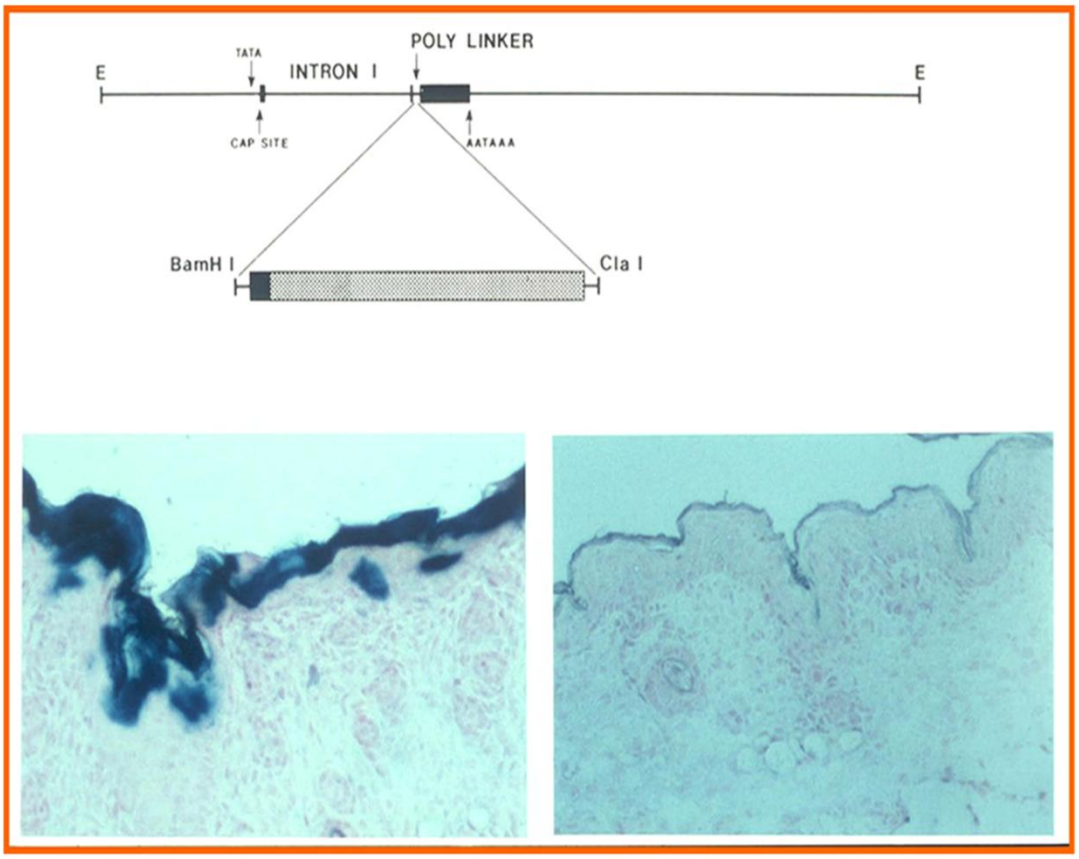

Figure 1-5 Structure of the human keratin 1 (HK)1 targeting vector A 12kb EcoR1 fragment of the human HK1 gene was engineered to remove the coding sequences and insert a BamH1/ClaI cloning site where the LacZ reported gene was inserted to create the *HK1.βgal* mouse. Frozen *HK1.βgal* newborn mouse skin section was stained by Xgal for LacZ/βgal activity, showing expression in the basal layers and suprabasal layers [blue] (Greenhalgh unpublished).

1.4.2 HK1.ras transgenic mouse phenotypes

Ras proteins are key regulators of cellular processes, including cell differentiation, proliferation, and survival. Encoded by three widely expressed genes (*HRAS, K-ras* and *N-ras*), these proteins exhibit substantial sequence similarity and perform overlapping functions. Their activation triggers signalling networks (Hobbs et al., 2016; Huang & Balmain, 2014). Ras acts as a key regulator of downstream effectors that are important for cellular growth and differentiation (Hobbs et al., 2016).

Ras proteins are localised at the cell membrane and act to facilitate cell signalling. Guanine nucleotide exchange factors (GEF) and GTPase-

activating proteins (GAP) switch the activity of ras on and off. Under normal conditions, ras GTPases are strictly controlled, with GEFs exchanging a bound GDP for a GTP. GEFs affect ras activation by exchanging a bound GDP for a GTP. GAPs will then bind to, stabilise, and accelerate enzyme activity. This terminates with the cleavage of the terminal phosphate, returning ras to its inactive, GDP-bound state. The oncogenic mutation influencing ras genes compromises ras GTPase activity, keeping the protein in an active form (Hobbs et al., 2016; Huang & Balmain, 2014).

In the context of skin biology, activation of ras pathways occurs through epidermal growth factor receptor (EGFR) signalling, which is crucial for maintaining cellular homeostasis (Doma et al., 2013; Kern et al., 2011). This activation switches the ras pathway from an inactive state into an active state, initiating the ras/ MAPK pathway (Figure 1-6). This pathway involves the activation of Raf, which phosphorylates mitogen-activated protein kinase (MEK) and (ERK), resulting in activation of various transcriptional targets, including the AP-1 complex (Deng & Karin, 1994; Doma et al., 2013; Kern et al., 2011; Roberts & Der, 2007).

These downstream signalling events regulate genes involved in cell cycle progression, apoptosis. In this process, PI3K plays a central role. Upon activation by receptor tyrosine kinases (RTK), PI3K phosphorylate Phosphoinositide bisphosphate (PIP2) to generate PIP3, a key signalling molecule that activates AKT, which in turn promotes cell survival by inhibiting apoptosis and enhancing cell proliferation, survival, migration, and invasion (Qi et al., 2022; Wang et al., 2014; Wen et al., 2021). Activation of PI3K/AKT relies on the E-cadherin-ß-catenin complex (Kim & Lee, 2010). AKT signalling activation, inhibits GSK3ß, leads to stabilisation and nuclear translocation of ß-catenin, thereby enhancing ß-catenin signalling (Lau et al., 2011), which further supports cell survival and promotes tumorigenesis (Figure 1-6). When PTEN is functional, it inhibits the production of PIP3 from PIP2 by PI3K, thereby suppressing the activation of the AKT and cell proliferation (Chen et al., 2016; Xu et al., 2024). When PTEN is lost, PI3K/AKT signalling becomes hyperactive, contributing to tumour progression and cell survival (Figure 1-6). Additionally, ras also activates the PI3K/AKT pathway, which promotes cellular proliferation and enhances resistance to apoptosis (Hopkins & Parsons, 2014; Martini et al., 2014). Thus,

the deregulation of this PI3K/AKT pathway, negatively regulated by PTEN (Hopkins & Parsons, 2014), links the ras/fos/MAPK pathway to PTEN signalling (Figure 1-6). This interaction could contribute to reduced E-cadherin expression in transgenic mouse skin carcinogenesis, a hypothesis addressed in Chapter 3.

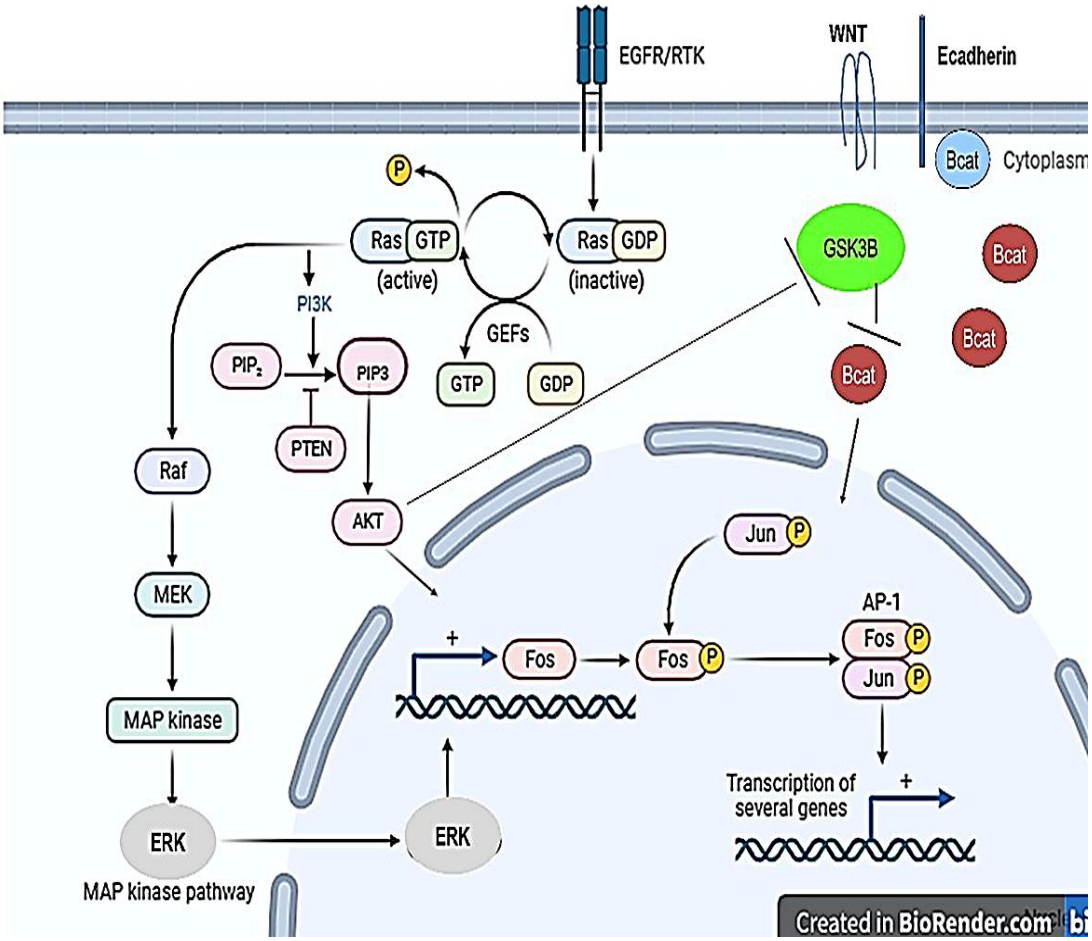

Figure 1-6 Schematic diagram shows PI3K/AKT& Ras/MAPK signalling pathways The diagram illustrates the PI3K/AKT pathway and the ras/MAPK pathway in cell survival and signalling. The ras/MAPK pathway is initiated by the RTK receptor, triggers activation of RasGTPase, and subsequent recruitment of raf (Khosravi-Far et al., 1996). This triggers the activation of MAPK kinase (MEK), which further activates proteins like fos and Jun, which are components of AP-1 transcription factor complex. PTEN inhibits the PI3K/AKT pathway, regulating cell proliferation. AKT activation, through E-cadherin/β-catenin complex, stabilises β-catenin, promoting nuclear translocation. (Original).

The presence of *ras* mutations in various signalling pathways has prompted extensive research into the development of anti-ras therapies, as these mutations are prevalent in around 30% of human tumours (Prior et al., 2012). Human SCCs exhibit a high frequency of *HRAS* mutations, with the mutation at codon 61 being the most common (Huang & Balmain, 2014). When the Harvey murine sarcoma virus (Ha-MSV) gene, which encodes v-HRAS, was introduced into mouse primary keratinocytes, it led to the transformation of the cells, promoting increased cell proliferation upon activation of *v-HRAS*. Additionally, when transformed cells were grafted onto nude mice skin, it resulted in the formation of benign papillomas (Roop et al., 1986). This study demonstrated that *v-HRAS* can mimic the DMBA two-stage chemical carcinogenesis initiation step; however, it still requires a promotional factor, such as wounding, to induce papilloma formation.

The activation of the ras gene using a keratin promoter HK1 in transgenic mouse skin has been investigated (Greenhalgh et al., 1993c; Greenhalgh et al., 1993a). By introducing exclusive epidermal *v-HRAS* expression under the control of the HK1 promoter, the researchers created a transgenic mouse model known as *HK1.ras* (Greenhalgh et al., 1993a). Two strains of *HK1.ras* mice, *HK1.ras*^{1205} and *HK1.ras*^{1276}, were used in this study (Greenhalgh et al., 1993a), with *HK1.ras*^{1205} having the ability to develop benign papillomas in response to wound promotion from ear tagging, whereas *HK1.ras*^{1276} mice did not tend to develop papillomas without additional mutation, such as *fos* activation or *PTEN* mutation (Greenhalgh et al., 1993c; Greenhalgh et al., 1993a; Greenhalgh et al., 1993b).

HK1.ras transgenic mice exhibit papillomas around 10-12 weeks of age, usually following ear tag wounding (see Chapter 3). Although the newborns initially displayed a wrinkled phenotype, adult mice generally appeared normal. However, their epidermis consistently showed a hyperplastic pathology, even in the absence of wound-induced promotion. The papillomas formed by *HK1.ras* persist and do not spontaneously convert into malignancy, and do not undergo spontaneous progression either (Greenhalgh et al., 1993a). This makes the model valuable for studying the genetic mutations involved in malignant conversion and tumour progression, which is essential to enable proper investigation and assessment of multistage events (Greenhalgh et al., 1993c).

Thus, the HK1 targeting vector was employed to target activated *ras* and *fos* oncogenes (*HK1.ras, HK1.fos*). By employing a HK1 keratin promoter, epidermal *v-HRAS* or *v-FOS* expression (Greenhalgh et al., 1993b) elicited keratinocyte hyperplasia and benign papillomas, while *v-FOS* co-expression with *v-HRAS* resulted in autonomous papillomas, but further events are required for malignant conversion (Greenhalgh et al., 1993c). This characteristic makes papillomas ideal for studying the causal roles of other oncogenes in tumour progression and the conversion to carcinoma (Greenhalgh et al., 1995; Macdonald et al., 2014; Masre et al., 2020; Yao et al., 2006).

1.4.3 Fos in skin carcinogenesis

In the *HK1 ras* experiments above, transformation by *ras* induced papillomas; however, it was the introduction of activated *fos* that induced their transformation (Greenhalgh et al., 1990; Greenhalgh et al., 1989; Greenhalgh & Yuspa, 1988) a result consistent with DMBA initiation (Balmain et al., 1984) and confirmed in later TPA experiments (Schlingemann et al., 2003), and thus *HK1.fos* transgenic mice were developed.

The *fos* gene was first identified as the Finkel-Biskis-Jenkins FBJ osteosarcoma virus (Curran & Teich, 1982). It was originally derived through retroviral sequence recombination with the cellular *c-FOS* gene (human homologue). It plays a crucial role in tumorigenesis. Several studies demonstrated that *fos* acts as a nuclear transcription factor. However, *fos* is unable to bind to DNA by itself, but forms an AP-1 complex through heterodimerization with genes from the *jun* family (Malnou et al., 2007). The AP1 complex is a significant target of the ras/MAPK signalling pathway, as previously mentioned. *Fos* expression is associated with cell proliferation, differentiation and apoptosis. It has been shown to be overexpressed in a variety of cancers (Morgan & Curran, 1991) and is one of the major components of epidermal differentiation (Fisher et al., 1991; Greenhalgh et al., 1993b; Guinea-Viniegra et al., 2012; Wang et al., 1995).

In skin physiology and cancer, the role of *fos* as an oncogene is widely recognised (Wang et al., 1995), and in human SCCs, *fos* is known to be induced by UV-B (Christmann et al., 2007). Although the molecular mechanisms by which *fos* contributes to skin tumorigenesis are still unknown

(Guinea-Viniegra et al., 2012). *Fos* is required for *ras*-induced benign and malignant changes in skin progression (Greenhalgh et al., 1990; Greenhalgh & Yuspa, 1988; Saez et al., 1995).

In previous studies using transgenic mice, it was observed that the fusion of lacZ/FOS genes led to continuous expression of *fos* with ß-galactosidase staining in all interfollicular epidermis (IFE) layers, including the hair follicle (Smeyne et al., 1992). In normal human epidermal skin, *fos* was found to be expressed in the proliferative basal cell layers (Basset-Séguin et al., 1990), indicating its involvement in both proliferation and differentiation processes (Fisher et al., 1991). These findings suggest that alterations in *fos* expression may contribute to the development of tumours, making it a potential target in tumorigenesis.

Another *in vitro* study investigated the role of the FBJ murine osteosarcoma virus *v-FOS* gene in tumorigenesis. The study involved transfecting the *v-FOS* gene into papilloma cells (Greenhalgh & Yuspa, 1988), derived from DMBA/TPA promotion, which expressed activated *HRAS* (Strickland et al., 1988). The results showed that co-operation of *v-FOS* and *v-HRAS* led to the formation of malignant SCCs when transplanted into nude mouse skin (Greenhalgh & Yuspa, 1988). Further work demonstrated that the combination of *v-FOS* and *v-HRAS*, achieved through infecting primary mouse keratinocytes and grafting them into the skin of nude mice, led to the development of highly aggressive SCCs (Greenhalgh et al., 1990). This indicates the oncogenic potential of *fos* when combined with *ras* activation and their co-operation in promoting tumorigenesis and malignant transformation of skin cells.

In the context of investigating the role of *c-FOS* in SCC, a transgenic model was developed using the viral form of *v-FOS* derived from FBJ osteosarcoma virus to create the *HK1.fos* transgene, which led to constitutive expression of *c-FOS* in the epidermis.

Delayed development of a hyperplastic histotype with notable keratosis was observed in *HK1.fos* mice (see Chapter 3), typically becoming prominent around 6-8 months following wounding, which eventually progresses into highly keratotic papillomas approximately 8-12 months post-ear-tagging, although they remain benign (Greenhalgh et al., 1993b). Further progression required an additional secondary event. Treatment with TPA resulted in the

appearance of papillomas containing an activated *ras*, which serves as an initiating event (Greenhalgh et al., 1995).

As detailed below in the HK1 transgenic mouse model of skin carcinogenesis, promotion of malignancy required the application of TPA for an extended period (over 1 year), where activation of endogenous *c-HRAS* was found to be involved in the conversion of papilloma to SCC (Greenhalgh et al., 1995; Sutter et al., 1994). The study indicates that the expression of *c-Fos* alone, even when amplified and combined with *HK1.fos*, is insufficient for progression, emphasising the requirement for multiple oncogenic events such as *HK1.ras* or long-term promotion from wounding or TPA to induce papilloma formation and subsequent malignant conversion.

Malignancy in *HK1.fos* mice was achieved by chemical promotion with TPA (Greenhalgh et al., 1995; Hennings et al., 1993; Yuspa, 1994). These experiments indicated that firstly, HK1 progression was seldom spontaneous, requiring specific additional genetic or epigenetic events; and secondly, that premalignant phenotypes possessed the genetic stability necessary to study the progression mechanism *in vivo*.

To induce the development of squamous cell benign papilloma in the HK1.ras genotypes, wound promotion was necessary, which was achieved by ear-tagging. As a result, all *HK1.ras*^{1205} mice developed benign papilloma within 8-10 weeks following ear-tagging, while *HK1.fos* genotypes exhibited delayed papilloma formation occurring 8-12 months following ear-tagging (Greenhalgh et al., 1993a; Greenhalgh et al., 1993b). However, the *HK1.ras*^{1205} mice showed high sensitivity to wound or TPA promotion. Due to ethical considerations in the UK, the *HK1.ras*^{1276} strain was used instead of the *HK1.ras*^{1205} strain (Greenhalgh et al., 1993c), which does not develop papilloma on its own. However, when crossed with *HK1.fos* mice, the bi-genic *HK1.ras*^{1276}*/fos* progeny developed papillomas over a period of 4-6months (Greenhalgh et al., 1993c), allowing for further experiments involving *HK1.ras, HK1.fos*, and Phosphatase and tensin homolog (*PTEN*) loss (Macdonald et al., 2014; Yao et al., 2008; Yao et al., 2006).

When *HK1.ras*^{1205} mice were crossed with *HK1.fos*, the resulting bi-genic pups exhibited severe hyperplasia and hyperkeratosis shortly after birth, leading to restricted movement and incompatibility with life. Breeding *HK1.fos* with the milder *HK1.ras*^{1276} line produced pups with a slightly more

pronounced phenotype, allowing for characterisation of the bi-genic phenotype. The wound-sensitive *HK1.ras* line produced larger papillomas when compared to age-matched *HK1.ras*^{1276}*.fos* mice. However, if the tag is lost in the *HK1.ras*^{1205} line, the papillomas typically regress, while those in *HK1.ras*^{1276}*.fos* persist. Despite this, the tumours did not spontaneously progress to malignancy, even when maintained for 12-16 months, unlike in many other models (Brown et al., 1998). The histological analysis of *HK1.ras.fos* papillomas revealed a typical papilloma structure with orderly differentiation. K1 expression remained strongly suprabasal, reflecting the benign nature of the tumour.

The phenotypic stability of this model was ideal for examining the additional genetic events required for malignant conversion. The induction of the malignant phenotype necessitates additional genetic abnormalities that should be very specific to the tissue involved and should be introduced at specific stages of development to control the timing of new mutations. This requirement ensures that the genetic alterations contribute to the progression of malignancy in a controlled and tissue-specific manner.

Therefore, *HK1.ras* and *HK1.fos* are good candidates for generating the stages of initiation and promotion of pre-malignant phenotypes and papillomas, as detailed previously. However, the lack of spontaneous mutation makes this HK1 model ideal to study the genes driving conversion and malignant progression (Greenhalgh et al., 1993c). This approach has been successful in investigating various combinations of oncogenes and the loss of TSGs, including p53, p21 (unpublished by Greenhalgh) and PTEN (Macdonald et al., 2014) which play crucial roles in the development of malignancies.

1.4.4 Phosphatase and tensin homomlog (PTEN)

One of the first TSGs investigated for a role in malignant conversion was PTEN, a tumour suppressor gene that regulates several cellular processes, including cell death and proliferation, and acts as a negative regulator of the PI3K/AKT signalling pathway. PTEN is a lipid phosphatase that antagonises the action of PI3K by dephosphorylating phosphoinositide triphosphate (PIP3) to generate phosphoinositide bisphosphate (PIP2) (Figure

1-6). PI3-kinase and PTEN are major positive and negative regulators of the PI3K/AKT pathway, respectively (Hopkins & Parsons, 2014).

Furthermore, regulation of this pathway is crucial for maintaining the integrity of fundamental cellular processes, including cell growth, survival, death, and metabolism. Conversely, dysregulation of this pathway is associated with the development and progression of cancers. Receptor tyrosine kinases (RTKs) are major upstream regulators of PI3K/AKT signalling (Hopkins & Parsons, 2014). Loss or inactivation of PTEN accumulates PIP3, which activates AKT anti-apoptotic signalling and permits cells to proliferate uncontrollably (Figure 1-6). Germline PTEN mutation leads to Cowden's Disease, a condition characterised by epidermal hyperkeratosis and a high risk of cancer, such as SCC (Yotsumoto et al., 2020). In some cases, PTEN mutations were associated with more advanced stages of growth, suggesting that overactivation of RTK/PI3K/AKT signalling is driving tumorigenesis (Guinea-Viniegra et al., 2012). E-cadherin loss is implicated, as a previous study demonstrated that the loss of E-cadherin leads to increased cell growth and activation of the PI3K/AKT signalling pathway through inhibition of PTEN transcription.

Another study revealed that the loss of E-cadherin is associated with enhanced nuclear signalling of ß-catenin and constitutive activation of PI3K/AKT signalling, further reinforcing nuclear ß-catenin signalling by inactivation of GSK3ß, indicating crosstalk between E-cadherin, PI3K/AKT and ß-catenin (Georgopoulos et al., 2010). PTEN mutations have been implicated in PTEN hereditary syndromes (PHTS) like Cowden disease (Fistarol et al., 2002; Liaw et al., 1997), which are characterised by initial manifestation of multiple cutaneous keratosis and hamartomas, followed by subsequent development of tumours in various internal organs, including breast, endometrial, thyroid, colon, and kidney cancer (Tan et al., 2012). This keratosis suggests that PTEN has a significant involvement in keratinocyte differentiation and maintenance of the epidermal barrier (Tan et al., 2012), and plays crucial roles beyond its known function in the epidermis, making it a relevant target to investigate in the HK1 mouse model. However, modelling PTEN loss in transgenic mice proved to be challenging due to the lethality associated with PTEN knockout (Suzuki et

al., 1998). The use of the cre-loxP system to induce PTEN loss during embryogenesis led to a rapid progression of SCCs in response to chemical carcinogenesis (Suzuki et al., 1998; Suzuki et al., 2003).

Thus, an RU486-inducible cre-loxP system was employed to mutate PTEN and assess the consequences in the HK1 model (Berton et al., 2000; Macdonald et al., 2014; Yao et al., 2006). Analysis of this study was based on tissue samples derived from two previously established strains of mice, the first strain expressed the keratin K14 promoter-driven cre recombinase protein ligand-binding domain (PLDB), and the second strain was the target, consisting of LoxP-flanked exons or stop codons, allowing for precise, conditional gene manipulation. Consequently, cre recombinase is broadly expressed in keratinocytes, but it initially remains within the cytoplasm (Figure 1-7 A). Upon RU486 application, cre recombinase enters the nucleus, where it ablates or deletes the flanked-LoxP sites, as shown in Figure 1-7 B. Thus, epidermal specificity is attained through the topical application of RU486, with the K14 promoter driving cre recombinase expression specifically in the basal layer of the epidermis and in the stem cells of hair follicles (Berton et al., 2000). The *K14.crePR1* transgene is employed to express *cre* in the basal layer (IFE) keratinocytes, together with (HF) bulge region stem cells (Kellendonk et al., 1996).

Thus, an inducible cre-mediated ablation of PTEN exon 5, known as *Δ5PTEN*, was performed. The process involves the presence of cre-Progesterone fusion protein, which then enters the nucleus to excise the stop codon in exon 5, flanked by loxP ($\Delta 5PTEN^{flx}$). The result of this regulator transgene is illustrated in Figure 1-7. Following topical treatment (ears/dorsal surface) with RU486, cre removes the AKT regulatory phosphorylase activity of PTEN via ablation of exon 5 ($K14crePR/\Delta 5PTEN^{flx}$) (Wu et al., 2003; Yao et al., 2006), resulting in hyperplasia/hyperkeratosis and a model for Cowden's Disease (Ming & He, 2009). Initially, studies utilising a PTEN conditional knockout were assessed and provided multistage tumours to evaluate the roles of E-cadherin. The same gene switch system will be employed to investigate E-cadherin loss in stage-specific carcinogenesis.

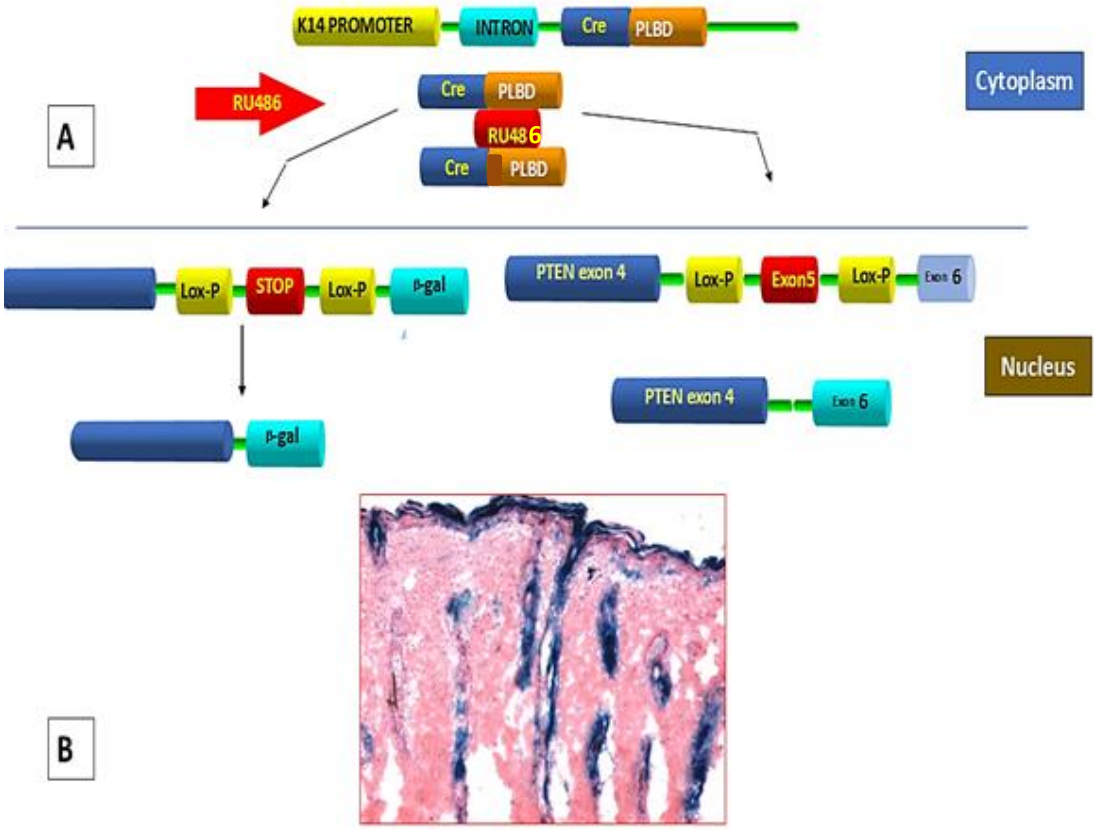

Figure 1-7 A diagram of the Cre/LoxP system with RU486 treatment in bi-genic *K14.creP/Δ5PTEN*$^{flx/flx}$ mice (A) The inactivation of PTEN-mediated AKT regulation is achieved by removing a specific part of the PTEN gene called exon 5, which is responsible for its phosphatase activity. The cre protein, driven by the K14 promoter, is used to specifically express in the epidermis and hair follicle. By treating with RU486, the cre protein is fused to PLBD. Upon treatment with RU486, the creP dimerises and is translocated into the nucleus, where it deletes sequences flanked by loxP sites, including PTEN exon 5. (B) 8/9 weeks post initial RU486 treatment shows β-gal staining expression in interfollicular epidermis and follicles, thus indicating expression in follicular stem cells (Greenhalgh et al., 1995).

Initial experiments using the mouse model demonstrated that cooperation with *ras* activation in RU486-treated *HK1.ras-K14creP/Δ5PTEN*$^{flx/flx}$ mice promoted rapid papillomatogenesis, but malignant conversion was very rare due to elevated p53/p21 expression unless negated by TPA (Yao et al., 2006). An additional study on mice was conducted relating to *fos* activation. RU486-treated *HK1.fos-K14creP/Δ5PTEN*^{flx} transgenic mice exhibited hyperplasia, hyperkeratosis, with tumours becoming highly differentiated and progressing into keratoacanthomas (KAs) instead of carcinoma, due to the high expression of p53/p21 induced by increased levels of GSK3β inactivation (Yao et al., 2006). *Fos* cooperation with PTEN loss was associated with a benign context where GSK3β–induced p53/p21 expression through β-catenin signalling (Grigoryan et al., 2008) and p53/p21 expression continually switched on AKT-associated proliferation, thereby promoting differentiation and preventing further progression. This compensatory mechanism requires normal availability of p53 and/or p21; otherwise, deregulated fos, AKT and GSK3β are associated with malignant progression (Yao et al., 2008; Macdonald et al 2014).

Taken together, this GSK3β inactivation data suggests that increased, cytoplasmic β-catenin was a critical element that triggered compensatory p53/p21 responses. As outlined above, β-catenin has dual functions in the regulation of cells via integration of Wnt signalling and in cell-cell adhesion via maintenance of adhesion junctions alongside *E-cadherin* (and *PTEN*). Hence, E-cadherin signalling to cytoplasmic β-catenin levels dictates which role is activated, and this is dependent on cytoplasmic β-catenin being translocated to the membrane or phosphorylated by the GSK3β/APC complex for subsequent ubiquination (outlined above). The analysis of keratoacanthoma (KA) data, particularly in relation to the cooperation between *fos* and *PTEN*, led to an investigation into the role of E-cadherin loss and its impact on β-catenin activation/inhibition in the *HK1.ras*/fos/PTEN carcinogenesis model (Yao et al., 2008).

Another study investigated the collaboration between *Δ5PTEN* and the oncogenes *ras* (*HK1.ras*) and *fos* (*HK1.fos*), and results showed that RU486-treated *HK1.ras.fos-K14creP/Δ5PTEN*$^{flx/flx}$ skin mice exhibited increased hyperplasia and the development of proliferating cysts. Interestingly, RU486 treatment accelerated papillomatogenesis but delayed malignant

progression. Tumours appeared to halt at a wdSCC histotype (Macdonald et al., 2014; Yao et al., 2006). This investigation sheds light on the intricate interplay between PTEN, ras, and fos oncogenes in skin carcinogenesis. Furthermore, in the presence of various oncogenic effectors, the progression to malignancy necessitated the additional loss of p53, rendering papillomas susceptible to conversion. The sustained expression of p21 appeared to counteract AKT1, thereby restricting the progression towards a wdSCC state for a specific duration. This state persisted until the loss of p21, which led to heightened p-AKT activity and a subsequent transition to a more aggressive SCC (Macdonald et al., 2014). These data sparked interest in conducting this project to investigate the role of E-cadherin loss in *HK1.ras.fos-K14creP/Δ5PTEN*$^{flx/flx}$ transgenic skin mouse and investigate its influence on the activation/inhibition of ß-catenin.

1.4.5 E-cadherin molecular mechanism and crosstalk

The E-cadherin gene, a known tumour suppressor, is located on chromosome 16q22.2, and encodes the E-cadherin protein, which is a 120-kDa transmembrane glycoprotein (Shenoy, 2019). E-cadherin glycoprotein, a key component of cell adhesion, is composed of three structural domains: a transmembrane domain, an intracellular domain, and an extracellular domain with calcium-dependent repeats, enabling homophilic binding between adjacent cells and providing stability, architecture, and inhibition of individual cell motility (Gall & Frampton, 2013; Lilien et al., 2002).

E-cadherin is a crucial component of calcium-dependent cell adhesion, facilitating the formation and maintenance of epithelial cell layers by forming molecular complexes with catenins and connecting to the actin cytoskeleton (Conacci-Sorrell et al., 2002; Gall & Frampton, 2013) (See Figure 1-2). E-cadherin cytoplasmic tails attach to ß-catenin, which in turn connects to α-catenin, forming the E-cadherin-catenin complex (Figure 1-2), which plays a vital role in the function and organisation of epithelial cells by linking to the actin cytoskeleton. This linkage provides mechanical stability to the cell layer, transmits intercellular tension, allows for the coordination of cell shape, and establishes apical-basal polarity, thereby maintaining the integrity of the epithelial cell layer. Its disruption leads to significant

consequences on the differentiation and homeostasis of epithelial structure (Davis et al., 2003; Hinck et al., 1994).

The actin cytoskeleton, especially F-actin, serves as the main link to the active cytoskeleton due to its crucial role in connecting the cadherin-catenin complex to the cellular framework (Bajpai et al., 2009). While α-catenin and ß-catenin play a crucial role in binding E-cadherin to F-actin, they cannot bind directly to F-actin. This limitation underscores the significance of other actin-binding proteins in mediating this connection. One such protein is Epithelial protein lost in neoplasm (EPLIN), which interacts with α-catenin, enabling the E-cadherin-ß-catenin complex to link to F-actin (Abe & Takeichi, 2008).

The exact mechanism by which E-cadherin mutation contributes to carcinogenesis is still under investigation. The role of E-cadherin in both specific developmental processes and carcinogenesis is shaped by the intricate interplay of various signalling pathways. The E-cadherin-catenin complex plays a crucial role in cell-cell adhesion. It is regulated at various levels, including transcription, translocation, trafficking, and post-translational regulation of cadherin proteins. It serves as a signalling hub that transmits signals to the nucleus and cytoskeleton and interacts with various pathways, including ß-catenin, Wnt signalling (Nelson & Nusse, 2004), RhoGTase, nuclear factor kappa light chain enhancer of activated B cells (NF-KB) , and EGFR signalling , in a manner that is independent of adhesion. This complex interplay enables the regulation of diverse cellular processes and contributes to tumorigenesis (Vleminckx et al., 1991).

The adhesive function of E-cadherin depends on extracellular calcium ions, which stabilise its extracellular domains and enable homophilic binding between adjacent cells. A reduction in calcium weakens these interactions, promoting cell detachment, a mechanism relevant to EMT and enhanced migratory behaviour during metastasis. The loss of E-cadherin expression is consistently observed in highly aggressive and less differentiated malignant cells (Nguyen et al., 2011; Shu et al., 2013), and its downregulation is commonly observed in malignant epithelial cancers (Li et al., 2017). Various mechanisms, such as mutation, proteolytic cleavage, and epigenetic regulation, contribute to the functional impairment of E-cadherin in the

development of gastric, breast, kidney, pancreas, and skin malignancies (Bozdogan et al., 2016; Gao et al., 2019; Jang, 2012; Liu et al., 2014). Thus, understanding the complex interplay between E-cadherin and signalling pathways is essential for comprehending the pathogenesis and potential therapeutic strategies for these cancers.

1.4.6 Signalling pathways and crosstalk, regulated by E-cadherin

1.4.6.1 E-cadherin/β-catenin/Wnt pathway:

Beyond its structural role in maintaining cell adhesion, E-cadherin also participates in key intercellular signalling pathways, notably by modulating the Wnt/ß-catenin pathway through its interaction with ß-catenin (Hartsock & Nelson, 2008). Under normal conditions, cytoplasmic ß-catenin is maintained at a low level via its degradation by the APC-GSK3ß-Axin- Casein kinase 1 (Ck1) complex (Lau et al., 2011). However, activation of Wnt signalling inhibits this complex, leading to accumulation and translocation of ß-catenin into the nucleus to activate the Wnt target genes.

Under certain Wnt-activating conditions, such as the presence of paracrine factors, cytokines, and TNF-α, ß-catenin escapes degradation and translocates into the nucleus, where it binds to TCF-4/LEF-1 proteins (Chen & Hu, 2023). This binding induces the expression of Wnt target genes, including c-Myc, cyclins, and MMP, leading to uncontrolled cell proliferation and growth (Volpini et al., 2018). Loss of E-cadherin disrupts ß-catenin sequestration at the membrane, leading to cytoplasmic accumulation and enhanced nuclear signalling. This not only promotes uncontrolled cell proliferation but also contributes to oncogenesis by repressing PTEN, a key inhibitor of the PI3K/AKT pathway. Reduced PTEN expression allows for increased PI3K/AKT activity via GSK3ß inhibition, further supporting tumour growth and survival (Lau et al., 2011). Collectively, E-cadherin loss facilitates tumour progression by enhancing both Wnt/ß-catenin signalling and PI3K/AKT pathway activation (Figure 1-3).

Thus, E-cadherin plays a crucial role in regulating the levels of cytoplasmic ß-catenin. By maintaining low levels of cytoplasmic ß-catenin, E-cadherin inhibits ß-catenin signalling and induces growth inhibition (Gottardi et al., 2001). However, a study carried out in human ovarian cancer showed that E-cadherin downregulation leads to the loss of ß-catenin from cell-cell contact sites (Lau et al., 2011). This study investigated the involvement of the PI3K/AKT/GSK3ß signalling pathway in changing the subcellular localisation of ß-catenin caused by E-cadherin depletion. The results showed that the activity of the LEF/TCF promoter, which indicates the transactivation activity of ß-catenin, is increased in ovarian carcinoma with E-cadherin depletion, suggesting the involvement of PI3K/AKT/GSK3ß signalling in this process (Lau et al., 2011). However, the exact mechanism by which E-cadherin loss regulates ß-catenin signalling is still not fully understood.

The translocation of ß-catenin into the nucleus also suppresses the expression of PTEN; therefore, investigation of E-cadherin/PTEN cooperativity is needed, as there is a potential for cooperation between E-cadherin and PTEN/ras and fos. Additionally, the interaction of PTEN with ras and fos proteins indicates a connection to MAPK pathways (Hopkins & Parsons, 2014). These findings highlight the interconnectivity of these molecular pathways and their role in cellular processes related to cancer development and progression.

Understanding the role of E-cadherin in cellular signalling pathways provides insight into how disruptions in these pathways can lead to cancer development. E-cadherin plays a crucial role in regulating the AKT/MTOR pathway, which is involved in cell growth and survival (Wei et al., 2018). Thus, the balance of the Wnt/ß-catenin/E-cadherin pathway, which regulates cell proliferation, is disrupted in favour of uncontrolled cell growth, leading to the promotion of oncogenesis (Kalluri & Weinberg, 2009; Nelson & Nusse, 2004). Additionally, E-cadherin plays a role in inhibiting EGFR pathways by interacting with EGFR (Li et al., 2018). However, mutation of E-cadherin can lead to the activation of EGFR, along with downstream effectors through pathways such as RAS/RAF/MEK, and PI3K/AKT/MTOR (Perrais et al., 2007), promoting enhanced cell proliferation and motility, which are associated with tumorigenesis (Jeanes et al., 2008).

1.4.7 E-cadherin in skin cancer

In addition to its role in cell-cell adhesion, E-cadherin plays a crucial function in inhibiting EGFR pathways by co-localising with EGFR at cell-cell contacts. This interaction has a negative effect on the activation of these receptors by their respective ligands, leading to suppression of this signalling pathway (Perrais et al., 2007). However, mutation of E-cadherin leads to activation of EGFR and downstream effectors through RAS/RAF/MEK pathways (Kim et al., 2019), as well as pro-tumorigenic pathways like FAK/c-Src and AKT/MTOR (Kourtidis et al., 2015; Zhang et al., 2015), results in increased cell proliferation and motility (Zhang et al., 2015). Thus, this study aimed to investigate the loss of E-cadherin in stage-specific mouse skin carcinogenesis.

An inducible gene switch is essential, as in previous studies, classical gene targeting has shown that embryos lacking E-cadherin do not survive beyond the blastocyst stage of development (Boussadia et al., 2002). This suggests that E-cadherin is crucial for early embryonic development, underscoring its significance in cell-cell adhesion. Previously, to investigate the role of E-cadherin in organogenesis, a non-inducible cre/loxP system was employed to delete the *E-cadherin* gene in the epithelial cells of mammary glands in transgenic mice. The mutant mammary gland exhibited a significant phenotype, with an extreme reduction in milk protein production, leading to the inability of the mother to nurse their offspring (Boussadia et al., 2002), suggesting that E-cadherin is needed for the terminal differentiation process, and its absence results in significant cell death during parturition (Boussadia et al., 2002).

A non-inducible targeted loss of E-cadherin in the skin epithelium in utero resulted in hyperplasia in juveniles, as the epidermal basal layer compensated by expressing multiple cadherins to maintain adherens junctions (AJs) (Tinkle et al., 2004). Without the correct cadherins, terminal differentiation was impaired, resulting in hyperplasia rather than ulceration, which would have otherwise maintained the barrier functions (Tinkle et al., 2004). However, this study did not progress to investigate carcinogenesis, e.g., via DMBA /TPA treatments or crossing with other mouse strains. Whilst the lack of E-cadherin affected the terminal differentiation program of the

lactating mammary gland in mouse, i.e. E-cadherin is a survival factor for mammary gland (Boussadia et al., 2002), a more recent study demonstrated that loss of E-cadherin not only increased invasion, but also reduced cancer cell proliferation survival and decreased circulating tumour cell numbers in invasive ductal carcinomas (Padmanaban et al., 2019). These findings highlight the complex and multifaceted role of E-cadherin. Thus, the role of E-cadherin remains unclear and was investigated in this project (Boussadia et al., 2002).

To investigate the activation/role of E-cadherin in multi-stage carcinogenesis, as outlined above, the same conditional gene inactivation scheme driven by keratin K14 promoter was employed to achieve cre expression in the basal epidermal layers and hair follicles, including the stem cells (Berton et al., 2000). The cre recombinase gene was again ligated with a progesterone ligand binding domain (PLBD), and then RU486 was added, which antagonises progesterone and activates the cre recombinase gene (Kellendonk et al., 1996) exclusively in treated epidermal cells- including the stem cells. Topical treatment with RU486 ablates the functional exon sites flanked by LoxP sites of exon 6-10 for *E-cadherin* (Boussadia et al., 2002), resulting in E-cadherin ablation and loss of E-cadherin function, which was achieved by ablation of exons 6-10 (Ab epitope in exon-5) (Figure 1-8).

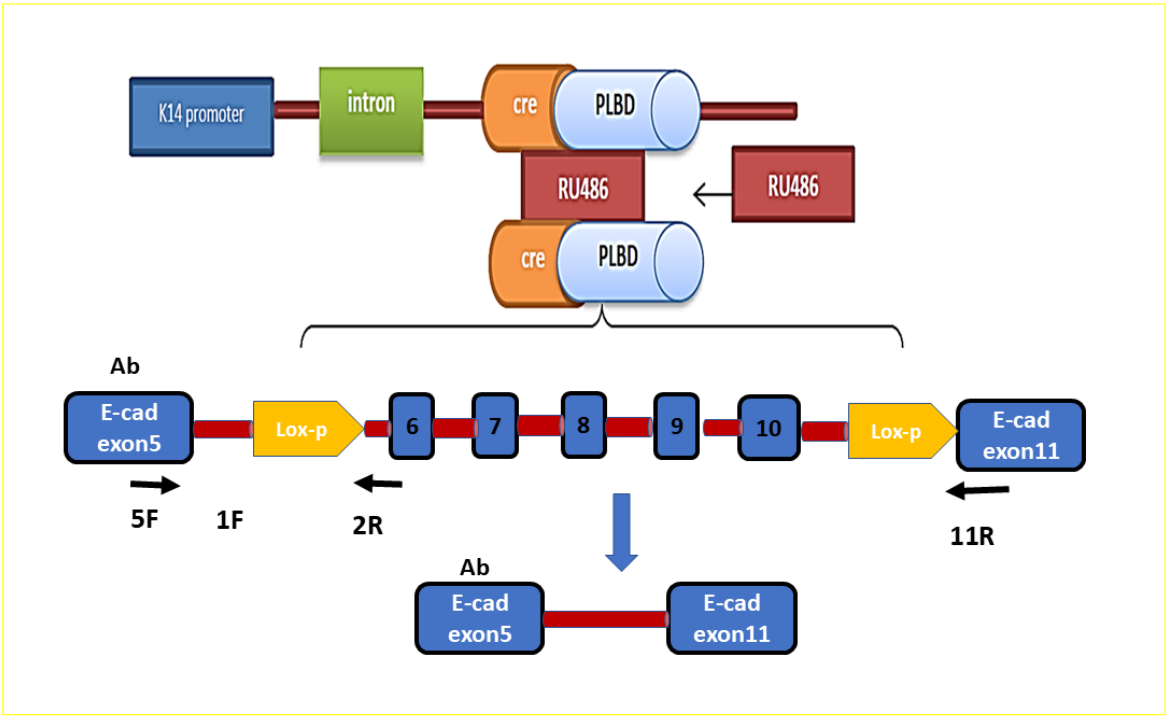

Figure 1-8 Generation of the E-Cadherin floxed gene. The figure depicts the conditional removal of exons 6-10 of E-cadherin in *K14creP/Δ6-10Ecad*$^{flx/flx}$ mouse model. Following the topical application of RU486, cre recombinase fused to PLBD, under the control of the K14 promoter, specifically ablates exons 6-10 of the *E-cadherin* gene. This targeted excision results in tissue-specific knockout of E-cadherin in keratinocyte lineages, allowing for the study of E-cadherin function in these cells. Ab: Anti-E-cadherin epitope in exon 5 detects non-functional Δ6-10E-cadherin protein (Original).

1.5 Hypothesis

It is hypothesised that inducible loss of E-cadherin contributes directly to the malignant conversion of premalignant papillomas into aggressive SCC, particularly when combined with oncogenic activation of ras or fos and/ or the loss of tumour suppressor gene PTEN. This transition is expected to be mediated through the distribution of epithelial integrity and deregulation of ß-catenin signalling and associated downstream molecular pathways that govern proliferation, adhesion, and invasion. Furthermore, it is hypothesised that while the epidermis may initially deploy intrinsic protective mechanisms to suppress carcinogenesis at early stages, these defences are ultimately insufficient to counteract the combined oncogenic insults and the loss of E-cadherin function, thereby facilitating tumour progression.

1.6 Aims

- To determine the endogenous E-cadherin status at every stage of *HK1.ras.fos-K14creP/Δ5PTEN*$^{flx/flx}$ multistage carcinogenesis, and to explore its interactions with the expression of other relevant genes as the underlying mechanisms progress.
- To determine if inducible E-cadherin loss will trigger stage-specific progression of papillomas in conjunction with exclusive epidermal ras activation, ultimately leading to malignant conversion.
- To determine whether inducible E-cadherin loss can cooperate with fos and PTEN mutation, altering the development of KAs and leading to carcinomas.
- To determine whether inducible E-cadherin loss can collaborate with ras and fos activation, along with PTEN mutation, to drive malignant conversion and progression.

Chapter 2 Materials and Methods

2.1 Materials

2.1.1 Chemicals used in the study

Reagents/Chemicals	Manufacturer (Cat. Number)
Taq DNA Polymerase • 10X PCR buffer • $MgCl_2$ (50mM) • deoxynucleoside triphosphate (dNTP)	Invitrogen (Cat No: 10342053)
Ethylenediaminetetra-acetate (EDTA)	Sigma (Cat No: E5134)
Sodium dodecyl sulfate (SDS)	Thermo Fisher Scientific (Cat No: BP166-500)
Sodium Chloride (NaCl)	Sigma (Cat No: S3014)
Proteinase K	Thermo Fisher Scientific Cat No: EO0491
Certified ™ Molecular Biology Agarose	Bio-Rad Laboratories
Ethidium Bromide	Sigma (Cat No: E1510)
Ethanol	VWR chemicals (Cat No: 20821.330)
Xylene	Sigma (Cat No: 534056-1L)
Bovine serum albumin	Sigma (Cat No: A8806-1G)
Normal goat serum	Thermo Fisher Scientific (Cat No: 16210064))
Permafluor™ Aqueous Mounting Medium	Thermo Fisher Scientific (Cat No: TA-006-FM)
Vectashield Antifade mounting media	Vector Laboratories (Cat No: H-1000-10.)
3,3'-diaminobenzidine (DAB) staining	Dako (Cat No: K3468)
Haematoxylin	Sigma (Cat No: H3136-25G)

Table 2-1 A table of reagents/chemicals and manufacturers used in this study.

2.1.2 Buffers and solutions

Buffers/Solution	Manufacturer (Cat. Number)
DNA Lysis Buffer	(prepared in-house)
DNA loading buffer	(prepared in-house)
1X Tris-Acetate-EDTA (TAE) Buffer	(prepared in-house)
Phosphate Buffered Saline (PBS) PBS tablet	(prepared in-house) Sigma (Cat No. P4417)
Sodium Citrate Buffer (10mM, pH 6.0)	LabVision (Cat No. AP-9003-050)
30% Hydrogen Peroxide Solution	Sigma (Cat No: H1009)

Table 2-2 A table of commercial and in-house buffers and solutions.

2.1.3 Genetic and immunostaining materials

Genotypes	Worked as
HK1.ras^{1205}	Transgenic mice expressing *v-HRAS* from a modified K1 vector
HK1.fos	Transgenic mice expressing *v-fos* from a modified K1 vector
K14creP	Transgenic mice expressing RU486 responsive cre recombinase from a keratin K14 promoter.
Δ5PTEN $^{wt/flx,\ flx}$	Transgenic mice wild type, heterozygous or homozygous for LoxP-flanked exon 5 PTEN.
HK1.ras^{1276}*/fos*	Transgenic mice expressing *v-HRAS* and *v-fos* from a modified K1 vector
HK1.fos/K14creP.Δ5PTEN$^{flx/flx}$	Progeny of mating *HK1.fos* and *K14creP.Δ5PTEN*$^{flx/flx}$
HK1.ras.fos/K14creP.Δ5PTEN$^{flx/flx}$	Progeny of mating *HK1.ras.fos* and *K14creP.Δ5PTEN*$^{flx/flx}$
Δ6/10 E-cad$^{wt/flx,\ flx}$	Transgenic mice wild type, heterozygous or homozygous for LoxP-flanked exon 6-10 E-cadherin.
K14creP.Δ6/10 E-cad$^{wt/flx.flx}$	Progeny of mating K14creP and *Δ6/10 E-cad*$^{wt/flx,\ flx}$
HK1.ras-K14creP/Δ6-10E-cad$^{wt/flx.flx}$	Progeny of mating *HK1.ras* and *K14creP/Δ6-10E-cad*$^{wt/flx.flx}$
HK1.fos/K14creP/Δ6-10E-cad$^{wt/flx.flx}$	Progeny of mating *HK1.fos* and *K14creP/Δ6-10E-cad*$^{wt/flx.flx}$
HK1.ras.fos-K14creP/Δ6-10E-cad$^{wt/flx.flx}$	Progeny of mating *HK1.ras.fos* and *K14creP/Δ6-10E-cad*$^{wt/flx.flx}$
HK1.ras.fos-K14creP/Δ5PTEN/Δ6-10E-cad$^{wt/flx.flx}$	Progeny of mating *HK1.ras.fos* and *K14creP/Δ5PTEN/Δ6-10E-cad*$^{wt/flx.flx}$

Table 2-3 Lists of genotypes used in this study.

Gene	Forward (F) and Reverse (R) Primer Sequence		Band size
K14.creP	F	5’ CGGTCGATGCAACGAGTGAT 3'	650bp
	R	5’ CCACCGTCAGTACGTGAGAT 3'	
E-cadherin	F	5’ GGGTCTCACCGTAGTCCTCA 3'	Floxed allele~350bp Wt allele~245bp
	R	5’ GATCTTTGGGAGAGCAGTCG 3'	
Δ6-10E-cadherin	F	5’ CGTGTTCCGGTCAGCGCAGG 3'	500bp
	R	5’CAACGCTATGTCCTGATAGCGGTCC3’	
PTEN	F	5’ ACTCAAGGCAGGGATGAGC 3’	Floxed allele~1300bp Wt allele 1200bp
	R	5’ GTCATCTTCACTTAGCCATTGG 3’	
Δ5PTEN	F	5’ ACTCAAGGCAGGGATGAGC 3’	~500bp
	R	5’ GGTTGATATCGAATTCCTGCAGC 3’	
HK1.fos	F	5’ GGATCCATGATGTTCTCGGGTTTC 3’	750bp
	R	5' CGATTATTGCCACCCTGCCATG 3'	
HK1.ras	F	5' GGATCCGATGACAGAATA CAAGC 3'	550bp
	R	5' ATCGATCAGGACAGCACACTTGCA 3'	

Table 2-4 Oligos sequences for transgenic detection.

Antibody	Dilution	Manufacturer (Cat. Number)
Rabbit anti-K1	1:100	Biolegend Cat No:905601
guinea pig polyclonal anti-K14	1:00	Progen Cat No. GP-CK14
Rabbit anti-ß-catenin	1:50 1:50	Abcam ab32572/Proteintech (Cat No: 20536-1.AP/Cell Signalling/Sigma-Prestige Ab)
Rabbit polyclonal anti-E-Cadherin	1:200 1:200	Proteintech (Cat No:20874-1-AP/ Sigma)
Rabbit anti-p53	1:150 1:150	Abcam ab31333 Proteintech (Cat No: 21891-1-APSigma SAB4503000/ SIGMA SAB4503015)
Biotinylated goat anti-guinea pig	1:100	Vector Labs (Cat No: BA-7000)
FITC-labelled anti-rabbit IgG	1:100	Jackson Labs (Cat No: 711-005-152)
HRP conjugated anti-rabbit	1:100	Vector Labs (Cat No: PI-1000)
Streptavidin-Texas Red	1:400	Vector Labs Cat No: SA-5006

Table 2-5 Immunofluorescence and immunohistochemistry antibodies, dilutions, and manufacturers.

2.2 Methods

2.2.1 Transgenic mice

Biopsies were taken from transgenic mice previously established and maintained by the animal unit at the University of Glasgow Central Research Facility (CRF). All experiments were undertaken according to UK Home Office Experimental Regulations and roles in accordance with procedure number 3 of the Licence # P82170325 (to DAG).

Several epidermal-specific genotypes were previously created by employing a truncated modified Human K1 keratin promoter to achieve exclusive epidermal expression of *v-HRAS* (*HK1.ras1205&1276*) (Greenhalgh et al., 1993a), or *v-FOS* oncogenes, which elicited keratinocyte hyperplasia and benign (papillomas) (Greenhalgh et al., 1993b), while their co-expression resulted in papillomas only without conversion (Greenhalgh et al., 1993c) to carcinoma, thus they were ideal to assess the genes involved.

Experiments were designed to assess PTEN knockout. Conditional deletion of exon5 of PTEN (Δ5PTEN) (Macdonald et al., 2014; Yao et al., 2006) was carried out by employing the RU486-inducible Cre-LoxP system through topical administration of RU486, which results in the loss of the phosphatase domain of PTEN and the ability to downregulate AKT expression. This system was adopted to conditionally delete exons 6-10 of E-cadherin, turning it into a constitutively inactive protein (Boussadia et al., 2002).

2.2.2 DNA extraction

Approximately 3mm of tail tip biopsies were snap frozen immediately and stored at -20 °C. Biopsies were digested in 500 µl of tail extraction buffer (50mM Tris- Hydrochloride pH 8.0, 100 mM), EDTA pH 8.0, 100mM NaCl, 1% SDS and 200 µg/ml fresh proteinase K (Sigma) for 24 hours at 55 °C and occasionally were vortexed to degrade the tails. The next day, the digested tails were centrifuged for 10-12 minutes at 13,000 rpm. Then, an equal volume (500µl) of ice-cold 100% ethanol was gently added to precipitate the tail genomic DNA at the interface, which was carefully collected by rolling onto a pipette tip. The extra buffer was carefully removed by blotting on a paper towel. Any remaining ethanol was allowed to evaporate, and the DNA

was transferred into a new, labelled Eppendorf tube containing 280 µl of water. The precipitated DNA was left to dissolve in dH_2O at 55 °C for 20 minutes and stored at 4 °C.

2.2.2.1 Polymerase Chain Reaction analysis

DNA was set up as a template in a 25µl reaction volume for each sample, using the following reagents: 10X PCR buffer (2.5 µl) (Invitrogen), 25mM $MgCl_2$ (Invitrogen), 200ng/µl forward primer (Sigma), 200ng/µl reverse primer (Sigma), 10mM of each dNTP and 5U/ml DNA Taq Polymerase (Table 2-6). The specific primers used against *Cre, E-cadherin, PTEN*, *HK1.fos* or *HK1.ras* are detailed in Table 2-4. The master mix was added into tubes (23 µl), and then 2.5 µl of extracted DNA was added. The samples were processed using a thermal cycler under conditions optimised for each transgene (see Table 2-7).

2.2.2.2 Agarose Gel Electrophoresis

After the PCR cycle had been completed, 5 µl of loading dye was added to each sample. The DNA loading buffer contained:0.25% bromophenol blue, 0.25% xylene, 30% glycerol (Sigma-Aldrich). The samples were then loaded on an agarose gel (1% for single bands ~ 400- ~700 e.g. *HK1.ras*, *K14.creP* and *HK1.fos* and up to 1.5% for better separation of small doublet bands). Electrophoresis was carried out in 1x TAE buffer, and the gels were stained with ethidium bromide. Bands were visualised under UV light to verify the successful amplification of DNA corresponding to each transgene.

Reagent	Volume (µL)
dH2O	17.0
dNTP mix (20 mM)	0.25
Taq DNA Polymerase (5 U/µL)	0.25
Forward primer	0.50
Revers primer	0.50
MgCl2 (25Mm STOCK)	2.00
10X PCR buffer	2.50

Table 2-6 Master mix reagents and volumes.

Gene	Cycling conditions					
	Denaturation		Primer Annealing	Extension		Cycle
K14.creP	94ºC/5min	94ºC/30Sec	58ºC/45sec	72ºC/1min	72ºC/5min	35
E-cadherin	94ºC/5min	94ºC/1min	62ºC/1min	72ºC/1min	72ºC/10min	35
PTEN	95ºC/2min	95ºC/30sec	64ºC/1min	72ºC/1.30 min	72ºC/10min	36
HK1.fos	95ºC/2min	95ºC/3sec	62ºC/30sec	72ºC/1min	72ºC/10min	35
HK1.ras	95ºC/2min	95ºC/30sec	56ºC/1min	72ºC/1min	72ºC/10min	35

Table 2-7 Polymerase chain reaction conditions.

2.2.3 Immunofluorescence analysis

For immunofluorescence analysis, all Formalin-Fixed Paraffin-Embedded Sections (FFPE) (5-7μm) were cut using a Leica RM2235 rotary microtome, incubated at 60°C for 45min to melt the paraffin, and then immediately immersed in xylene for 45min to remove all paraffin. The tissue sections were briefly immersed in absolute ethanol to remove excess xylene, then washed in phosphate-buffered saline (PBS) (Sigma), pH 7, for 10 min. The sections were then placed in antigen retrieval buffer, 10mM sodium citrate buffer (pH 6.0) (Lab Vision, Fremont, CA) and heated (usually at 95-100°C) in a microwave oven. Sections were allowed to cool in buffer for at least 40 min. After the antigen retrieval step, sections were washed in PBS (5min) at room temperature. Then, nonspecific binding was blocked by incubation with an appropriate serum matched to the secondary antibody, diluted in PBS (IHC: 10% normal goat serum; IF: 10% normal goat or 10% normal horse serum, due to double labelling) for 10 minutes.

After washing and blocking, the sections were incubated overnight at 4°C in humidified conditions, with 100-150 μl per section of appropriate concentration of primary antibodies (Table 2-5).

The following day, the sections were washed in 1x PBS for 10 minutes and then incubated with biotinylated goat anti-guinea pig antibody, diluted in 10% Bovine Serum Albumin (BSA) in PBS, for 1hr in humidified conditions. Sections were washed with 1x PBS for 10 minutes and finally incubated with a combination of FITC-conjugated donkey anti-rabbit IgG (Jackson Labs and Texas Red-Streptavidin (to bind biotin) vector at room temperature for 1 hr. FITC was used to visualise the primary antibody targeted protein (green) and Streptavidin-Texas Red (Vector Labs) for the K14 counterstained keratinocytes (red). After final incubation, sections were washed in 1x PBS in the dark for 10 min and then dried before being coverslipped using PermaFluorTM Aqueous/Vectashield antifade mounting media. They were stored at 4°C, ready to be visualised under a microscope. The sections were visualised using a Carl Zeiss microscope with Axiovision software. All images were captured under consistent exposure and threshold settings to ensure standardised visual comparison across samples. The results were evaluated

through qualitative visual inspection. Each experiment was conducted using a cohort of *n*= 10.

2.2.4 Immunochemistry analysis

For IHC, a similar protocol to the IF analysis was followed. However, after antigen retrieval, the sections were incubated in 3% hydrogen peroxidase for 10 min at room temperature to exhaust endogenous peroxidase activity. After washing in PBS for 10 minutes, the sections were dried and blocked using the appropriate serum, matching the secondary antibody, which was made in PBS, e.g., 10% normal goat serum (NGS) for 10 minutes.

Sections were then incubated overnight in a humidified atmosphere at 4°C with 100-150 µl of primary antibody per section, diluted to the appropriate concentration in 10% NGS. The sections were then washed in 1x PBS for 10 minutes and incubated with HRP-conjugated anti-rabbit antibody (Vector Labs) (diluted at 1:100) in 10% BSA in PBS for 1 hr at room temperature. The DAB substrate solution (Dako) was prepared according to the manufacturer's instructions and was added (100-150 µl per section) to the sections. The sections were incubated with the DAB solution for a few minutes, followed by rinsing in distilled water dH_2O to stop the reaction. Each section was incubated for approximately 3-5 min, depending on the antibody. Sections were counterstained with haematoxylin (20-30 seconds), washed in water, then decolourised by dipping in acid-alcohol (99ml 70% ethanol and 1ml 1M HCl). Then sections were immersed in Scott's tap water for 1 min to blue the hamatoxylin after a quick wash with running tap water. Sections were dehydrated by immersion in absolute ethanol for 5 minutes, followed by xylene for 5 minutes. They were then left to dry before being mounted with Permount solution and coverslipped. Finally, sections were visualised using Carl-Zeiss microscope Axio Vision 3.1 imaging software. Each experiment was conducted using a cohort of *n*= 10.

Chapter 3 The analysis of endogenous E-cadherin expression in transgenic mouse skin carcinogenesis

3.1 Introduction

In order to investigate the role of E-cadherin loss in a multistage skin carcinogenesis model, *HK1.ras.fos-K14creP/Δ5PTEN$^{flx/flx}$* tumours were recreated, and stage-specific tumours were analysed for E-cadherin. As previously outlined in the methods, *HK1.ras* and *fos* oncogenes were targeted to the epidermis using the HK1 vector, and PTEN mutation specifically in the epidermis was confirmed by topical administration of RU486 to activate cre. The keratin K14 promoter was used to drive cre expression in the basal layer of the epidermis and hair follicles, including the stem cells. (Berton et al., 2000).

In previous studies, the activation of p-AKT by Δ5PTEN has been shown to cooperate with *ras* and *fos* activation to induce malignant conversion following p53 loss and malignant progression following p21 loss. This resulted in increased AKT activity and initial formation of wdSCC soon after p53 loss in *HK1.ras.fos-K14creP/Δ5PTEN$^{flx/flx}$* mice that progressed to aggressive SCC over time (Macdonald et al., 2014; Yao et al., 2006). These findings highlighted the potential role of cell-cell adhesion loss in facilitating the development of malignancy. Accordingly, this study aimed to assess the specific role of E-cadherin loss in this multistage skin carcinogenesis model, particularly its interaction with oncogenic ras and fos activation with concurrent PTEN loss.

3.2 Confirmation of transgenic mice genotype by PCR analysis

The genotype of transgenic mice was determined using PCR analysis of DNA samples obtained from tail tips and tumour biopsies, which also confirmed the activity of RU486-mediated cre recombinase. An inducible *cre/loXP gene switch system was utilised* to control the activation of *PTEN* or *E-cadherin* in specific areas of mouse skin. This was achieved through the fusion of *cre* recombinase with PLBD, enabling dimer formation and nuclear translocation upon topical application of RU486. In experiments involving *PTEN* mutations, *K14creP* regulator transgenic mice were employed to induce cre activity in the epidermis. Following the cre-mediated removal of the

LoxP-flanked stop cassette, exon 5 was lost in the epidermal cells. Additionally, the same mice were used to induce *E-cadherin* ablation in exon6-10. Specific primers were used to analyse the transgenic mice DNA for genotyping confirmation (Chapter 2 Table 2-3) of *ras, fos, PTEN*, and *E-cadherin* for *HK1.ras, HK1.fos, K14creP*, wild type, and LoxP-flanked exon5 *PTEN* alleles and LoxP-flanked *E-cadherin*.

For *HK1.ras* analysis, a band at 550bp was previously observed (Figure 3-1 A), while *HK1.fos* DNA has a 750bp band (Figure 3-1 B). The RU486-Inducible *K14cre* regulator transgene produces a 650bp band (Figure 3-2 A). Tissues with a floxed *PTEN* allele were verified with primers 1 & 2 (Chapter 2 Table 2-3), which span the loxP sites in exon 5 (Figure 3-2 B). DNA from *Δ5PTEN* transgenic mice showed a 1300bp band indicative of the floxed allele and a 1200bp band indicative of the wild type allele. For confirmation of *PTEN* exon 5 loss, primers 1 & 3 were designed specifically for intron 4 and intron 6 and showed a band of 500bp in *K14creP/Δ5PTEN*$^{flx/flx}$ lanes (1-4) (Figure 3-2 C) but not in mice untreated with RU486 nor in those without the cre regulator or wild type PTEN lanes (5-12) (Figure 3-2 C).

Subsequently, PCR analysis of E-cadherin mice that had previously been created by mating K14cre recombinase mice showed successful ablation of exons 6-10, producing a band at 500bp in RU486-treated *K14creP/Δ6-10E-cad*$^{flx/flx}$ samples lanes (1-4) but not in mice untreated with RU486 nor in those without the cre regulator or wild type E-cadherin lanes (5-12) (Figure 3-2 E).

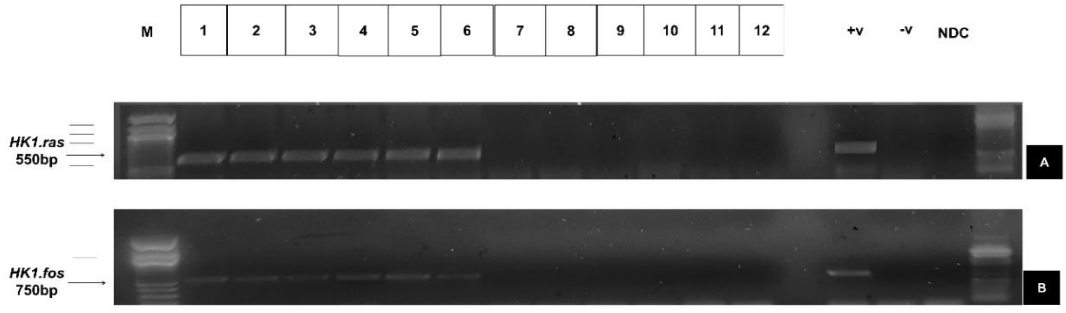

Figure 3-1 PCR analysis of HK1.ras and HK1.fos genotypes (A) Analysis of *HK1.ras* positive mice exhibits a band of 550bp in lanes (1-6), while the negative control DNAs from non-transgenic ICR mice in lanes (7-12) do not exhibit this band. (B) Similarly, *HK1.fos* positive mice exhibit a band of 750bp in lanes (1-6) and it is absent in negative control DNA from non-transgenic ICR mice in lanes (7-12). Lanes 13, 14, and 15 are positive, negative and no DNA controls, respectively. Lower bands visible in the gel correspond to primer-dimers, which result from primers binding to each other rather than to the target DNA.

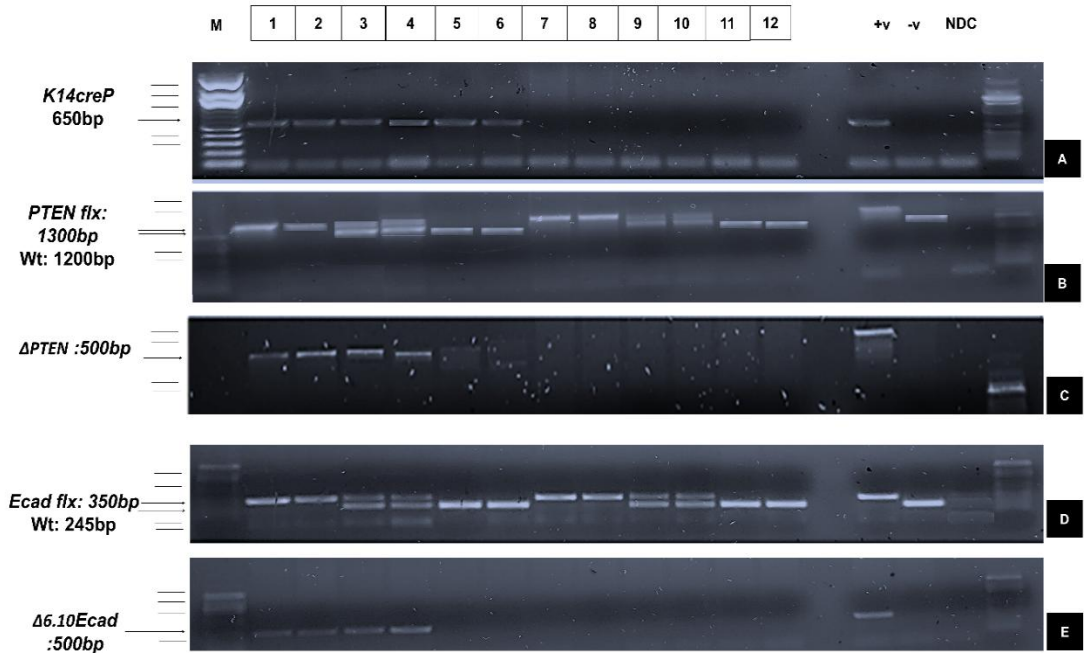

Figure 3-2 PCR analysis of K14.creP, PTEN and E-cadherin transgenes in skin and tumours: (A) The 650bp band indicates the presence of K14creP in positive transgenic mice in lanes (1-6), while its absence in negative controls confirms their non-transgenic status. (B) PCR oligo set 1&2 identifies the floxed PTEN allele by a band at 1.3kbp (lanes 1,2,7 & 8), a doublet of 1.3/1.2-kbp bands indicates heterozygous PTEN (lanes 3,4,9 &10), and a 1.2-kbp band indicates the wild type PTEN allele (lanes 5,6,11&12). (C) Using PCR oligo set1&3 shows a band of 500bp, indicating the truncated exon 5 in RU846 treated K14cre mediated ablation (lanes 1-4), which is absent in controls (lanes 5-12). (D) Using the primer pair (5&11), E-cadherin analysis gives the E-cadherin floxed allele at 350bp, whilst heterozygous mice also possess the wild type allele at 245bp (lanes 1-6). (E) RU846 treated lanes with K14.creP cause ablation of exons 6-10 and give a band at 500bp using the primer pair (1 & 2). While lanes 7-12 are RU846-treated skin with no DNA K14.creP, this gives no bands. Lanes 12, 13, and 14 are positive, negative, and no DNA PCR controls, respectively.

3.3 Analysis of endogenous E-cadherin expression status in multistage *HK1.ras.fos-K14creP/∆5PTEN$^{flx/flx}$* mouse skin carcinogenesis

To investigate the potential roles of E-cadherin at multiple stages of tumorigenesis, the expression of endogenous E-cadherin was assessed in re-established tri-genic *HK1.ras.fos-K14creP/Δ5PTEN$^{flx/flx}$* mice as well as other combinations of mouse strains, including *HK1.ras.fos* (Macdonald et al., 2014; Yao et al., 2006) to serve as comparison controls after E-cadherin loss. The new tri-genic *HK1.ras.fos-K14creP/Δ5PTEN$^{flx/flx}$* model yielded phenotypes identical to those previously published (Greenhalgh et al., 1993c;

Greenhalgh et al., 1993a; Greenhalgh et al., 1993b; Macdonald et al., 2014; Yao et al., 2006). This mechanism typically progresses from normal epidermis to epidermal hyperplasia due to the activation of *HK1.ras* or *HK1.fos*, which induces excess proliferation, causing the epidermis to expand and become folded. The co-operation of *HK1.ras*/*fos* increases the proliferation and progression into benign squamous cell papilloma (see below). These papillomas do not become malignant (Greenhalgh et al., 1993c; Greenhalgh et al., 1993a; Greenhalgh et al., 1993b) unless another mutation is introduced, such as the inactivation of PTEN. This was achieved in *HK1.ras.fos-K14creP/Δ5PTEN*$^{flx/flx}$ mice via topical application of RU486.

As demonstrated in Figure 3-3, the novel combination of *HK1.ras.fos-K14creP/Δ5PTEN*$^{flx/flx}$ mice yielded results consistent with those observed in previous studies (Greenhalgh et al., 1993c; Greenhalgh et al., 1993a; Greenhalgh et al., 1993b; Yao et al., 2008; Yao et al., 2006). The initiation was completed by *HK1.ras* activation, causing thickened scaly skin in newborn pups that resolved in adults (Chapter 1, Figure 1-1). The *ras* activation also induced a histopathology of epidermal hyperplasia characterised by the expansion of basal and suprabasal keratinocytes (Figure 3-3 A), which persisted in adult ears and acted as a precursor to the development of overt papilloma in the *HK1.ras*^{1205} strain (Greenhalgh et al., 1993a). As previously mentioned in the Introduction (Introduction 1.4.2), there are two distinct strains of *HK1.ras* mice. The 1205 strain and 1276 strain. The 1205 strain demonstrates a high susceptibility to tumour promotion, leading to the formation of papillomas in 100% of mice within 6-8 weeks of ear tag wounding. Conversely, the 1276 strain predominantly exhibits simple hyperplasia as a result of p53 induction (Masre et al., 2020). *HK1.ras*^{1205} papillomas resemble *HK1.ras.fos* papillomas (Figure 3-3 B) and do not show signs of malignant transformation (Greenhalgh et al., 1993c; Greenhalgh et al., 1993a; Greenhalgh et al., 1993b) due to induction of compensatory p53 (Macdonald et al., 2014; Yao et al., 2006). The H&E image in Figure 3.3 B shows a clear basal cell layer at the base of the papilloma, with overlying differentiated keratinocyte layers, indicating normal stratification and keratinisation. However, upon loss of the ear tag, *HK1.ras*^{1205} papillomas undergo regression. Conversely, *HK1.ras*^{1276}*.fos* papillomas remain autonomous due to the promotion stimulus provided by

HK1.fos. The *HK1.fos* mice develop a thickened and hyperplastic epidermis in their ear skin, indicating a role in keratinocyte differentiation (Chapter 5). This phenotype is consistent with previous studies and suggests that the *HK1.fos* gene plays a significant role in the differentiation process of keratinocytes (Greenhalgh et al., 1993b). However, due to the severity of the phenotype observed with crossing 1205 and *HK1.fos* mice, further experimentation in the UK is not feasible.

In the initial experiments *PTEN* mutation was introduced into the *HK1.ras* (*HK1.ras-K14creP/Δ5PTEN*$^{flx/flx}$) model, resulting in accelerated growth of benign papillomas, as in previous models (Greenhalgh et al., 1995). To induce malignant conversion, TPA promotion was required, leading to the development of aggressive and poorly differentiated SCCs. Later studies revealed that the promotion of tumour growth by TPA was necessary to overcome a protective response triggered by the increased level of p53 and p21 in cells lacking AKT regulation due to PTEN loss (Macdonald et al., 2014). Previous studies investigating the co-operation of *HK1.fos* and *PTEN* loss have shown that the development of KA was dependent on the compensatory expression of p53 and p21. This initially inhibits proliferation, as shown by BRDU labelling analysis, and subsequently induces keratinocyte differentiation via p21 (Topley et al., 1999), as indicated by premature K1 expression, as shown in Figure 3-3 G. It also demonstrated co-expression of K1 and K14 in the basal layer, suggesting aberrant differentiation within the basal keratinocyte population.

The interaction between HK1.fos and Δ5PTEN initially determined the role of E-cadherin in this model, revealing its function in the compensatory response of the epidermis to maintain homeostasis and inhibit tumour progression at each stage. In the context of HK1.fos and Δ5PTEN cooperation, novel benign keratoacanthomas developed. These tumours are characterised by a tendency to regress and exhibit histological features that include a significant degree of keratosis, characterised by thickening of the stratum corneum, often associated with terminal differentiation of keratinocytes (Figure 3-3 C).

In the context of *HK1.ras.fos-K14creP/Δ5PTEN*$^{flx/flx}$ genotypes, along with additional *ras* activation, the mice exhibited malignant progression, following p53 loss in late-stage papillomas, then rapidly progressed to poorly

differentiated SCC (pdSCC) with invasive characteristics (Figure 3-3 D). This progression was associated with uniform activation of p-AKT1 and was marked by an increasingly aggressive tumour phenotype characterised by pronounced invasion and a highly disorganised epidermis (Macdonald et al., 2014).

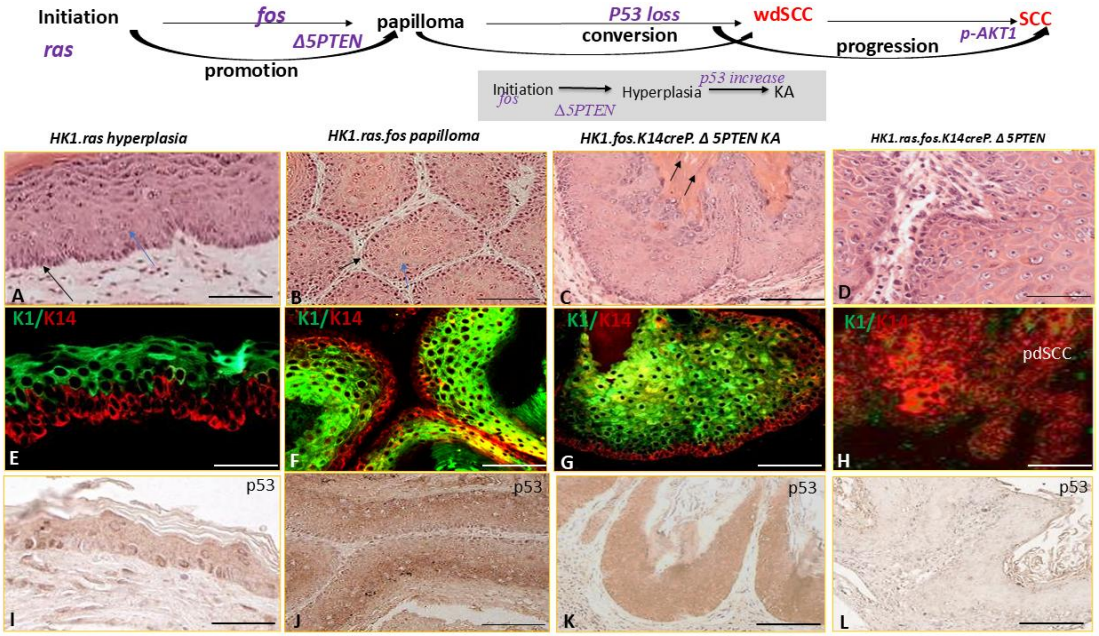

Figure 3-3 Phenotypes in *HK1.ras.fos-K14creP/Δ5PTEN*$^{flx/flx}$ carcinogenesis The upper schematic diagram illustrates the sequence of events in carcinogenesis, where the activation of *ras* gene initiates the process, followed by the promotion of *fos* genes. The conversion into malignancy requires the loss of *PTEN* and *p53* genes. (A) Histopathology of *HK1.ras* hyperplasia, showing expansion of the basal layer (black arrow) and the suprabasal differentiated keratinocyte layer (blue arrow). (B) *HK1.ras.fos* papilloma with clear expansion of the basal layer (black arrow) and overlying differentiated keratinocyte layer (blue arrow). (C) The *HK1.fos-K14creP/Δ5PTEN*$^{flx/flx}$ model exhibits KA characterised by hyperkeratosis (arrow) and disorganised epidermal differentiation. (D) Aggressive *HK1.ras.fos-K14creP/Δ5PTEN*$^{flx/flx}$ SCC. (E-H) Double-label immunofluorescence analysis for keratin K14 (red) and K1 (green). (E) *HK1.ras* hyperplasia and (F) *HK1.ras.fos* papilloma shows strong K1 expression in the suprabasal layer, indicative of normal differentiation. (G) *HK1.fos-K14creP/Δ5PTEN*$^{flx/flx}$ KA exhibit accelerated differentiation with keratinocytes expressing K1. Notably, co-expression of K1 and K14 in the basal layer indicates disrupted stratification or aberrant differentiation during KA formation. (H) *HK1.ras.fos-K14creP/Δ5PTEN*$^{flx/flx}$ SCC shows K1 expression is gradually reduced, indicating an aggressive nature of conversion, where K1 is completely absent in pdSCC areas. (I-L) Immunohistochemistry analysis of p53 expression. (I) In *HK1.ras* hyperplasia, p53 expression is seen in sporadic dividing cells. (J) Stronger p53 expression appears in *HK1.ras.fos* papillomas, and the expression is very strong in (K) *HK1.fos-K14creP/Δ5PTEN*$^{flx/flx}$ KAs. (L) In aggressive *HK1.ras.fos-K14creP/Δ5PTEN*$^{flx/flx}$ pdSCCs p53 expression is lost. (Scale bars: A&B: 100 μm; C: 75 μm: D: 50 μm; E: 150 μm; F&G: 75 μm; H: 50 μm; I: 75 μm; J: 50 μm; K&L: 100 μm).

To confirm the classification of skin tumours, double-labelled immunofluorescence (IF) analysis was used to assess expression of keratin K1; loss of which is a marker for tumour progression, and keratin K14 was employed to highlight the epidermis or tumour from the stroma. The presence or absence of these markers helps distinguish between late-stage papilloma and early-stage well-differentiated squamous cell carcinoma (wdSCCs), as during carcinogenesis, suprabasal K1 expression is observed in normal and hyperplasia and remains strong in benign papilloma. However, on conversion to carcinoma, initially wdSCC still possessed some K1, but it was gradually reduced and was absent in aggressive, invasive SCC (Greenhalgh et al., 1993c; Greenhalgh et al., 1993a; Greenhalgh et al., 1993b; Macdonald et al., 2014; Yao et al., 2006).

This is summarised in Figure 3-3 E&F, where typical hyperplasia and papillomas exhibit a relatively normal suprabasal K1 expression. However, the basal layer indicated by K14 (red) expands due to an increased proliferative response triggered by the activation of ras and/or fos oncogenes. This suggests the basal layer undergoes increased cell division (proliferation) in response to these gene activations.

In KAs produced by *HK1.fos-K14creP/Δ5PTEN*$^{flx/flx}$ co-operation, strong K1 expression was observed, and on occasion, there was an accelerated and premature differentiation pattern observed (Deng & Karin, 1994). This was indicated by strong and novel expression of K1 in the basal layers (see Figure 3-6 below). This finding aligns with an early commitment to cellular differentiation, leading to the excessive accumulation of keratinocytes associated with this specific tumour type, and is consistent with recent findings regarding the response to abnormal expression of basal layer E-cadherin (see below). However, in the *HK1.ras.fos-K14creP/Δ5PTEN*$^{flx/flx}$ SCCs, K1 expression is greatly reduced, indicating malignant conversion. In areas of pdSCC, K1 expression is either greatly diminished or entirely absent (Figure 3-3 H).

An investigation into p53 expression was conducted, and surprisingly, the initial stages of hyperplasia caused by HK1.ras exhibited weak and sporadic p53 expression. (Figure 3-3 I). This suggests that the epidermis may have a mechanism to tolerate excessive cell proliferation, such as during wound healing, where transient hyperproliferation is required for tissue

repair without immediate activation of tumour suppressive responses such as p53-mediated apoptosis or cell cycle arrest. In this context, dampening p53 activation may allow the tissue to maintain its protective barrier and minimise damage by avoiding premature or excessive apoptosis mediated by p53 (Calautti et al., 2005). In the RU486-treated *HK1.ras.fos* papillomas model, the expression of p53 became stronger. This was observed as the model progressed to papilloma, where p53 was expressed in the nuclei of most basal layer keratinocytes (Figure 3-3 J). This increased p53 played an initial role in preventing further malignant progression. Indeed, *HK1.fos-K14creP/Δ5PTEN$^{flx/flx}$* KA exhibited strong p53 expression in the basal layer, which correlated with a significant increase in differentiation (Figure 3-3 K). Thus, in KAs, the absence of PTEN results in elevated levels of p-AKT1, which subsequently inactivates GSK3ß; this inactivation leads to a compensatory increase in p53 expression, as observed in previous studies. Additionally, E-cadherin might have a potential role in the compensatory responses of the epidermis to maintain its normal function and prevent tumour progression. However, in RU486-treated *HK1.ras.fos-K14creP/Δ5PTEN$^{flx/flx}$* SCC, p53 loss was observed (Figure 3-3 L). This loss increased the aggressiveness of the tumour and susceptibility to malignant conversion to pdSCC.

3.3.1 Analysis of E-cadherin expression in *HK1.ras.fos-K14creP/Δ5PTEN$^{flx/flx}$* carcinogenesis

E-cadherin expression was examined in stage-specific *HK1.ras.fos-K14creP-Δ5PTEN$^{flx/flx}$* phenotypes. In *HK1.ras* hyperplasia, E-cadherin expression remained suprabasal, resembling the expression pattern seen in normal controls (Figure 3-4 I-L), indicating its role in maintaining cell-cell adhesion and epidermal barrier function (Figure 3-4). However, in *HK1.ras.fos* papillomas, E-cadherin was still detectable in the suprabasal cell layers as in hyperplasia (Figure 3-5 C&D). This suggests that there is some maintenance of cell adhesion in papillomas, where E-cadherin is expressed throughout the suprabasal layers. Thus, E-cadherin expression may have implications for maintaining the tissue architecture and behaviour of the cells in these conditions. Elevation of p53 expression in papillomas (Figure 3-5 G&H) suggests that p53 might have a role in inhibiting the conversion process as a compensatory mechanism.

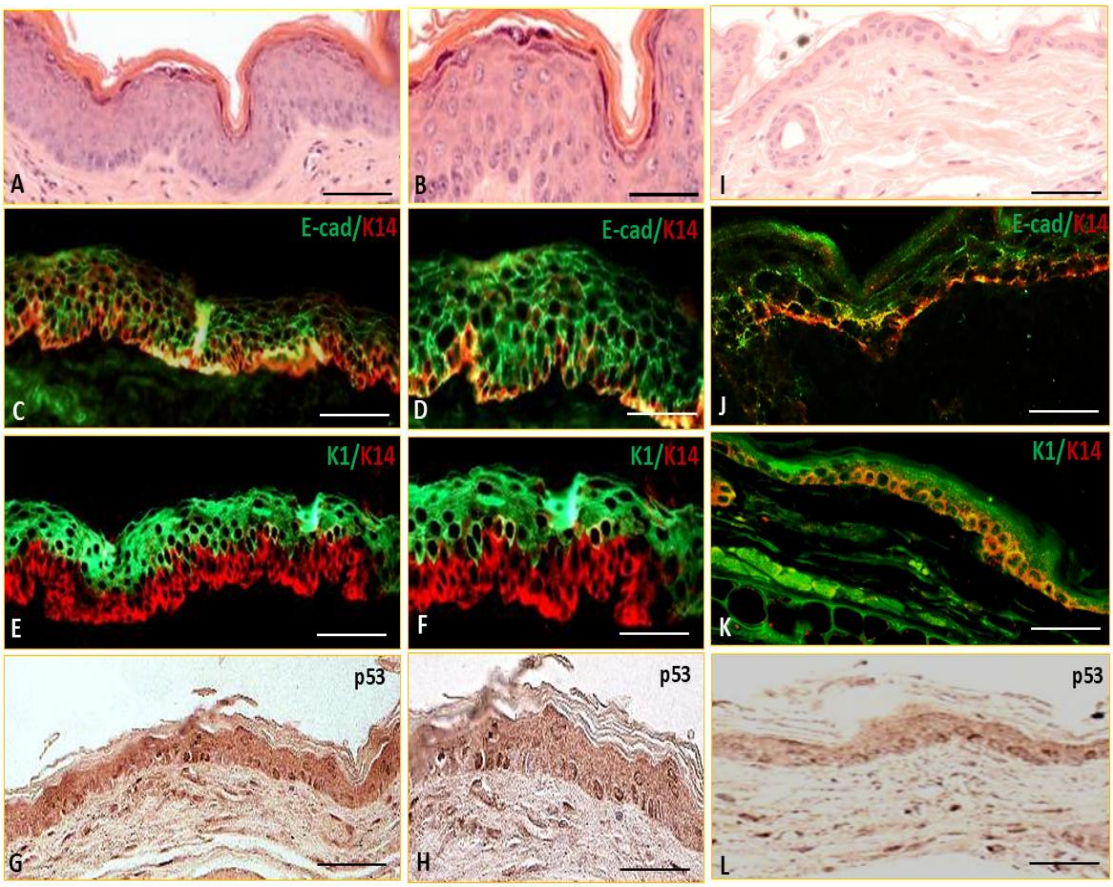

Figure 3-4 Analysis of E-cadherin and p53 expression in *HK1.ras* hyperplasia (A&B) Show the histopathology of *HK1.ras* hyperplasia at low and high magnification, respectively. (C&D) Show IF analysis of E-cadherin expression that is predominantly in the suprabasal cell layer, but it is still detectable in the basal cell layer as indicated by the yellow signal resulting from co-localisation of red (K14) and green (E-cadherin) fluorescence, shown at low and high magnification, respectively. (E&F) Show IF analysis of strong K1 expression in the suprabasal layer at low and high power, respectively. (G&H) IHC analysis reveals cytoplasmic p53 expression at low and high magnification, respectively. (I-L) Comparable corresponding normal controls. (I) H&E staining of normal skin, (J) IF staining of E-cadherin in normal epidermis, (K) IF staining of K1 in normal epidermis, (L) IHC staining for p53 in normal skin (Scale bar: A, C, E&G: 100μm; B, D, F&H: 50μm; I-L: 100 μm).

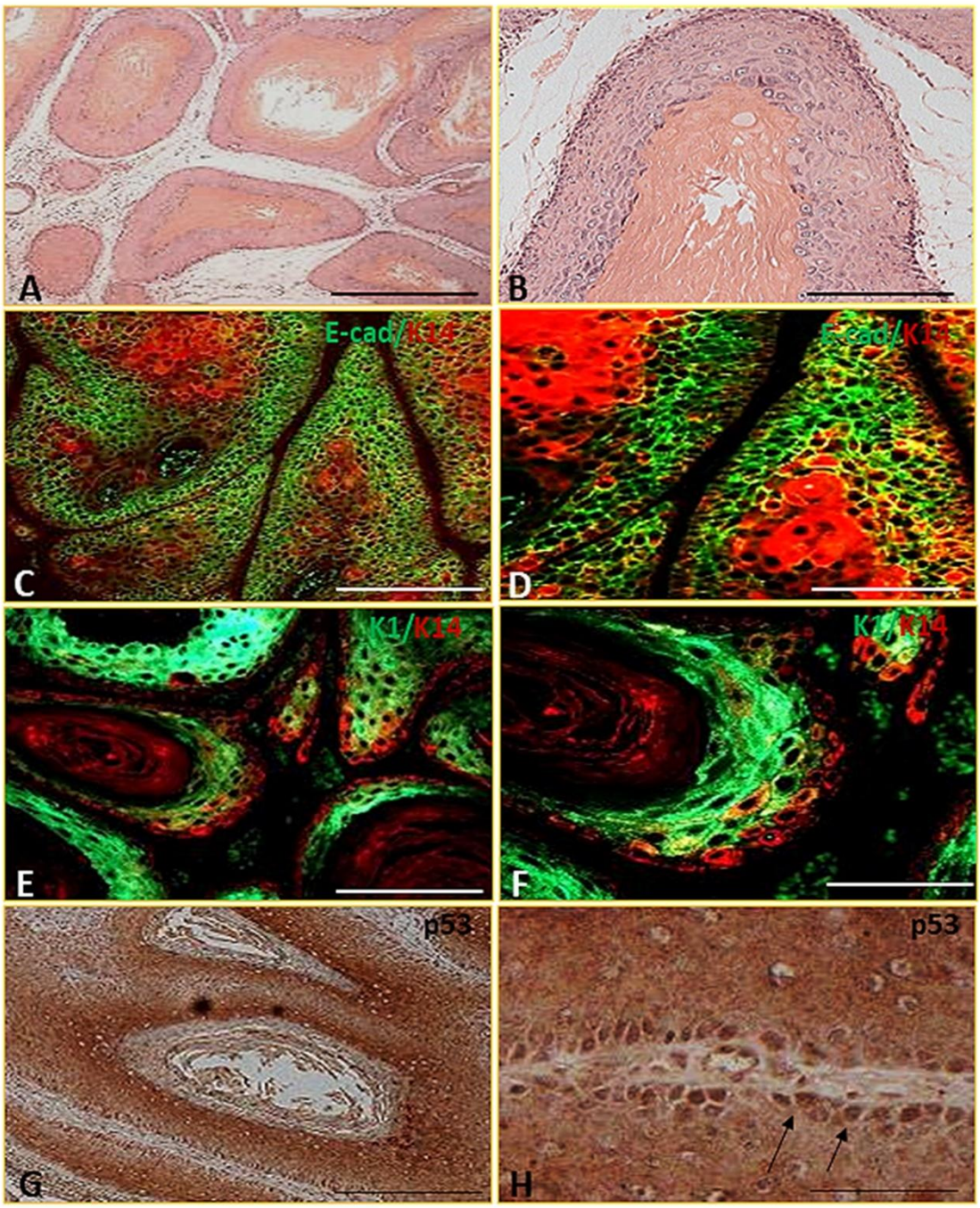

Figure 3-5 Analysis of E-cadherin and p53 expression in *HK1.ras.fos* papilloma (A&B) Show low and high magnifications of the histopathology of *HK1.ras.fos* papilloma. (C&D) IF analysis at low and high magnification of E-cadherin shows that expression remains suprabasal. (E&F) Show IF analysis at low and high magnification of K1 expression that is suprabasal. (G&H) IHC analysis of p53 expression at low and high magnification shows strong and nuclear staining, which becomes more prominent in all basal layer keratinocytes (arrows). (Scale bar: A, C, E, & G: 100μm; D, F, H: 50μm).

The cooperation between *HK1.fos* and *Δ5PTEN* has shed light on the crucial involvement of E-cadherin in orchestrating compensatory mechanisms within the epidermis to maintain homeostasis and impede tumour advancement at each developmental phase. The *HK1.fos-K14creP/Δ5PTEN*$^{flx/flx}$ cooperation led to the emergence of novel benign KAs characterised by distinctive histological alterations similar to papillomas but distinguished by pronounced hyperkeratosis (Figure 3-6 A&B) resulting in the classical appearance of KA.

In the context of *HK1.fos-K14creP/Δ5PTEN*$^{flx/flx}$ KAs, the observation that there is an increase in E-cadherin expression in the basal and suprabasal keratinocytes, suggests an upregulation of this cell adhesion protein at the basal/suprabasal level (Figure 3-6 C&D). As E-cadherin is crucial for maintaining connections between adjacent cells, this increased expression in the basal layer may indicate a reinforcement of cell adhesion, potentially influencing the structural integrity and organisation of the cells within the KAs (Figure 3-6 G&H). This increased expression is associated with elevated differentiation and enhanced cell-cell adhesion (Chiles et al., 2003; Jeanes et al., 2008), which helps protect against tumour invasion, ultimately preventing invasion of tumour cells.

Expression of E-cadherin was associated with a compensatory increase in the expression of p53. This suggests that there is a correlation between the expression of E-cadherin and an induced compensatory increase in p53 expression. A previous study illustrated that the compensatory activation of p53 observed was triggered by elevated levels of p-AKT1 due to the absence of PTEN exon 5, as well as AKT-mediated levels of inactivated p-GS3Kß, which were previously observed in *HK1.fos-K14creP/Δ5PTEN*$^{flx/flx}$ KA development (Yao, et al 2008) could result in failure of GS3K-ß mediated ß-catenin ubiquitination, resulting in anomalous ß-catenin signalling and dysregulation of E-cadherin signalling. This suggests that the membranous E-cadherin expression in both basal and suprabasal keratinocyte layers during a specific stage in the development of KAs may trigger strong compensatory p53 expression responses that halt proliferation and induce irregular differentiation.

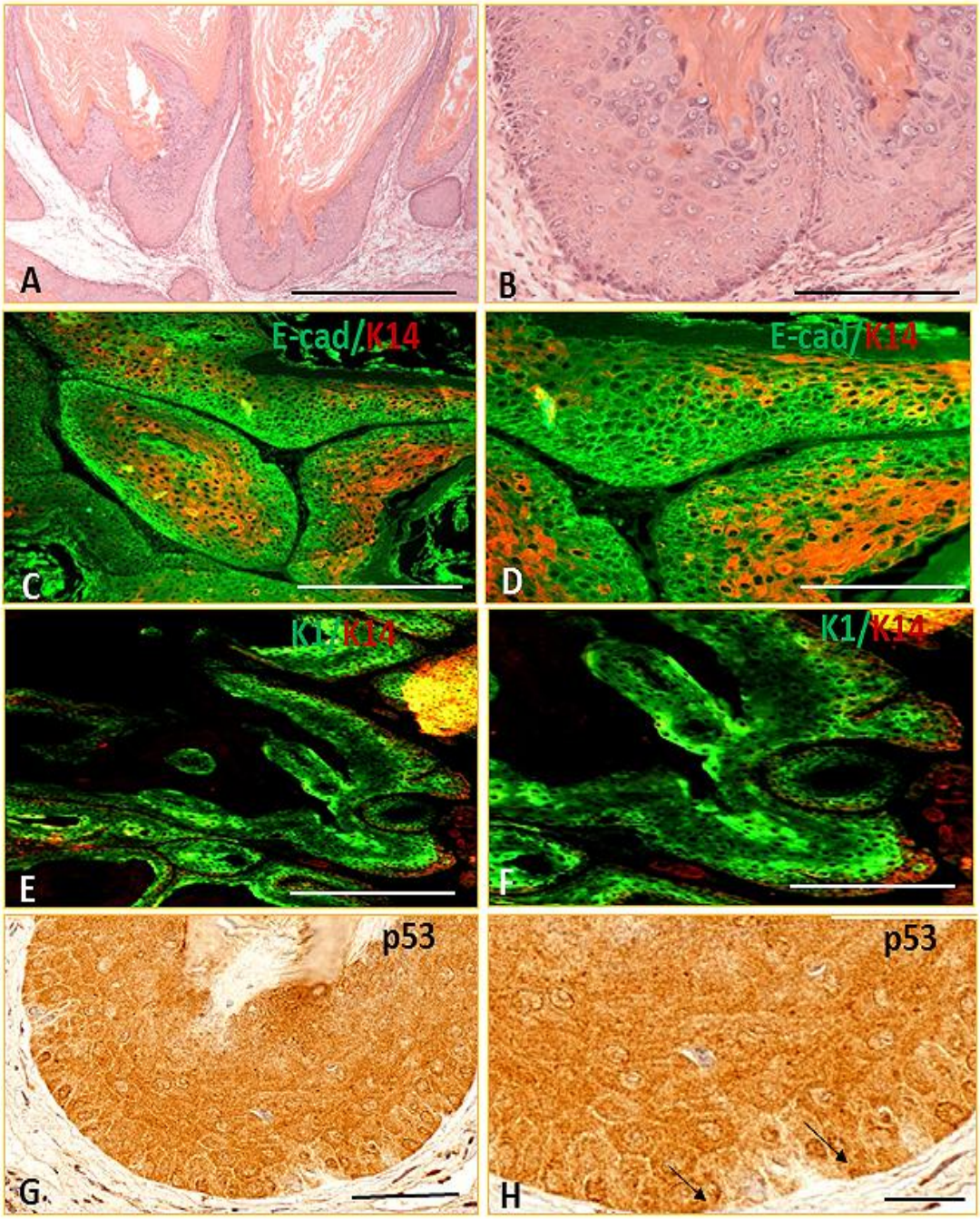

Figure 3-6 Analysis of E-cadherin and p53 expression in *HK1.fos-K14creP/Δ5PTEN*$^{flx/flx}$ keratoacanthoma (A&B) Histopathology of the *HK1.fos-K14creP/*∆*5PTEN*$^{flx/flx}$ model exhibits KA characterised by extensive layers of keratin and disorganised epidermal differentiation at low and high magnifications, respectively. Panel B shows the same image as presented in Figure 3-3 C. (C&D) Show low and high magnification of immunofluorescence analysis that revealed a strong E-cadherin expression in the basal layers in KAs. Also, in (E&F) KA accelerated differentiation is exhibited with basal keratinocytes expressing K1 at low and high magnification, respectively. (G&H) IHC analysis demonstrates that clear nuclear and basal keratinocyte p53 expression in KAs (arrows) at low and high power, respectively. (Scale bars: A: 100μm; B: 50μm; C: 75μm; D: 50μm; E: 100μm, F: 75μm; G: 75μm; H: 50μm).

In the *HK1.ras.fos-K14creP/Δ5PTEN$^{flx/flx}$* SCC model, histological progression from wdSCC to pdSCC was observed. In wdSCC, well-defined nests of tumour cells were observed (Figure 3-7 A arrows), and the cells showed an organised structure (Figure 3-7 A&B). However, as the carcinomas progressed, as shown in Figure 3-8 A&B, the histological appearance became more chaotic, the cells lost their structure, becoming more irregular and invasive (Figure 3-8 B).

IF analysis of *HK1.ras.fos-K14creP/Δ5PTEN$^{flx/flx}$* SCC progression showed that membranous E-cadherin expression gradually disappeared in the invasive basal layers along with progression from wdSCC (Figure 3-7 C&D) into SCC/pdSCC (Figure 3-8 C&D), suggesting a loss of cell-cell adhesion. This loss suggests a breakdown in the connections between neighbouring cells, primarily mediated by adhesion molecules such as E-cadherin, which could contribute to the invasive nature of the tumour by allowing cells to detach from the primary mass, degrade the surrounding extracellular matrix, and migrate into adjacent tissues, a key step in EMT (Onder et al., 2008).

Effective cell-cell adhesion is crucial for maintaining tissue structure, and its disruption in the case of aggressive SCC may facilitate tumour invasion by allowing cells to detach and invade surrounding tissues more easily. Concomitantly, p53 expression was reduced in wdSCC (Figure 3-7 G&H) and was completely lost in pdSCC areas (Figure 3-8 G&H). This could potentially contribute to uncontrolled cell growth, genomic instability, and resistance to apoptosis. The correlation between the loss of p53 and E-cadherin expression downregulation in aggressive SCC suggests a potential interplay between these two factors in the development and progression of the cancer. The concurrent loss of p53 and E-cadherin expression may indicate a complex relationship where disruptions in both tumour suppressor function and cell adhesion mechanisms contribute to the aggressive characteristics of the cancer cells. These findings suggest that E-cadherin plays a role in aiding malignant progression by affecting the ability to form focal adhesion junctions in the invasive layer.

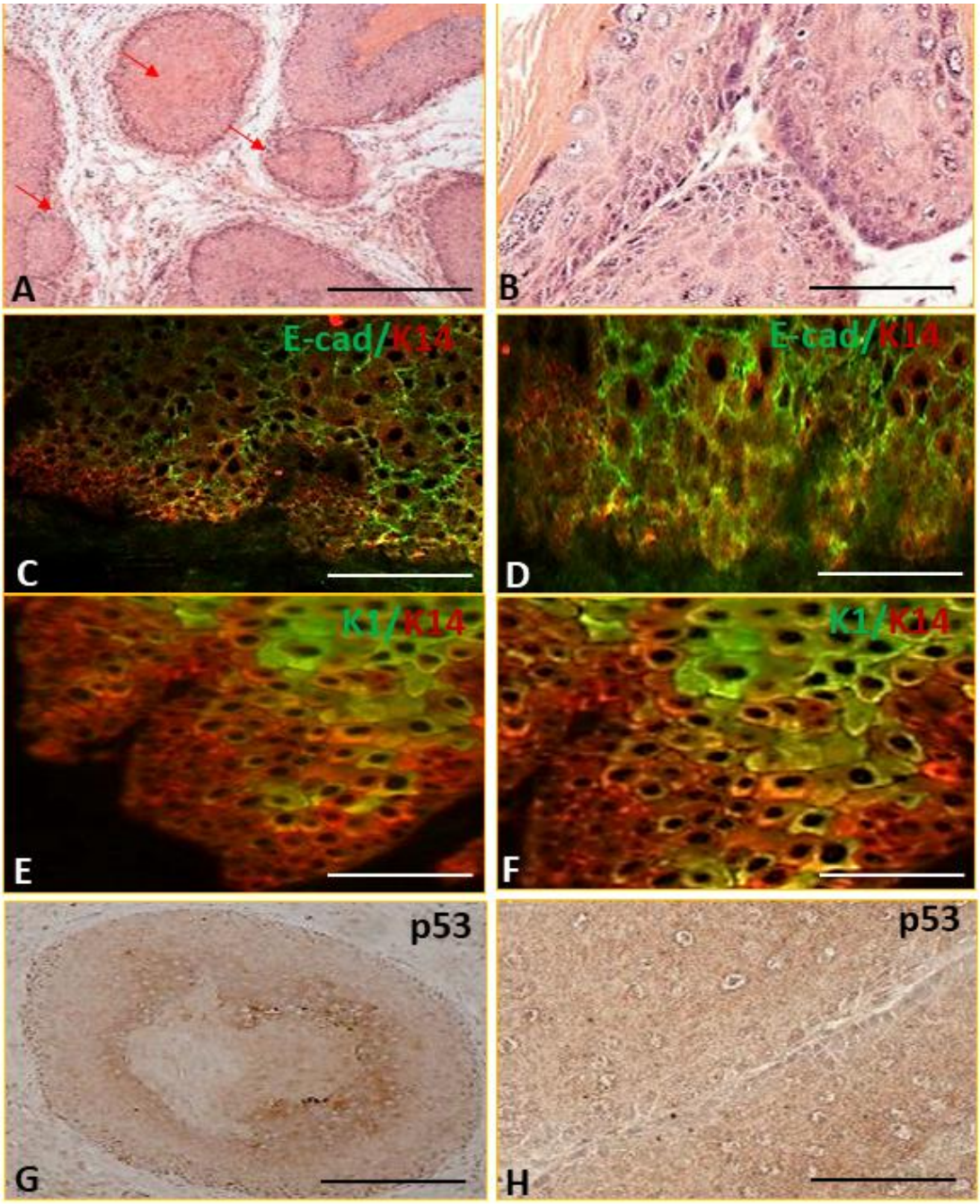

Figure 3-7 Analysis of E-cadherin and p53 expression in RU486-treated *HK1.ras.fos-K14creP/Δ5PTEN*$^{flx/flx}$ wdSCC during early progression (A&B) Histopathology of *HK1.ras.fos-k14creP/Δ5PTEN*$^{flx/flx}$ tumours exhibit wdSCC progression at low and high magnification, respectively. In Panel A, red arrows indicate tumour nests. (C&D) IF analysis of *HK1.ras.fos-K14creP/Δ5PTEN*$^{flx/flx}$ wdSCCs exhibit reduced E-cadherin expression at the invasive basal layers at low and high magnification, respectively. (E&F) Low and high magnification show a gradual reduction of K1 expression, but some K1 expression remains consistent with the wdSSC histology. (G&H) IHC analysis shows reduced p53 expression at low and high magnification, respectively, suggesting p53 loss is an early event. (Scale bars: A: 100μm; B: 50μm; C: 75μm; D: 50μm; E: 100μm, F: 75μm; G: 75μm; H: 50μm).

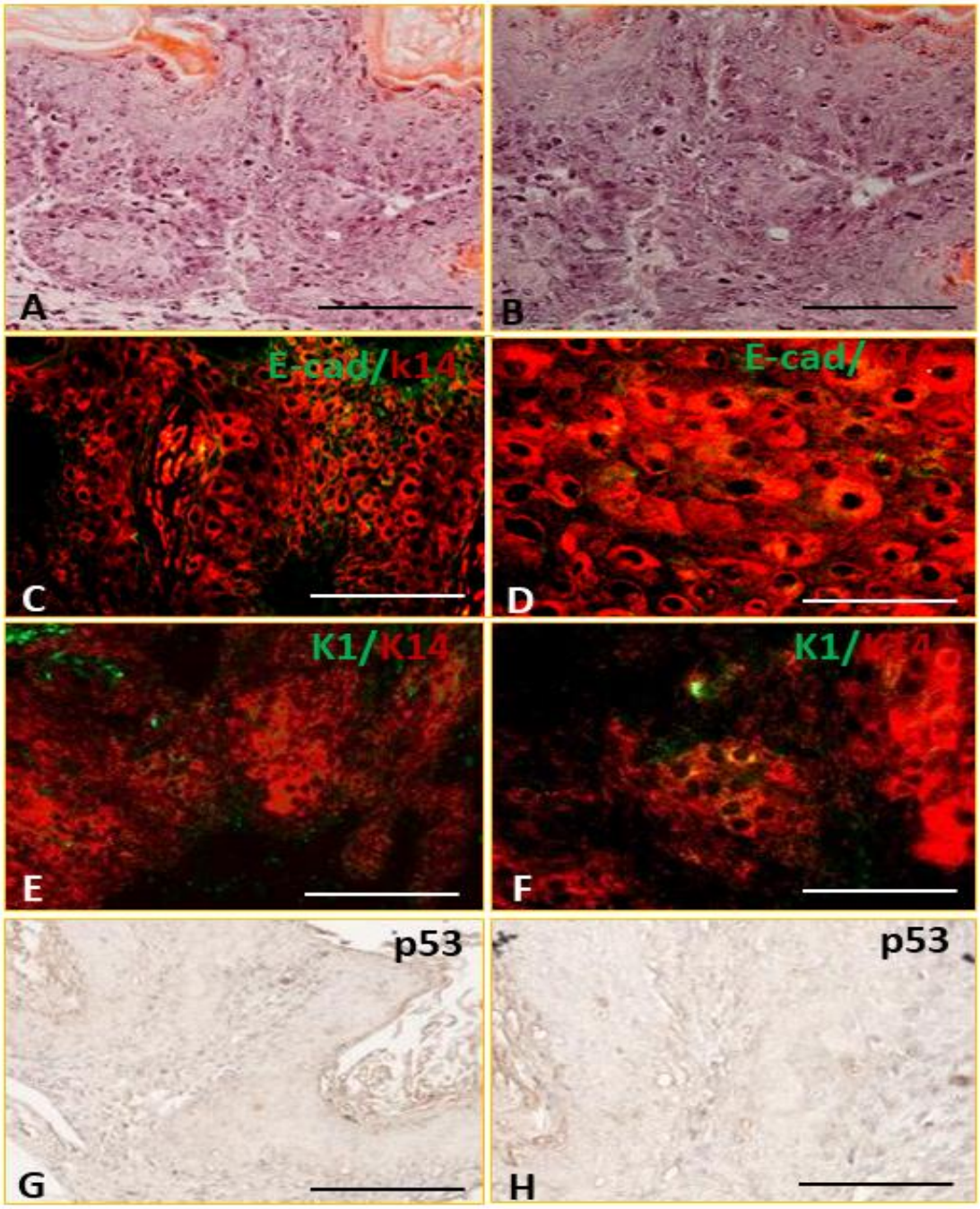

Figure 3-8 Analysis of E-cadherin and p53 expression in RU486-treated *HK1.ras.fos-K14creP/Δ5PTEN$^{flx/flx}$* SCC progression (A&B) Histopathological analysis of older *HK1.ras.fos-K14creP/Δ5PTEN$^{flx/flx}$* tumours demonstrate pdSCC progression. (C&D) IF analysis reveals loss of E-cadherin expression at both low and high magnifications, respectively. (E&F) IF analysis reveals loss of K1 expression at both low and high magnifications, respectively. (G&H) IHC analysis reveals a loss of p53 expression at both low and high magnifications. (Scale bar: A, C, E&G: 75μm; B, D, F&H: 50μm).

3.4 Summary

This chapter examined the endogenous expression pattern of E-cadherin during multistage skin carcinogenesis in the *HK1.ras.fos-K14creP/Δ5PTEN*$^{flx/flx}$ mouse models. In the early stages of hyperplasia, E-cadherin expression was preserved and membranous, particularly in the suprabasal layers, supporting its role in maintaining epithelial integrity and cell-cell adhesion. In benign papillomas, E-cadherin expression increased, suggesting a potential protective role by enhancing intercellular adhesion and possibly activating p53 via ß-catenin signalling.

However, in wdSCC, expression became noticeably reduced, particularly in the invasive basal layers. In pdSCC, E-cadherin expression was lost entirely. This loss coincided with reduced p53 expression, indicating a breakdown in epithelial architecture and an increase in invasive potential. Collectively, these findings suggest a context-dependent role for E-cadherin, being protective in early stages and wdSCC but promoting malignant progression when lost in pdSCCs. A summary figure (Figure 3-9) illustrates these dynamic changes in E-cadherin and p53 expression throughout multistage skin carcinogenesis *in HK1.ras.fos-K14creP/Δ5PTEN*$^{flx/flx}$ mouse model.

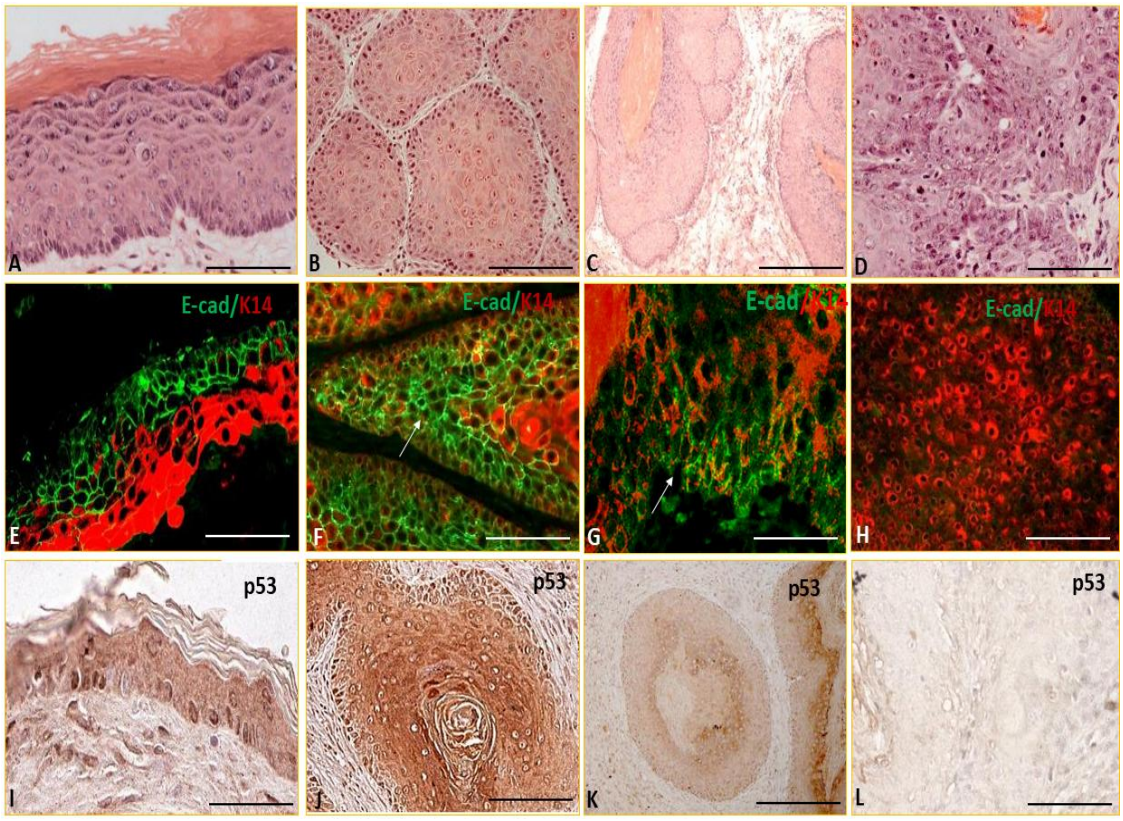

Figure 3-9 Summary of E-cadherin expression and p53 expression in HK1.ras.fos-K14creP/Δ5PTEN$^{flx/flx}$ carcinogenesis: The figure shows the E-cadherin expression pattern in *HK1.ras.fos-K14creP/Δ5PTEN$^{flx/flx}$* carcinogenesis. (A-D) Show the histopathology of *HK1.ras.fos-K14creP/Δ5PTEN$^{flx/flx}$* model. (E-H) IF analysis shows E-cadherin expression is observed to be located in the membrane of the suprabasal cell layer in (E) hyperplasia. This suggests that there is an increased production of E-cadherin, which may contribute to the maintenance of cell-cell adhesion and tissue integrity. (F) E-cadherin expression in papilloma is still present suprabasally but with less expression. However, (G) in *HK1.ras.fos-K14creP/Δ5PTEN$^{flx/flx}$* wdSCC exhibits decreased E-cadherin expression at the invasive basal layer, indicating a loss of cell-cell adhesion. However, they still retain some expression of E-cadherin. Unlike in (H) SCC/pdSCC progression, where E-cadherin expression disappeared. (I-L) The IHC analysis of p53 reveals that the p53 expression is sporadically increased in (I) hyperplasia. This elevated expression becomes more prominent in (J) papilloma, indicating a potential correlation between p53 level and the progression. However, in (K) wdSCC, the p53 expression is diminished and absent in (L) pdSCC, which correlates with E-cadherin loss in the invading cells and potentially contributes to the invasive behaviour of SCC. (Scale bars: &B; 100μm; C: 75 μm: D: 50 μm; E: 150 μm; F&G: 75 μm; H: 50 μm; I&J: 75 μm; K&L: 50 μm). Note: A&B images in this figure are repeated from (Figure 3- 3 A&B) and are included here for summary purposes.

Chapter 4 The effect of inducible E-cadherin loss in HK1.ras transgenic mouse skin

4.1 Introduction

E-cadherin is a critical epithelial-specific cell adhesion molecule that maintains tissue integrity through the formation of adherens junctions (Olson et al., 2019). It interacts with ß-catenin to anchor the cytoskeleton to the cell membrane, thereby stabilising cell-cell contacts (Fujii et al., 2020). In addition, E-cadherin regulates cellular behaviours such as migration, invasion, and intercellular signalling. Disruption of the E-cadherin-ß-catenin complex can compromise epithelial cohesion and contribute to tumour development. Although distinct from Wnt/ß-catenin signalling pathway, E-cadherin functionally intersects with it through its regulatory relationship with ß-catenin (Jolly et al., 2019).

However, changes in E-cadherin expression or function can influence Wnt signalling indirectly (Hakim et al., 2023). For instance, reduced E-cadherin levels may impact cell-cell adhesion, potentially affecting the cellular environment and Wnt pathway activity (Hakim et al., 2023), which is known to be crucial for proper hair follicle morphogenesis (Bennett et al., 2021; Fukunaga et al., 2005). This, in turn, could affect hair follicle formation and development by disrupting cell-cell adhesion, a process in which ß-catenin plays a crucial role as a key component of adherens junctions, ensuring the structural integrity and proper communication between cells necessary for hair follicle morphogenesis (Watt & Collins, 2008).

In the previous results chapter, the analysis of *HK1.ras.fos-K14creP/Δ5PTEN*$^{flx/flx}$ skin carcinogenesis mouse models revealed that endogenous E-cadherin expression in papillomas was mainly membranous and localised in suprabasal keratinocytes, similar to *HK1.ras* papillomas. However, in KA formation, E-cadherin expression moved to the basal layer, which was accompanied by increased p53 expression, suggesting a possible correlation rather than a direct regulatory relationship. This change in E-cadherin expression pattern contributes to the development of KA rather than SCC (Yao et al., 2008).

In tri-genic *HK1.ras.fos-K14creP/Δ5PTEN*$^{flx/flx}$ tumours, E-cadherin expression became more basal and less membranous. The expression also

diminished as the tumour progressed from wdSCC to pdSCC, and the E-cadherin expression was paralleled by p53 expression (Chapter 3 Figure 3-8).

However, following p53 loss, there is a reduction in E-cadherin membrane expression, leading to a progressive loss of cell-cell adhesion at the invasive basal layer, alongside the p53 loss, which contributed to the drive to malignant conversion via loss of the guardian role (Macdonald et al., 2014), resulting in increased mutations and invasion (Chapter 3). Previous studies indicated that conditional ablation of E-cadherin in skin results in loss of adherens junctions and altered epidermal differentiation in keratinocytes, with no evident sign of inflammation (Young et al., 2003). This results in abnormalities in skin hair follicles, leading to progressive loss and disrupting the ongoing hair cycle, which is dependent on E-cadherin (Young et al., 2003) loss of terminal differentiation, lack of correct hair follicle formation, and hair growth. Further investigation is still ongoing to fully elucidate the precise contribution of E-cadherin to coordinating keratinocyte cohesion, polarisation and differentiation during hair follicle development and epidermal homeostasis.

E-cadherin is well-known for its dual role in cell adhesion and intercellular signalling. However, distinguishing between these two functions (adhesion and signalling) has posed a significant challenge in research. The intracellular tail of E-cadherin plays a crucial role in binding to ß-catenin, and the absence of ß-catenin significantly affects hair follicle morphogenesis, terminal differentiation of keratinocytes, and the equilibrium between cell death and proliferation (Fukunaga et al., 2005; Huelsken et al., 2001; Hülsken & Behrens, 2000; Ordóñez-Morán et al., 2015).

The purpose of this analysis was to investigate cooperation between conditional E-cadherin ablation and *ras* activation in the mechanism that drives the benign tumour into malignant conversion and subsequent progression to pdSCC. The findings indicated no apparent effect on *HK1.ras*-driven papillomatogenesis; however, when combined with E-cadherin loss and ras activation, it triggered malignant transformation in 100% of cases. Subsequently, these tumours rapidly progressed into aggressive SCC, often linked with p53 loss (and ß-catenin activation). Therefore, these findings suggest that the loss of E-cadherin associated with *ras* activation contributes to the malignant transformation and rapid tumour progression, potentially

attributed to disruptions in cell-cell adhesion (and nuclear ß-catenin activation), following p53 loss. Initially, the study explored the phenotypic similarities between the inducible ablation of E-cadherin in *K14creP/Δ6-10Ecad*$^{flx/flx}$ and earlier studies. The primary emphasis was on assessing the impact of E-cadherin loss in epidermal terminal differentiation and the expression of TSGs.

4.2 The effect of E-cadherin heterozygosity

To analyse the effect of E-cadherin loss in *HK1.ras.fos-K14creP/Δ5PTEN*$^{flx/flx}$ models, *Δ6-10E-cadherin* was created by mating *K14creP* with *K14creP/Δ6-10E-cad*$^{flx/flx}$. As shown in Figure 4-1, exons 6-10 are flanked by *loxP* sites. K14-driven cre recombinase excises these exons, deleting sequences that encode key extracellular cadherin repeat domains. This results in a truncated, non-functional E-cadherin protein, effectively modelling E-cadherin loss of function *in vivo*.

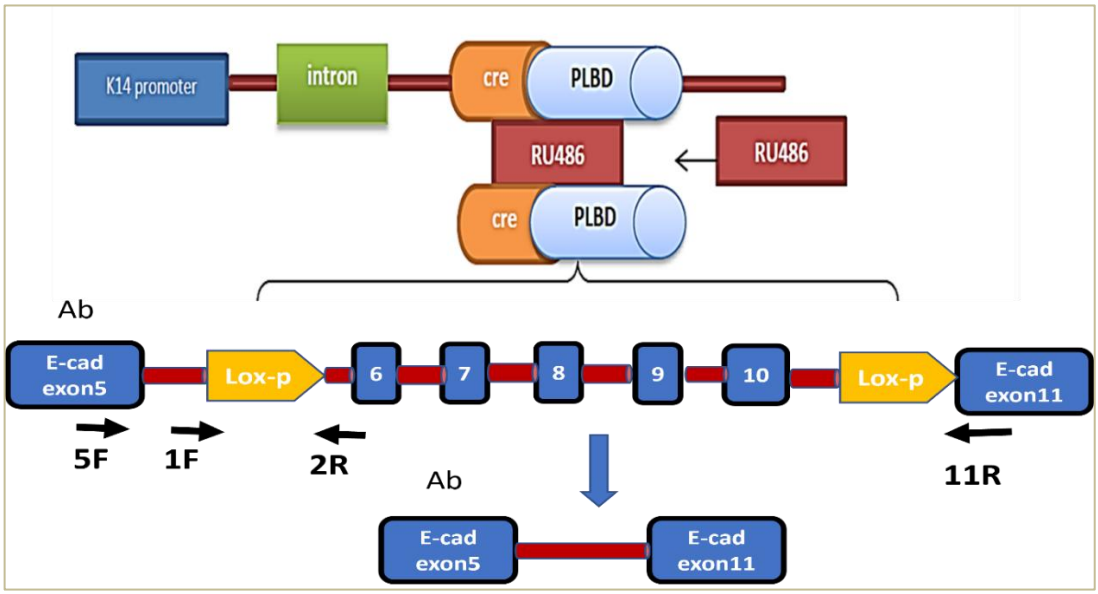

Figure 4-1 Inducible *E-cadherin* gene switch and confirmation of *cre* activity Functional E-cadherin ablation is mediated by epidermal-targeted cre recombinase, expressed by RU486-inducible cre recombinase fused with the progesterone-ligand-promoter binding domain (PLBD). It is expressed from the K14 keratin promoter, triggered by RU486 after skin application. The functional loss of E-cadherin results from the targeted ablation of exons 6-10. Ab is an anti-E-cadherin epitope in exon 5 that detects the non-functional Δ6-10E-cadherin protein.

Routine PCR analysis was performed to validate the genotype of *K14creP/Δ6-10E-cad*$^{flx/flx}$ mice, as shown in Figure 4-2. This analysis involved using specific oligo primers (Chapter 2 Table 2-3). Figure 4-2 A shows the presence of a 650bp K14creP regulator transgene in lanes 1, 2, 5, &6 of the positive mouse samples. The Δ6-10E-cadherin flox allele was detected at 350bp in lanes 6-9, and the heterozygous E-cadherin mice carried the wild-type allele at 245bp, which was detected in lanes 1-3, &5 (Figure 4-2 B). The identification of Δ6-10E-cadherin at 500bp in lanes 1 &5 in response to RU486 treatment, which induces E-cadherin ablation see (Figure 4-2 C). However, the band was absent in K14creP-negative siblings and RU486-untreated mice.

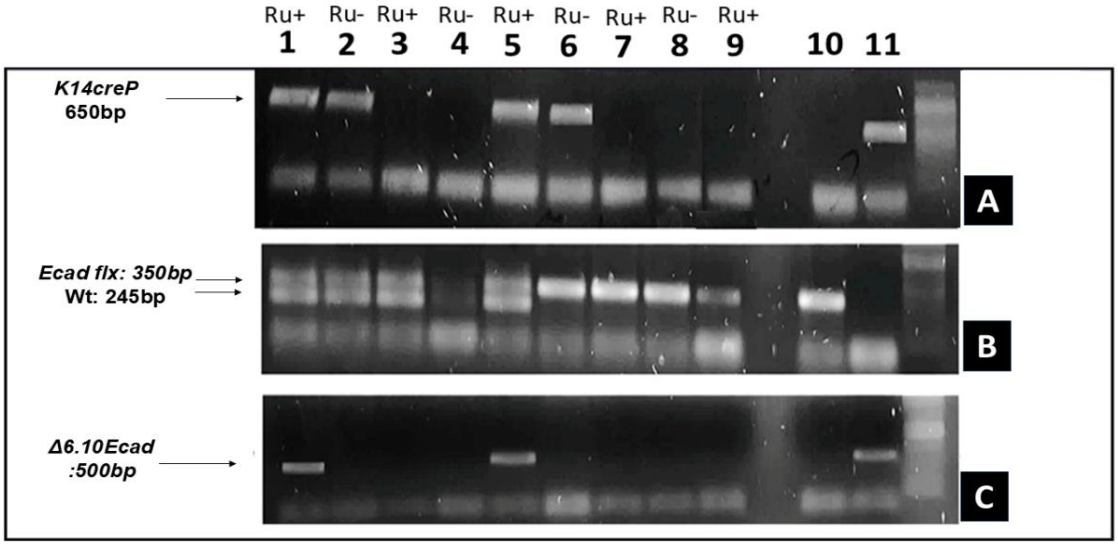

Figure 4-2 PCR analysis of *K14creP/Δ6-10E-cad* skin confirms genotypes and ablation of E-cadherin exons 6-10 (A) Shows a band at 650bp for the K14creP regulator transgene (lanes 1,2, 5, &6), and no bands from the control in lanes 3, 4, 7, 8, & 9. Lanes 10&11 are negative and positive controls. (B) In E-cadherin analysis, using the primer pair (5&11), the Δ6-10E-cad^{flx} allele is detected at 350bp (lanes 6-9), while heterozygous mice carry the wild-type allele at 245bp (lanes 1-3, & 5). Lanes 10&11 are positive and negative controls. (C) Topical RU486 treatment induces K14cre-mediated ablation of exon 6-10, using primer pair (1 & 2), resulting in a 500bp band in lanes 1 & 5 and absent in RU486-untreated mice or K14creP-negative siblings.

After 20 weeks of RU486 treatment, biopsies were taken. The mice appeared normal and showed no cutaneous abnormalities, suggesting that a single functional allele was sufficient to maintain adequate E-cadherin function, with no detectable changes in cell-cell contact formation. Similarly, the transgenic control mice (n=6 per cohort) that received RU486 treatment for the same duration also showed no noticeable effects (Figure 4-3 B&D). In contrast, RU486-treated *K14creP/Δ6-10Ecad*$^{flx/flx}$ mice (n=6 each cohort) showed altered hair growth compared to their heterozygous control siblings and wild type Philadelphia Institute of Cancer Research (ICR) mice, leading to a dishevelled appearance (Figure 4-3 A&C). This change in hair phenotype may be attributed to the loss of E-cadherin function in the epidermis, which disrupts epithelial cell adhesion and the normal structure of hair follicles, potentially impairing hair recycling and regeneration. *K14creP/Δ6-10Ecad*$^{flx/flx}$ mice also exhibited sparse fur along the dorsal treated areas (Figure 4-3 A). These images also show that K14creP/Δ6-10E-cad$^{flx/flx}$ mice have a thick ear phenotype, with the beginnings of keratosis compared to control siblings and normal ICR mice (Figure 4-3 B left &D).

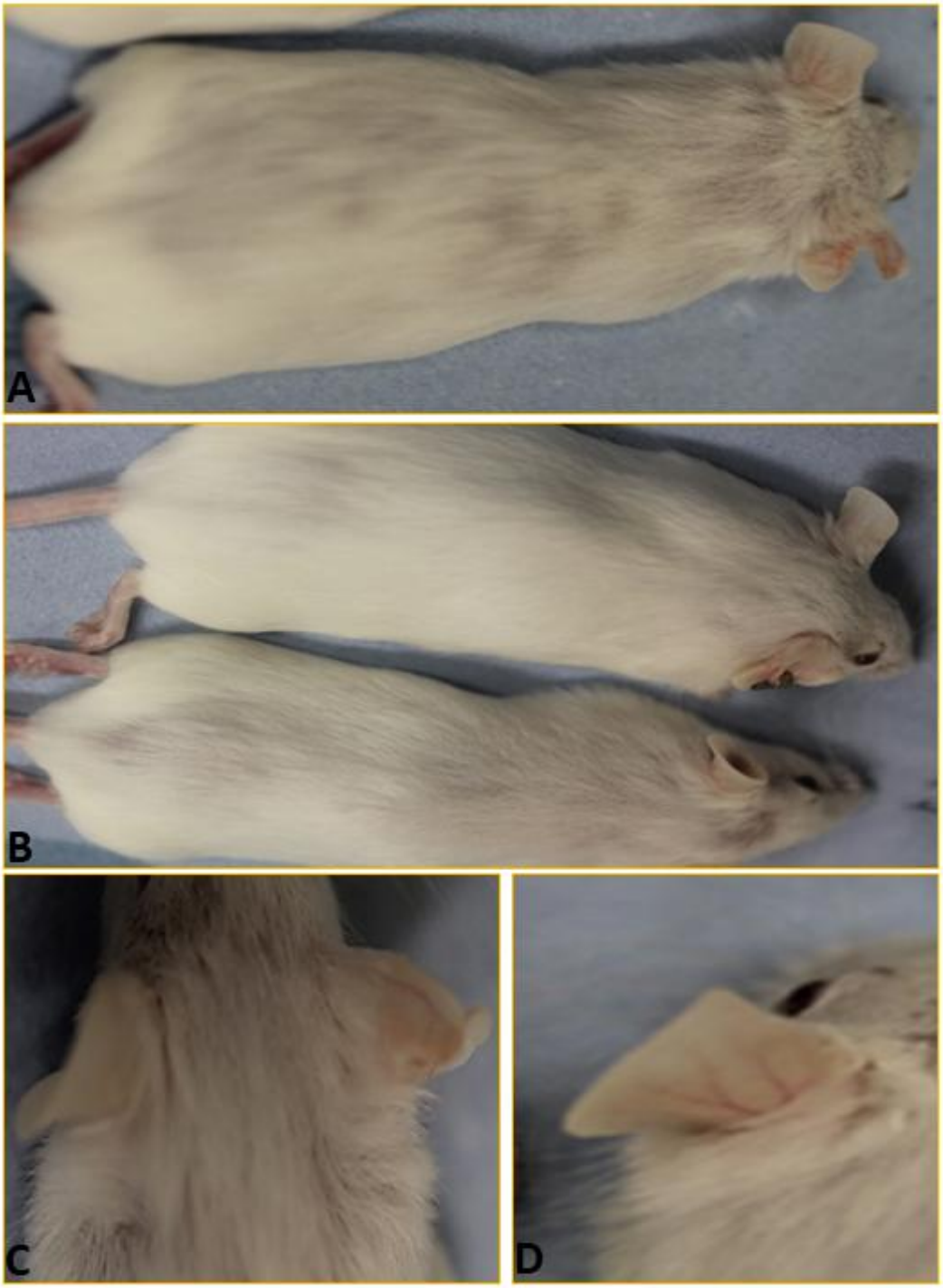

Figure 4-3 Phenotypes of RU486-treated *K14creP/Δ6-10-E-cad$^{flx/flx}$* and *K14creP/Δ6-10Ecad$^{flx/het}$* mice (A) RU486-treated *K14creP/∆6-10-Ecad$^{flx/flx}$* mice exhibit incorrect hair growth, resulting in a scruffy appearance, and the fur is noticeably sparse in treated areas. (B) Comparison of treated control *K14creP/∆6-10Ecad$^{flx/het}$* siblings (Left; mouse is normal) and RU486-treated *K14creP/∆6-10-Ecad$^{flx/flx}$* sibling with incorrect hair growth. (C) Shows treated *K14creP/∆6-10Ecad$^{flx/flx}$* mice also have an enlarged and thick ear phenotype with keratosis compared to (D) control siblings which is it a control untreated or an ICR wild type mouse ear.

The histological analysis of a normal anagen follicle is presented first as a control to illustrate the baseline morphology (Figure 4-4). This is followed in the histological analysis of RU486-treated *K14creP/Δ6-10Ecad*$^{flx/flx}$ skin, which revealed an abnormal epidermis accompanied by mild hyperplasia (Figure 4-5). In Figure 4-5 A, the epidermis displays mild hyperplasia with irregularities in the basal layer and obvious intercellular gaps, suggesting a disruption in cell-cell adhesion. The hyperplasia seen in these panels appeared to compensate for potential barrier loss via differentiation and obvious keratosis (Figure 4-5 C). These gaps became more apparent in consistent with early stages of failed adhesion, a phenomenon that is particularly noticeable in *ras/Ecad*^{flx} mice (see below). The disruption observed in the basal layer reflects an early loss of tissue integrity, potentially setting the stage for further pathological changes.

The follicular histology depicted in Figure 4-5 B, D&F, demonstrate a similar pattern of structural disruption. Far fewer anagen follicles were observed, compared to normal anagen follicle controls (Figure 4-4), and this may account for the overt dishevelled appearance.

The associated hyperplasia and altered hair follicle bulb structure may be due to failed E-cadherin signalling to ß-catenin in *K14creP/Δ6-10Ecad*$^{flx/flx}$ mice, a phenomenon not seen in heterozygous mice. However, the interfollicular epidermis was not hyperplastic, as the hair follicles still provide barrier functions, unlike the epidermis of the ear, which has fewer hair follicles.

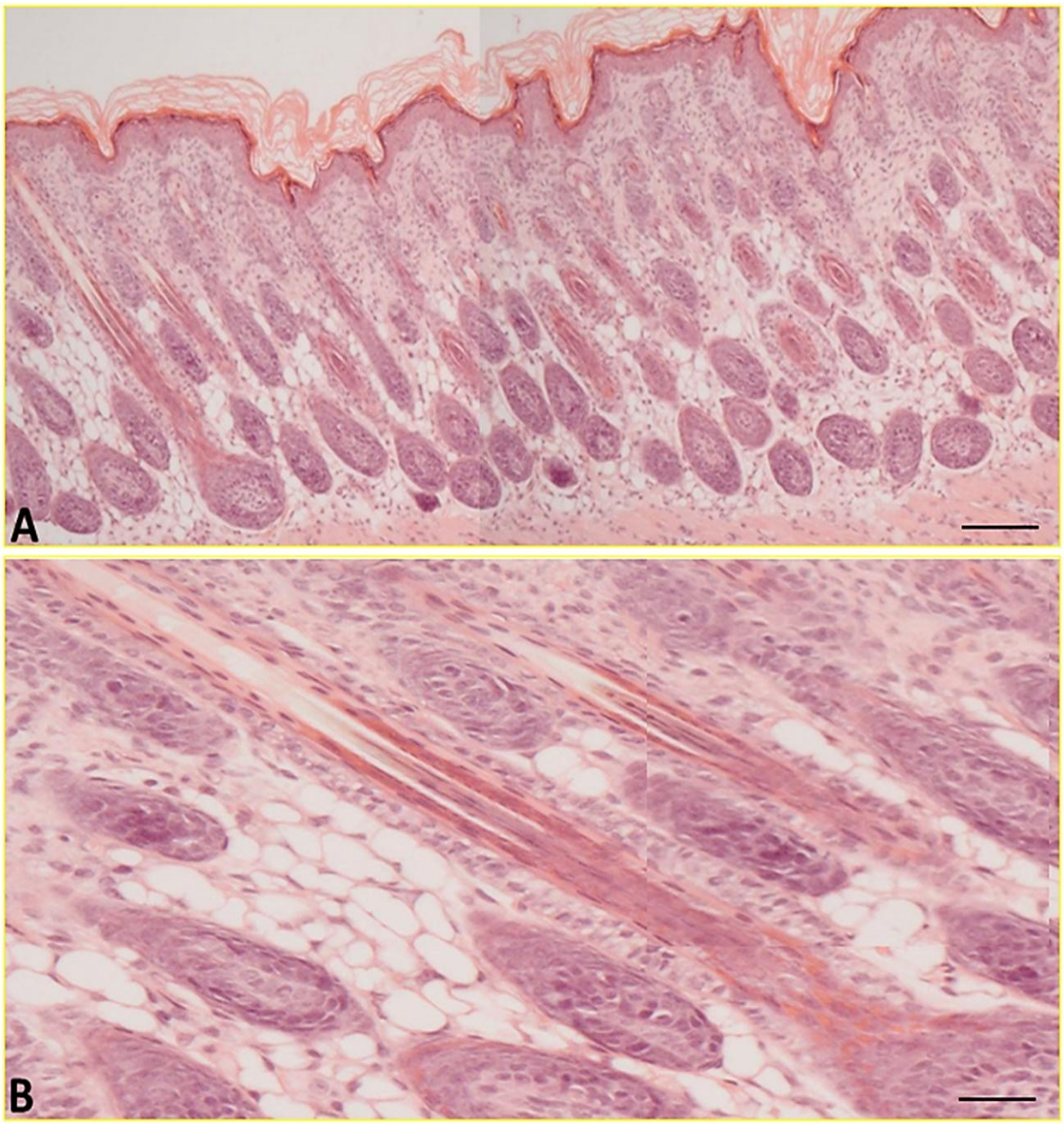

Figure 4-4 Histology of normal anagen follicles (A&B) low and high magnifications of normal anagen follicles in RU486-untreated mice. (Scale bars: A: 100μm; B: 50μm).

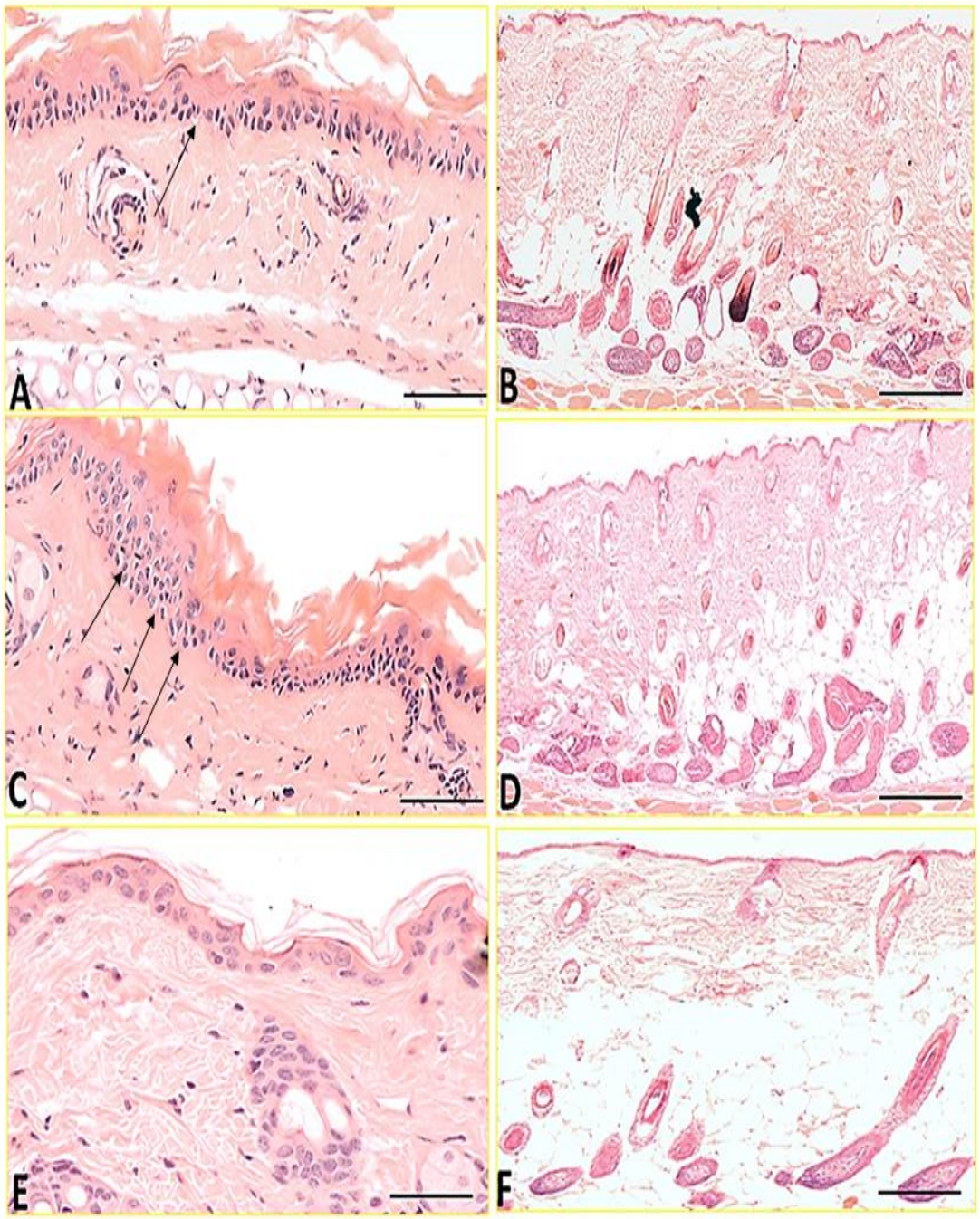

Figure 4-5 Histology of RU486-treated *K14creP/Δ6-10Ecad*$^{flx/flx}$ genotypes (A&C).RU486-treated *K14creP/Δ6-10E-cad*$^{flx/flx}$ genotype exhibits mild hyperplasia, intercellular gaps (arrows), and increased basal keratinocyte layers that display more differentiation compared to (E) normal control. (B) Telogen phase RU486-treated *K14creP/Δ6-10E-cad*$^{flx/flx}$ skin with irregular follicles, indicative of reduced anagen phase activity. (D) RU486-treated *K14creP/Δ6-10E-cad*$^{flx/flx}$ skin shows fewer follicles. (F) Normal control. (Scale bars: A, C&E: 75μm; B, D&F: 100 μm).

However, the interesting aspect is that despite E-cadherin loss, it does not trigger tumorigenic transformation in keratinocytes. This suggests that while E-cadherin plays a role in cell-cell adhesion, its absence alone is not sufficient to induce the tumorigenic transformation of keratinocytes.

Other factors or molecular pathways may be involved in regulating the balance between cell-cell adhesion and tumorigenesis in this specific context. Thus, the next step was to investigate the cooperation between E-cadherin conditional ablation and ras activation.

4.2.1.1 E-cadherin heterozygosity induces papilloma conversion to an early wdSCC in *HK1.ras-K14creP/Δ6-10Ecad$^{flx/het}$* mice.

To further validate and explore the effects of E-cadherin ablation, initial experiments began by generating *HK1.ras-K14creP/Δ6-10Ecad$^{flx/het}$* mice. Thus, *K14creP/Δ6-10E-cad$^{flx/flx}$* were bred with a strain of *HK1.ras^{1205}* mice that developed papilloma in 100 % of mice, which have been widely used in studying papilloma formation (Greenhalgh et al., 1995), and have the genetic requirements for malignant conversion (Masre et al., 2017; Wang et al., 2000).

As described in the Introduction (Introduction1.4.2) *HK1.ras^{1205}* mice develop papillomas in the wounded (tagged) ear in all cases, depending on the timeframe and the individual genetic background of these outbred ICR mice. The papillomas develop from a thickened, hyperplastic tag on the ear within 6-7 weeks and grow over 8-10 weeks to a diameter of 3-6mm, and by 12-14 weeks to a diameter of 7-10mm, well within the 1.5cm UK limits. However, in some instances, a small percentage (0.1%) of *HK1.ras* mice develop papillomas in areas other than the ears. This occurrence is random and limited to areas of scratching and biting (not shown).

Initially, RU486-treated *HK1.ras-K14creP/Δ6-10Ecad$^{flx/het}$* (n=6 per cohort) mice displayed a similar thickening of the ear at the tag site, and papillomas appeared within a similar timeframe of 6-8 weeks, with tumours showing similar initial sizes (Figure 4-6 A). However, by 10 -12 weeks, these tumours became noticeably larger (Figure 4-6 B Top animal) compared to aged-matched control littermates that were RU486-untreated and biopsied simultaneously (Figure 4-6 B Bottom animal). While such controls were consistently observed in all *HK1.ras* and all (non-cre) genotypes (regardless

of RU486 treatment) (Figure 4-6 C), this pattern of increased tumour size was observed in all RU486-treated *HK1.ras-K14creP/Δ6-10Ecad*$^{flx/het,}$ and histological analysis showed that these tumours had started to progress towards malignancy.

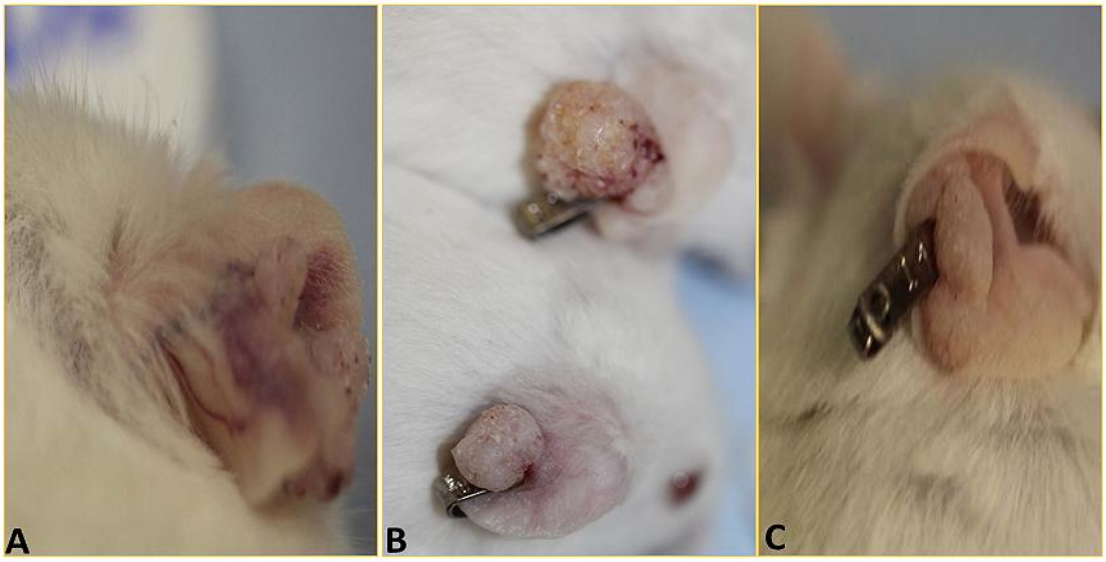

Figure 4-6 Phenotype of *HK1.ras-K14creP/Δ6-10Ecad*$^{flx/het}$ mice tumour development (A) RU486-treated *HK1.ras-K14creP/Δ6-10-Ecad*$^{flx/het}$ mouse developed papilloma by 6-8 weeks. (B) Top mouse shows the E-cadherin heterozygosity in *HK1.ras-K14creP/Δ6-10-E-cad*$^{flx/het}$ genotype by 10-12 weeks that can induce malignant conversion but is restricted to an early wdSCC pathology, bottom mouse is no RU486-treated control that mimics (C) *HK1.ras* littermate controls papilloma.

4.2.1.2 The histological analysis of E-cadherin heterozygosity in *HK1.ras-K14creP/Δ6-10Ecad$^{flx/het}$* mice show effects on keratinocyte differentiation and increased hyperplasia

The histological analysis of RU486-treated *HK1.ras-K14creP/Δ6-10Ecad$^{flx/het}$* mice exhibited hyperplasia that was notably more pronounced than in controls (Figure 4-7), with more pronounced proliferation. Despite this proliferation, the overall differentiation of cells appeared relatively normal; however, these mice exhibited intercellular spaces in the basal layers (Figure 4-7 A&C), indicating a failure in cell-cell adhesion as an early event in tumour progression. This feature was less obvious in *HK1.ras* control mice with hyperplasia (Figure 4-7 B&D).

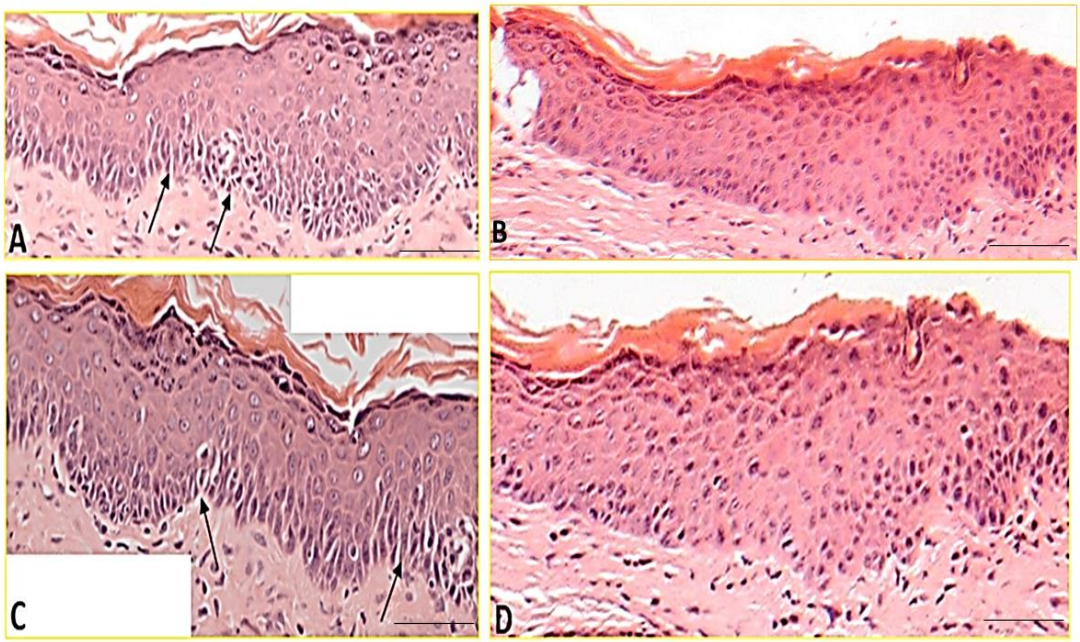

Figure 4-7 Histology of RU486-treated *HK1.ras-K14creP/Δ6-10Ecad*$^{flx/het}$ hyperplasia (A&C) *HK1.ras-K14creP/Δ6-10Ecad*$^{flx/het}$ hyperplasia displays intracellular gaps (arrows) in the basal layers compared to (B&D) *HK1.ras* hyperplasia with less obvious intercellular gaps. (Scale bars: A: 50μm; B: 100μm; C: 50μm; D: 50μm).

4.2.2 E-cadherin heterozygosity induces papilloma conversion to an early wdSCC in *HK1.ras-K14.creP/Δ6-10E-cad*$^{flx/het}$ mice.

HK1.ras-K14creP/Δ6-10Ecad$^{flx/het}$ mice exhibited papillomas similar to those observed in the control *HK1.ras* mice by 8-10 weeks (see above). However, histological analysis revealed that *HK1.ras-K14creP/Δ6-10Ecad*$^{flx/het}$ papillomas exhibited pronounced intercellular gaps between basal layer keratinocytes (Figure 4-8 A&B), which were not observed in the controls (Figure 4.8 C&D). These gaps suggest a disruption of cell-cell adhesion and the beginning of conversion. By 10 weeks, areas of carcinoma *in situ* were identified within *HK1.ras-K14creP/Δ6-10Ecad*$^{flx/het}$ *tumours*, characterised by the presence of mitotic figures (Figure 4-8 B) (arrows).

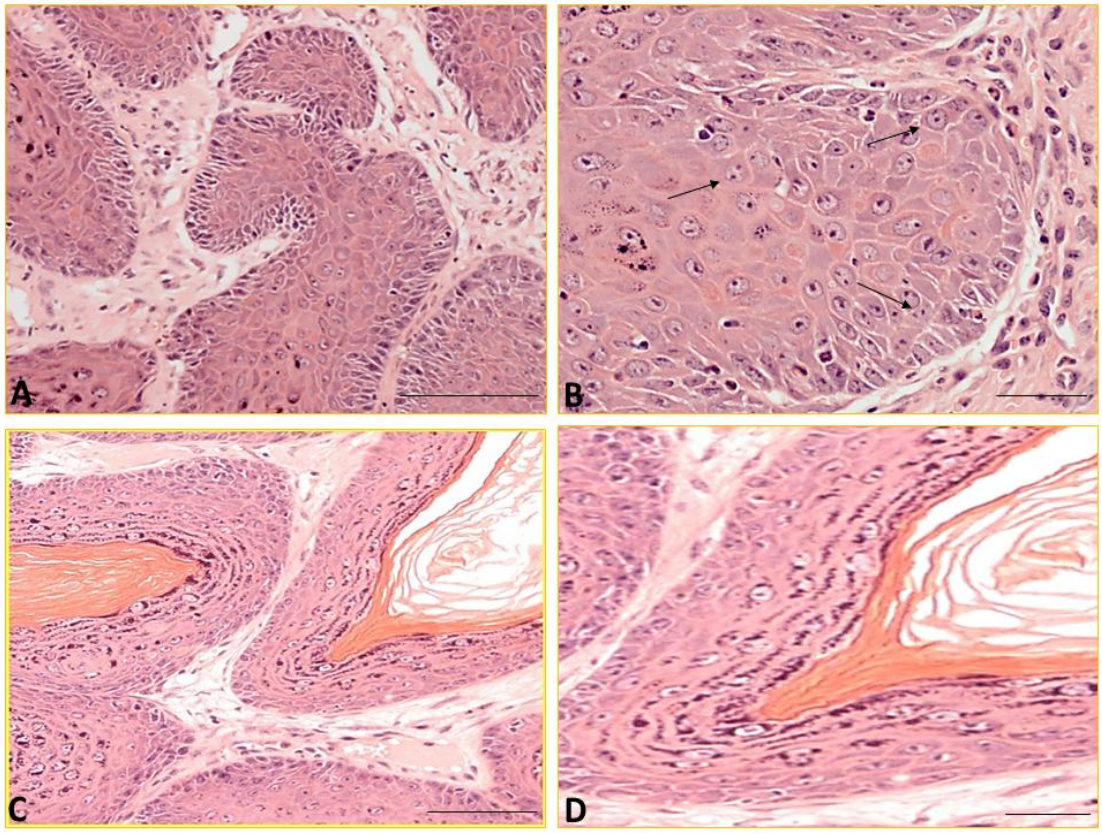

Figure 4-8 Histology of *RU486-treated HK1.ras-K14creP/Δ6-10Ecad*$^{flx/het}$ papillomatogenesis and beginnings of conversion by 10 weeks (A) RU486-treated *HK1.ras.K14creP/Δ6-10Ecad*$^{flx/het}$ mice exhibit papillomas by 10 weeks. (B) Shows areas of carcinoma *in situ* that possess mitotic figures (arrows) and intercellular gaps. (C&D) Control *HK1.ras* mice with fewer intercellular gaps and have normal differentiation. (Scale bars: A&C: 75μm; B&D: 25 μm).

A distinct correlation emerged between *HK1.ras-K14creP/Δ6-10Ecad*$^{flx/het}$ within papillomas and the development of carcinoma *in situ* (Figure 4-9 A&C) by weeks 12-14, marking the initiation of malignant transformation. These cellular changes culminated in the formation of early-stage wdSCC (Figure 4-9 B) that collectively invaded the surrounding tissues (Figure 4-9 D), but the tumour progression was limited to an early stage of wdSCC pathology, suggesting that this genotype still retains a functional E-cadherin allele, which contributed to the restricted progression.

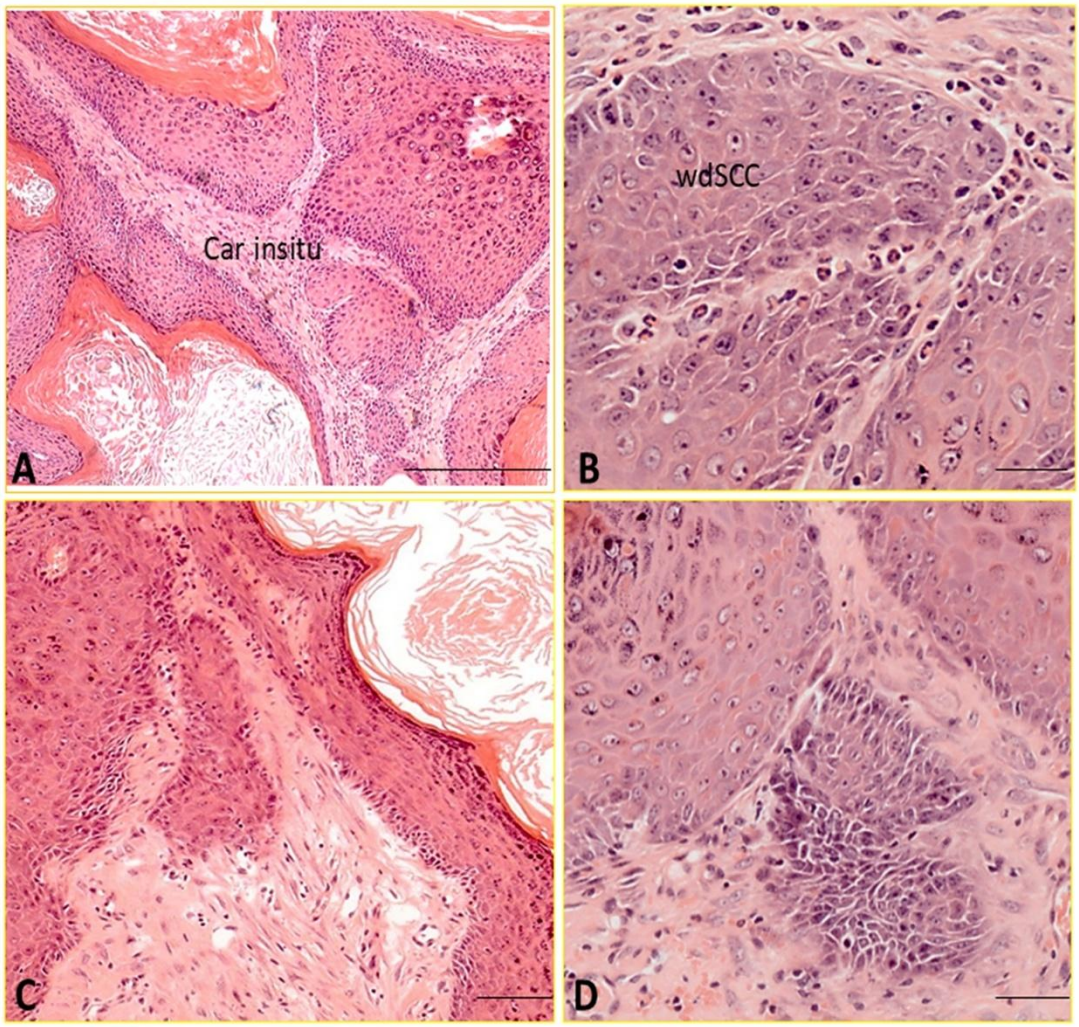

Figure 4-9 Histopathology of RU486-treated *HK1.ras-K14creP/∆6-10Ecad*$^{flx/het}$ tumour progression into carcinoma *in situ* and limited early-stage wdSCC at 12-14 weeks (A&C) low and high magnifications of RU486-treated *HK1.ras-K14creP/Δ6-10Ecad*$^{flx/het}$ that show carcinoma *in situ* development. (B) RU486-treated *HK1.ras-K14creP/Δ6-10Ecad*$^{flx/het}$ model, which exhibits wdSCC with mitotic figures and is collectively invading in (C). (Scale bars: A&B: 100μm; C&D: 50μm).

4.2.3 Effects of E-cadherin heterozygosity on differentiation and β-catenin signalling in *HK1.ras-K14creP/Δ6-10Ecad*$^{flx/het}$ mice

To further investigate the pathological backgrounds associated with the HK1.ras-*HK14creP/Δ6-10E-cad*$^{flx/het}$ genotype, a comprehensive analysis was undertaken of the differentiation and possible mechanisms that affect HF development and malignant progression. This examination initially aimed to elucidate variations in the expression profiles of key markers, specifically early differentiation keratin K1, to assess its effect on differentiation and exploit K1 expression to confirm malignant conversion.

Assessment of relative and positional expression in *HK1.ras-K14creP/Δ6-10Ecad*$^{flx/het}$ mice were used, as these mice may have reduced E-cadherin expression, leading to alterations in ß-catenin signalling that affect HF formation compared to control *HK1.ras* genotypes.

4.2.3.1 Analysis of K1 expression in *HK1.ras-K14cereP/Δ6-10Ecad*$^{flx/het}$ mice

As shown in Figure 4-10 A&B, K1 expression in *HK1.ras-K14creP/Δ6-10Ecad*$^{flx/het}$ papillomas were observed in the differentiated suprabasal layers, consistent with its role as an early marker of differentiation (Fuchs & Green, 1980). This was similar to the control *HK1.ras* papillomas, which also displayed intense and strong suprabasal K1 expression (Figure 4-10 E& F). However, by 10 weeks, the K1 expression had transitioned from basal to suprabasal keratinocytes, appeared disordered and irregular in *HK1.ras-K14creP/Δ6-10Ecad*$^{flx/het}$ compared to equivalent control papillomas (Figure 4-10 C&D).

This suggests that while initial Δ6-10E-cadherin heterozygosity in *HK1.ras-K14creP/Δ6-10Ecad*$^{flx/het}$ papilloma did not disrupt the normal differentiation of keratinocytes; however, with time, reduced E-cadherin levels (see below) began to affect progression to early-stage carcinoma as observed histologically (above).

This effect may be due to conflicting proliferative signals from E-cadherin reduction, which affected ß-catenin deregulation (Chakraborty et al., 2010; Di Cunto et al., 1998; Topley et al., 1999). These changes may lead to altered HF formation and susceptibility to malignant conversion, possibly via effects on p53 expression, such as disrupted cell cycle arrest or impaired apoptosis.

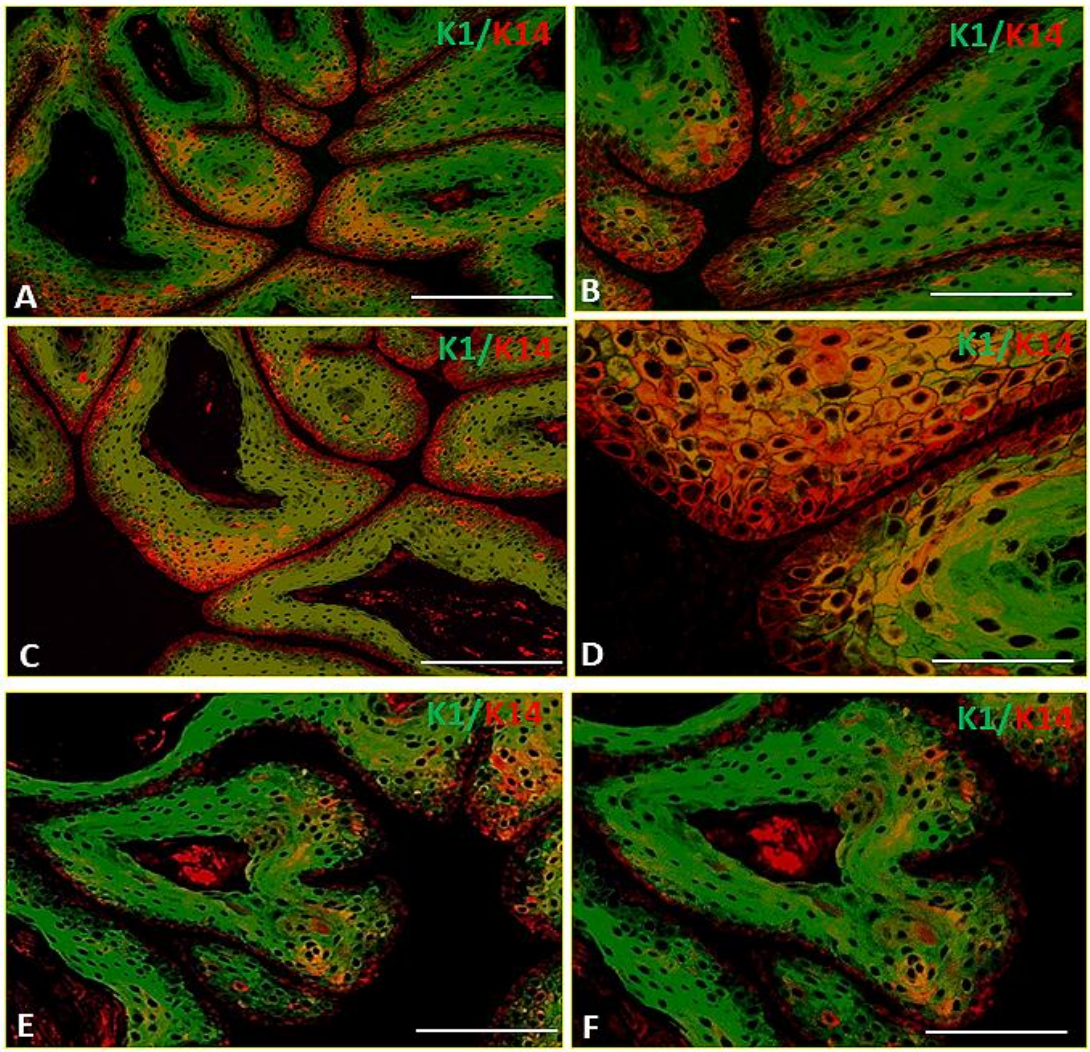

Figure 4-10 Analysis of K1 expression in RU486-treated *HK1.ras-K14creP/Δ6-10Ecad$^{flx/het}$* tumour progression at 10-12 weeks (A&B) Show *HK1.ras-K14creP/Δ6-10Ecad$^{flx/het}$* papilloma with strong K1 expression in the suprabasal layers. (C) Shows reduced K1 expression in some areas during conversion from papilloma into (D) wdSCC. (E&F) Typical K1 expression in HK1.ras papilloma, which exhibits ordered differentiation and smooth basal to suprabasal interactions. (Scale bars: A-C: 100μm, D-F: 50μm).

4.2.3.2 Analysis of Δ6-10E-cadherin expression in *HK1.ras-K14creP/Δ6-10Ecad$^{flx/het}$* mice

The *HK1.ras-K14creP/Δ6-10E-cad$^{flx/het}$* papillomas exhibited reduced Δ6-10E-cadherin expression patterns within the basal keratinocytes (Figure 4-11 A&B). This suggests that reduced E-cadherin expression contributes to progression toward wdSCC and the development of carcinoma *in situ* (Figure 4-11 B). The partial reduction in E-cadherin disrupts cell-cell adhesion, leading to the formation of intercellular gaps, which reflect a breakdown in epithelial integrity, facilitating increased cellular proliferation and malignant conversion. The progression toward wdSCC in this model indicated that while some E-cadherin is present, it is insufficient to fully suppress tumour progression. The compromised adhesion and resulting cellular changes contribute to the development of a more aggressive phenotype. However, despite these changes, the progression was limited and restricted to early wdSCC.

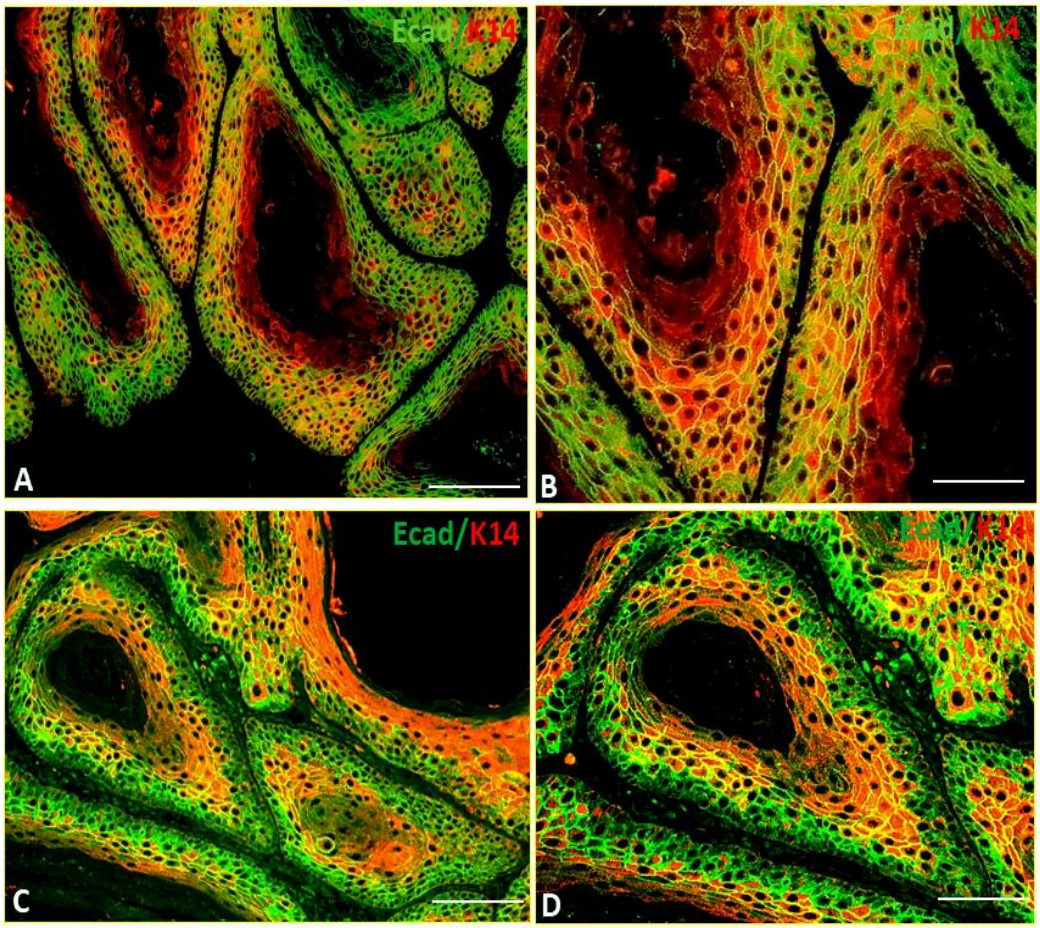

Figure 4-11 Analysis of E-cadherin expression in RU486-treated *HK1.ras-K14creP/*∆*6-10Ecad*$^{flx/het}$ and *HK1.ras* papilloma at 10-12 weeks (A&B) Show low and higher magnifications of reduced membranous ∆6-10E-cadherin expression, reduced in the basal cell keratinocytes, are obvious in (B) carcinoma *in situ*. (C&D) Low and high magnifications of *HK1.ras* papilloma control that show strong membranous suprabasal Ecadherin expression. (Scale bar: A&C: 100µm; C&D: 50µm).

4.2.3.3 Analysis of β-catenin expression in *HK1.ras-K14creP/Δ6-10Ecad$^{flx/het}$* mice

In the context of *HK1.ras-K14creP/Δ6-10E-cad$^{flx/het}$* mice, ß-catenin plays a critical role in both normal tissue homeostasis and tumour dynamics. The results indicated a shift in ß-catenin expression, with less membranous suprabasal expression, and only sporadic expression in the basal layer keratinocytes (Figure 4-12 A&B). This could potentially destabilise ß-catenin in basal cells, leading to impaired adhesion, loss of proliferative control, and the development of hyperplasia. In contrast, the control *HK1.ras* papillomas exhibited typical membranous ß-catenin expression predominantly in the suprabasal layer (Figure 4-12 C&D). This reduction in membrane-associated-ß-catenin alongside E-cadherin may have a minimal impact on ß-catenin-mediated nuclear transcription. This suggests that disruption in ß-catenin signalling can lead to altered hair follicle dynamics (Watt & Collins, 2008), potentially contributing to promoting progression to early wdSCC. These findings imply that the role of ß-catenin in cell adhesion is crucial for limiting tumour progression in this model.

Analysis of *HK1.ras-K14creP/Δ6-10Ecad$^{flx/het}$* tumours revealed that heterozygous E-cadherin ablation resulted in little change in papilloma formation and is similar to the HK1.ras genotype. However, the increasing intercellular gaps suggest failed cell-cell adhesion and thus *HK1.ras-K14creP/Δ6-10E-cad$^{flx/het}$* tumours developed first into carcinoma in situ and later into early malignant wdSCC, with reduced functional E-cadherin expression at the basal layers, suggesting a partial failure in cell-cell adhesion.

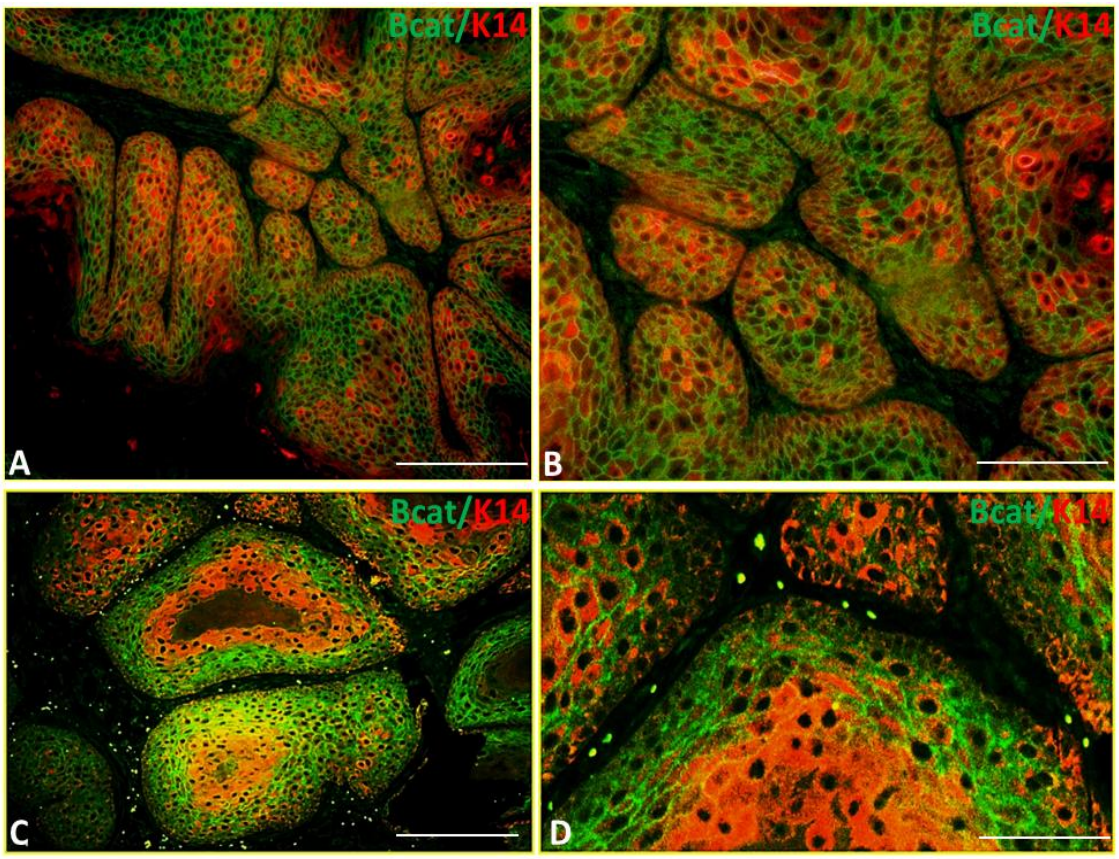

Figure 4-12 Analysis of β-catenin expression in RU486-treated *HK1.ras-K14creP/Δ6-10E-cad*$^{flx/het}$ papilloma progression at 10-12 weeks (A&B) *HK1.ras-K14creP/Δ6-10E-cad*$^{flx/het}$ papilloma at a low and higher magnification, reveals less membranous suprabasal β-catenin expression with sporadic nuclear expression in the basal layer. (C&D) *HK1.ras* papillomas, where the expression of β-catenin is mainly in the membranous and suprabasal layers. (Scale bars: A&C: 100μm; B&D: 50μm).

To understand the molecular mechanisms underlying the regression-prone nature of papillomas upon E-cadherin ablation, this study analysed histopathological changes in samples from the RU486-inducible conditional ablation E-cadherin model that has been previously introduced into regression-prone papilloma models (Berton et al., 2000) using by the *cre/loxP* system (*K14creP/Δ6-10E-cad*$^{flx/flx}$).

4.3 E-cadherin loss in *HK1.ras-K14creP/Δ6-10Ecad$^{flx/flx}$* mice induces malignant conversion and progression to aggressive SCC consistent with cell-cell adhesion failure.

E-cadherin loss is a critical event in epithelial cell adhesions, and it has been strongly implicated in the malignant conversion and progression to a more aggressive SCC (Zhitnyak et al., 2020). In the current study, using the *HK1.ras-K14creP/Δ6-10E-cad$^{flx/flx}$* model, E-cadherin loss led to an earlier onset of malignant conversion and rapid progression to a more aggressive tumour phenotype

In the *HK1.ras-K14creP/Δ6-10E-cad$^{flx/flx}$* model, the deletion of E-cadherin leads to disruption of cell-cell adhesion (Zhitnyak et al., 2020), which is characterised by increased cell motility, invasiveness, and resistance to apoptosis. The loss of E-cadherin also promotes the activation of various signalling pathways involved in tumour progression, such as Wnt/β-catenin (Saydam et al., 2009). The loss of E-cadherin in this model triggers a cascade of events that drive malignant conversion and aggressive tumour behaviour, highlighting the crucial role of E-cadherin in maintaining normal epithelial function and suppressing tumour progression.

Initial observations in RU486-treated HK1.ras-*K14creP/Δ6-10Ecad$^{flx/flx}$* models demonstrated that complete E-cadherin ablation induced greater hyperplasia than the heterozygote model, with evidence of impaired basal keratinocytes differentiation, which suggests that the ablation of Δ6-10E-cadherin leads to hyperplasia (Figure 4-13 A-D) and intercellular spaces. However, it was found that the genetic alteration did not affect the kinetics of papillomatogenesis, as tumours still appeared over an 8–10-week period, similar to those in the controls (Figure 4-13 E&F). Although E-cadherin loss in *HK1.ras-K14creP/Δ6-10Ecad$^{flx/flx}$* mice did not appear to alter *HK1.ras*-mediated papillomatogenesis kinetics, *HK1.ras-K14creP/Δ6-10E-cad$^{flx/flx}$* mice had more intercellular spaces at the basal layer (Figure 4-13 B&D (arrows)), suggesting that failure in cell-cell adhesion is an early event. Consequently, this facilitated the earlier onset and further progression towards pdSCC (see below).

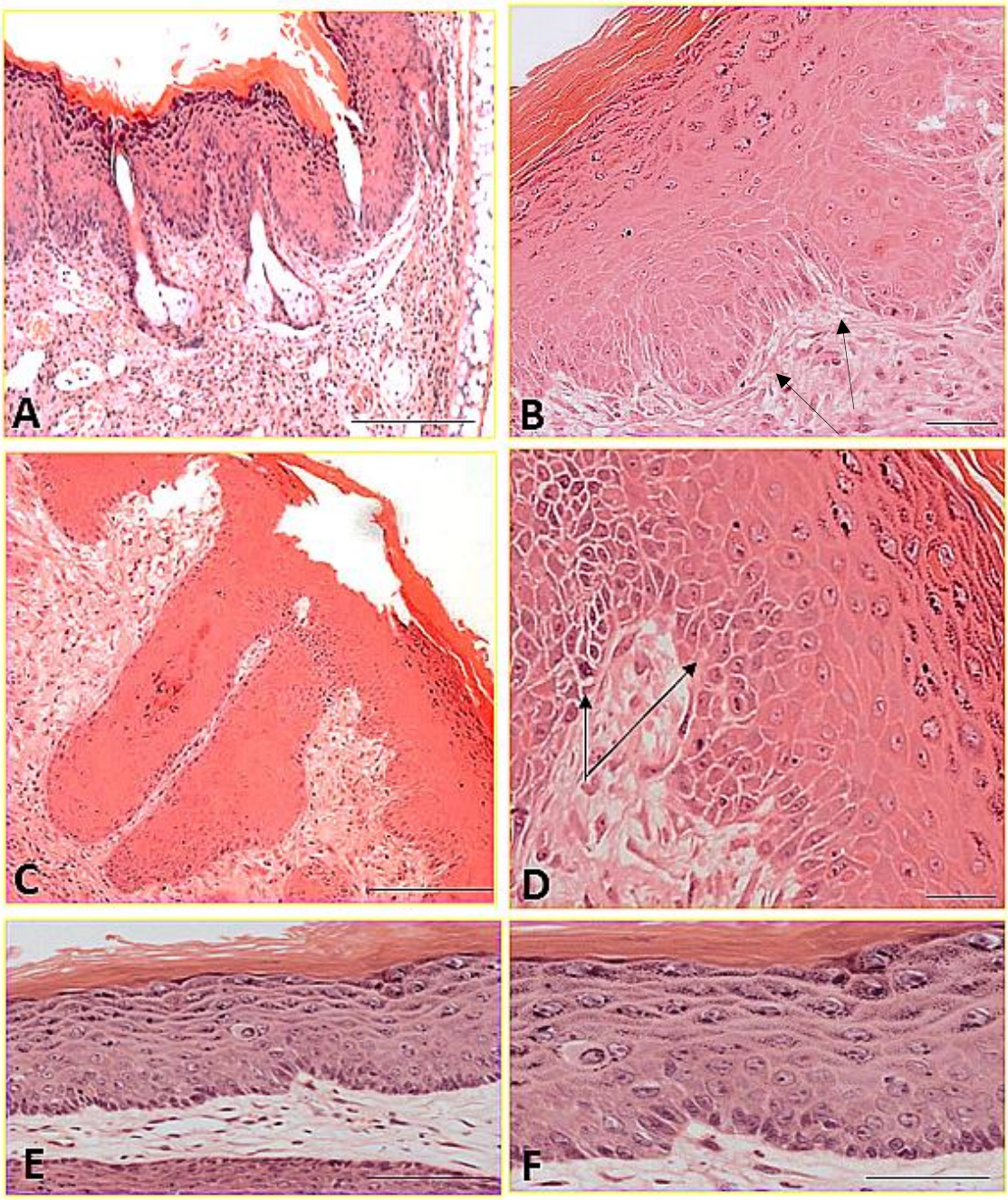

Figure 4-13 Histopathology of RU486-treated *HK1.ras-K14creP/Δ6-10Ecad$^{flx/flx}$* hyperplasia and papilloma over 8-10 weeks (A) RU486-treated *HK1.ras.K14creP/Δ6-10Ecad$^{flx/flx}$* mice display increased hyperplasia. (B) A higher magnification shows intracellular gaps in the basal layers (arrows). (C&D) Low and high magnification images of RU486-treated *HK1.ras.K14creP/Δ6-10Ecad$^{flx/flx}$* papilloma, respectively. At higher magnification (D), intercellular gaps are more obvious (arrows). (E&F) Low and high magnification images of *HK1.ras* control, panel E, are previously presented in (Figure 3-3 A & Figure 3-9 A) and are included here for comparison reference. (Scale bar: A, C&E: 100μm; B, D&F: 50μm).

At 10–12-weeks, some regions within the RU486-treated *HK1.ras-K14creP/Δ6-10Ecad*$^{flx/flx}$ papillomas (Figure 4-14 A) showed signs of conversion into wdSCC (Figure 4-14 B). This gradual conversion exhibited mitotic figures, particularly in areas where the basal layers had extensive intercellular spaces (Figure 4-14 C). These changes were more pronounced in the homozygous model (Figure 4-14 C), which displays a wdSCC, compared to the heterozygous models (Figure 4-14 D&E), where only carcinoma *in situ* and limited early-stage wdSCC were observed. These observations suggest a direct correlation between the disrupted cell-cell adhesion and early malignant conversion, highlighting the importance of early cellular changes in driving tumour progression, with the loss of E-cadherin-mediated adhesion playing a pivotal role in the development of wdSCC.

By 12-14 weeks, further malignant progression was observed, with the subsequent SCCs showing rapid progression to aggressive SCC (pdSCC) (Figure 4-15). This progression was characterised by a distinctive pattern of invasion. Initially, SCC invaded collectively, with clusters of cells grouping together to invade the surrounding stroma (Figure 4-15 A-C). However, as the malignancy advanced, the invasion progressed into an individual cell invasion pattern (Figure 4-15 D-F) and this transition was evidenced by IF analysis (see below). This suggests activation of signalling pathways that influence this mode of invasion. Studies have illustrated that E-cadherin loss plays a crucial role in the malignant conversion and individual invasion of pdSCC (Hesse et al., 2016). In aggressive cancer cells, the downregulation or complete loss of E-cadherin leads to disruption of cell-cell adhesion, enabling the tumour cells to detach and acquire invasive properties (Kang et al., 2017; Strumane et al., 2006).

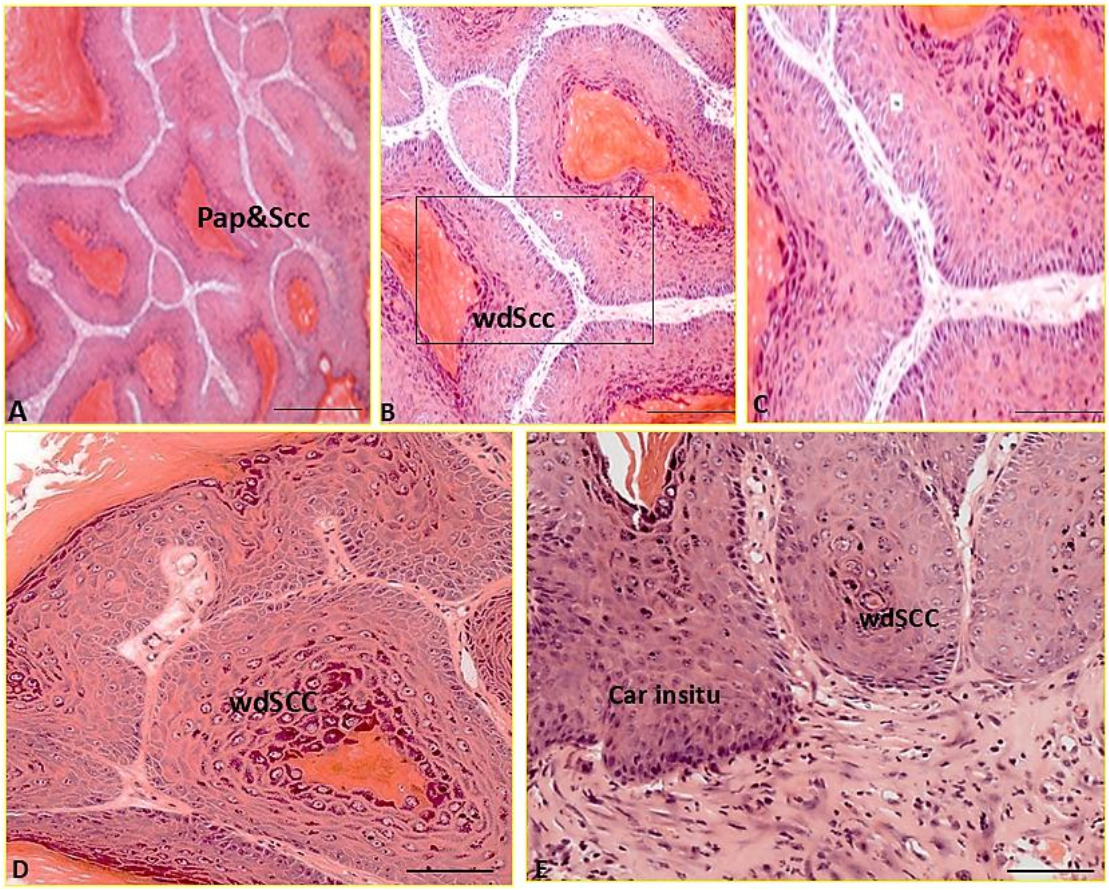

Figure 4-14 Histopathology of *HK1.ras-K14creP/Δ6-10Ecad*$^{flx/flx}$ papilloma &wdSCC at 10-12 weeks (A) Shows low magnification of RU486-treated *HK1.ras-K14creP/Δ6-10Ecad*$^{flx/flx}$ papilloma already exhibits intercellular spaces in the basal layers, suggesting a failure in cell-cell adhesion is an early event leading to areas of (B) wdSCC conversion (box). (C) High magnification of the boxed area in B confirms conversion to wdSCC. (D&E) At this time, RU486-treated *HK1.ras-K14creP/Δ6-10Ecad*$^{flx/het}$ tumours show restricted areas of early wdSCC and mainly carcinoma *in situ*. (Scale bars: A: 100μm; B: 75μm; C: 50μm; D: 75μm; E: 50μm).

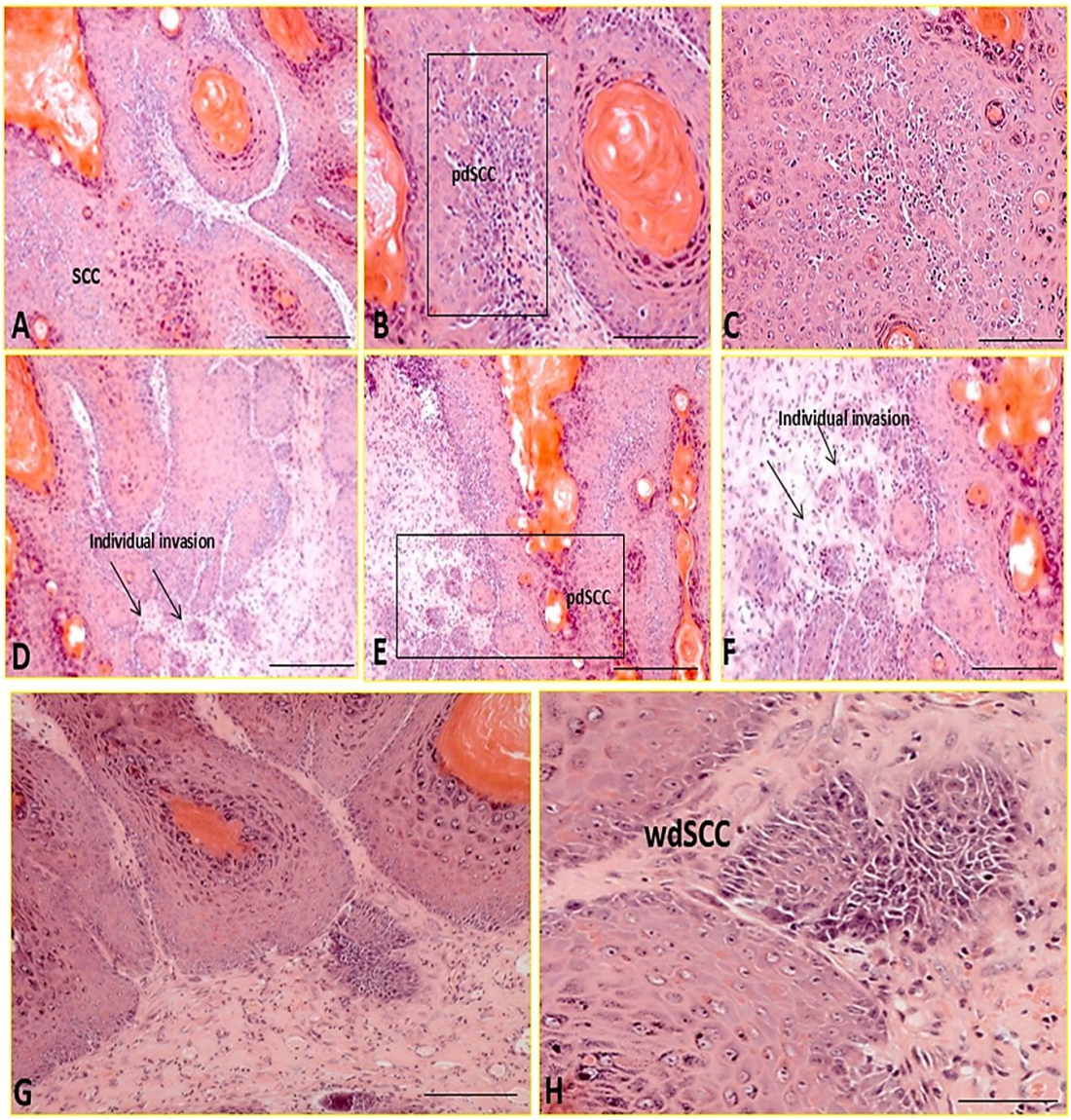

Figure 4-15 Histopathology of RU486-treated *HK1.ras-K14creP/Δ6-10Ecad*$^{flx/flx}$ SCC progression at 12-14 weeks (A-C) show different magnifications of RU486-treated *HK1.ras-K14creP/Δ6-10Ecad*$^{flx/flx}$ SCC/pdSCC that initially invade in a collective group mode, but then, in (D-F), the malignancy progresses into pdSCC with an individual mode of invasion, giving rise to islands of pdSCC (arrows). (G&H). RU486-treated *HK1.ras-K14creP/Δ6-10Ecad*$^{flx/het}$ that shows an early wdSCC nest that invades in collective group mode. (Scale bars: A: 100μm; B: 75μm; C: 50μm; D: 100μm; E: 75μm; F: 50μm; G: 75μm; H: 50μm).

4.3.1 Analysis of K1 expression in RU486-treated *HK1.ras-K14creP/Δ6-10Ecad$^{flx/flx}$* tumour progression

In the *HK1.ras-K14creP/Δ6-10Ecad$^{flx/flx}$* model, IF analysis revealed that the expression of K1 underwent changes that confirmed the histotype analysis over time (see above), reflecting the evolving nature of tumour cells. Initially, K1 expression was prominent in papilloma areas (Figure 4-16 A (arrows)) but began to decrease as the lesion progressed towards wdSCC (Figure 4-16 A-C). This reduction continued rapidly along with progression to pdSCC, where K1 expression was eventually lost (Figure 4-16 E-H). Interestingly, in regions where a collective mode of invasion was observed, K1 expression remained detectable within the invading tumour clusters (Figure 4-16 D). In contrast, in SCC/pdSCC areas, K1 was negative in the stroma, where individual invading cells, identified by their positive K14 expression, were observed (Figure 4-16 E&H). This pattern suggests that K1 downregulation is associated with more aggressive, individual cell invasion, while its retention in clusters may indicate a less aggressive, collective invasion mode. These findings highlight the importance of K1 expression in maintaining epithelial integrity in this model.

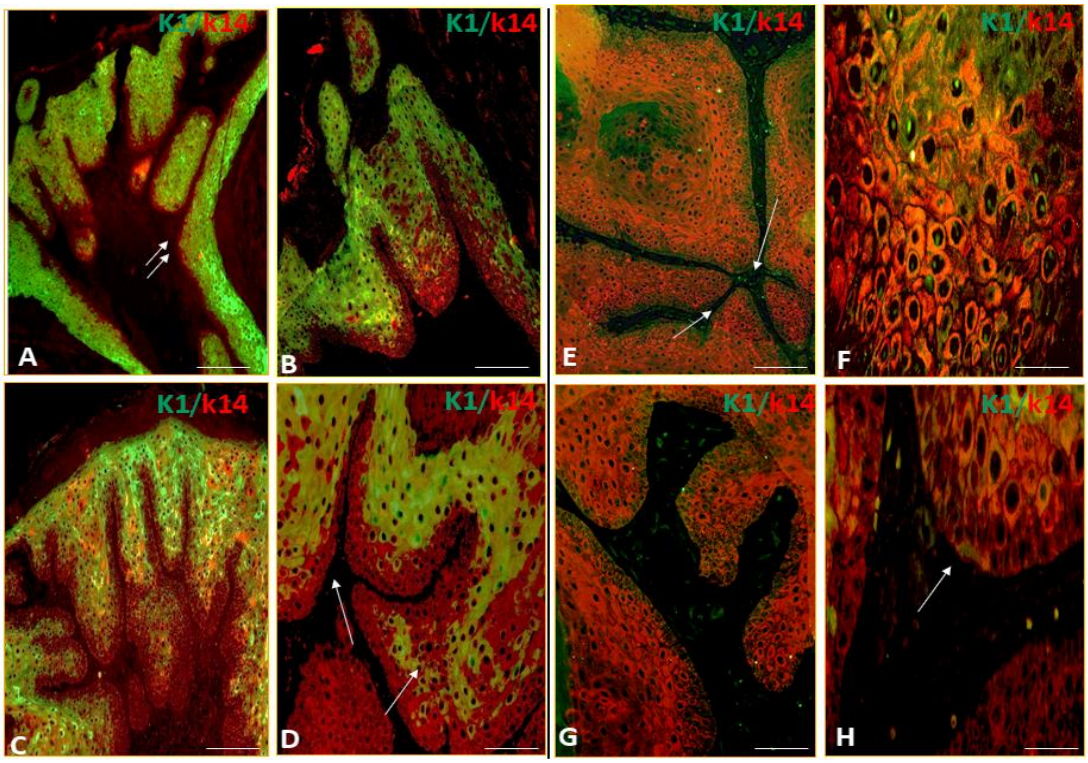

Figure 4-16 Analysis of K1 expression in RU486-treated *HK1.ras-K14creP/∆6-10Ecad$^{flx/flx}$* tumour progression (A-D) Show different magnifications of K1 expression in wdSCC with residual papilloma, which is initially strong in (A) papilloma area (arrows), but gradually reduces as the tumour progresses to (B&C) wdSCC, where (D) shows evidence of a focal K1 negative/K14-positive cell accumulation (arrows). (E-H) K1 expression is lost in SCC progression to pdSCC, where K1 expression is completely faded. (G&H) Show low and high-magnification images of regions of K14-positive cell clusters, potentially indicative of early individual-mode invasion (arrow). (Scale bars: A-C: 100µm; D-H: 50µm).

4.3.2 Analysis of truncated ∆6-10E-cadherin expression in RU486-treated *HK1.ras-K14creP/Δ6-10Ecad$^{flx/flx}$*

The analysis of truncated Δ6-10E-cadherin expression was conducted in the RU486-treated *HK1.ras-K14creP/Δ6-10Ecad$^{flx/flx}$* model. Typical expected results were observed in both experimental and control groups during initial papilloma formation, where Δ6-10E-cadherin expression remained suprabasal (Figure 4-17 A-C). However, an unexpected finding was made in the RU486-treated *HK1.ras-K14creP/Δ6-10Ecad$^{flx/flx}$* model. As papillomas progressed, basal Δ6-10E-cadherin expression was detected (Figure 4-17 D&E), suggesting an attempt to compensate for cell-cell disruption. This led to the development of wdSCC, where positive basal expression for truncated Δ6-10E-cadherin was detected (Figure 4-17 D&E). This expression was attributed to the epitope of the antibody being located outside the deleted

region, specifically binding to an epitope in exon 5. As a result, new insights into the signalling regulation of E-cadherin were gained, suggesting that signalling to E-cadherin persists during this stage; however, the mutant protein is non-functional, leading to malignant conversion. The subsequent figure shows reduced Δ6-10E-cadherin expression (Figure 4-18), indicating disruption of this protective mechanism. In SCC and pdSCC, Δ6-10E-cadherin expression disappeared (Figure 4-18), suggesting that the signalling to E-cadherin no longer existed, contributing further to tumour progression.

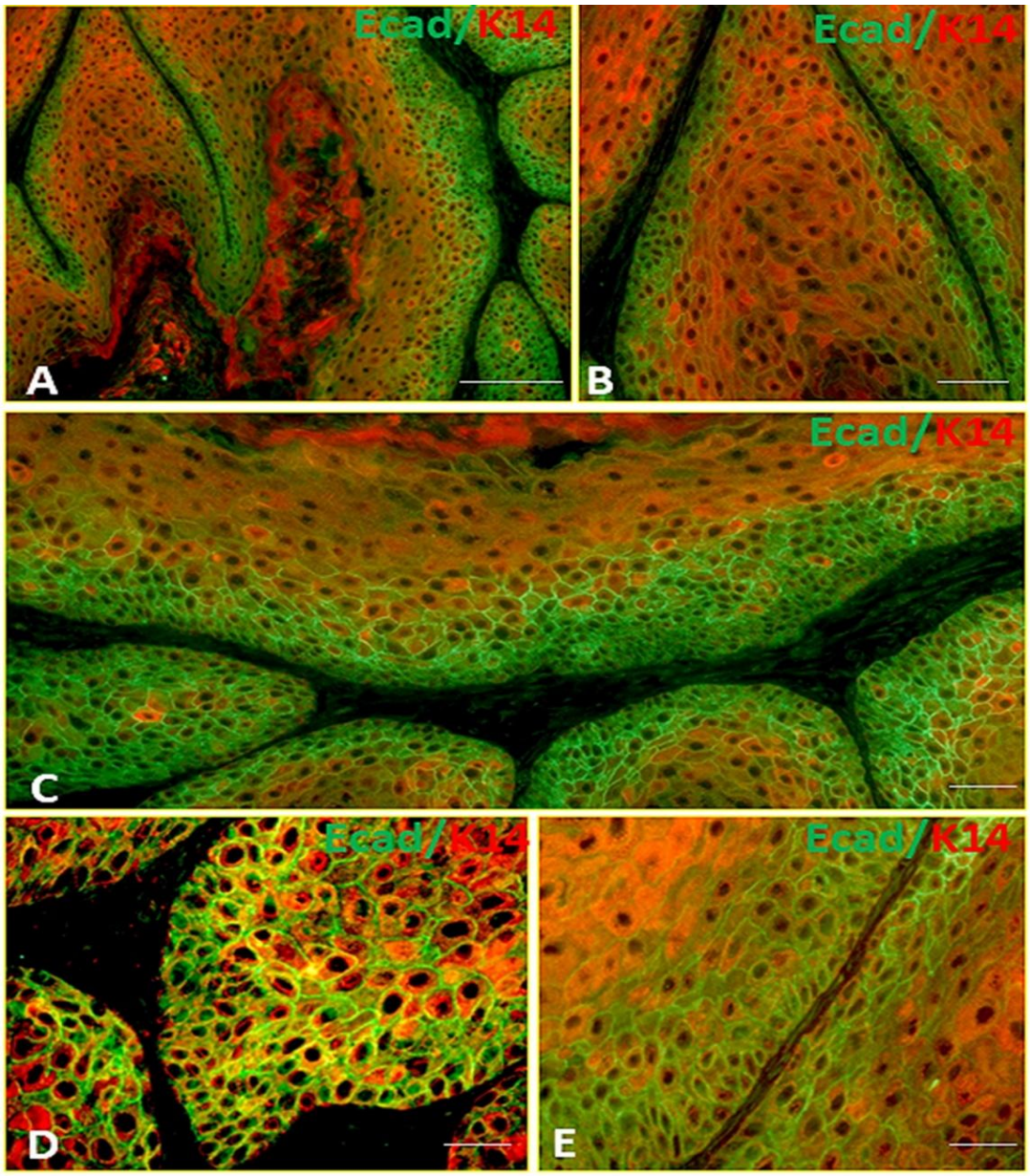

Figure 4-17 Analysis of truncated E-cadherin expression in RU486-treated *HK1.ras-K14creP/Δ6-10Ecad*$^{flx/flx}$ papilloma progression and conversion at 10-12 weeks (A-C) show different magnifications of Δ6-10E-cadherin expression in RU486-treated *HK1.ras-K14creP/Δ6-10Ecad*$^{flx/flx}$, and suprabasal expression gradually becomes basal as the papilloma progresses into (D & E) wdSCC, where basal Δ6-10E-cadherin expression is detected. (Scale bars: A: 100μm; B: 75μm; C: 50μm; D: 75μm; E: 50μm).

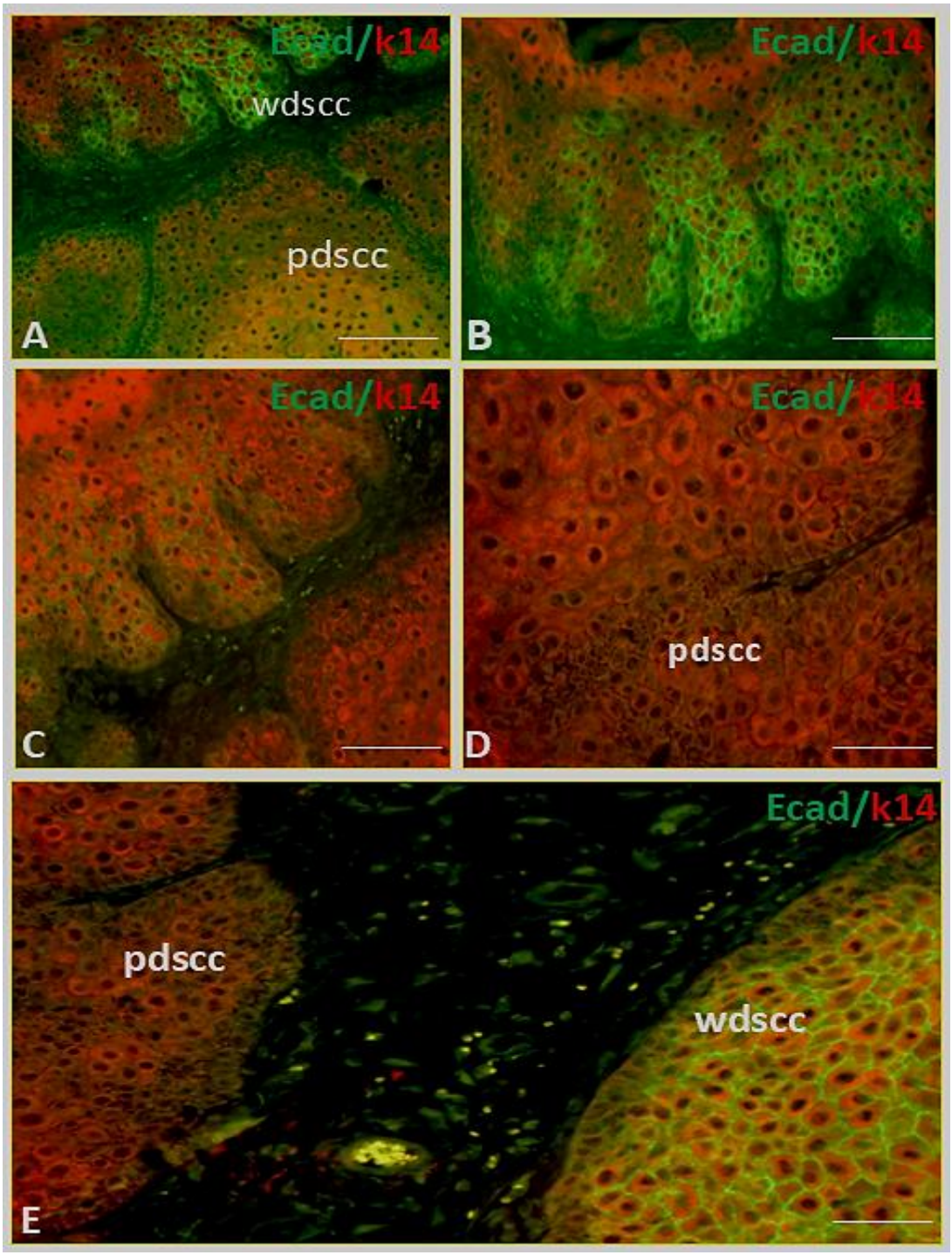

Figure 4-18 Analysis of truncated E-cadherin expression in RU486-treated *HK1.ras-K14creP/Δ6-10Ecad$^{flx/flx}$* SCC progression at 12-14 weeks (A&B) Δ6-10E-cadherin expression is detected in wdSCC areas, but the expression is gradually reduced along with increasing intercellular spaces as these wdSCC begin to progress. (C&D) Δ6-10E-cadherin expression is lost during the progression into aggressive SCC (pdSCC). Thus, on progression, non-functional Δ6-10E-cadherin protein is lost, suggesting that compensatory signalling to E-cadherin has failed. (E) Shows that Δ6-10E-cadherin expression is reduced in pdSCC areas compared to wdSCC areas, reflecting loss of cell-cell adhesion during progression. (Scale bars: A&C: 75μm; B, D&E: 50μm).

This unexpected Δ6-10E-cadherin expression was explored further by IHC. The expression of Δ6-10E-cadherin in *HK1.ras-K14creP/Δ6-10Ecad*$^{flx/flx}$ was assessed to determine the impact of altered E-cadherin expression on the development and progression of SCC, and to visually assess the localisation and abundance of Δ6-10E-cadherin expression. Any changes in the expression indicate potential disruptions in cell-cell adhesion, promoting skin SCC progression through impaired epithelial integrity and induction of EMT-related β-catenin signalling.

The results found that Δ6-10E-cadherin expression was predominantly suprabasal and membranous in papillomas, as shown in Figure 4-19 A&B. This pattern suggests that Δ6-10E-cadherin plays a role in maintaining cell-cell adhesion in early stages of tumour development. However, as the tumour progressed to wdSCC, the expression became basal (Figure 4-19 C), indicating a shift in the localisation of the protein. This basal expression suggests dysregulation of cell-cell adhesion and driving progression towards a more aggressive SCC, in which Δ6-10E-cadherin expression was reduced (Figure 4-19 D&E). Eventually, in pdSCC, Δ6-10E-cadherin expression was completely lost (Figure 4-19 F&G). This loss of expression suggests that the signalling to E-cadherin had ceased, further contributing to the progression into pdSCC.

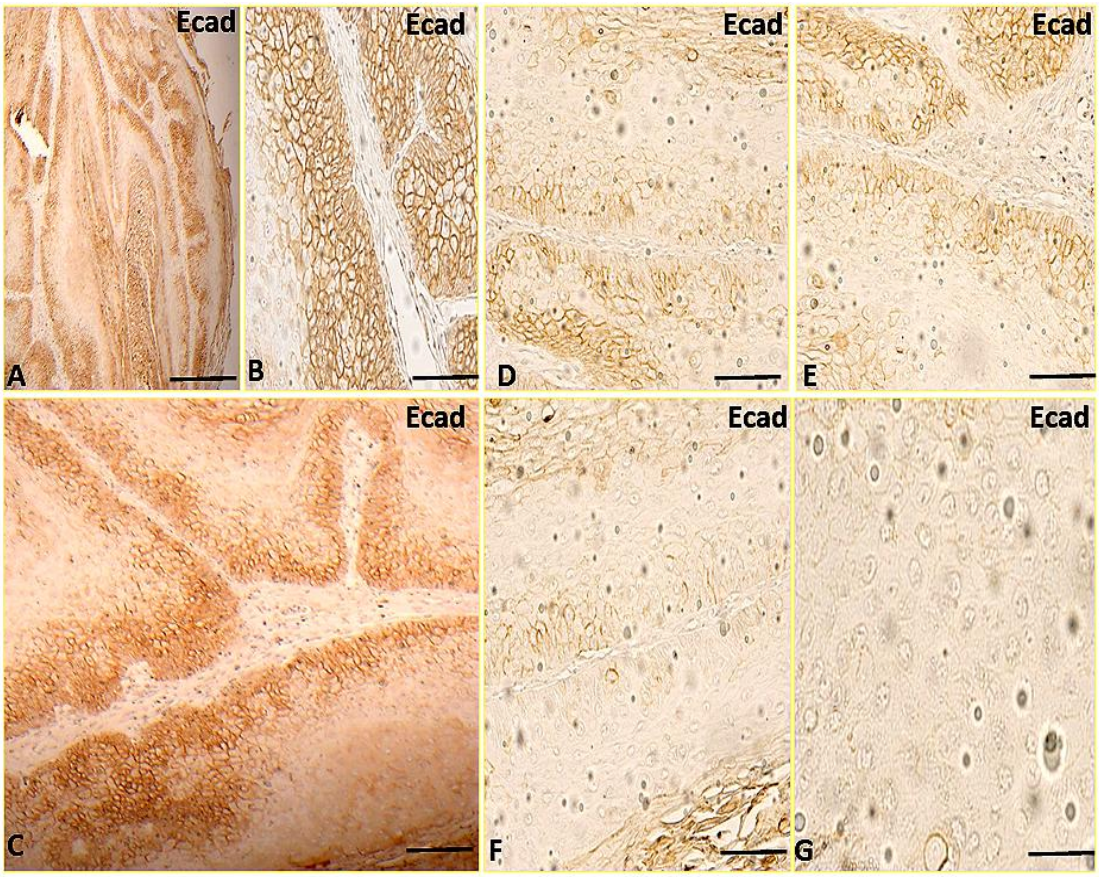

Figure 4-19 IHC analysis of truncated E-cadherin expression in RU486-treated *HK1.ras.K14creP/Δ6-10Ecad*$^{flx/flx}$ papilloma and carcinoma (A&B) low and high magnification images, respectively, of RU486-treated *HK1.ras.K14creP/Δ6-10Ecad*$^{flx/flx}$ papilloma show membranous suprabasal Δ6-10E-cadherin expression, but the expression becomes basal in some areas as the tumour progresses to (C) wdSCC. Whereas, in (D&E), Δ6-10E-cadherin expression is reduced in malignant progression to SCC, and (F&G) show pdSCC areas where the Δ6-10E-cadherin expression is almost lost. (Scale bars: A&B: 100μm; C: 75μm; D-G: 50μm).

4.3.3 Analysis of p53 expression in RU486-treated *HK1.ras-K14creP/Δ6-10Ecad*$^{flx/flx}$ tumour progression

The assessment of p53 expression was conducted using IHC in *HK1.ras-K14creP/Δ6-10E-cad*$^{flx/flx}$ models to evaluate its role during different stages of tumorigenesis. In papillomas, p53 expression was prominent, with nuclear localisation observed throughout the epidermal layers (Figure 4-20 A&B). This widespread nuclear p53 expression suggested a potential conversion to wdSCC. As these tumours progressed towards wdSCC, a gradual reduction in suprabasal p53 expression was observed, and loss was observed in many areas of the basal keratinocytes (Figure 4-20 C&D), indicating a shift in the molecular landscape associated with tumour differentiation. In pdSCC, p53

expression was noticeably reduced, with only occasional sporadic positive cells, correlating with the increased aggressiveness and loss of cellular control mechanisms in these advanced lesions (Figure 4-20 E&F).

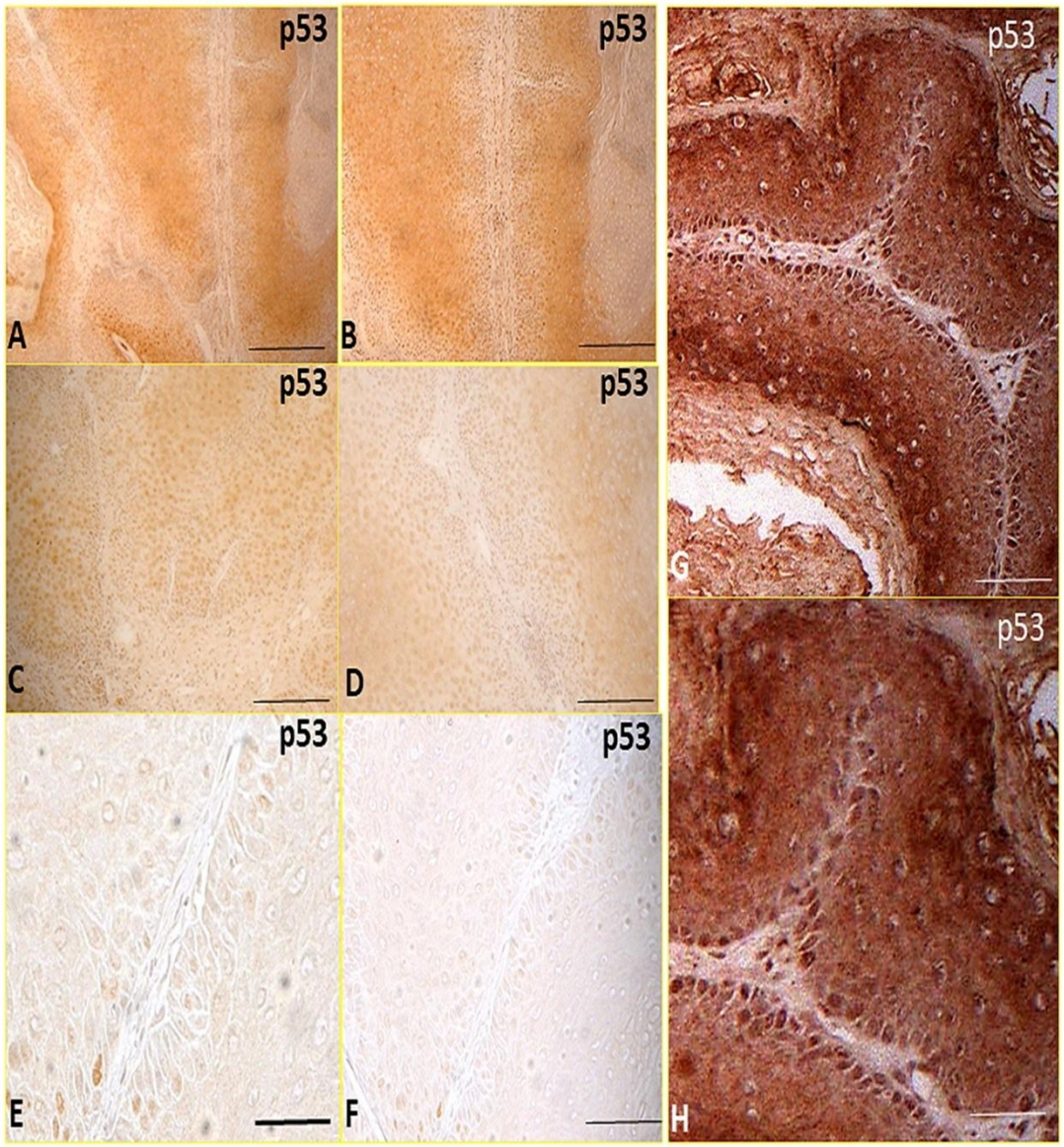

Figure 4-20 Analysis of p53 expression in RU486-treated *HK1.ras-K14creP/Δ6-10Ecad*$^{flx/flx}$ papilloma and carcinoma (A&B) RU486-treated *HK1.ras-K14creP/Δ6-10Ecad*$^{flx/flx}$ papilloma show high p53 expression in all epidermal layers. (C) Shows converting papilloma where p53 is still expressed. (D) In wdSCC, p53 expression persists in the suprabasal layers, the basal and nuclear expression is reduced and lost in many strands of basal keratinocytes. (E) SCC progression and (F) pdSCCs show marked reduction of p53 expression, with only occasional sporadic p53-positive cells visible. (G&H) Show *HK1.ras* benign papilloma exhibits strong and uniform p53 expression throughout the epidermal layers, but is particularly strong in the basal nuclei, although the staining appears overstained. (Scale bars: A&B: 100μm; C-F: 50μm; G: 75μm; H: 50μm).

4.3.4 Analysis of β-catenin expression in RU486-treated *HK1.ras-K14creP/Δ6-10Ecad$^{flx/flx}$* tumour progression

In the context of the RU486-treated *HK1.ras-K14creP/Δ6-10Ecad$^{flx/flx}$* tumour progression model, the status of ß-catenin, whether it remained membranous or shifted to a nuclear location, may indicate the degree of malignancy and disruption of cellular adhesion.

In benign papillomas, the more sensitive IHC analysis showed basal layer ß-catenin was primarily membranous (Figure 4-21 A&B; Figure 4-23 A&B), reflecting intact E-cadherin-mediated adhesion. As tumours progressed to wdSCC, ß-catenin was observed to become less membranous in basal layers (Figure 4-21 C&D) in comparison to papilloma to wdSCC (Figure 4-23 C&D (arrows)), and remained low in the nucleus (Figure 4-23 C&D), suggesting a breakdown in cell adhesion was associated with conversion.

This trend became more obvious in SCC progression, where ß-catenin expression became obviously less membranous and more nuclear (Figure 4-23 E&F), consistent with the role of deregulated ß-catenin in gene transcription, which is often associated with tumour proliferation, which may drive a more aggressive and invasive SCC behaviour. The reduction in membranous ß-catenin suggests a failure in the E-cadherin/ß-catenin interaction, leading to reduced cell-cell adhesion.

This suggests that ß-catenin dysregulation may play a crucial role in the progression and development of SCC. The observed loss of E-cadherin points to disrupted cell adhesion, which likely impacts ß-catenin signalling. Early tumour invasion may occur through collective cell movement, but as E-cadherin loss progresses, cells may adopt a more aggressive, individual mode of invasion. In advanced SCC, this ß-catenin regulation is linked to increased cell proliferation and invasion.

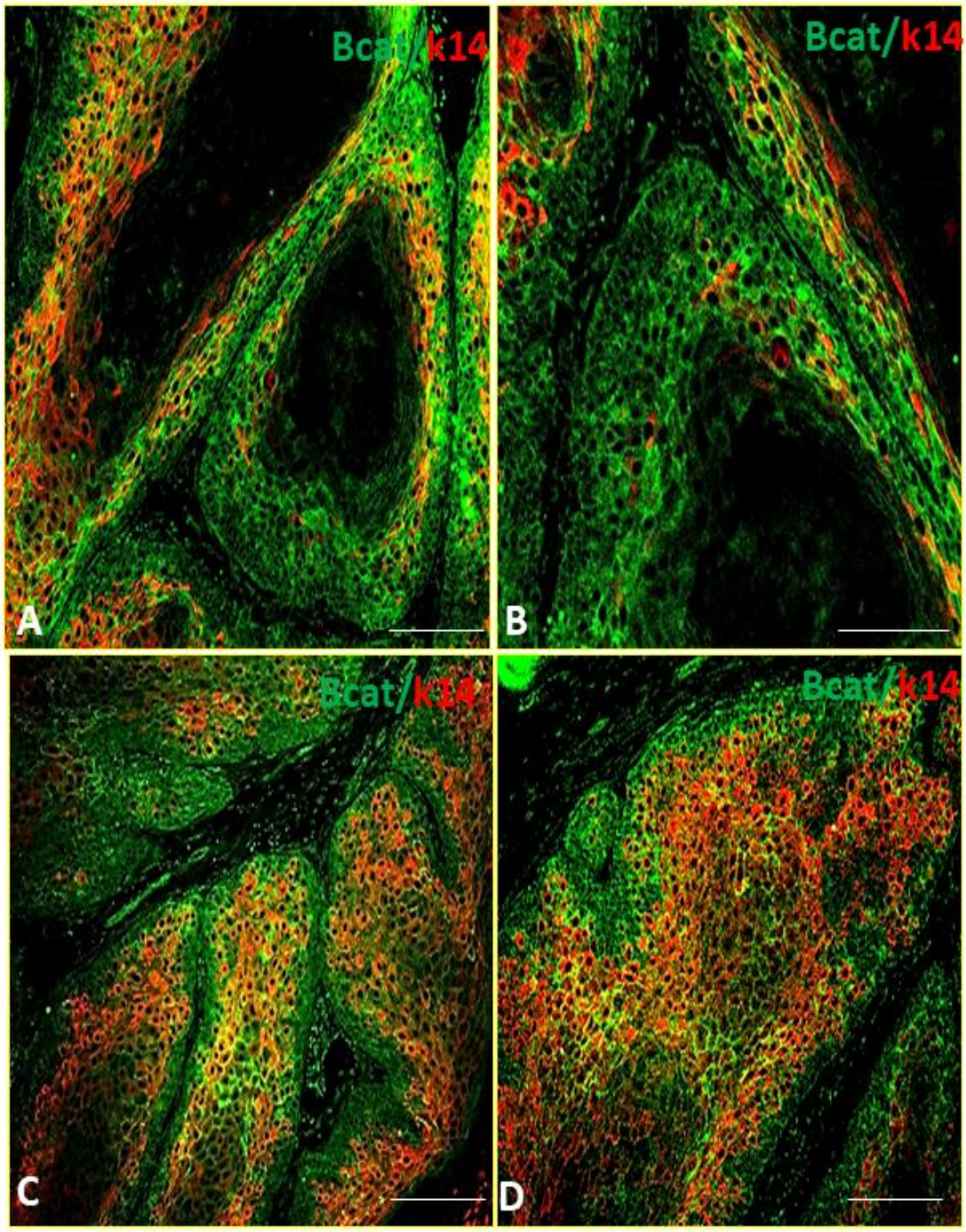

Figure 4-21 Analysis of β-catenin expression in RU486-treated *HK1.ras-K14creP/Δ6-10Ecad$^{flx/flx}$* papilloma and wdSCC (A&B) Show β-catenin expression is membranous and suprabasal in papilloma and less suprabasal in (C&D) wdSCC areas. (Scale bars: A&C: 100μm; B&D: 50μm).

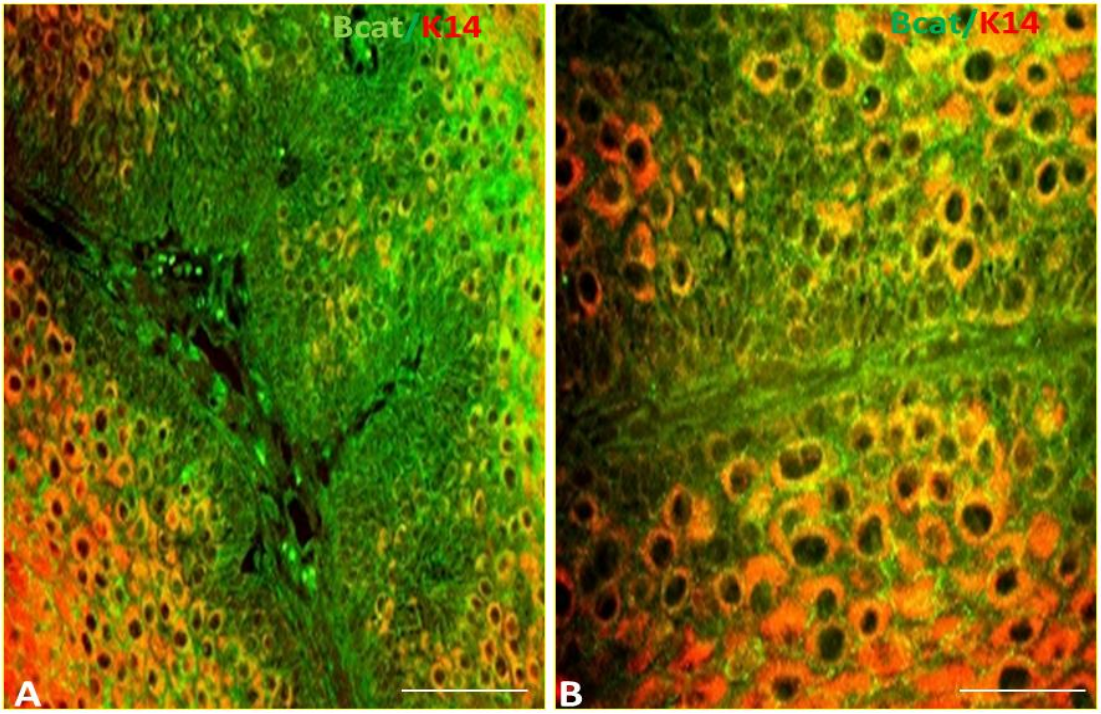

Figure 4-22 Analysis of β-catenin expression in RU486-treated *HK1.ras-K14creP/Δ6-10Ecad*$^{flx/flx}$ SCC progression (A&B) Low and high magnification images of RU486-treated *HK1.ras-K14creP/Δ6-10Ecad*$^{flx/flx}$ SCC that show less membranous β-catenin expression as the tumour progresses to SCC/pdSCC, indicating reduced cell-cell adhesion (Scale bars: A: 75μm; B: 50μm).

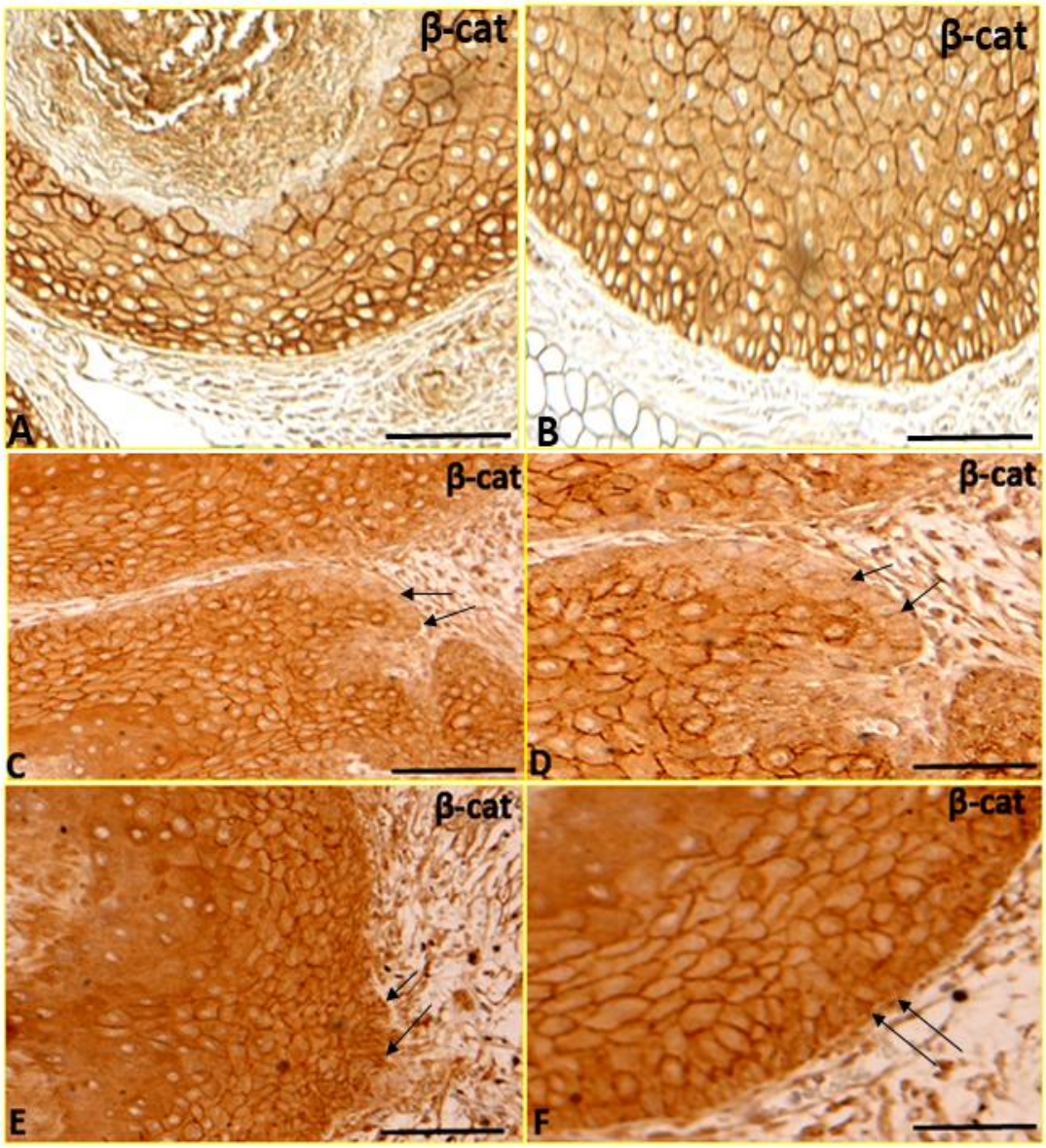

Figure 4-23 IHC analysis of β-catenin expression in RU486-treated *HK1.ras-K14creP/∆6-10E-cad*$^{flx/flx}$ papilloma and carcinoma (A&B) RU486-treated *HK1.ras-K14creP/∆6-10E-cad*$^{flx/flx}$ papilloma shows β-catenin expression in both basal and suprabasal layers, predominantly membranous with occasional nuclear staining. (C&D) In wdSCC, β-catenin expression remains membranous in the upper suprabasal layer, whereas the lower suprabasal and basal layers lack membranous β-catenin expression (arrows), yet with little nuclear expression. While in (E&F), β-catenin expression is becoming more nuclear and less membranous in SCC/pdSCC progression (arrows). (Scale bars: A&B: 100μm; C-F: 50μm).

4.4. Summary

E-cadherin has a pivotal function within the epidermis and is implicated in the governance of hair follicles and as an adhesive component of adherens junctions (Young et al., 2003).

As shown in the results section, the histological analysis of RU486-treated *K14creP/Δ6-10E-cad*$^{flx/flx}$ skin revealed a phenotype with noticeably sparse fur along the back. In the *HK1.ras-K14creP/Δ6-10Ecad*$^{flx/het}$ model, while the remaining E-cadherin was sufficient to maintain normal differentiation, it failed to protect against malignant transformation in cooperation with ras. This insufficiency led to the development of more aggressive tumours, indicating that even partial loss of E-cadherin in the presence of ras activation is inadequate to prevent malignancy.

This finding was consistent with the histological results, which revealed mild hyperplasia characterised by an increased number of basal cell layer keratinocytes and a lack of differentiation. The RU486-treated *K14creP/Δ6-10Ecad*$^{flx/flx}$ genotype exhibited altered hair follicle physiology, with incomplete HFs and follicular hyperplasia, compared to normal *E-cadherin* floxed mice, which lacked either creP or RU486. The hair follicle changes observed could be due to disruptions in ß-catenin signalling, which is consistent with its role in epithelial cell adhesion and tumorigenesis (Watt & Collins, 2008).

It was anticipated that conditional E-cadherin ablation in cooperation with ras activation would potentially change the hyperplasia pattern, accelerate tumour progression, and conversion. In heterozygous mice, the reduced expression of E-cadherin in *HK1.ras-K14creP/Δ6-10Ecad*$^{flx/het}$ tumours led to the development of papillomas, similar to those observed in the *HK1.ras* genotype. However, these tumours exhibited noticeable intercellular gaps in the basal keratinocytes, indicating that a failure in cell-cell adhesion is an early event. Consequently, these tumours progressed to carcinoma *in situ* and eventually to early-stage malignant wdSCC. This progression underscores the critical role of the normal functional allele of E-cadherin present in *HK1.ras-K14creP/Δ6-10Ecad*$^{flx/het}$ model, which is essential for maintaining cellular adhesion and preventing further tumour progression.

In ß-catenin and E-cadherin expression analysis across *HK1.ras-K14creP/Δ6-10Ecad*$^{flx/het}$ tumorigenesis model, distinct patterns were observed. In papillomas, ß-catenin was located at the cell membrane, reflecting stable cellular adhesion, while E-cadherin was strongly expressed, maintaining epithelial integrity. In wdSCC, ß-catenin expression was less membranous with sporadic expression in the basal keratinocytes, but E-cadherin expression was reduced, emphasising the breakdown of cell-cell adhesion.

The early differentiation marker K1 shows a disrupted, irregular pattern in *HK1.ras-K14creP/Δ6-10E-cad*$^{flx/het}$ papillomas compared to equivalent control *HK1.ras* papillomas, possibly due to opposing proliferative signals from E-cadherin/Wnt and ß-catenin deregulation (Chakraborty et al., 2010; Di Cunto et al., 1998; Topley et al., 1999).

These data suggest that reduced functional E-cadherin in heterozygous *HK1.ras-K14creP/Δ6-10E-cad*$^{flx/het}$ papillomas correlates with malignant conversion to carcinoma in situ and early-stage wdSCC that collectively invade the surroundings, but does not appear to contribute to papillomatogenesis, as detailed in the histological and marker expression analysis.

The role of E-cadherin loss in HK1.ras-K*14creP/Δ6-10E-cad*$^{flx/flx}$ transgenic mice carcinogenesis was investigated. It was found that the genetic alterations have no effect on papillomatogenesis. Despite the loss of E-cadherin in *HK1.ras-K14creP/Δ6-10E-cad*$^{flx/flx}$ mice, there was no apparent change in *HK1.ras*-mediated papillomatogenesis. However, malignant conversion occurred earlier and was more aggressive than in the *HK1.ras-K14creP/Δ6-10E-cad*$^{flx/het}$ model. As wdSCCs rapidly progress to aggressive SCC, detailed histological analysis and examination of marker expression revealed a shift in the mode of invasion. Initially, wdSCC exhibited a collective mode of invasion; however, as the tumours advanced to aggressive SCC, the invasion pattern transitioned to an individual mode (Figure 4-16 & Figure 4-17), which suggests involvement of signalling pathways that influence invasion. This is consistent with a previous study that showed the loss of E-cadherin plays a vital role in the malignant conversion and individual invasion of pdSCC in human skin and lymph nodes (Hesse et al., 2016).

The expression of E-cadherin and ß-catenin was investigated to identify any potential changes in cell-cell adhesion in the *HK1.ras-K14creP/Δ6-10E-cad*$^{flx/flx}$ skin model. Δ6-10E-cadherin expression was detected in late-stage papillomas and became basal as the papilloma progressed to wdSCC, where the anti-E-cadherin epitope detected the non-functional Δ6-10E-cadherin. This suggests that failed E-cadherin signalling aids progression. Eventually, Δ6-10E-cadherin expression faded, and the SCC progressed into an aggressive SCC (pdSCC), indicating that the truncated Δ6-10E-cadherin induces conversion and progression.

ß-catenin expression was observed to be membranous in benign papilloma basal layers, with no nuclear localisation. Upon conversion to wdSCC, membranous ß-catenin expression appeared reduced, whereas in pdSCC, ß-catenin became more nuclear in invasive basal cells. This transition from membranous to nuclear localisation highlights the progressive loss of cell-cell adhesion and the corresponding increase in failed transcriptional activity (particularly in p53) associated with tumour progression and invasion. Similarly, ß-catenin expression was observed to be strongly membranous in less aggressive ovarian cancer (Bodnar et al., 2014). Another study reported that ß-catenin is membranous in well-differentiated areas in colorectal carcinoma but becomes nuclear in poorly differentiated cells undergoing invasion.

The results showed that loss of E-cadherin was associated with loss of p53 expression, alongside an increase in nuclear ß-catenin expression in SCC, driving malignant progression to pdSCC. This is consistent with studies using the *HK1.ras.fos-K14creP/Δ5PTEN*$^{flx/flx}$ transgenic mouse model, where p53 loss is observed, which contributes to the malignant progression of SCC (Macdonald et al., 2014; Masre et al., 2020).

Collectively, these data show that conditional ablation of E-cadherin cooperates with ras activation and p53 loss at later stages following the malignant conversion of papillomas with nuclear ß-catenin expression, inducing rapid tumour progression due to cell-cell adhesion failures.

Chapter 5 Effect of inducible E-cadherin loss in *HK1.fos-K14creP/Δ5PTEN$^{flx/flx}$* transgenic mouse skin carcinogenesis

5.1 Introduction

The differential adhesion hypothesis, which attributes the cell sorting phenomena to differentially expressed adhesion molecules, provides a theoretical framework for understanding how cells segregate based on quantitative differences in adhesion strengths (Iijima et al., 2020; Rossbach et al., 2021). This hypothesis underscores the importance of adhesion.

As mentioned previously, E-cadherin expression in *HK1.ras* or *HK1.ras/fos* papillomas appeared suprabasal and membranous, mirroring normal levels (Chapter 3 Figure 3-3). In early-stage *HK1.ras/fos-K14creP/Δ5PTEN$^{flx/flx}$* tumorigenesis (hyperplasia and papillomas), despite additional *HRAS* activation, the basal layer cells still showed detectable E-cadherin expression, and these lesions also exhibited elevated p53 and p21 expression (Macdonald et al., 2014).

However, with time following p53 loss, E-cadherin expression was progressively lost at the invasive front as the tumour progressed to malignancy, thus disturbing cell-cell adhesion and aiding tumour progression and invasion. In the aetiology of *HK1.fos-K14creP/Δ5PTEN$^{flx/flx}$* KAs, the loss of PTEN regulation allowed E-cadherin expression to become strongly basal (Chapter 3 Figure 3-6). This alteration triggered compensatory p53, potentially influencing the progression of KAs by modulating the expression levels of these key regulatory proteins (Chapter 3 Figure 3-5). This compensatory p53 expression diverted the expected papillomatogenesis from *HK1.fos-K14creP/Δ5PTEN$^{flx/flx}$* cooperation into a process of massive differentiation, ultimately contributing to the aetiology of KAs (Chapter 3 Figure 3-7).

Thus, the increased expression of E-cadherin in *HK1.fos-K14creP/Δ5PTEN$^{flx/flx}$* basal layers, with nuclear localisation correlating with activation of p53/p21, played a crucial role, as this strong membranous E-cadherin expression would help facilitate cell-cell adhesion, leading to a KA outcome instead of invasive SCC. This analysis suggested that E-cadherin plays a significant role in the formation of *HK1.fos-K14creP/Δ5PTEN$^{flx/flx}$* KAs and may have cooperated with the loss of PTEN regulation in this process, along with a compensatory increase in p53 expression. Thus, the effects of

E-cadherin loss on *HK1.fos-K14creP/Δ5PTEN$^{flx/flx}$* models were assessed to see if this also happened.

As per the hypothesis in the research aims, the crossbreeding of *K14creP/Δ6-10E-cad$^{flx/flx}$* mice with *HK1.fos* mice (below) were expected to result in accelerated papilloma formation through cooperation with *HK1.ras^{1276}*. This idea was based on genetic factors likely to influence the tumour development process, such as the interaction between E-cadherin, possibly acting as an initiator, and fos as a promoter. For example, fos, a component of the AP1 complex (Saadeddin et al., 2009; Toualbi et al., 2007), and it is a target gene of Wnt signalling, shows increased expression due to ß-catenin accumulation. This elevated fos expression participates in gene regulation and ultimately impacts cellular processes, including proliferation and differentiation (Toualbi et al., 2007).

The interaction between ß-catenin and fos in the context of E-cadherin loss can have significant implications for tumorigenesis and tumour progression. ß-Catenin interacts with E-cadherin, forming a complex that is crucial for cell-cell adhesion and tissue integrity. Dysregulation of this complex, often associated with E-cadherin loss, can lead to aberrant signalling to ß-catenin, impacting downstream pathways such as the Wnt/ß-catenin pathway, PI3K/AKT pathway, and MAPK pathway, which are involved in cell proliferation, differentiation, and migration (Zhu et al., 2001).

The activation of fos can modulate the expression of genes associated with tumorigenesis. The link between fos activation and E-cadherin loss may further exacerbate the disruption of cell-cell adhesion and promote tumour progression. Studies have shown that fos activation can influence the expression of E-cadherin and ß-catenin, potentially altering their functional interactions and contributing to the malignant transformation of cells (Canel et al., 2013).

In the scenario where KA arises due to E-cadherin loss in mice with fos activation and PTEN loss, the involvement of ß-catenin becomes crucial (Gottardi et al., 2001). KAs may progress towards malignancy when E-cadherin loss is coupled with dysregulated ß-catenin signalling. This complex interplay between E-cadherin, ß-catenin, fos, and PTEN can drive the transformation of benign lesions into more aggressive forms, such as SCC, by promoting cell proliferation, invasion, and progression (Li et al., 1998; Zhu

et al., 2001). Thus, the intricate relationship between E-cadherin, ß-catenin, fos, and PTEN highlights the complexity of signalling pathways involved in tumorigenesis.

Dysregulation of these molecules can lead to aberrant cell behaviours, impacting tumour progression and aggressiveness. Understanding the crosstalk between these key players in cancer development is essential for elucidating the mechanisms underlying tumour transformation (Canel et al., 2013; Li et al., 1998; Zhu et al., 2001).

In *HK1.fos-K14creP/Δ5PTEN$^{flx/flx}$/Δ6-10E-cad$^{flx/het}$* mice, E-cadherin loss has minimal early effects as observed in *HK1.ras* carcinogenesis. This was further supported by results elicited in KAs, which were similar to those observed in *HK1.fos-K14creP/Δ5PTEN$^{flx/flx}$*. However, with time due to lack of cell-cell adhesion in *HK1.fos-K14creP/Δ5PTEN$^{flx/flx}$/Δ6-10Ecad$^{flx/flx}$* mice, possibilities of conversion were observed due to changes in differentiation (and K1 expression), with some alteration in proliferation and cell-cell adhesion that led to conversion into wdSCC/SCC with abnormal ß-catenin expression, loss of K1 and nuclear p53 expression. This suggests that the interaction between *Δ5PTEN* and *Δ6-10E-cadherin* mutation drives malignant conversion to wdSCC/SCC, not KA.

5.2 The cooperation of E-cadherin loss and *HK1.fos* in transgenic mouse skin carcinogenesis

The transcriptional factor fos plays a significant role in regulating the proliferation and differentiation of keratinocytes. Proper regulation of fos is essential for controlling the proliferation and differentiation of keratinocytes to prevent tumorigenesis (Liu et al., 2018; Seo et al., 2023; Zanconato et al., 2015). The dysregulation of fos has been linked to skin tumorigenesis (Greenhalgh et al., 1993c; Greenhalgh et al., 1993b), and its role in skin pathology through interactions with other signalling pathways and transcriptional factors (Liu et al., 2018). The interaction between the nuclear transcription factor fos and the regulation of E-cadherin signalling arises from fos being a downstream target of the ras/MAPK pathway. This relationship suggests possible crosstalk between fos and E-cadherin signalling

pathways, an indication that the regulation of fos activity may influence E-cadherin signalling and its downstream effects (Gavert & Ben-Ze'ev, 2007).

The findings from bi-genic E-cadherin/ras experiments emphasise the essential role of promotion (wounding) in conjunction with the fos oncogene in the multistage chemical carcinogenesis model, particularly as fos is a significant effector of chemical promotion by TPA (Schlingemann et al., 2003). This suggests that the interplay between E-cadherin and ras, along with the involvement of the fos oncogene, is crucial in the promotion phase of carcinogenesis, shedding light on the molecular mechanisms underlying tumour development (Schlingemann et al., 2003). However, more pertinent to these studies, the involvement of activated *v-FOS* in promoting papillomatogenesis and autonomous papilloma formation in the HK1 model through cooperation between *v-FOS and v-HRAS* underscores their synergistic effect in driving the development of papillomas, emphasising the significance of these oncogenes in the progression of skin tumours (Greenhalgh et al., 1993c). Interestingly, fos activation alone induces a hyperplastic histotype after prolonged latency and is reliant on a wound-promoting stimulus. This observation underscores the significance of fos activation in driving hyperplasia and highlights the requirement of the wound promotion stimulus for its manifestation (Greenhalgh et al., 1993b). The *HK1.fos* mouse appears indistinguishable from a typical mouse, except for its double mitotic index, as revealed by BRDU labelling. Consequently, accelerated differentiation likely offsets this heightened proliferation, resulting in a normal histotype (Greenhalgh et al., 1993b).

The role of fos in the later events of cancer formation has been demonstrated in the HK1 model, where v-FOS provided a constitutive promotion role for *HK1.ras*, resulting in papilloma formation (Greenhalgh et al., 1993c). Additionally, using a knockout c-FOS mouse infected with v-HRAS, no tumours were produced, (Saez et al., 1995), further highlighting the significance of fos in papilloma formation.

Thus, a study of cooperation between E-cadherin and fos in a transgenic mouse model would be valuable for examining the potential effects of such a combination in tumour formation and keratinocyte differentiation. To investigate this cooperation in tumorigenesis, *K14creP/Δ6-10E-cad*$^{flx/flx}$ mice were crossed with *HK1.fos* mice to produce bi-genic E-cadherin/fos cohorts.

5.2.1 E-cadherin cooperates with fos to elicit hyperplasia.

As subsequent sections will investigate tri-genic *HK1.fos-K14creP/Δ5PTEN$^{flx/flx}$/Δ6-10Ecad$^{flx/flx}$* cooperation studies focusing on the E-cadherin genotype and keratoacanthoma aetiology, these mice were included in the bi-genic study. Consequently, the phenotypes observed in the bi-genic *HK1.fos-K14.creP/Δ6-10Ecad$^{flx/flx}$* mice served as valuable comparison controls. The mice utilised the K14creP regulator (Berton et al., 2000) for Δ6-10E-cadherin expression following RU486 topical treatment. Initially, *HK1.fos* and their aged-matched *HK1.fos-K14creP/Δ6-10E-cad$^{flx/flx}$* mice littermates were treated with RU486 at 5/6weeks of age.

After 12-weeks of treatment with RU486, mice with *HK1.fos-K14creP/Δ6-10Ecad$^{flx/flx}$* and *HK1.fos* genotypes exhibited similar phenotypes (Figure 5-1). Every mouse exhibited scaly, thickened ears, with no signs of tumour formation. This observation echoed the results reported for *HK1.fos* (Greenhalgh et al., 1993b). However, histological analysis of *HK1.fos-K14creP/Δ6-10Ecad$^{flx/flx}$* mice revealed an increased hyperplasia (Figure 5-2 A) with areas of acanthosis (spinous layer) (Figure 5-2 B), and intercellular spaces compared with HK1.fos mice (Figure 5-2 C&D), suggesting the potential effect of E-cadherin loss in suprabasal keratinocytes. This may contribute to epidermal strength and cell-cell adhesion, while also implicating a role for fos in commitment to differentiation (Fisher et al., 1991; Greenhalgh et al., 1993b); (Wheelock & Jensen, 1992).

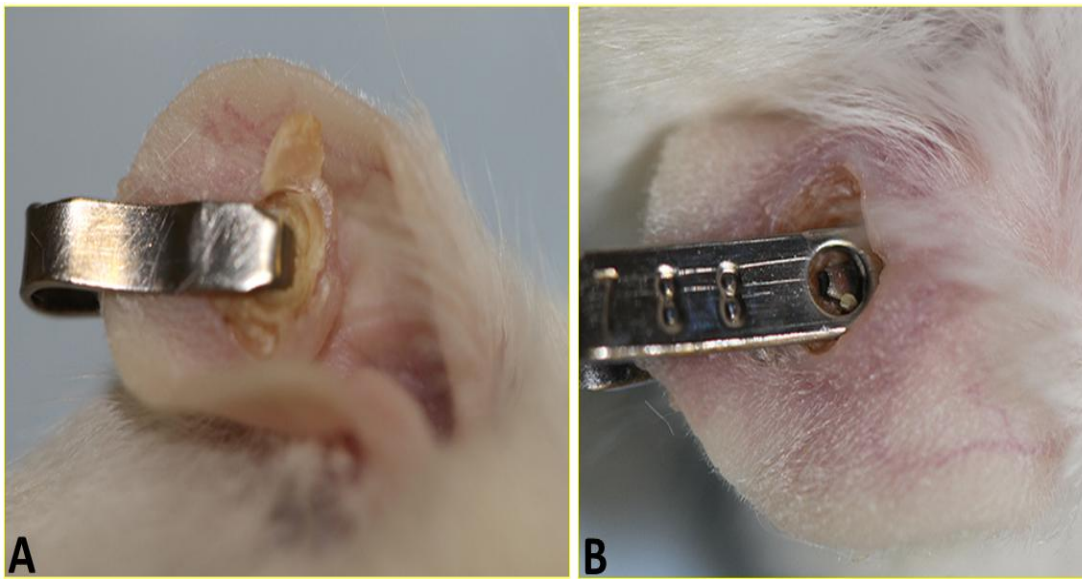

Figure 5-1 Phenotypes of *HK1.fos-K14creP/Δ6-10Ecad*$^{flx/flx}$ and HK1.fos mice at 12 weeks (A) RU486-treated *HK1.fos-K14creP/Δ6-10Ecad*$^{flx/flx}$ mice and (B) RU846-treated *HK1.fos* mice show broadly similar phenotypes, although Panel A exhibits slightly increased keratosis compared to Panel B.

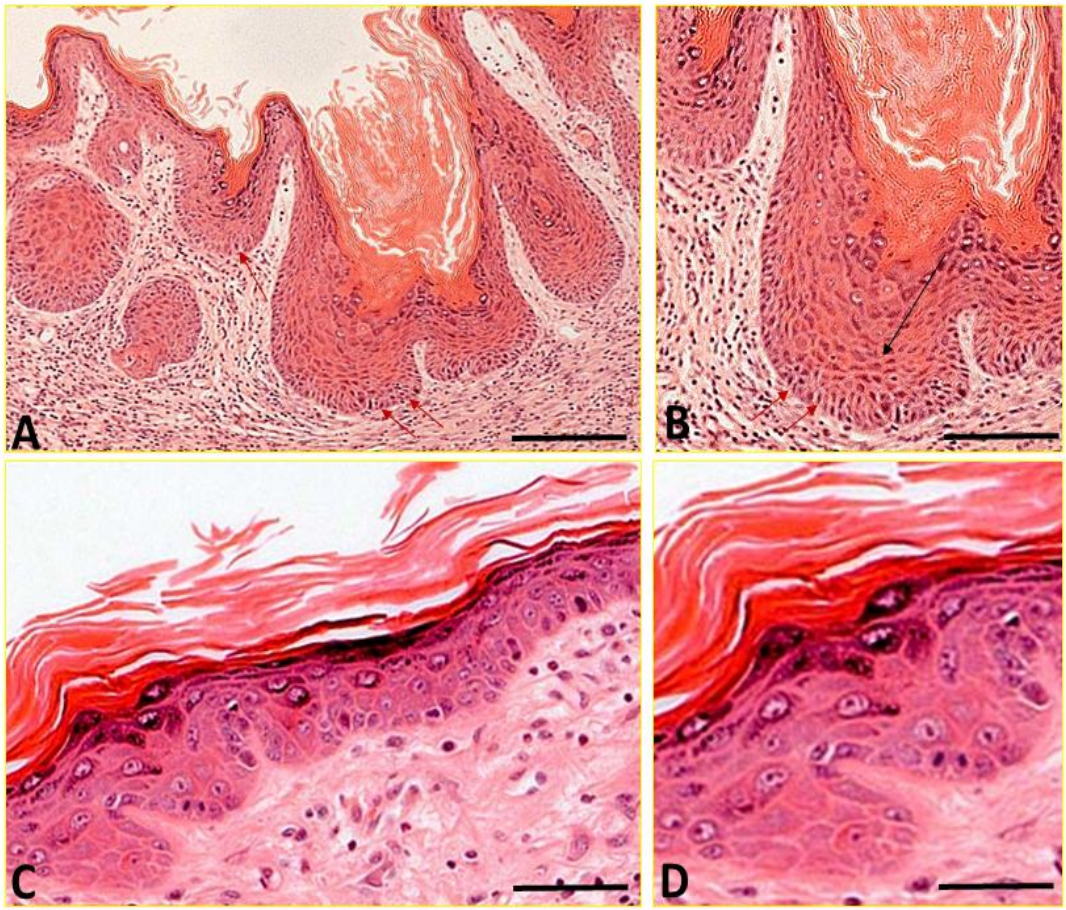

Figure 5-2 The histotype of *HK1.fos-K14creP/Δ6-10Ecad*$^{flx/flx}$ and *HK1.fos* mice at 12 weeks (A) RU486-treated *HK1.fos-K14creP/Δ6-10Ecad*$^{flx/flx}$ mice showed hyperplasia with an increase in keratinocyte proliferation, leading to thicker epidermal layers, and intercellular gaps in the basal keratinocytes (red arrows). (B) A higher magnification of RU486-treated *HK1.fos-K14creP/Δ6-10Ecad*$^{flx/flx}$ mice shows acanthosis (black arrow) and an increased number of cells compared to (C) RU486-treated *HK1.fos* and (D) a higher magnification of RU486-treated *HK1.fos* mice. (Scale bars: A:150μm; B: 100μm; C: 75 μm; D: 50 μm).

The *HK1.fos-K14creP/Δ6-10Ecad*$^{flx/flx}$ genotypes facilitated an investigation into the potential collaboration between E-cadherin and fos deregulation in keratinocyte differentiation, in relation to the observed keratosis. Expression of K1 using double-labelled immunofluorescence was investigated using skin biopsies (Figure **5-3**). The results of the analysis revealed robust K1 expression in both *HK1.fos-K14creP/Δ6-10Ecad*$^{flx/flx}$ and *HK1.fos* hyperplasia in a typical suprabasal pattern.

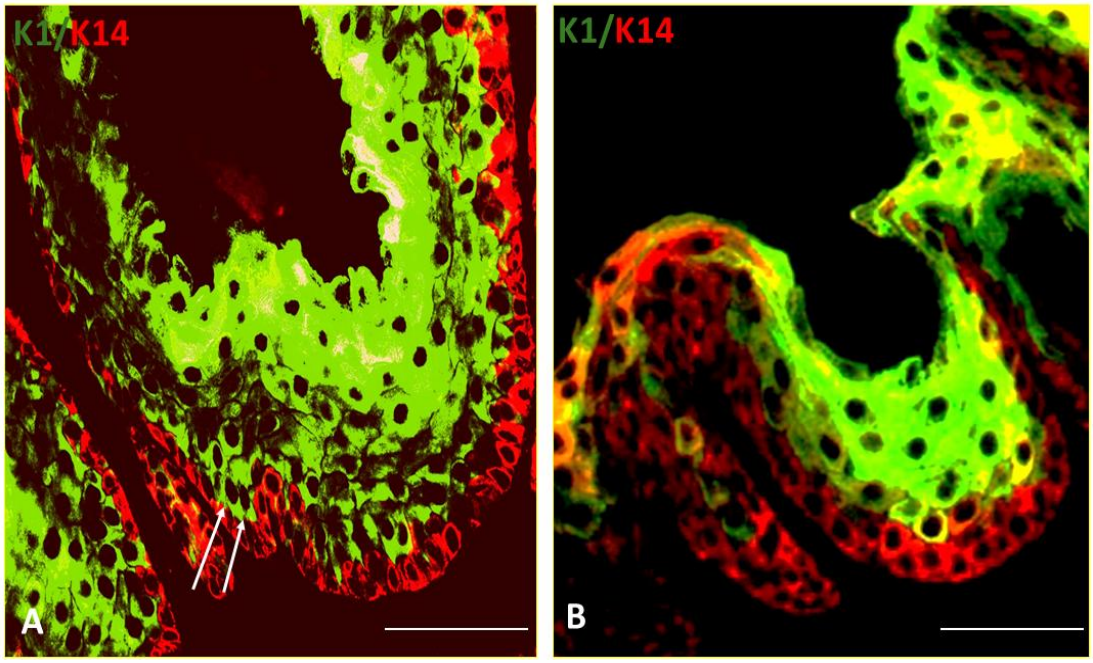

Figure 5-3 K1 expression analysis of RU486-treated *HK1.fos-K14creP/Δ6-10Ecad*$^{flx/flx}$ mice and *HK1.fos* mice at 12 weeks (A) *HK1.fos-K14creP/ Δ6-10Ecad*$^{flx/flx}$ and (B) *HK1.fos* mice hyperplasia show K1 expression in suprabasal layers. The reference standard appears faint due to a low fluorescence signal, yet the relative K1 expression in the samples remains visible. (Scale bars: 100μm).

Collectively, there were no discernible phenotypic variations between bi-genic *HK1.fos-K14creP/Δ6-10Ecad*$^{flx/flx}$ and *HK1.fos* mice, and they did not develop any tumours. Thus, inducible E-cadherin loss in cooperation with fos activation was not sufficient to trigger tumorigenic transformation in keratinocytes. As a result, the subsequent cohort of tri-genic *HK1.fos-K14creP/Δ5PTEN*$^{flx/flx}$*/Δ6-10Ecad*$^{flx/flx}$ mice were established to study the cooperation of E-cadherin with fos and PTEN in keratinocyte differentiation.

5.3 The cooperation of inducible E-cadherin loss in *HK1.fos-K14creP/Δ5PTEN$^{flx/flx}$* mouse skin

As previously mentioned, this study aimed to understand how these signalling pathways interact and influence the function of E-cadherin in skin tumorigenesis within the experimental model. This approach enables a direct comparison of the role of Δ6-10E-cadherin in tumour formation and response mechanisms across different genetic contexts.

These experiments were designed to investigate the effects of E-cadherin loss in the *HK1.fos-K14creP/Δ5PTEN$^{flx/flx}$* model by studying the collaborative effects of PTEN loss (Macdonald et al., 2014; Yao et al., 2008).

E-cadherin loss, in the *HK1.fos-K14creP/Δ5PTEN$^{flx/flx}$* model, can disrupt cell-cell adhesion and enhance motility, as loss of E-cadherin-mediated cell-cell adhesion can promote a more motile phenotype (Ma et al., 2012) through various pathways, including the MAPK pathway, Rho GTPases, and EGFR activation (Mateus et al., 2007). These interactions and signalling cascades contribute to the regulation of cell motility and invasiveness. This disruption, along with PTEN loss, which can activate signalling pathways associated with cell migration and invasion, may synergistically promote the ability of keratoacanthoma cells to migrate and invade surrounding tissues.

The cooperation of E-cadherin loss in *HK1.fos-K14creP/Δ5PTEN$^{flx/flx}$* mice can alter the tumour environment in ways that promote tumour progression and conversion (see below).

Overall, these experiments tested the idea that the cooperation between inducible loss of E-cadherin, fos activation, and PTEN loss can synergistically promote the development of KAs by disrupting cell-cell adhesion, promoting proliferation, and facilitating tumour progression into wdSCC.

5.3.1 E-cadherin ablation cooperation in *HK1.fos-K14creP/Δ5PTEN$^{flx/flx}$* keratoacanthoma aetiology.

The initial findings in RU486-treated *HK1.fos-K14creP/Δ5PTEN$^{flx/flx}$/Δ6-10Ecad^{flx}* mice showed tumours with rapid growth, exhibiting a dome-shaped appearance consistent with the clinical and histological features of KA (Yao et al., 2008). KAs typically exhibit rapid growth, forming a raised, dome-

shaped nodule with a central keratin plug (Schwartz, 2004). The hallmark histological feature of KA is keratosis, characterised by abundant keratin columns resulting from p53 halting proliferation and fos inducing differentiation. In pre–KA lesions, the larger the proliferative bulb, the more prominent the keratin column, which refers to epidermal hyperplasia that is characterised by thickening of the stratum spinosum layer of the epidermis with changes in cell proliferation and adhesion, which could manifest as a unique histological characteristic in the skin lesion (Schwartz, 2004; Yao et al., 2008). Thus, the appearance of this skin phenotype in all genotypes associated with *HK1.fos-K14creP/Δ5PTEN$^{flx/flx}$* cooperation suggest that these epidermal responses were a result of the synergic effect of fos cooperation with PTEN loss, paradoxical activation of MAPK signalling, and the differential effects of p53/p21 and fos (Fisher et al., 1991; Greenhalgh et al., 1993b).

5.3.2 E-cadherin expression in heterozygous *HK1.fos-K14creP/Δ5PTEN$^{flx/flx}$/Δ6-10Ecad$^{flx/het}$* elicit KA as in *HK1.fos-K14creP/Δ5PTEN$^{flx/flx}$*

The expression of E-cadherin in heterozygous *HK1.fos-K14creP/Δ5PTEN$^{flx/flx}$/Δ6-10E-cad$^{flx/het}$* mice elicited KAs similar to *HK1.fos-K14creP/Δ5PTEN$^{flx/flx}$* KAs (Figure 5-4 B), with features typically associated with accelerated and premature differentiation (Figure 5-4 A). This phenomenon can be explained by the synergistic effect of fos cooperation with PTEN loss, which promotes a benign tumour environment where GSK3β-induced p53 expression consistently regulates AKT-associated proliferation into differentiation stages, ultimately preventing further tumour progression. Additionally, the molecular mechanism underlying this process is consistent with the activation of MAPK signalling, leading to the accelerated growth of the proliferative bulb that underlies a K1 histotype and is the source of subsequent differentiation and keratosis (Su et al., 2012).

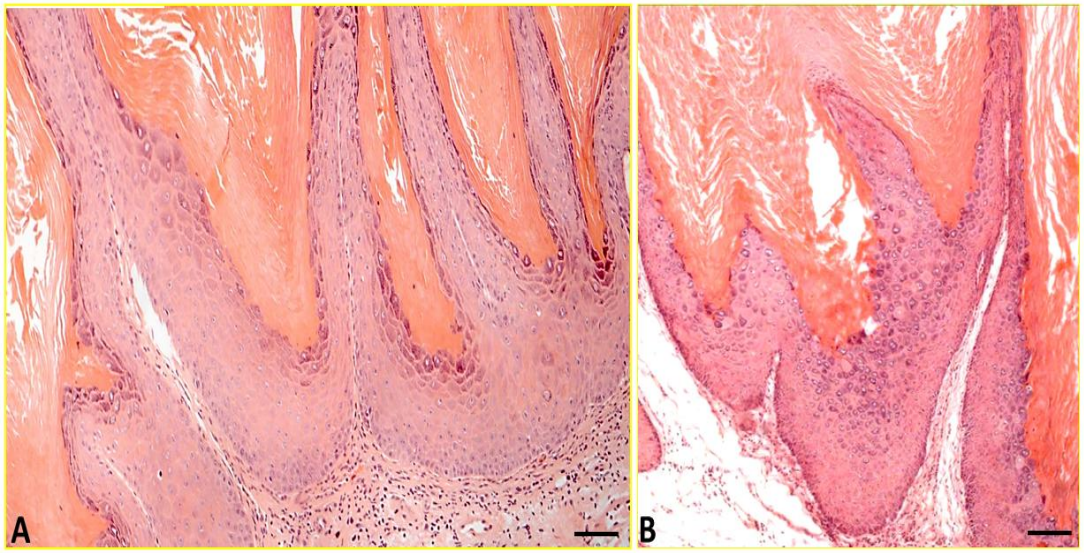

Figure 5-4: The histology of RU486-treated *HK1.fos-K14creP/Δ5PTEN$^{flx/flx}$/Δ6-10Ecad$^{flx/het}$* KA at 12 weeks (A) RU486-treated *HK1.fos-K14creP/Δ5PTEN$^{flx/flx}$/Δ6-10Ecad$^{flx/het}$* mice developed KAs at 12 weeks associated with accelerated and premature differentiation, similar to those in (B) KAs shown in *HK1.fos-K14creP/Δ5PTEN$^{flx/flx}$* mice. Panel B was previously shown in (Figure3-6 A). (Scale bars: A&B: 100μm).

In RU486-treated *HK1.fos-K14creP/Δ5PTEN$^{flx/flx}$/Δ6-10Ecad$^{flx/het}$* mice that developed KAs at 12weeks, the heterozygous E-cadherin expression was strong, membranous and predominantly found in the basal layers, as shown in Figure 5-5 A-D. This pattern closely resembles the endogenous E-cadherin expression in *HK1.fos-K14creP/Δ5PTEN$^{flx/flx}$* KAs, as depicted in Figure 5-5 E&F. This expression pattern was crucial for mediating intercellular adhesion and promoting cell-cell adhesion. The strong, membranous, and basal expression of E-cadherin observed in both immunofluorescence and IHC analyses suggests that the E-cadherin heterozygosity may lead to slightly diminished expression in some areas (Figure 5-5 B&C arrows). This phenomenon could be attributed to the presence of one functional allele of the E-cadherin gene, which may result in a partial reduction in E-cadherin expression levels compared to the wild-type (Figure 5-5 B&D).

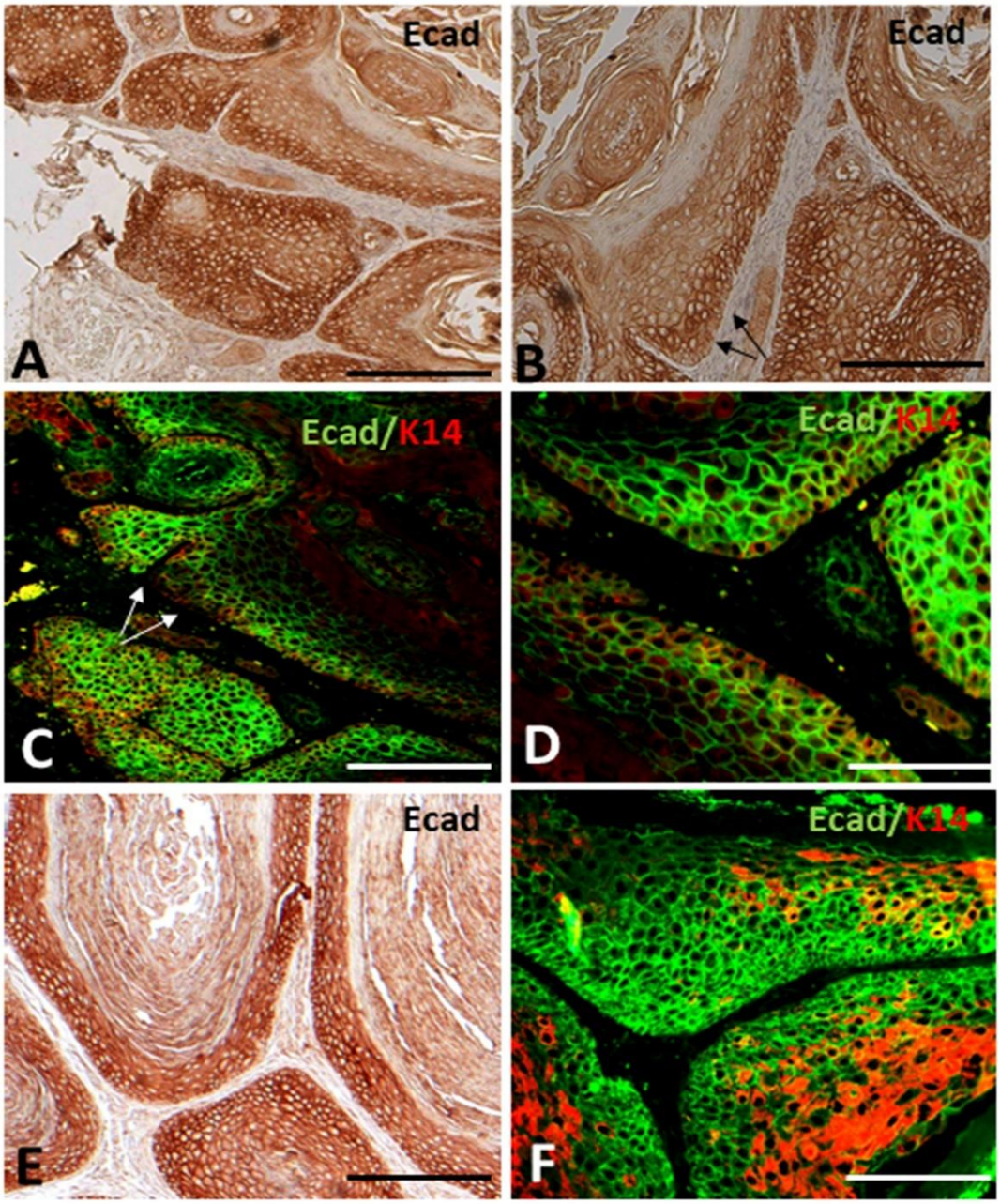

Figure 5-5 Analysis of E-cadherin expression in RU486-treated *HK1.fos-K14creP/Δ5PTEN$^{flx/flx}$/Δ6-10Ecad$^{flx/het}$* KA at 12 weeks (A-D) Show low and high magnification of IF E-cadherin analysis and IHC E-cadherin analysis in *HK1.fos-K14creP/Δ5PTEN$^{flx/flx}$/Δ6-10Ecad$^{flx/het}$* KAs, where the expression is strong, membranous and basal, similar to E-cadherin expression in (E-F) *HK1.fos-K14creP/Δ5PTEN$^{flx/fx}$* KAs. However, the heterozygosity in *HK1.fos-K14creP/Δ5PTEN$^{flx/flx}$/Δ6-10Ecad$^{flx/het}$* KAs, E-cadherin expression appears slightly diminished compared to controls and sporadically, the expression is faint in some areas (arrows). (Scale bars: A, C&E: 100μm, B, D&F: 50μm).

5.3.2.1 Analysis of β-catenin expression in *HK1.fos-K14creP/Δ5PTEN$^{flx/flx}$/Δ6-10Ecad$^{flx/het}$* KAs

Basal ß-catenin expression in RU486-treated *HK1.fos-K14creP/Δ5PTEN$^{flx/flx}$/Δ6-10Ecad$^{flx/het}$* KAs was observed, but its expression appeared cytoplasmic rather than nuclear (Figure 5-6), suggesting that E-cadherin can sequester ß-catenin to its cytoplasmic tail, preventing its nuclear translocation and promoting cell adhesion and differentiation (Kawahara et al., 2011; Kowalski et al., 2003).

KAs exhibit a unique life cycle, characterised by phases of rapid growth followed by spontaneous regression. This cycle appears to involve the activation of Wnt/ß-catenin signalling during physiological regeneration, which stabilises ß-catenin, leading to downstream effects on gene expression. These molecular events may contribute to the natural progression of the lesion (Joshi et al., 2020); (Wend et al., 2013). The interplay between ß-catenin and E-cadherin is essential for maintaining tissue architecture and regulating cell behaviour.

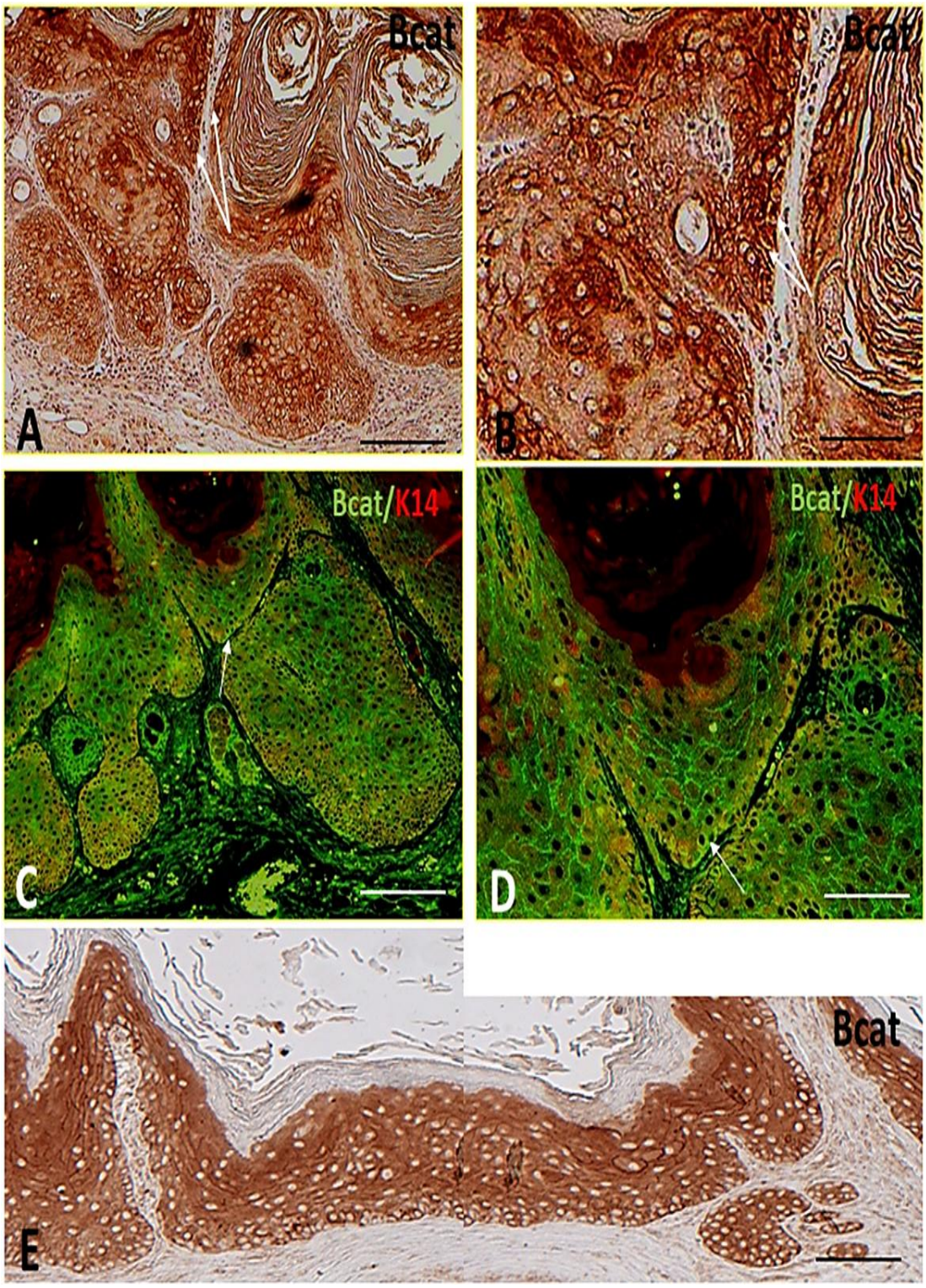

Figure 5-6 β-catenin expression analysis in RU486-treated *HK1.fos-K14creP/Δ5PTEN$^{flx/flx}$/Δ6-10Ecad$^{flx/het}$* KAs. (A&B) Low and high magnification of IHC for β-catenin expression in *HK1.fos-K14creP/Δ5PTEN$^{flx/flx}$/Δ6-10Ecad$^{flx/het}$* the β-catenin shows cytoplasmic expression at the basal cell layer (arrows). (C&D) Low and high magnification of β-catenin IF expressed in the basal cell cytoplasm (arrows), the cytoplasmic expression of β-catenin is similar to (E) β-catenin expression in *HK1.fos-K14creP/Δ5PTEN$^{flx/flx}$* KA. (Scale bars: A, C&E: 100μm; B&D: 50μm).

The observation of basal ß-catenin expression in RU486-treated *HK1.fos-K14creP/Δ5PTEN$^{flx/flx}$/Δ6-10Ecad$^{flx/het}$* KAs, with cytoplasmic localisation rather than nuclear, indicates a role for E-cadherin in sequestering ß-catenin to its cytoplasmic tail. This sequestration mechanism prevents the nuclear translocation of ß-catenin, thereby promoting cell adhesion and differentiation (Tian et al., 2011).

The interplay between E-cadherin and ß-catenin signalling has been shown to regulate differentiation in acute myeloid leukaemia (Kühn et al., 2015). It has been suggested that certain interactions, promoting the formation of E-cadherin clusters that stabilise ß-catenin within the complex, prevent its nuclear translocation and subsequent target expression (Kühn et al., 2015). This further supports the notion that the localisation and stability of ß-catenin are regulated by its interactions with other cellular components, such as E-cadherin.

Studies have also demonstrated that tyrosine phosphorylation of ß-catenin can disrupt its interaction with E-cadherin, leading to the disruption of cadherin-based cell-cell adhesion (Sheth et al., 2007). This phosphorylation-dependent mechanism underscores the intricate regulatory mechanisms that modulate the adhesive properties of cells through the E-cadherin/ß-catenin complex.

Collectively, the complex interplay between adhesion molecules, such as E-cadherin and ß-catenin, and other regulatory factors influences cellular processes, including adhesion, differentiation, and signalling pathways. Understanding these interactions is essential for unravelling the mechanisms underlying cell behaviours and tissue development.

5.3.2.2 K1 and p53 expression in the *HK1.fos-K14creP/Δ5PTEN$^{flx/flx}$/Δ6-10Ecad$^{flx/het}$* KAs

Analysis of keratin K1 expression in RU486-treated *HK1.fos-K14creP/Δ5PTEN$^{flx/flx}$/Δ6-10Ecad$^{flx/het}$* showed similar results to wild-type E-cadherin mice. Due to abnormal differentiation, K1 was observed in the basal keratinocyte layers of KAs. This expression contributes to the KA outcome by accelerating commitment to differentiation and inhibiting further progression, as shown in Figure 5-7.

Thus, basal layer K1 expression indicated a sudden commitment to differentiation, which played a key role in inhibiting further tumour progression and inhibited the malignant phenotype, underscoring the importance of differentiation in controlling tumour progression.

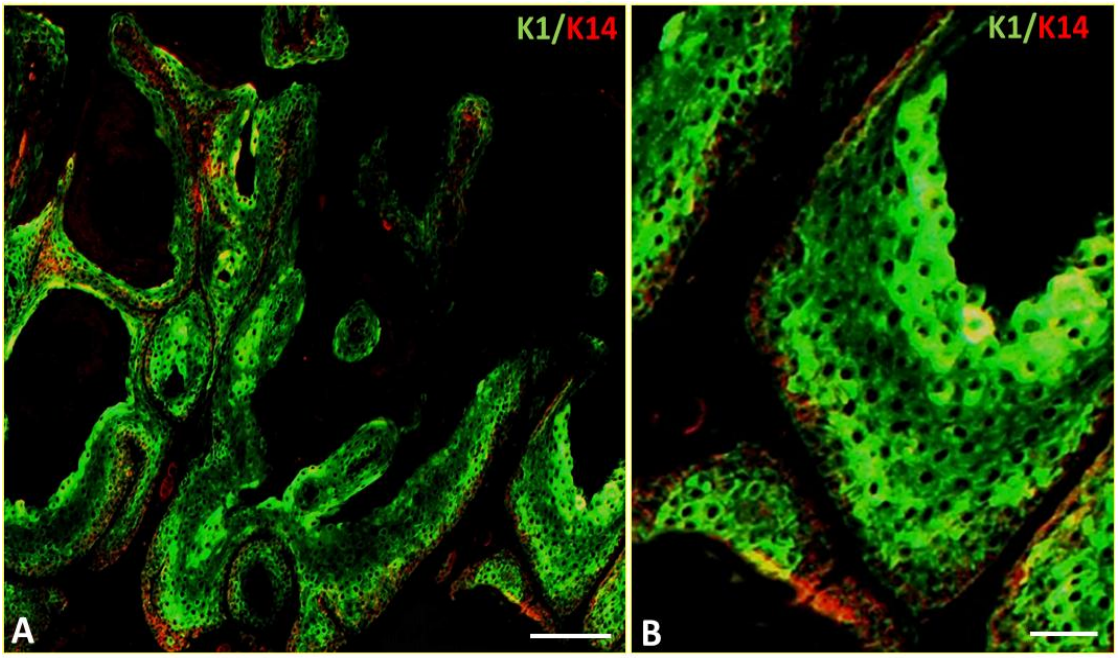

Figure 5-7 K1 analysis of RU486-treated *HK1.fos.K14creP/Δ5PTEN$^{flx/flx}$/Δ6-10Ecad$^{flx/het}$* KAs at 12 weeks (A&B) Low and high magnification of HK1.fos.K14creP/Δ5PTEN$^{flx/flx}$/Δ6-10Ecad$^{flx/het}$ demonstrating strong basal K1 expression. (Scale bars: A: 100μm; B: 50μm).

The co-expression of K1 in the basal layers of *HK1.fos-K14creP/Δ5PTEN$^{flx/flx}$/Δ6-10Ecad$^{flx/het}$* KAs, along with elevated nuclear levels of p53 (Figure 5-8), plays a crucial role in enhancing keratinocyte differentiation and promoting the development of KAs. This is in conjunction with the strong membranous basal E-cadherin expression and the cytoplasmic ß-catenin expression in *HK1.fos-K14creP/Δ5PTEN$^{flx/flx}$/Δ6-10Ecad$^{flx/het}$* mice (Figure 5-7). Collectively, these factors contribute to the intricate molecular mechanisms involved in KA development. Specifically, the basal expression of ß-catenin acts as a trigger for the activation of p53, which in turn plays a pivotal role in regulating cellular differentiation and growth.

The interplay between E-cadherin heterozygosity and these key proteins highlights their roles in cell adhesion, differentiation and signalling pathways within the tumour environment. Thus, there was a minimal change

observed in heterozygous E-cadherin mice, indicating that a full loss of E-cadherin is needed to achieve a phenotype.

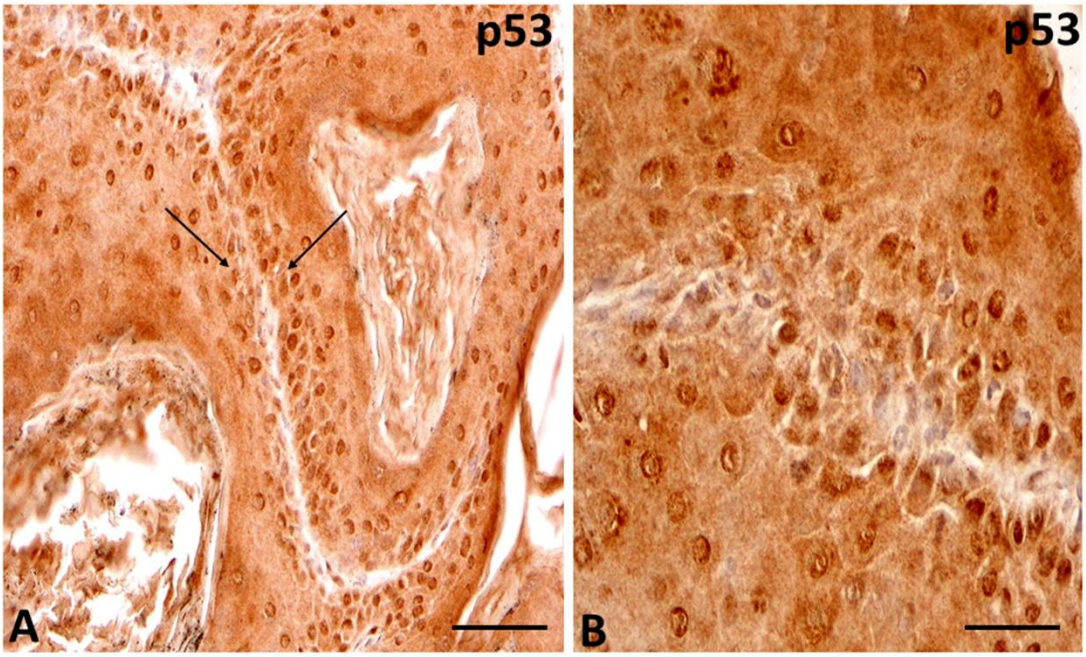

Figure 5-8 P53 analysis in RU486-treated *HK1.fos-K14creP/Δ5PTEN$^{flx/flx}$/Δ6-10Ecad$^{flx/het}$* KAs. (A) Shows the basal and suprabasal expression of p53 (arrows). (B) Shows nuclear p53 expression. (Scale bars: A: 75μm; B: 50μm).

5.3.3 Δ6-10E-cadherin expression in *HK1.fos-K14creP/Δ5PTEN$^{flx/flx}$/Δ6-10Ecad$^{flx/flx}$* mice drives malignant conversion to wdSCC/SCC

Expression of Δ6-10E-cadherin in *HK1.fos-K14creP/Δ5PTEN$^{flx/flx}$/Δ6-10Ecad$^{flx/flx}$* mice initially led to the development of KA-like tumours, often lacking well-formed microcysts (Figure 5-9 A). However, over time, these tumours progressed into wdSCC (Figure 5-9 B). This transition from a benign KA-like phenotype to SCC (Figure 5-9 C) highlights the potential role of Δ6-10E-cadherin in altering cell-cell adhesion and downstream signalling pathways, contributing to the distinct phenotypic changes observed during tumour progression. This progression to wdSCC/SCC indicates a shift towards a more aggressive phenotype with increased potential for invasion. The tumours progressed to aggressive SCC through mechanisms such as p53 loss, β-catenin alterations, as observed in *HK1.ras.fos-K14creP/Δ5PTEN$^{flx/flx}$/Δ6-10Ecad$^{flx/flx}$* models (see Chapter 6). However, in *HK1.fos-K14creP/Δ5PTEN$^{flx/flx}$/Δ6-10Ecad$^{flx/flx}$* models, the conversion appeared to be

slower, likely due to the absence of ras, which typically drives benign tumour formation.

This transformation highlights the significance of understanding the molecular mechanisms underlying tumour progression and the role of E-cadherin in regulating tumour behaviour.

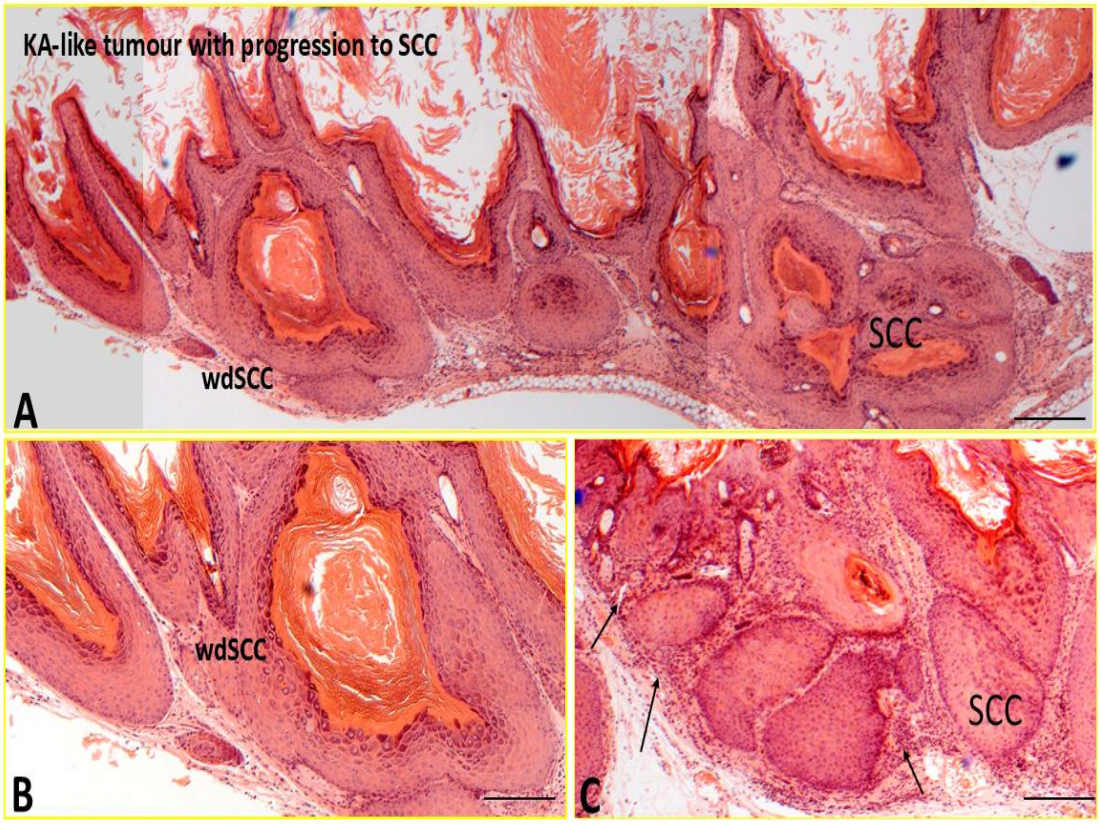

Figure 5-9 The histotype of RU486-treated *HK1.fos-K14creP/Δ5PTEN$^{flx/flx}$/Δ6-10Ecad$^{flx/flx}$* mice shows malignant conversion to wdSCC/SCC at 12 weeks. (A) The RU486-treated *HK1.fos-K14creP/Δ5PTEN$^{flx/flx}$/Δ6-10Ecad$^{flx/flx}$* mice showing the progression from KA-like tumour to (B) wdSCC, and further into (C) SCC that shows disorganisation with patches of invasion (arrows). (Scale bars: A: 150μm; B: 100μm; C: 75μm).

5.3.3.1 Analysis of Δ6-10 Ecadherin expression in RU486-treated *HK1.fos-K14creP/Δ5PTEN$^{flx/flx}$/Δ6-10Ecad$^{flx/flx}$* genotypes

The expression of Δ6-10E-cadherin in RU486-treated *HK1.fos-K14creP/Δ5PTEN$^{flx/flx}$/Δ6-10Ecad$^{flx/flx}$* tumours remained detectable throughout the progression. IHC analysis (Figure 5-10 A) showed that the expression appeared more diffuse and less tightly localised to the membrane, indicating early changes in adhesion characteristics. Higher magnification images (Figure 5-10 B&C) confirmed that Δ6-10E-cadherin was still present,

including areas of wdSCC and SCC. However, the distribution pattern appeared altered, suggesting ongoing attempts to maintain cell adhesion. Therefore, rather than a complete fading, the expression appeared to persist, with possible variation in signal strength. Complementary IF analysis further supported these observations, Δ6-10E-cadherin retained membranous localisation in some regions (Figure 5-10 D-E), while in others, particularly within areas of progression, it was reduced (Figure 5-10 F). Together, these findings suggested that although Δ6-10E-cadherin was still detectable, its localisation became disrupted during tumour progression, reflecting a transition in epithelial architecture and adhesion dynamics.

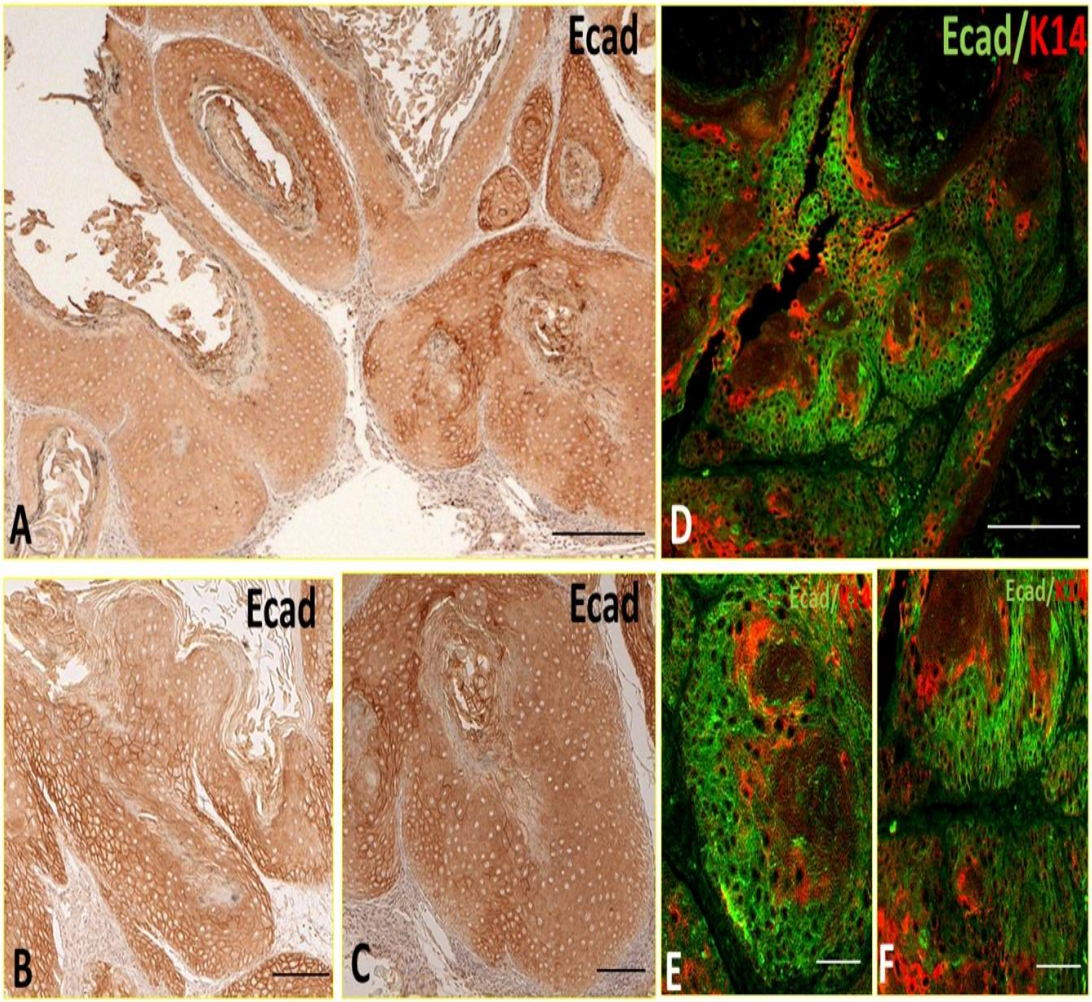

Figure 5-10 Analysis of Δ6-10E-cadherin expression in RU486-treated *HK1.fos-K14creP/Δ5PTEN$^{flx/flx}$/Δ6-10Ecad$^{flx/flx}$* wdSCC at 12 weeks. (A-C) Show IHC analysis of Δ6-10E-cadherin expression in *HK1.fos-K14creP/Δ5PTEN$^{flx/flx}$/Δ6-10Ecad$^{flx/flx}$*. (A) Low magnification of *HK1.fos-K14creP/Δ5PTEN$^{flx/flx}$/Δ6-10Ecad$^{flx/flx}$* mice, where Δ6-10E-cadherin expression is still detectable. (B) High magnification image of RU486-treated *HK1.fos-K14creP/Δ5PTEN$^{flx/flx}$/Δ6-10Ecad$^{flx/flx}$* confirms the continued presence of Δ6-10E-cadherin expression in (wdSCC), although the distribution is noticeably reduced in (C) progression to SCC . (D-F) IF analysis of Δ6-10E-cadherin expression in *HK1.fos-K14creP/Δ5PTEN$^{flx/flx}$/Δ6-10Ecad$^{flx/flx}$*. (D) Low magnification of Δ6-10E-cadherin expression that retains membranous expression in some regions, while in (E), Δ6-10E-cadherin expression is reduced during the progression to (F) SCC. (Scale bars: A: 150μm; B&C: 50μm; D: 100μm; E&F: 50μm).

5.3.3.2 Analysis of β-catenin expression of RU486-treated *HK1.fos-K14creP/Δ5PTEN$^{flx/flx}$/Δ6-10Ecad$^{flx/flx}$* genotype

In RU486-treated *HK1.fos-Δ5PTEN$^{flx/flx}$/Δ6-10Ecad$^{flx/flx}$* tumours, ß-catenin was mainly detected at the membrane in both basal and suprabasal layers. The staining was most intense and continuous in the basal layer, while suprabasal layers showed slightly reduced and occasionally discontinuous signals (Figure 5-11 A). Cytoplasmic ß-catenin expression was occasionally seen in some cells, but no nuclear localisation was observed (Figure 5-11 B). This pattern indicates preservation of ß-catenin's junctional function without activation of the Wnt signalling pathway via nuclear translocation.

Thus, the partial loss of Δ6-10-E-cadherin, together with maintained membranous ß-catenin, suggests an intermediate state in SCC progression where cell-cell adhesion is partially compromised but not completely disrupted. This may reflect early alterations in epithelial integrity that facilitate tumour growth and invasion while retaining some epithelial characteristics typical of wdSCC.

The dysregulation of E-cadherin and ß-catenin has been observed in breast carcinogenesis, where changes in their expression are implicated in tumour differentiation and acquisition of an invasive phenotype (Bankfalvi et al., 1999). Additionally, in gastric carcinoma, abnormal E-cadherin and ß-catenin expression have been identified as potential markers of submucosal invasion and lymph node metastasis (Liu et al., 2019). Thus, the interplay between Δ6-10E-cadherin expression, ß-catenin dynamics, and the loss of E-cadherin in various cancers underscores the critical role of cell adhesion molecules in tumour progression. The modulation of these adhesion molecules can influence cell behaviour and invasive potential.

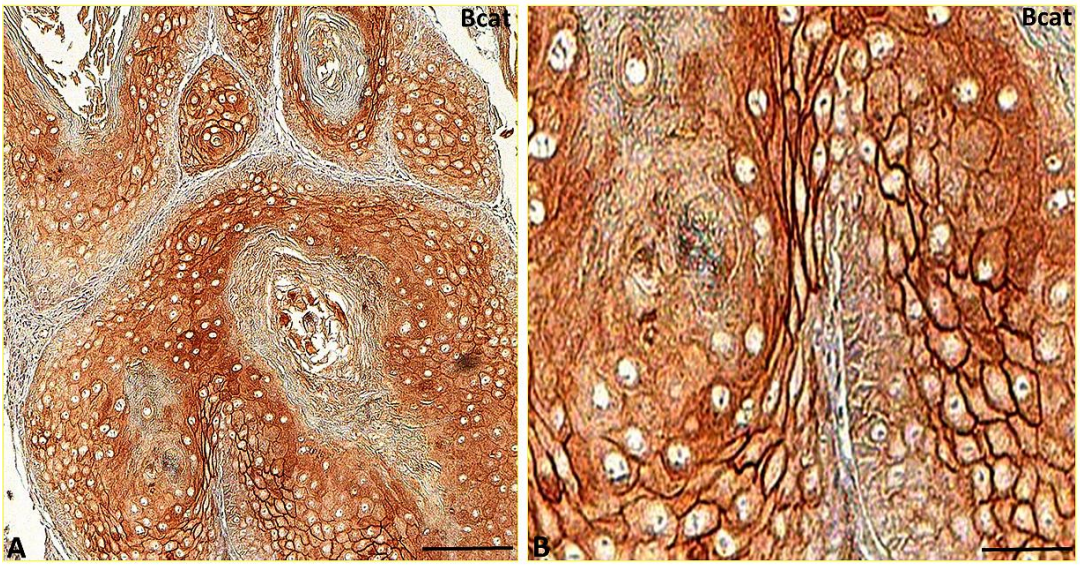

Figure 5-11 IHC analysis of β-catenin expression in RU486-treated *HK1.fos-K14creP/Δ5PTEN$^{flx/flx}$/Δ6-10E-cad$^{flx/flx}$* tumours at 12 weeks. (A) Low magnification shows β-catenin expression on cell membranes, with signal present in both basal and suprabasal layers. (B) Higher magnification shows membranous β-catenin localisation in the basal and suprabasal layers, with occasional cytoplasmic expression and no nuclear staining. (Scale bars: A: 75μm; B: 25μm).

5.3.3.3 p53 expression and K1 analysis in the *HK1.fos-K14creP/Δ5PTEN$^{flx/flx}$/Δ6-10Ecad$^{flx/flx}$* wdSCC/SCC

p53 expression in RU486-treated *HK1.fos-K14creP/Δ5PTEN$^{flx/flx}$/Δ6-10Ecad$^{flx/flx}$* mice were analysed at 12 weeks. The results showed a reduction in p53 expression (Figure 5-12 A), with a reduction in nuclear p53 expression (Figure 5-12 B&C). This finding suggests that alterations in p53 may potentially influence tumour progression and conversion dynamics. This observed alteration in the p53 expression pattern underscores its significance in the regulatory mechanisms governing tumorigenesis.

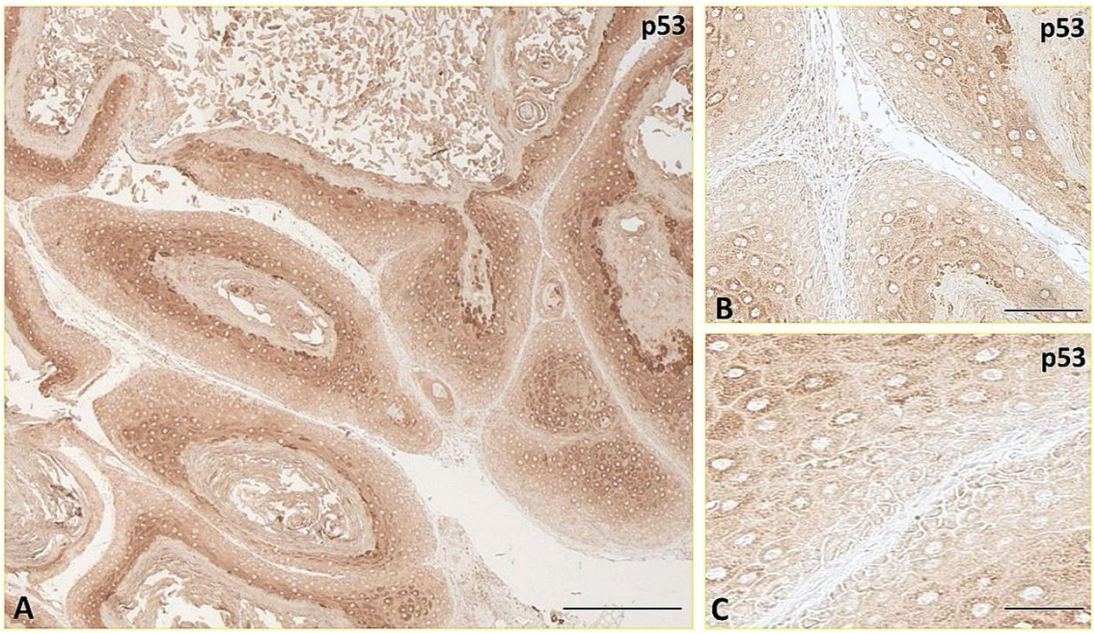

Figure 5-12 the analysis of p53 expression in RU486-treated *HK1.fos-K14creP/Δ5PTEN$^{flx/flx}$//Δ6-10Ecad$^{flx/flx}$* wdSCC/SCC at 12 weeks. (A) Shows low magnification of RU486-treated *HK1.fos-K14creP/Δ5PTEN$^{flx/flx}$/Δ6-10Ecad$^{flx/flx}$* wdSCC, where p53 expression is notably reduced. (B&C) Show high magnification of diminished nuclear p53 expression. (Scale bars: A: 150μm; B: 100μm; C: 50μm).

The interplay between the expression of Δ6-10E-cadherin variant, dysregulation of ß-catenin signalling, and loss of p53 in *HK1.fos-K14creP/Δ5PTEN$^{flx/flx}$/Δ6-10Ecad$^{flx/flx}$* tumours underscores the critical role of cell adhesion molecules in tumour progression. While E-cadherin remained detectable in these tumours, the presence of altered Δ6-10E-cadherin may compromise its adhesive and signalling functions. This functional disruption may contribute to epithelial disorganisation and increase invasive potential. Previous studies have shown that the combined loss of E-cadherin and p53 can accelerate tumour invasion, resembling human invasive lobular carcinoma (Derksen et al., 2006). Similarly, p53 loss and ß-catenin dysregulation were evident, supporting the idea that even in the presence of Δ6-10E-cadherin, functional impairment of adhesion pathways can promote malignant progression.

While p53 expression was consistently reduced, K1 expression remained detectable, although some regions showed diminished staining intensity (Figure 5-13). This focal variation suggests potential alterations in keratinocyte differentiation and proliferation processes that are essential for maintaining epidermal homeostasis and skin morphology. The observed

changes in K1 staining may reflect underlying modulation of signalling pathways involved in epidermal differentiation dynamics during tumour progression.

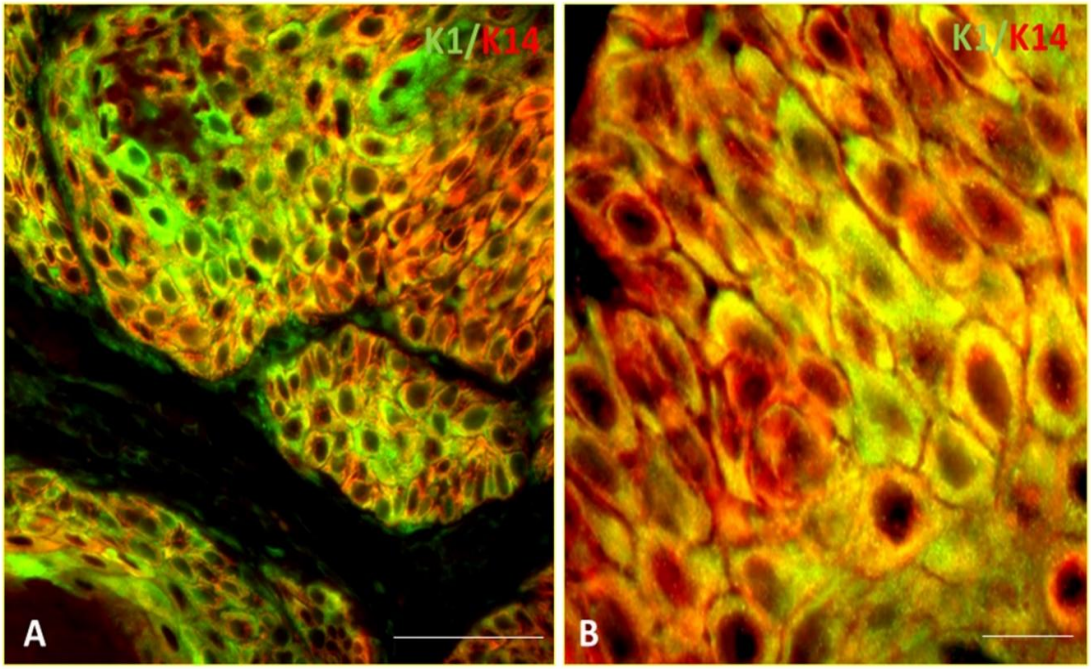

Figure 5-13 K1 analysis in RU486-treated *HK1.fos-K14creP/Δ5PTEN$^{flx/flx}$/Δ6-10Ecad$^{flx/flx}$* wdSCC/SCC at 12 weeks (A) Displays a low magnification image demonstrating that K1 expression remains broadly detectable. (B) Shows a high magnification view of the wdSCC area, where K1 staining is retained, with non-uniform expression observed. Yellow fluorescence indicates co-localisation of K1 and K14, highlighting overlapping expression. (Scale bars: A: 100μm; B: 50μm).

5.4 Summary:

As outlined above, the loss of E-cadherin in RU486-treated *HK1.fos-K14creP/Δ6-10Ecad*$^{flx/flx}$ mice showed hyperplasia with expanded epidermal compartments with elevated areas of acanthosis and intercellular spaces, suggesting the potential effect of E-cadherin in suprabasal keratinocytes proliferation, leading to thicker epidermal layers (Figure 5-1). The loss of E-cadherin may also contribute to the epidermal strength and cell-cell adhesion and signalling pathways, potentially promoting abnormal keratinocyte differentiation, while also implicating the role of fos in commitment to differentiation (Jensen & Wheelock, 1992). This dysregulation may result in the expansion of epidermal compartments and the development of hyperplasia, characterised by an increase in the number of cells within the epidermis.

This suggests that E-cadherin has a crucial role in maintaining epidermal homeostasis and regulating keratinocyte behaviour. This phenotype revealed an increase in hyperplasia associated with an increase in K1 expression in a basal/suprabasal pattern (Figure 5-7). This observation suggests a potential link between the genetic alterations in the *HK1.fos-K14creP/Δ6-10Ecad*$^{flx/flx}$ model and enhanced K1 expression, which may be indicative of altered keratinocyte differentiation and proliferation. The upregulation of K1 expression in the basal layers could signify changes in the differentiation responses of keratinocytes, potentially contributing to the observed hyperplasia in this genotype.

The results of E-cadherin expression in RU486-treated *HK1.fos-K14creP/Δ5PTEN*$^{flx/flx}$*/Δ6-10Ecad*$^{flx/het}$ mice demonstrate a nuanced impact on tumour progression and differentiation dynamics, where E-cadherin expression may contribute to the anomalous differentiation. The KAs observed in this model resemble those in *HK1.fos-K14creP/Δ5PTEN*$^{flx/flx}$ KAs, characterised by micro-cysts indicative of accelerated and premature differentiation (Figure 5-4). These features included the consistent presence of strong basal/suprabasal K1 expression, as well as continuous strong basal E-cadherin expression. This increase in E-cadherin expression in the basal cell layers may enhance the cell-cell adhesion process and promote the

structural integrity of the tissue, which may contribute to maintaining the organisation of KAs (Chiles et al., 2003; Jeanes et al., 2008).

Elevated nuclear p53 expression was also observed, which potentially halts proliferation and induces irregular differentiation, along with cytoplasmic basal ß-catenin expression. This underscores the role E-cadherin heterozygosity contributes to protecting against tumour progression and in the maintenance of morphological features (Berx et al., 1995). These data suggest E-cadherin may collaborate with fos activation and PTEN loss to sustain KA formation and prevent malignant conversion.

Conversely, in the context of Δ6-10E-cadherin expression in RU486-treated *HK1.fos-K14creP/Δ5PTEN*$^{flx/flx}$*/Δ6-10Ecad*$^{flx/flx}$ mice, a distinctive trajectory emerges. Initial tumour formation resembling KA-like lesions was observed (Figure 5-9). However, these lesions progressed into wdSCC interspersed with patches of SCC (Figure 5-9). This suggests that a more aggressive and invasive behaviour was associated with E-cadherin ablation. As shown in Figure 5-10, Δ6-10E-cadherin expression remained detectable despite signs of disturbed cell-cell adhesion. This suggests that signalling attempts to maintain cell-cell adhesion through signalling pathways have failed, resulting in potential progression to wdSCC and subsequent invasion by SCC.

This result was concomitant with less membranous ß-catenin expression (Figure 5-11 A&C), and more nuclear localisation within the basal layer (Figure 5-11 B&D), indicating facilitation of conversion into wdSCC. However, this nuclear localisation of ß-catenin exhibited variability, with instances of its absence in certain regions (Figure 5-11 A) while persisting in others. In essence, nuclear ß-catenin was not uniformly sustained, with its presence observed selectively across distinct areas (Figure 5-11 B). This suggests that the loss of E-cadherin led to a deregulation of signalling to ß-catenin. However, compensatory mechanisms exist that attempt to inhibit further progression.

The interplay between genetic alterations, such as PTEN loss and E-cadherin ablation, may influence the K1 expression contribution to the development of skin lesions, including keratoacanthomas and SCCs; since PTEN loss leads to activation of the PI3K/AKT pathway (Hopkins & Parsons, 2014), which can directly or indirectly affect K1 expression by inducing

cellular proliferation and resistance to apoptosis. Altered signalling pathways resulting from both PTEN and E-cadherin loss may modulate K1 gene expression, as E-cadherin loss disrupts cell differentiation, which could impact K1 expression in keratinocytes.

Overall, Δ6-10E-cadherin expression in *HK1.fos-K14creP/Δ5PTEN$^{flx/flx}$/Δ6-10Ecad$^{flx/flx}$* mice has been implicated in driving conversion to wdSCC or SCC rather than KA.

Chapter 6 The E-cadherin loss in *HK1.ras.fos-K14creP/Δ5PTEN$^{flx/flx}$/Δ6-10Ecad$^{flx/flx}$* transgenic mouse drives malignant conversion and progression into poorly differentiated squamous cell carcinoma

6.1 Introduction

In previous chapters, the investigation of endogenous E-cadherin in transgenic mice carrying activated ras and fos oncogenes expressed exclusively in the epidermis, along with conditional PTEN loss to drive carcinogenesis, revealed a reduction in E-cadherin expression at the invasive front of wdSCC shortly after p53 loss (Chapter 3). This sheds light on the dynamic interplay between genetic alterations and signalling pathways in the development of skin lesions, particularly wdSCC and SCCs. The findings suggest that the modulation of E-cadherin expression, in conjunction with the activation of oncogenes and loss of TSGs, plays a crucial role in driving the progression of skin carcinomas towards more aggressive phenotypes (Li et al., 2006).

The downregulation of E-cadherin, often associated with genetic alterations such as PTEN loss and oncogene activation, can disrupt cell-cell adhesion and promote cell motility, which are key processes in tumour invasion and metastasis. The intricate relationship between E-cadherin and signalling molecules like fos activation can enhance cell motility through mechanisms involving the MAP kinase pathway. This process also engages downstream effectors such as Rho GTPases that regulate cytoskeletal dynamics (Mack & Georgiou, 2014). These interactions contribute to the regulation of cell motility and invasiveness, highlighting the complexity of E-cadherin-mediated cellular behaviours in the context of tumorigenesis (Imamichi & Menke, 2007).

The dysregulation of E-cadherin and PTEN signalling pathways can impact the expression of keratin proteins, such as K1, which are essential for maintaining skin integrity. The disruption of E-cadherin-mediated cell-cell contacts, coupled with genetic alterations, can lead to altered K1 expression patterns, influencing the development of skin lesions with varying differentiation states, including wdSCC and SCCs. This molecular interplay highlights the significance of E-cadherin and its downstream effects on K1 expression in the development of skin carcinomas (Silye et al., 1998).

Thus, analysis of endogenous E-cadherin in transgenic mice with activated ras and fos oncogenes and conditional PTEN loss provides valuable insights into the molecular mechanisms underlying the development of skin lesions, particularly wdSCC and SCC. The modulation of E-cadherin expression, in conjunction with genetic alterations and signalling pathways, plays a critical role in driving the progression of skin carcinomas towards more aggressive phenotypes, highlighting the intricate interplay between these factors in tumorigenesis. Previous research has highlighted the tumour-suppressive role of E-cadherin in various cancers, emphasising its significance in inhibiting tumour progression through multiple mechanisms. E-cadherin has been implicated in regulating contact-mediated inhibition of proliferation by suppressing ß-catenin/Wnt signalling (Wijshake et al., 2021). When cells are in contact with each other, E-cadherin molecules on adjacent cells interact, forming AJs. This interaction stabilises the cell-cell adhesion and prevents the dissociation of ß-catenin from the cell membrane. As a result, ß-catenin is unable to translocate into the nucleus to activate Wnt signalling, which is involved in cell proliferation. Therefore, E-cadherin indirectly suppresses ß-catenin/Wnt signalling, contributing to contact inhibition in cell proliferation (Wijshake et al., 2021).

Previous studies have demonstrated that in certain contexts, such as hyperplasia/papillomas, the loss of E-cadherin can be tolerated through increased differentiation (Nurismah et al., 2008). However, in the context of carcinogenesis and following the appearance of overt tumours, the conditional ablation of E-cadherin drives invasion and malignant progression, highlighting its involvement in cell-cell adhesion and aberrant signalling to ß-catenin (Salon et al., 2004). These findings emphasise the dual role of E-cadherin in different biological contexts, where its loss can lead to distinct outcomes depending on the cellular environment and disease stages.

An immediate elevated expression of p53 was observed in *HK1.ras.fos-K14creP/Δ5PTEN*$^{flx/flx}$ hyperplasia, and papillomas. While malignant conversion necessitated p53 loss, leading to further progression of wdSCC into more aggressive carcinomas (Macdonald et al., 2014). This underscores the intricate interplay between E-cadherin, p53, and cooperation with ras, and fos activation in regulating tumour progression and transition into malignancy in skin carcinogenesis.

In this results chapter, the focus was on investigating the inducible ablation of E-cadherin function using cre/LoxP technology. Specifically, *K14creP/Δ6-10Ecad*$^{flx/flx}$ mice were utilised to introduce a RU486-inducible, conditional E-cadherin knockout into *HK1.ras.fos-K14creP/Δ5PTEN*$^{flx/flx}$ genotypes (Pugach et al., 2015). Thus, by employing this technology, the role of E-cadherin in *HK1.ras.fos-K14creP/Δ5PTEN*$^{flx/flx}$ */Δ6-10Ecad*$^{flx/flx}$ model can be examined in a controlled and inducible manner.

The results revealed that the conditional ablation of E-cadherin facilitated the rapid malignant conversion and progression of wdSCC into SCC after the appearance of overt tumours. This observation is consistent with the pivotal roles of E-cadherin in cell-cell adhesion and dysregulated signalling to β-catenin (Jeanes et al., 2008).

The dysregulation of E-cadherin function can have profound implications for disease progression, emphasising the importance of understanding the molecular mechanisms underlying E-cadherin-mediated signalling pathways in cancer biology.

6.2 Inducible gene switch in *HK1.ras.fos-K14creP/Δ5PTEN* $^{flx/flx}$*/Δ6-10Ecad*$^{flx/flx}$ transgenic mouse skin carcinogenesis model

The specific ablation of PTEN exon 5 and E-cadherin exons 6-10 was targeted in *HK1.ras.fos/Δ5PTEN*$^{flx/flx}$*/Δ6-10Ecad*$^{flx/flx}$ epidermis. This ablation was achieved by topical application of RU486 weekly for 3 weeks to activate the cre recombinase expressed by the K14 promoter (Macdonald et al., 2014). This method allowed for precise and controlled deletion of PTEN and E-cadherin in epidermal cells, facilitating the study of their roles in skin carcinogenesis and tumour progression. Following the cre-mediated excision of the LoxP-flanked stop cassette, inducible loss of PTEN exon 5 and E-cadherin exons 6-10 was initiated in the same epidermal cells (Figure 6-1).

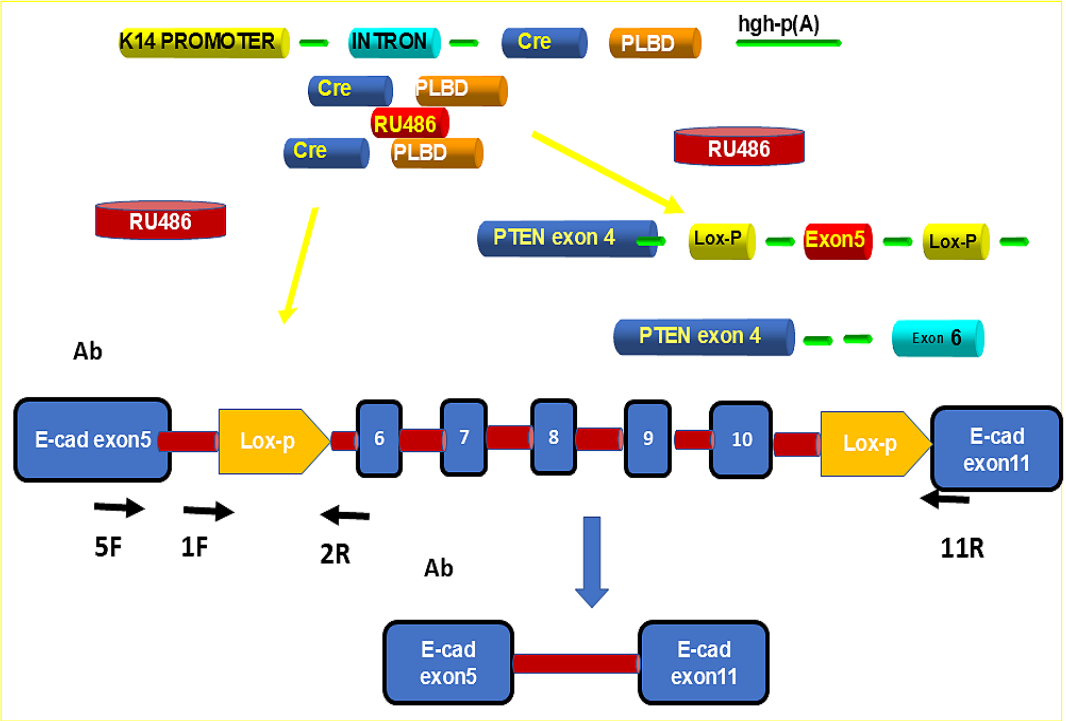

Figure 6-1 The inducible gene switch in RU486-treated *HK1.ras.fos-K14creP/Δ5PTEN$^{flx/flx}$/Δ6-10Ecad$^{flx/flx}$* transgenic mouse skin carcinogenesis model. This figure shows that PTEN exon 5 & E-cadherin exons 6-10 are ablated exclusively in *HK1.ras.fos-K14creP/Δ5PTEN$^{flx/flx}$/Δ6-10Ecad$^{flx/flx}$* epidermis following topical application of 15 µL of 2mg/mL RU486 weekly for 3 weeks to activate cre recombinase expressed by a K14 promoter.

6.2.1 Analysis of the co-operation between E-cadherin loss and the loss of PTEN in transgenic mouse carcinogenesis

In this experimental design, mice from cohorts (n=10) of *K14creP/Δ5PTEN$^{flx/flx}$/Δ6-10Ecad$^{flx/flx}$* and aged-matched *K14creP/Δ5PTEN$^{flx/flx}$* controls were treated topically with RU486 on both ears. This treatment induces cre activation specifically in the epidermal cells, targeting and eliminating genetic elements to examine the effects of PTEN and E-cadherin loss within the same cellular population. As a result, exon 5 of PTEN and the transcriptional stop cassette for Δ6-10E-cadherin were excised, ablating the expression of these transgenes. Each bi-genic control genotype (n=5) and a cohort of *K14creP/Δ5PTEN$^{flx/flx}$/Δ6-10Ecad$^{flx/flx}$* (n=5) underwent identical RU486 treatment for up to 7 months.

The *K14creP/Δ5PTEN$^{flx/flx}$/Δ6-10Ecad$^{flx/flx}$*, inducible ablation of E-cadherin, in conjunction with the loss of PTEN-mediated AKT regulation, did

not reveal any observable cooperative effects, with cellular behaviour as expected. Both RU486-treated *K14creP/Δ5PTEN$^{flx/flx}$/Δ6-10Ecad$^{flx/flx}$* and RU486-treated *K14creP/Δ5PTEN$^{flx/flx}$* mice exhibited some skin thickening accompanied by mild keratosis as early as 10-12 weeks. However, these conditions exhibited minimal alteration by the 7th month of observation (Figure 6-2), aligning with earlier studies involving *K14creP/Δ5PTEN$^{flx/flx}$* models (Yao et al., 2006).

The absence of tumour formation in the RU486-treated *K14creP/Δ5PTEN$^{flx/flx}$/Δ6-10Ecad$^{flx/flx}$* mice over a period of 7 months suggests a delayed or inhibited tumorigenic response in these models compared to the bi-genic *HK1.ras-K14creP/Δ6-10Ecad$^{flx/flx}$* mice that developed tumours within 12-14 weeks (Chapter 4). This lack of synergy was evident as there was no indication of tumour formation even after a prolonged period of 7 months (Chen et al., 2006).

This interplay between E-cadherin loss and PTEN loss in regulating tumorigenesis underscores the complexity of signalling pathways involved in tumour development. The study emphasised the importance of PTEN in modulating the PI3K/AKT pathway, a critical signalling cascade implicated in various cellular functions.

The role of PTEN as a negative regulator of PI3K signalling was underscored, demonstrating its significance in controlling AKT activation and downstream pathways. This regulation is essential in understanding the co-expression patterns observed between E-cadherin loss and PTEN loss in transgenic mouse models of carcinogenesis, highlighting how disruptions in these pathways contribute to tumour development (Kim et al., 2014). Overall, the simultaneous loss of E-cadherin and PTEN-mediated AKT regulation does not significantly enhance cooperative effects or induce tumour formation in this experimental context.

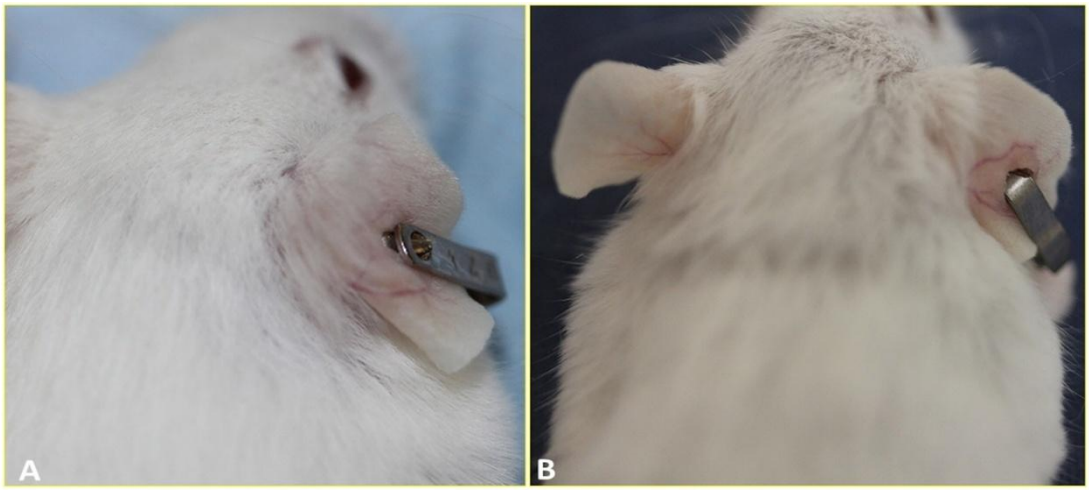

Figure 6-2 Phenotypes of RU486-treated *K14creP/Δ5PTEN$^{flx/flx}$/Δ6-10Ecad$^{flx/flx}$* and RU486-treated *K14creP/Δ5PTEN$^{flx/flx}$* mice at 27 weeks. (A) RU486-treated *K14creP/Δ5PTEN$^{flx/flx}$/Δ6-10Ecad$^{flx/flx}$* mice exhibit slight ear thickening, similar to the changes observed in (B) RU486-treated *K14creP/Δ5PTEN$^{flx/flx}$* mice display scaly ear and slightly thickened.

Histologically, ear skin biopsies from RU486-treated *K14creP/Δ5PTEN$^{flx/flx}$/Δ6-10Ecad$^{flx/flx}$* mice at 27 weeks revealed mild epidermal hyperplasia with a slightly folded appearance and mild keratosis (Figure 6-3 A&B), similar to the observations in RU486-treated *K14creP/Δ5PTEN$^{flx/flx}$* mice (Figure 6-3 C&D) (Yao et al., 2006). However, in RU486-treated *K14creP/Δ5PTEN$^{flx/flx}$/Δ6-10Ecad$^{flx/flx}$* hyperplasia was associated with more prominent intercellular spaces (Figure 6-3 A&B), although intercellular spaces were also occasionally visible in RU486-treated *K14creP/Δ5PTEN$^{flx/flx}$* mice (Figure 6-3 C&D). By contrast, RU486-untreated control mice exhibited normal epidermis with no evidence of hyperplasia. This histological presentation suggests that the genetic modifications induced by RU486 treatment led to specific changes in the skin structure, characterised by increased epidermal thickness and keratinocyte proliferation, indicative of hyperplasia and keratosis (Yao et al., 2006). These findings align with the notion that PTEN loss, in combination with other genetic alterations such as E-cadherin modifications, can influence skin morphology and cellular behaviour, leading to hyperplastic changes in the epidermis (Yao et al., 2006). The observed histological features are consistent with the effect of PTEN loss on skin homeostasis and development of hyperkeratosis, resembling characteristics associated with conditions such as Cowden disease (Yao et al., 2006).

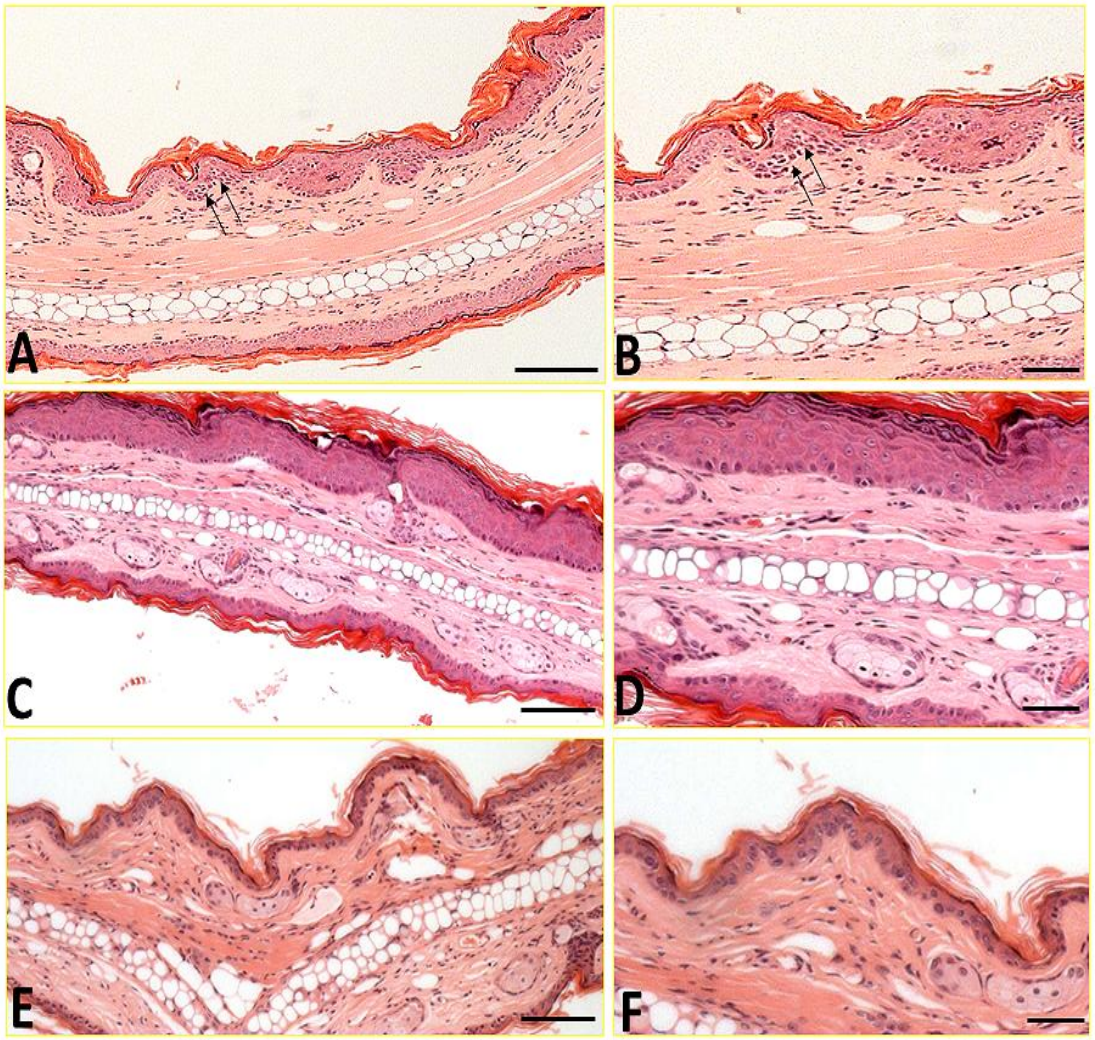

Figure 6-3 The histotype of RU486-treated *K14creP/Δ5PTEN$^{flx/flx}$/Δ6-10Ecad$^{flx/flx}$* and RU486-treated *K14creP/Δ5PTEN$^{flx/flx}$* mice at 27 weeks. (A&B) RU486-treated *K14creP/Δ5PTEN$^{flx/flx}$/Δ6-10Ecad$^{flx/flx}$* epidermis, showing mild hyperplasia with obvious intercellular spaces (arrows). The exhibited hyperplasia is identical to (C&D) RU486-treated *K14creP/Δ5PTEN$^{flx/flx}$* hyperplasia. Occasional intercellular spaces are also observed in (E&F) corresponding to RU486-untreated *K14creP/Δ5PTEN$^{flx/flx}$/Δ6-10Ecad$^{flx/flx}$* controls, indicating a normal epidermis. (Scale bars: A, C&E: 100 μm; B, D&F: 50 μm).

RU486-treated *HK1.ras^{1276}-K14creP/Δ5PTEN$^{flx/het}$/Δ6-10Ecad$^{flx/het}$* control mice (n=6) exhibited a normal appearance, with mild keratotic changes, without signs of tumour changes (Figure 6-4) characteristic of their parental bi-genic phenotypes (Yao et al., 2006). This observation suggests that treatment with RU486 did not lead to changes in the skin phenotype of these mice at this stage, as compared to more aggressive tumorigenic phenotypes observed in other genotypes.

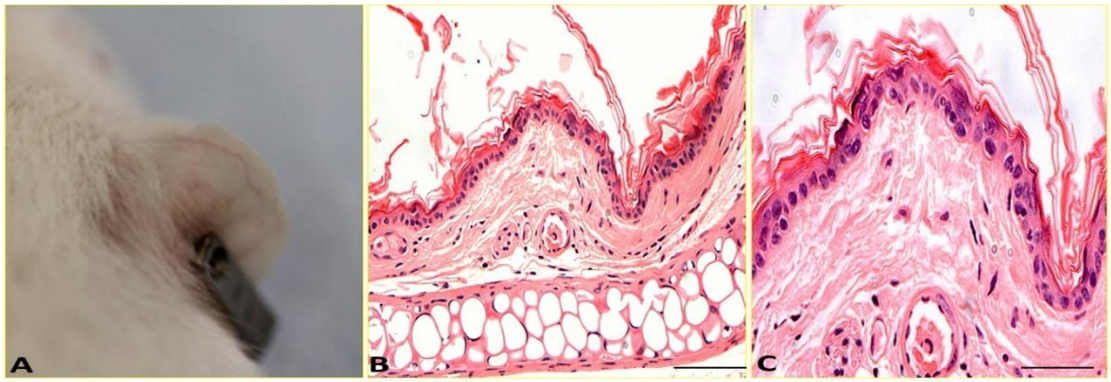

Figure 6-4 The RU486-treated *HK1.ras^{1276}-K14creP/Δ5PTEN$^{flx/het}$/Δ6-10Ecad$^{flx/het}$* phenotype and histotype (A) Shows RU486-treated *HK1.ras^{1276}-K14creP/Δ5PTEN$^{flx/het}$/Δ6-10Ecad$^{flx/het}$* phenotype. (B&C) Low and high magnification of RU486-treated *HK1.ras^{1276}-K14creP/Δ5PTEN$^{flx/het}$/Δ6-10Ecad$^{flx/het}$* that show normal TEG with mild keratosis. (Scale bars: B: 100 μm; C: 50 μm).

6.3 E-cadherin loss in *K1.ras^{1276}.fos-K14creP/Δ5PTEN$^{flx/flx}$/Δ6-10Ecad$^{flx/flx}$* mice drives malignant conversion and progression to poorly differentiated SCC, consistent with cell-cell adhesion failure

In this study, experiments utilised the *HK1.ras^{1276}* line, which had previously been successfully crossed with *K14creP/Δ6-10Ecad$^{flx/flx}$* mice. *HK1.ras^{1205}* was not used in subsequent experiments, particularly in *HK1.fos* cooperation and PTEN loss (Greenhalgh et al., 1993c; Greenhalgh et al., 1993a), based on the severe skin phenotypes observed. This reflects careful consideration of genetic combinations to avoid excessive phenotypic outcomes that could impede research progress. This approach produced the *HK1.ras^{1276}-K14creP/Δ6-10Ecad$^{flx/flx}$* model, which facilitated breeding and provided additional controls for comparison. As the experiment progressed,

new insights emerged into the *HK1.ras*^{1276}*.fos-K14creP/Δ5PTEN*$^{flx/flx}$*/Δ6-10Ecad*$^{flx/flx}$ phenotype and its underlying mechanisms, shifting the focus back to exploring the cooperative effects of E-cadherin loss and PTEN loss in cooperation with ras^{1276} and fos oncogenes.

In the investigation of *HK1.ras*^{1276}*.fos-K14creP/Δ5PTEN*$^{flx/flx}$*/Δ6-10Ecad*$^{flx/flx}$ synergism, inducible E-cadherin ablation was studied in transgenic mice expressing *HK1.ras*^{1276}*.fos* and *K14creP/Δ5PTEN*$^{flx/flx}$. In subsequent experiments, sibling cohorts of 5- to 6-week-old *HK1.ras*^{1276}*.fos-K14creP/Δ5PTEN*$^{flx/flx}$*/Δ6-10Ecad*$^{flx/flx}$ mice (n=10) were treated with RU486 to induce conditional ablation of E-cadherin function (*Δ6-10Ecad*^{flx}) and PTEN mutation (*Δ5PTEN*^{flx}). This allowed for the examination of the combined effects of E-cadherin loss, ras^{1276}, fos expression, and PTEN mutation in the context of skin biology and tumorigenesis.

At 8-10 weeks, *HK1.ras*^{1276}*.fos-K14creP/Δ5PTEN*$^{flx/flx}$*/Δ6-10Ecad*$^{flx/flx}$ mice exhibited a distinctive phenotype that led to bilateral tumour formation in both TGE and NTGE (Non-tagged ear) (Figure 6-5 A&B). Signs of tumour formation were observed in *HK1.ras*^{1276}*.fos-K14creP/Δ5PTEN*$^{flx/flx}$*/Δ6-10Ecad*^{flx} genotypes, in contrast to age-matched RU486-treated *HK1.ras*^{1276}*-K14creP/Δ6-10Ecad*$^{flx/flx}$ cohorts (n=6) that showed no signs of tumour formation (Figure 6-5 C).

These tumours were independent of wound promotion, as they appeared simultaneously on both TGE and NTGE of *HK1.ras*^{1276}*.fos-K14creP/Δ5PTEN*$^{flx/flx}$*/Δ6-10Ecad*^{flx}. This observation indicates a potential synergistic effect of these genetic alterations on tumorigenesis. The appearance of the tumours, independent of wound promotion, further highlights the significance of the genetic interactions in driving tumour formation in this experimental model.

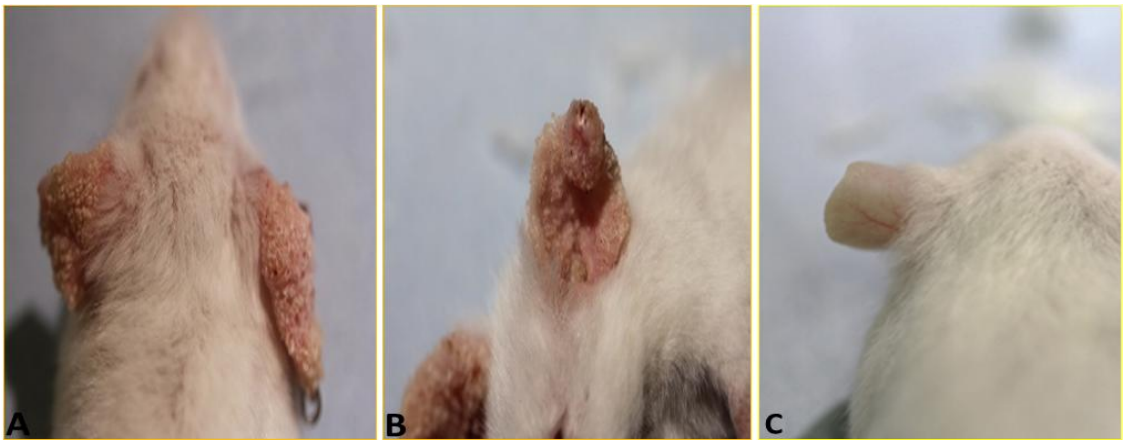

Figure 6-5 The phenotypes of RU486-treated *HK1.ras^{1276}.fos-K14creP/Δ5PTEN$^{flx/flx}$/Δ6-10Ecad$^{flx/flx}$* mice at 8-10 weeks (A&B) *HK1.ras^{1276}.fos-K14creP/Δ5PTEN$^{flx/flx}$/Δ6-10Ecad$^{flx/flx}$* mice show a specific phenotype characterised by bilateral tumours in TGE and NTGE. In contrast, (C) the age-matched *HK1.ras^{1276}-K14/Δ6-10Ecad$^{flx/flx}$* mice display no signs of tumour development.

Histologically, *HK1.ras^{1276}.fos-K14creP/Δ5PTEN$^{flx/flx}$/Δ6-10Ecad$^{flx/flx}$* mice at 8-10 weeks exhibited features consistent with malignant transformation, as observed at low power magnification (Figure 6-6). These features include cellular atypia, loss of normal architecture, rapid and progressive disorganisation in many regions of SCC relative to the surrounding epidermal architecture, and the presence of multiple irregular lobulated patterns infiltrating the surrounding dermal tissue, along with increased intercellular spaces. Immune cell infiltration was noted, indicating the invasive nature of the carcinoma and the transition into pdSCC (Figure 6-6).

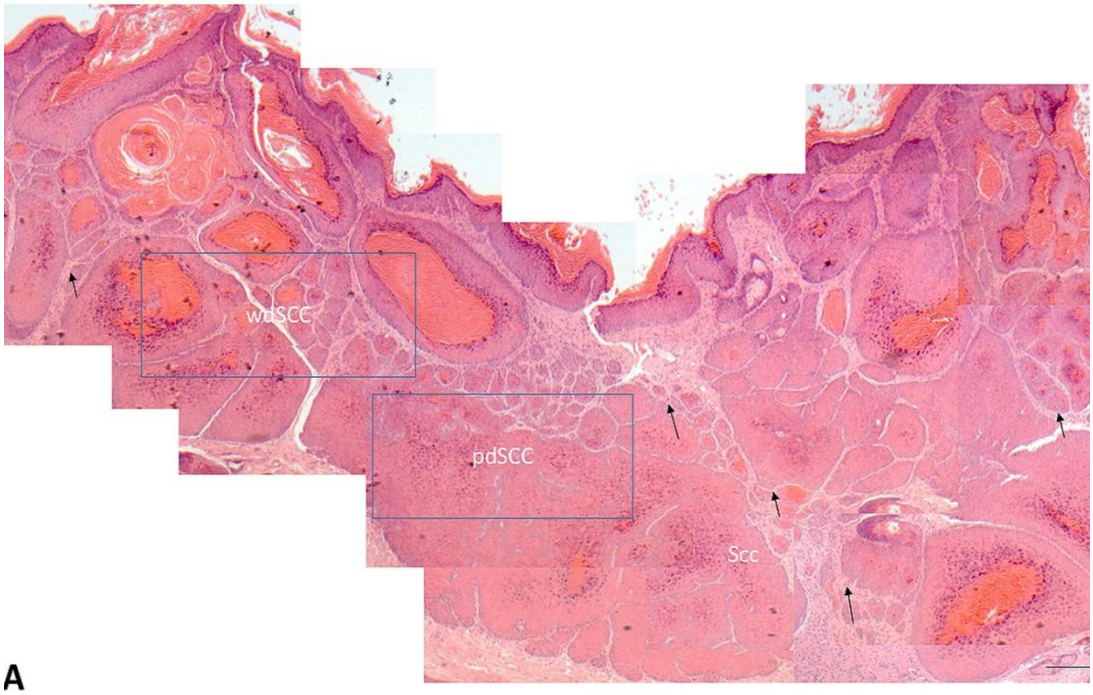

Figure 6-6 The histology of *HK1.ras^{1276}.fos-K14creP/Δ5PTEN$^{flx/flx}$/Δ6-10Ecad$^{flx/flx}$* SCC at 8-10 weeks *HK1.ras^{1276}.fos-K14creP/Δ5PTEN$^{flx/flx}$/Δ6-10Ecad$^{flx/flx}$* skin mice at low power magnification that shows features consistent with malignant transformation. These include cellular atypia, loss of normal architecture that many regions of wdSCC (box) display a rapid and progressive disorganisation relative to the surrounding epidermal architecture, and presence of multiple irregular lobulated patterns that infiltrate the surrounding dermal tissue (black arrows) along with immune cell infiltration, indicating the invasive nature of carcinoma and transition into SCC/pdSCC (box). (Scale bars: approx. 150 μm).

Higher magnification revealed that the tumours in these mice exhibited characteristics of an aggressive SCC histotype (Figure 6-7 A-C). This includes an increase in intercellular space, loss of cellular differentiation, increased pleomorphism, and more prominent mitotic activity. These features collectively suggest a more malignant and invasive phenotype compared to wdSCC.

In contrast, it was observed that the control *HK1.ras^{1276}.fos-K14creP/Δ5PTEN$^{flx/flx}$/Δ6-10Ecad$^{flx/het}$* mice exhibited wdSCC (Figure 6-7 D&E) similar to those observed in *HK1.ras.fos-K14creP/Δ5PTEN$^{flx/flx}$* mice. This suggests that the presence of the Δ6-10E-cadherin heterozygous mutation did not significantly alter the histopathological characteristics of the tumours and did not have a distinct impact on the tumour phenotype in this context.

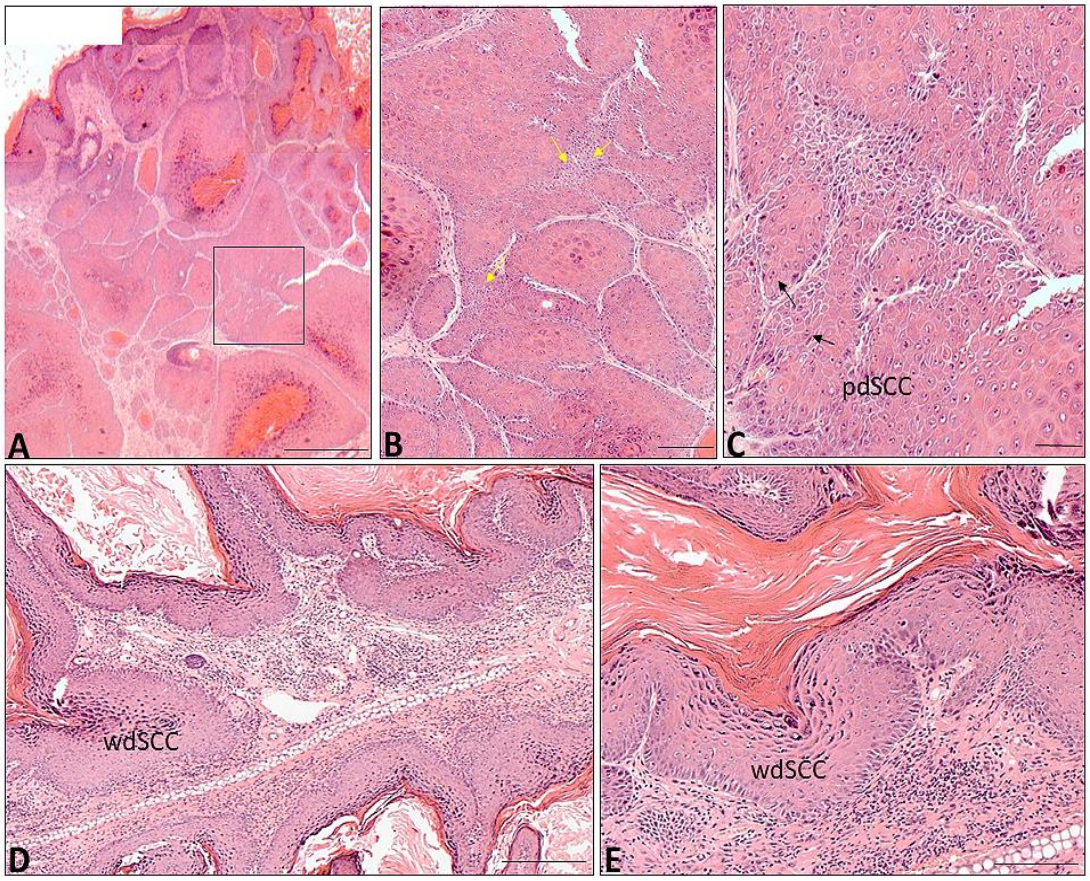

Figure 6-7 The histopathology of *HK1.ras^{1276}.fos-K14creP/Δ5PTEN$^{flx/flx}$/Δ6-10Ecad$^{flx/flx}$* mice at 8-10 weeks exhibits aggressive SCC compared to *HK1.ras^{1276}.fos-K14creP/Δ5PTEN$^{flx/flx}$/Δ6-10Ecad$^{flx/het}$* control that displays wdSCC (A-C) Different magnifications of RU486-treated *HK1.ras^{1276}.fos-K14creP/Δ5PTEN$^{flx/flx}$/Δ6-10Ecad$^{flx/flx}$* SCC/pdSCC progression. (A) Shows low magnification of *HK1.ras^{1276}.fos-K14creP/Δ5PTEN$^{flx/flx}$/Δ6-10Ecad$^{flx/flx}$* SCC with an area of progression into pdSCC (box). (B) Shows a higher magnification of *HK1.ras^{1276}.fos-K14creP/Δ5PTEN$^{flx/flx}$/Δ6-10Ecad$^{flx/flx}$* SCC/pdSCC keratinocytes exhibit infiltration into the dermis in tight finger-like projections, with clear intercellular spaces (yellow arrows), and in (C), at higher magnification, shows mitotic activity pdSCC (black arrows). (D&E) Low and high magnifications of *HK1.ras^{1276}.fos-K14creP/Δ5PTEN$^{flx/flx}$/Δ6-10Ecad$^{flx/het}$* histotype control that displays wdSCC similar to those in *HK1.ras.fos-K14creP/Δ5PTEN$^{flx/flx}$*. (Scale bars: A: 100μm; B: 75μm; C: 50μm; D: 100μm; E: 50μm).

These findings highlight the malignant progression in *HK1.ras^{1276}.fos-K14creP/Δ5PTEN$^{flx/flx}$/Δ6-10Ecad$^{flx/flx}$* mice by the development of an aggressive SCC histotype. The disorganisation in wdSCC areas indicates disrupted tissue architecture, a sign of tumour progression and invasion. The *HK1.ras^{1276}.fos-K14creP/Δ5PTEN$^{flx/flx}$/Δ6-10Ecad$^{flx/flx}$* SCC keratinocytes infiltrated the dermis in tight, finger-like projections, as shown in Figure 6-7 B and suggests a shift towards a highly invasive pdSCC. This histopathological feature is significant as it provides insights into the progression of malignancy and the invasive potential of tumour cells in this model. These tumours not only exhibit increased malignancy and aggressiveness but also show significant disorganisation, highlighting the dynamic and complex nature of tumour progression in this model.

These findings suggest an interplay between E-cadherin loss, PTEN loss, and oncogene activation in promoting tumour progression. The cooperation of these genetic alterations may contribute to the transformation of wdSCC into a more aggressive phenotype, characterised by pdSCC and enhanced invasion. The dysregulated signalling pathways associated with E-cadherin loss, such as the PI3K/AKT/mTOR pathway, may further drive the progression of SCC towards pdSCC. These molecular interactions may contribute to the differentiation patterns observed in the progression from wdSCC to pdSCC in the RU486-treated *HK1.ras.fos-K14creP/Δ5PTEN$^{flx/flx}$/Δ6-10Ecad$^{flx/flx}$* mice.

6.3.1 Analysis of Δ6-10 Ecadherin expression in *HK1.ras^{1276}.fos-K14creP/Δ5PTEN$^{flx/flx}$/Δ6-10Ecad$^{flx/flx}$* SCC

Immunofluorescence was used to determine Δ6-10E-cadherin expression in *HK1.ras^{1276}.fos-K14creP/Δ5PTEN$^{flx/flx}$/Δ6-10Ecad$^{flx/flx}$* genotypes at 8-10 weeks. Initially, positive Δ6-10E-cadherin expression was observed in areas of wdSCC (Figure 6-8 A), indicating an attempt to compensate for cell adhesion, as previously noted in earlier results chapters. However, as the tumour progressed to pdSCC, the mutant protein became non-functional, leading to rapid malignant progression. The subsequent reduction in Δ6-10E-cadherin expression correlated with the rapid progression from wdSCC to pdSCC (Figure 6-8 A&B) indicating a disruption of this compensatory response.

In contrast, in *HK1.ras*^{1276}*.fos-K14creP/Δ5PTEN*$^{flx/flx}$*/Δ6-10Ecad*$^{flx/het}$ controls (wdSCC), Δ6-10E-cadherin was strongly detected (Figure 6-8 C&D), indicating robust cell-cell adhesion and maintained epithelial integrity. This partial E-cadherin presence in the control aligns with a limitation in SCC progression to wdSCC, similar to that observed in the *HK1.ras.fos-K14creP/Δ5PTEN*$^{flx/flx}$ genotype.

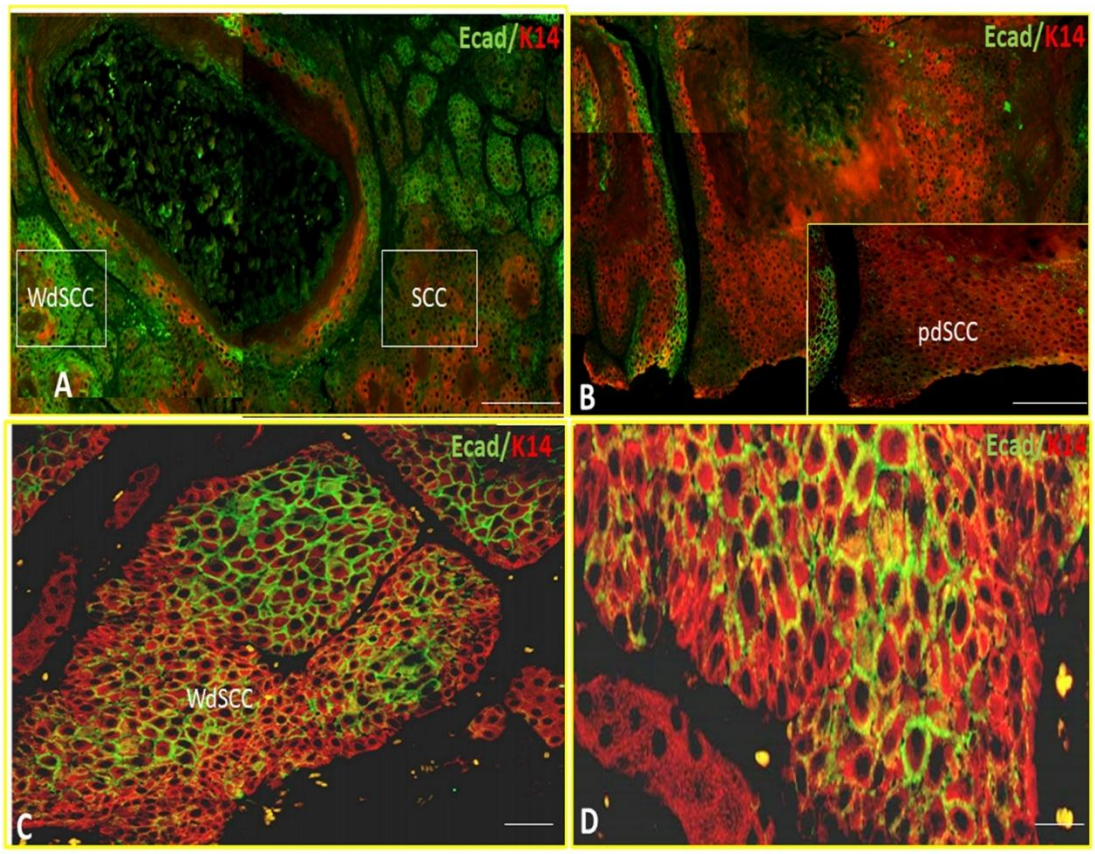

Figure 6-8 immunofluorescence analysis of Δ6-10E-cadherin expression in *HK1.ras*^{1276}*.fos-K14creP/Δ5PTENf*$^{lx/flx}$*/Δ6-10Ecad*$^{flx/flx}$ SCC progression at 8-10 weeks (A) Shows a reduction in Δ6-10E-cadherin as the tumour progresses, as expression is gradually reduced corresponding with the rapid progression from wdSCC (box) to (SCC) (box), and in (B) Δ6-10E-cadherin expression disappears in pdSCC areas. Conversely, in (C&D), low and high magnification of *HK1.ras*^{1276}*.fos-K14creP/Δ5PTEN*$^{flx/flx}$*/Δ6-10Ecad*$^{flx/het}$ wdSCC show that Δ6-10E-cadherin remains clearly membranous in the basal-suprabasal layer. (Scale bars: A: approx. 100 μm; B: 75 μm; C: 75 μm; D: 50 μm).

IHC was also used to determine Δ6-10E-cadherin expression in *HK1.ras*^{1276}*.fos-K14creP/Δ5PTEN*$^{flx/flx}$*/Δ6-10Ecad*$^{flx/flx}$ mice. A reduction in Δ6-10E-cadherin expression was observed in SCC as the tumour progressed from wdSCC to pdSCC (Figure 6-9 A-C), suggesting a loss of cell adhesion and increased invasion. Whereas in *HK1.ras*^{1276}*.fos-K14creP/Δ5PTEN*$^{flx/flx}$*/Δ6-10Ecad*$^{flx/het}$ controls wdSCC robust membranous-bound staining of Δ6-10E-cadherin (Figure 6-9 D&E) was observed, indicating attempts to maintain cell-cell adhesion and epithelial integrity. This study not only highlights the role of E-cadherin in maintaining cohesion but also positions it as a potential biomarker for EMT, useful in assessing SCC differentiation status and progression.

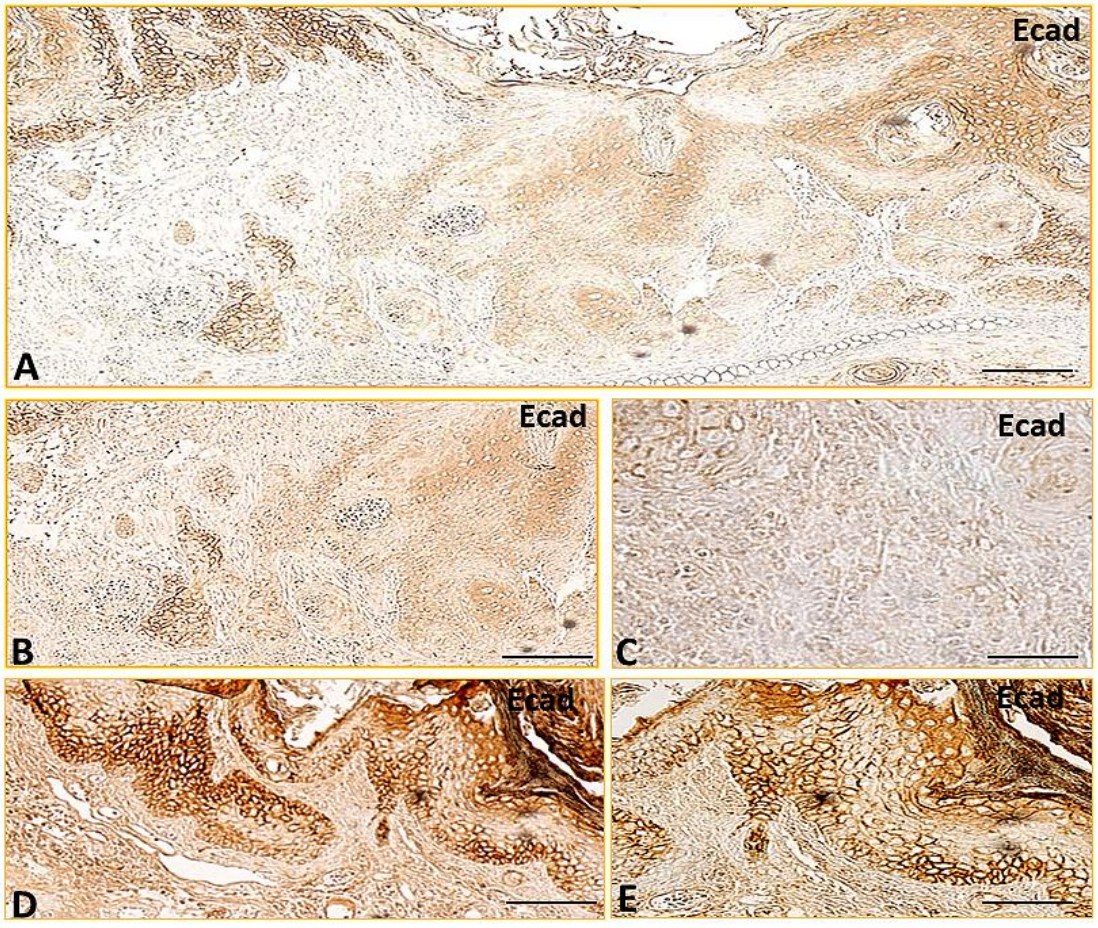

Figure 6-9 Immunohistochemistry analysis of Δ6-10E-cadherin expression in *HK1.ras*^{1276}*.fos-K14creP/Δ5PTEN*$^{flx/flx}$*/Δ6-10Ecad*$^{flx/flx}$ SCC at 8-10 weeks (A) Low magnification of *HK1.ras*^{1276}*.fos-K14creP/Δ5PTEN*$^{flx/flx}$*/Δ6-10Eacad*$^{flx/flx}$ SCC, where Δ6-10E-cadherin expression, with reduced visibility as SCC progresses rapidly into pdSCC. (B&C) Higher magnifications of *HK1.ras*^{1276}*.fos-K14creP/Δ5PTEN*$^{flx/flx}$*/Δ6-10Ecad*$^{flx/flx}$ SCC progression area, where Δ6-10E-cadherin expression further diminishes, compared to (D&E) *HK1.ras*^{1276}*.fos-K14creP/Δ5PTEN*$^{flx/flx}$*/Δ6-10Eacad*$^{flx/het}$ wdSCC control that shows Δ6-10E-cadherin expression prominently localised to the membranous regions of basal layer keratinocytes. (Scale bars: A: 150μm; B: 100μm; C: 50μm, D: 75μm; E: 50μm).

6.3.2 Analysis of β-catenin expression in *HK1.ras^{1276}.fos-K14creP/Δ5PTEN$^{flx/flx}$/Δ6-10E-cad$^{flx/flx}$* SCC

The expression and localisation of ß-catenin in *HK1.ras^{1276}.fos-K14creP/Δ5PTEN$^{flx/flx}$/Δ6-10Ecad$^{flx/flx}$* genotypes have been shown to be reduced, particularly in areas of pdSCC (Figure 6-10 C). ß-catenin typically plays a dual role in the cell, functioning in both cell adhesion and the Wnt signalling pathway (Gonzalez & Medici, 2014). In *HK1.ras^{1276}.fos-K14creP/Δ5PTEN$^{flx/flx}$/Δ6-10Ecad$^{flx/het}$* wdSCC controls, ß-catenin expression is often observed to be less nuclear and more membranous in the lower basal keratinocytes, which suggests a shift towards its role in cell adhesion via interactions with E-cadherin at the cell membrane (Jiang et al., 2007). This shift could be a compensatory response to maintain some degree of cellular adhesion in the presence of oncogenic signalling pathways.

Conversely, in SCC areas, where Δ6-10E-cadherin expression disappears, ß-catenin expression appears reduced (Figure 6-10 A-C). This reduction of ß-catenin could be attributed to the breakdown of the E-cadherin/ß-catenin complex, which is crucial for maintaining the stability and localisation of ß-catenin (Pires et al., 2017). The absence of Δ6-10E-cadherin in *HK1.ras^{1276}.fos-K14creP/Δ5PTEN$^{flx/flx}$/Δ6-10Ecad$^{flx/flx}$* SCC has been associated with destabilisation of ß-catenin, potentially leading to its degradation via proteasomal pathways or preventing its accumulation within the cells, resulting in its apparent reduction (Kim et al., 2019). When E-cadherin is lost, the stability of ß-catenin is compromised, affecting its intercellular levels and localisation, which can have profound implications on cellular functions and behaviour, particularly in the context of SCC progression. The reduction of ß-catenin suggests a disruption in Wnt signalling, which could contribute to the aggressive and undifferentiated phenotype observed in these tumours (Gonzalez & Medici, 2014).

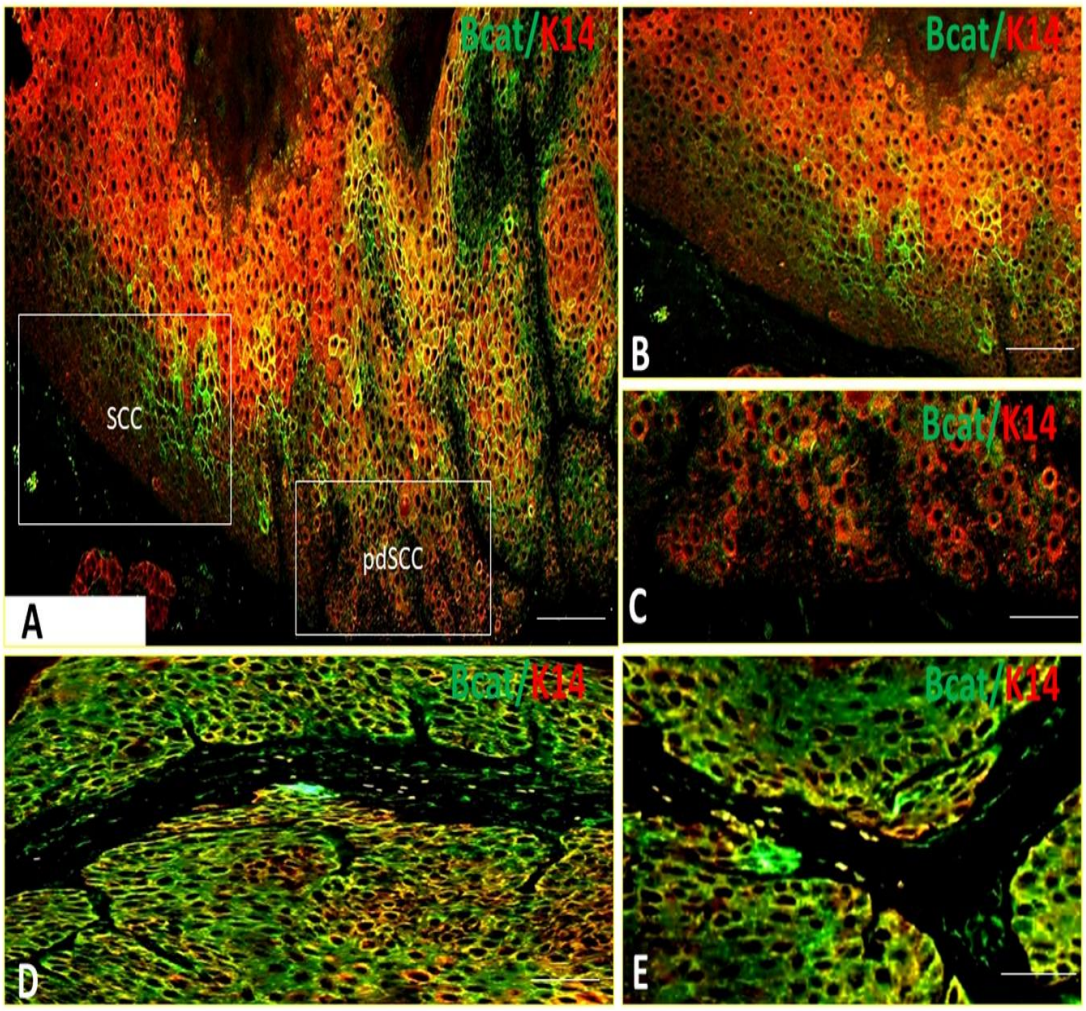

Figure 6-10 IF analysis of β-catenin expression in *HK1.ras^{1276}.fos-K14creP/Δ5PTEN$^{flx/flx}$/Δ6-10Ecad$^{flx/flx}$* SCC progression at 8-10 weeks (A) *HK1.ras^{1276}.fos-K14creP/Δ5PTEN$^{flx/flx}$/Δ6-10Ecad$^{flx/flx}$* shows β-catenin expression patterns during the progression of SCC into (B) pdSCC, where β-catenin expression appears to be reduced, and in (C) β-catenin expression is noticeably reduced and lost in the pdSCC region. (D&E) Low and high magnification of *HK1.ras^{1276}.fos-K14creP/Δ5PTEN$^{flx/flx}$/Δ6-10Ecad$^{flx/het}$* wdSCC controls show lower basal membranous B-catenin expression. (Scale bars: A: approx. 100μm; B-E: 75μm).

IHC demonstrated that ß-catenin expression was reduced, and this was associated with the progression of SCC. As the SCC advanced, ß-catenin expression was noticeably reduced (Figure 6-11 A&B), which was concurrently observed with the decrease in Δ6-10E-cadherin. This correlation implies that the loss of Δ6-10E-cadherin may lead to deregulation of ß-catenin, suggesting that their loss is an important factor in SCC pathogenesis (Kalluri & Weinberg, 2009).

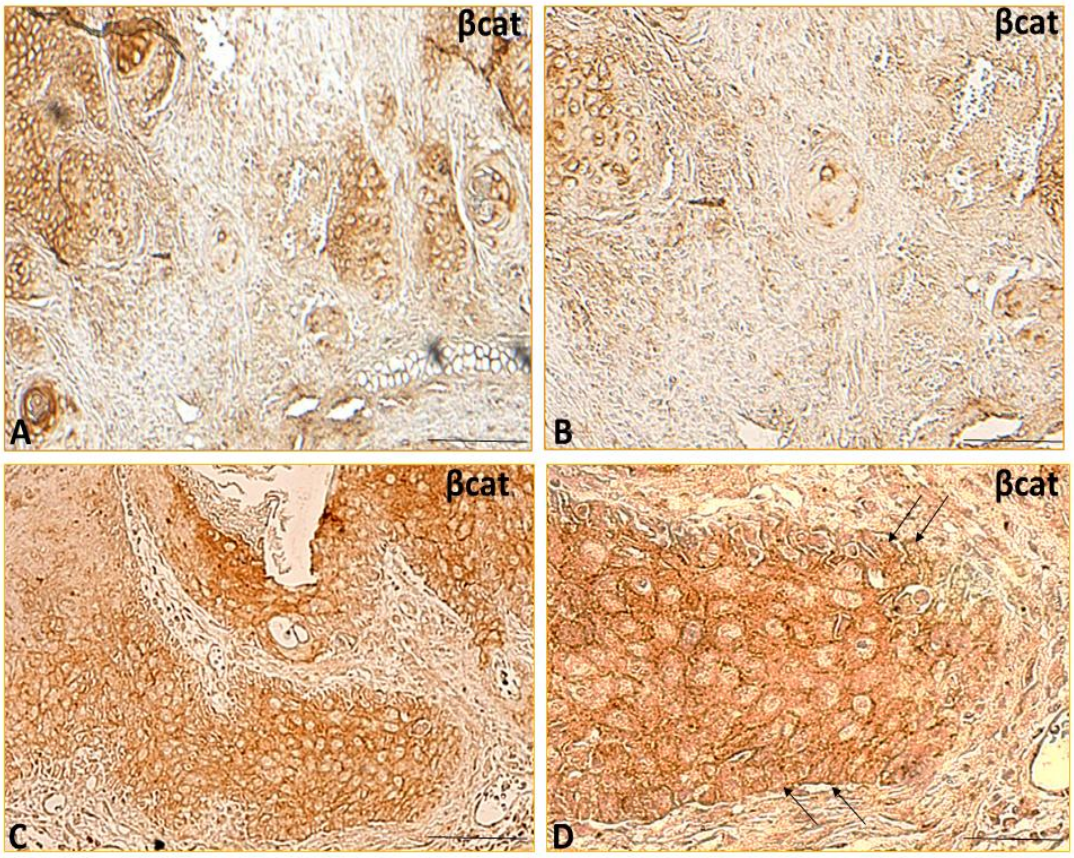

Figure 6-11 IHC analysis of β-catenin expression in *HK1.ras^{1276}.fos-K14creP/Δ5PTEN$^{flx/flx}$/Δ6-10Ecad$^{flx/flx}$* SCC progression at 8-10 weeks (A) Low magnification of *HK1.ras^{1276}.fos-K14creP/Δ5PTEN$^{flx/flx}$/Δ6-10Ecad$^{flx/flx}$* SCC progression that shows dysregulation of β-catenin localisation. (B) Shows higher magnification of *HK1.ras^{1276}.fos-K14creP/Δ5PTEN$^{flx/flx}$/Δ6-10Ecad$^{flx/flx}$* areas of pdSCC where β-catenin appears to be partially lost. (C&D) *HK1.ras^{1276}.fos-K14creP/Δ5PTEN$^{flx/flx}$/Δ6-10Ecad$^{flx/het}$* wdSCC control, where β-catenin expression becomes nuclear and basal (arrows). (Scale bars: A: 100μm; B: 50μm; C: 75μm, D: 50μm).

6.3.3 The analysis of K1 and p53 expressions in *HK1.ras^{1276}.fos-K14creP/Δ5PTEN$^{flx/flx}$/Δ6-10Ecad$^{flx/flx}$* SCC progression

The analysis of K1 expression in *HK1.ras^{1276}.fos-K14creP/Δ5PTEN$^{flx/flx}$/Δ6-10Ecad$^{flx/flx}$* SCC provides valuable insights into tumour progression and invasion, especially when combined with the results from Δ6-10E-cadherin and β-catenin expression studies. In *HK1.ras^{1276}.fos-K14creP/Δ5PTEN$^{flx/flx}$/Δ6-10Ecad$^{flx/het}$* wdSCC, K1 expression was robust and predominantly localised to the suprabasal/basal layers (Figure 6-11 C&D) reflecting the differentiation status of the SCC. However, in the *HK1.ras^{1276}.fos-K14creP/Δ5PTEN$^{flx/flx}$/Δ6-10Ecad$^{flx/flx}$* genotype, K1

expression became markedly reduced and disorganised, paralleling the loss of cellular differentiation and increased invasiveness (Figure 6-12 A&B).

This pattern of K1 expression was mirrored by changes in Δ6-10E-cadherin and ß-catenin expression. The deregulation of pathways involving ras and fos activation, combined with the loss of PTEN and E-cadherin function, exacerbates the partial loss of K1 and disorganisation of ß-catenin and Δ6-10E-cadherin expression, promoting aggressive tumour behaviour. The concurrent reduction and aberrant localisation of K1, Δ6-10E-cadherin, and ß-catenin serve as markers for the progression and invasive potential of SCC, highlighting the complex interplay of genetic alterations in tumour pathogenesis (Kalluri & Weinberg, 2009).

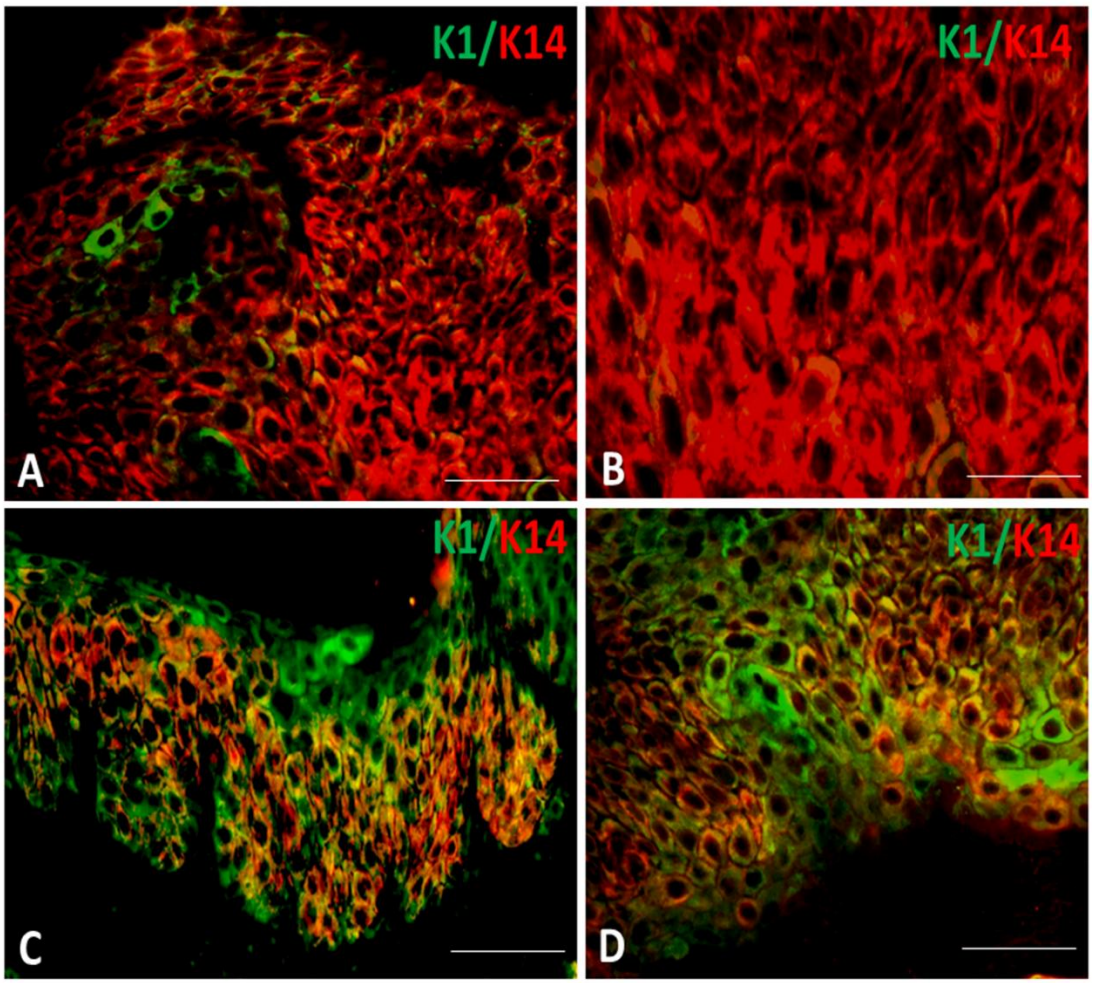

Figure 6-12 IF analysis of K1 expression in *HK1.ras^{1276}.fos-K14creP/Δ5PTEN$^{flx/flx}$/Δ6-10Ecad$^{flx/flx}$* SCC progression at 10 weeks (A&B) Show low and high magnifications of *HK1.ras^{1276}.fos-K14creP/Δ5PTEN$^{flx/flx}$/Δ6-10Ecad$^{flx/flx}$* pdSCC, where K1 expression is partially lost. While the expression is partially reduced in (C&D) low and high magnification of RU486-treated *HK1.ras^{1276}.fos-K14creP/Δ5PTEN$^{flx/flx}$/Δ6-10Ecad$^{flx/het}$* wdSCC. (Scale bars: A&C: 25μm; C&D: 50μm).

p53 expression was analysed in the *HK1.ras*^{1267}*.fos-K14creP/Δ5PTEN*$^{flx/flx}$*/Δ6-10Ecad*$^{flx/flx}$, model, and a progressive reduction in p53 expression was observed, correlating with SCC progression. At lower magnification (Figure 6-13 A), p53 expression appeared reduced, indicating the initial stage of downregulation of p53. This reduction became more pronounced at higher magnification (Figure 6-13 B). In contrast, *HK1.ras*^{1267}*.fos-K14creP/Δ5PTEN*$^{flx/flx}$*/Δ6-10Ecad*$^{flx/het}$ wdSCC retained partial p53 expression (Figure 6-13 C&D), suggesting that p53 may play a role in maintaining differentiation in these models.

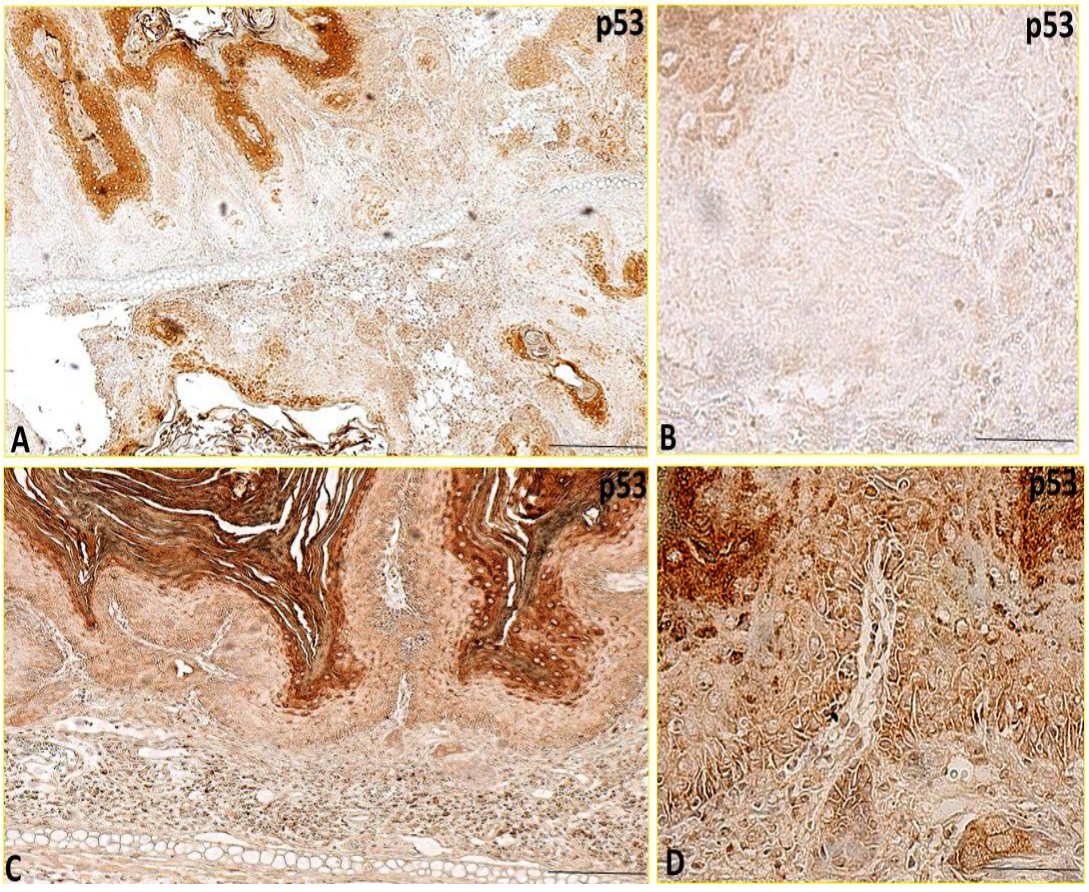

Figure 6-13 The analysis of p53 expression in *HK1.ras*^{1267}*.fos-K14creP/Δ5PTEN*$^{flx/flx}$*/Δ6-10Ecad*$^{flx/flx}$ SCC progression (A) Low magnification of *HK1.ras*^{1267}*.fos-K14creP/Δ5PTEN*$^{flx/flx}$*/Δ6-10Ecad*$^{flx/flx}$ SCC, showing a reduction in p53 expression, indicating the SCC progression. (B) Higher magnification of the same region, showing loss of p53 expression compared to (C&D) *HK1.ras*^{1267}*.fos-K14creP/Δ5PTEN*$^{flx/flx}$*/Δ6-10Ecad*$^{flx/het}$ wdSCC controls, p53 expression is partially maintained. (Scale bars: A&C: 100μm; B&D: 50μm).

6.4 summary

As detailed above, the loss of E-cadherin in RU486-treated *HK1.ras*^{1276}*.fos-K14creP/Δ5PTEN*$^{flx/flx}$*/Δ6-10Ecad*$^{flx/flx}$ mice has been demonstrated to play a crucial role in driving malignant conversion and progression to poorly differentiated SCC (pdSCC) (Figure 6-6), a phenomenon consistent with failure of cell-cell adhesion mechanisms (Figure 6-7) (Onder et al., 2008). This loss of E-cadherin has been associated with the induction of multiple downstream transcriptional pathways, including PIK3K/AKT, NF-KB, TGF-ß, and Wnt/ß-catenin, all of which contribute to increased tumour progression and invasiveness in this model. These findings highlight the importance of E-cadherin loss in SCC progression and emphasise its potential as a critical driver of tumour invasiveness (Onder et al., 2008).

Loss of E-cadherin in RU486-treated *HK1.ras*^{1276}*.fos-K14creP/Δ5PTEN*$^{flx/flx}$*/Δ6-10Ecad*$^{flx/flx}$ pdSCC is intricately linked to alterations in ß-catenin expression, which collectively contribute to the aggressive behaviour and progression of the SCC. This suggested that during E-cadherin loss in pdSCC, ß-catenin is no longer tethered to the cell membrane and can be phosphorylated and targeted for degradation by the destruction complex, which includes proteins such as APC and GSK-3ß (MacDonald et al., 2009). This also suggested that the loss of E-cadherin might disrupt the normal Wnt signalling dynamics, leading to inadequate nuclear translocation of ß-catenin and thus, its degradation. This loss of E-cadherin may also lead to changes in the expression of genes involved in ß-catenin regulation, further decreasing its levels.

Reduction of Δ6-10E-cadherin and ß-catenin expression in RU486-treated *HK1.ras*^{1276}*.fos-K14creP/Δ5PTEN*$^{flx/flx}$*/Δ6-10Ecad*$^{flx/flx}$ SCC progression may act as markers for the progression and invasive potential of SCC, underscoring the intricate interplay of genetic alterations in tumour pathogenesis (Mendonsa et al., 2018). The concurrent reduction in Δ6-10E-cadherin and ß-catenin, soon after p53 loss, has been linked to promoting the progression of SCC towards a more aggressive and invasive phenotype. The results suggest that the reduction of Δ6-10E-cadherin and ß-catenin contributes to the progression of SCC by potentially disrupting cell-cell adhesion mechanisms and promoting invasive behaviour.

These changes in E-cadherin and ß-catenin levels in cooperation with ras^{1276}, fos activation, and PTEN loss may induce alterations in downstream signalling pathways that propel tumour invasion, highlighting the significance of these molecules as markers for the aggressive nature of SCC. In contrast, the control RU486-treated *HK1.ras^{1276}.fos-K14creP/Δ5PTEN$^{flx/flx}$/Δ6-10Ecad$^{flx/het}$* mice displayed wdSCC similar to those in *HK1.ras.fos-K14creP/Δ5PTEN$^{flx/flx}$* mice, suggesting that the presence of the Δ6-10E-cadherin heterozygous mutation did not significantly alter the histopathological characteristics of the tumours or have a distinct impact on tumour phenotype in this context. This observation suggests that the heterozygous mutation in Δ6-10E-cadherin does not lead to substantial changes in tumour morphology or behaviour. This might be due to compensation by the remaining wild-type E-cadherin allele, which could preserve enough cell-cell adhesion and support wdSCC phenotype.

Studies have highlighted the significance of E-cadherin in maintaining contact inhibition and regulating cell motility, with the loss of E-cadherin expression linked to the loss of contact inhibition, increased cell motility, and progression to advanced stages of cancer (Mendonsa et al., 2018). The interplay between E-cadherin and ß-catenin at adherent junctions has been suggested to regulate the levels of free ß-catenin, impacting its ability to regulate target genes that support tumour invasion (Alice & Gumbiner, 2003). Thus, the loss of E-cadherin function may lead to alterations in the levels of free ß-catenin, affecting downstream signalling pathways and target gene expression related to tumour invasion (Alice & Gumbiner, 2003). The dysregulation of cell adhesion molecules, including E-cadherin, has been associated with tumour progression, emphasising roles for E-cadherin in cancer development.

Chapter 7 Discussion & future direction

The multi-stage skin carcinogenesis mouse model is a valuable tool for investigating the causality of E-cadherin and signalling pathways involved in carcinogenesis. This model, characterised by well-defined pathology associated with initiation, promotion, and malignant conversion, is particularly suitable for integration with transgenic technology to develop animal models for *in vivo* mechanistic studies. By utilising this model, research can identify systems that inhibit carcinogenesis at specific stages, to help elucidate the complex processes underlying tumour development (Yuspa, 2000). The epidermis deploys compensatory responses to maintain its homeostasis and inhibit tumour progression; a recurring theme observed across all findings in these experiments.

In this study, inducible E-cadherin ablation was introduced into a transgenic mouse skin model in conjunction with *ras* and/or *fos* oncogene activation, as well as inducible loss of the *PTEN* tumour suppressor gene. This approach aimed to elucidate the distinct stages of tumorigenesis and the impact of these mutations on tumour progression. It has also been used to identify the roles of E-cadherin in the formation of benign tumours, the transition to malignancy, and the progression to more aggressive tumours. Simultaneously, it investigates the role of E-cadherin in epidermal differentiation.

Carcinogenesis is a multifaceted process that progresses through various stages of tumour development. The conventional explanation of tumour progression involves the accumulation of driver mutations in cancer-related genes, which leads to successive waves of expansion of increasingly disordered cell clones (Jeanes et al., 2008). Tumorigenesis advances through a series of synergistic mutations that convert a normal cell into malignancy via premalignant intermediate stages (Hanahan, 2022). Among the critical changes in TSGs are alterations affecting cell-cell adhesion and signalling pathways, with E-cadherin playing a key role in maintaining cellular cohesion and tissue architecture. Its loss disrupts cell adhesion, contributing significantly to tumour progression and the invasive behaviour of cancer cells (Jeanes et al., 2008; Tinkle et al., 2008)

E-cadherin is a primary adhesion molecule in epithelia, and is frequently lost in human epithelial cancers, implicating its involvement in carcinogenesis (Christofori et al., 1998). Mutations in E-cadherin have been

shown to play a role not only in the later stages of carcinogenesis, progression, and invasion but also during the early stages of certain types of human cancer. For example, E-cadherin loss or mutation occurs in early-stage lobular breast carcinoma, where it disrupts cell adhesion and sets the stage for further tumorigenic changes (Berx et al., 1995). Similarly, in gastric cancer, E-cadherin mutations are found in initial lesions, contributing to tumour invasiveness as the tumour progresses (Becker et al., 1994). In ovarian cancer, altered E-cadherin expression has been associated with increased cell motility and invasion, even at relatively early stages of disease progression (Reddy et al., 2024). The loss of E-cadherin underscores its importance in tumour suppression, highlighting how its disruption facilitates tumour progression and invasion.

7.1 Endogenous E-cadherin expression in multistage *HK1.ras.fos-K14creP/Δ5PTEN*$^{flx/flx}$ skin mouse carcinogenesis is consistent with established scientific theories

The HK1 carcinogenesis model was optimal for investigating the potential roles of E-cadherin at various stages of tumour development (Greenhalgh et al., 1993c; Greenhalgh et al., 1993a; Greenhalgh et al., 1993b; Macdonald et al., 2014; Yao et al., 2006), due to the stage-specific stability of the induced phenotypes. Benign papillomas remain non-malignant (Greenhalgh et al., 1993c), unless additional oncogenic factors, like AKT activation through inducible PTEN loss at exon 5, are introduced (Macdonald et al., 2014).

In *HK1.ras* mice, the expression of E-cadherin in hyperplasia was observed and remained similar to that of normal controls, with consistent suprabasal layer membranous expression indicative of adherens junctions that contribute to epidermal barrier function. Conversely, in *HK1.ras.fos* papillomas, there was an increase in E-cadherin expression, primarily in the suprabasal layers, with occasional strands of positive basal-layer keratinocytes. This pattern may aid in inhibiting conversion in this model by facilitating appropriate cell-cell adhesion signalling to enhance adhesion and potentially signal the induction of p53 expression through β-catenin.

In RU486-treated *HK1.fos-K14creP//Δ5PTEN$^{flx/flx}$* KAs, there was an increase in the expression of E-cadherin, particularly transitioning from strong suprabasal expression to a strong basal expression. This pattern aligns with the protective function of E-cadherin against tumour invasion, contributing to its association with elevated levels of differentiation. The enhanced cell-cell adhesion resulting from this expression profile may contribute to the prevention of invasion in this model, potentially through signalling mechanisms that promote adhesion and involve p53-mediated regulation of ß-catenin, as supported by previous studies (Chiles et al., 2003; Jeanes et al., 2008). Thus, preserving membrane E-cadherin expression, which may contribute to the accelerated commitment to differentiation observed in these tumours. Sustained elevation of E-cadherin expression in KAs was associated with elevated basal levels of p53, which were further increased in parallel with the expression of basal K1. These compensatory mechanisms employed by the epidermis to preserve homeostasis, maintain cell-cell adhesion, and inhibit tumour progression are a consistent theme throughout the findings in these studies.

In *HK1.ras.fos-K14creP/Δ5PTEN$^{flx/flx}$* mice, the development of SCCs was observed. With the introduction of HK1.ras activation, the expression pattern differs from that of KAs, where E-cadherin displayed reduced levels (impacting cell-cell adhesion) following p53 loss within these SCCs. As the SCCs progress to poorly differentiated SCCs, E-cadherin expression was lost, coinciding with the loss of p53. Thus, the expression profile further supports the involvement of E-cadherin in facilitating malignant progression, as its loss in SCC impairs cell-cell adhesion at the invasive front. This observation aligns with the collective invasion patterns seen in human SCC (Hesse et al., 2016).

Analysis of endogenous E-cadherin expression indicates that its effects can vary depending on the context or stage of tumour development, as observed in early tumour stages in models such as *HK1.fos-K14creP/Δ5PTEN$^{flx/flx}$* KAs. Strong membranous E-cadherin expression appears to trigger a protective response mediated by TSGs such as p53, which acts to inhibit tumour progression. However, when the TSGs fail to prevent tumour progression, as observed in the later stages of *HK1.ras.fos-*

K14creP/Δ5PTEN$^{flx/flx}$ SCCs, E-cadherin loss appears to drive and enhance malignant progression.

These findings underscore the necessity for a more comprehensive understanding of the role of E-cadherin in tumorigenesis.

7.2 The cooperation of conditional ablation of E-cadherin and *HK1.ras* in transgenic mouse skin carcinogenesis

This study has highlighted the critical role of E-cadherin in driving malignant transformation of benign tumours, particularly in the context of ras activation. While activation of *HK1.ras* alone results in papilloma formation without progression to malignancy in 100% of animals, the additional loss of E-cadherin in the bi-genic RU486-treated *HK1.ras-K14creP/Δ6-10Ecad* cohorts exhibited signs of papilloma progression as early as 8-10weeks, accompanied by increasing intercellular gaps, suggesting cell-cell adhesion failure, which is an early event that drives malignant conversion and progression. The inducible loss of E-cadherin appears to facilitate an early onset of malignant progression and ultimately leads to the rapid conversion of papillomas into SCC (12 weeks). This finding highlights the pivotal role of conditional E-cadherin loss in tumour conversion, emphasising the essential contribution of wounding. In this context, wounding was a prerequisite for inducing papilloma formation, which subsequently allowed the conditional E-cadherin ablation to drive the transition of these late-stage papillomas into malignant tumours.

In RU486-treated *HK1.ras-K14creP/Δ6-10Ecad*$^{flx/het}$ models, the observation that reduced functional E-cadherin in *HK1.ras-K14creP/Δ6-10Ecad*$^{flx/het}$ papillomas correlated with the development of carcinoma *in situ* and early malignant wdSCC, but did not contribute to the initial papillomatogenesis, suggests a nuanced role for E-cadherin in the later stages of tumour progression. While the partial loss of E-cadherin did not influence the formation of papillomas, it appears to play a crucial role in the malignant transformation process, particularly in the transition from benign lesions to carcinoma *in situ* and early wdSCC. The collective mode of invasion in these lesions occurred in conjunction with a partial loss of E-cadherin expression (Onder et al., 2008). This partial loss of E-cadherin may

contribute to the organised yet invasive behaviour of cancer cells, as they retain some epithelial characteristics despite reduced E-cadherin expression (Onder et al., 2008).

Evidence supports this dual role of E-cadherin, with studies showing that its expression is sometimes maintained in invasive and metastatic carcinomas, where it paradoxically promotes tumour growth rather than inhibiting it (Onder et al., 2008). In these cases, cancer cells often invade surrounding tissues in a collective manner, as observed in this model, underscoring the complex role E-cadherin plays in cancer progression (Onder et al., 2008). In human pancreatic, colorectal, lung, and breast carcinomas, histopathological analysis revealed that groups of invading cancer cells have positive E-cadherin staining, suggesting that E-cadherin is retained during invasion (Kao et al., 2014). This retention is often associated with a partial epithelial-to-mesenchymal transition (P-EMT), where cancer cells acquire mesenchymal traits while maintaining epithelial markers such as E-cadherin, which allows them to migrate collectively (Aiello et al., 2018). Such observations further highlight the complex and multifaceted nature of the involvement of E-cadherin in cancer progression, suggesting that E-cadherin, while not fully lost, may contribute to tumour progression and collective invasion (Daulagala et al., 2019; Thiery & Sleeman, 2006). The specific correlation between reduced E-cadherin function and the advancement into carcinoma *in situ* highlights the importance of this protein in preventing further malignancy; however, its lack of involvement in papillomatogenesis suggests that other factors may be driving the initial tumour formation, with E-cadherin loss acting as a pivotal factor in the later, more aggressive stages of cancer development.

Progressing from the partial loss of E-cadherin observed in the heterozygous model, the complete loss in the RU486-treated *HK1.ras-K14creP/Δ6-10Ecad*$^{flx/flx}$ model further accelerated malignant conversion with rapid progression, leading to a more aggressive SCC. This is consistent with cell-cell adhesion failures by rapid progression from the collective mode of invasion, as observed in RU486-treated *HK1.ras-K14creP/Δ6-10Ecad*$^{flx/het}$ into the more aggressive individual mode of invasion in RU486-treated *HK1.ras-K14creP/Δ6-10Ecad*$^{flx/flx}$ model. Histological analysis, particularly

the expression of K1 and K14, suggests that invasion progresses from a collective mode of invasion in wdSCC to an individual mode of invasion.

Analysis of Δ6-10E-cadherin protein expression in *HK1.ras-K14creP/Δ6-10Ecad$^{flx/flx}$* papillomas, and carcinomas suggested ablation induces conversion, whereas the presence of Δ6-10E-cadherin expression suggested failed E-cadherin-mediated adhesion and associated signalling aids progression. The detected Δ6-10E-cadherin expression in papillomas and early wdSCC suggested that E-cadherin-dependent cell-cell adhesion is initially maintained, potentially preserving ß-catenin localisation and limiting early tumour progression. Likely as a compensatory mechanism to counteract the non-functional Δ6-10E-cadherin.

However, as SCCs progressed, the disappearance of Δ6-10E-cadherin indicated that this compensatory mechanism was no longer effective, resulting in complete loss of Δ6-10E-cadherin expression in pdSCC. The analysis also demonstrated that the complete functional E-cadherin ablation occurred in *HK1.ras-K14creP/Δ6-10Ecad$^{flx/flx}$* SCC progression was linked to a reduction in p53 expression, accompanied by increased nuclear ß-catenin expression in the invasive SCC basal layer, suggesting a failure in E-cadherin-mediated adhesion and associated signalling, which might be crucial for progression into pdSCC. These findings suggest that the failure of E-cadherin-mediated adhesion is a key event in the *HK1.ras-K14creP/Δ6-10Ecad^{flx}* model, driving malignant progression towards pdSCC. These results align with previous results using *HK1.ras.fos-K14creP/Δ5PTEN$^{flx/flx}$* models, where the loss of p53 was similarly associated with malignant progression (Macdonald et al., 2014; Masre et al., 2020).

The cooperation between E-cadherin loss and ras activation has been explored in various studies (Khan et al., 2016). In various human cancers, including pancreatic, colorectal, and lung cancers (Garinis et al., 2002; Khan et al., 2016; Winter et al., 2008). This correlation is often associated with a more aggressive tumour phenotype and poorer progression (Winter et al., 2008). The current study aligned with previous studies that showed conditional E-cadherin loss was associated with p53 loss, leading to the development of aggressive mammary tumours with metastatic potential in a mouse model (Derksen et al., 2006). Another study suggested that E-cadherin loss and p53 inactivation can cooperate to drive malignant

progression through enhanced Wnt/ß-catenin signalling, which in turn promotes the transcription of genes associated with cell proliferation and survival (Huang et al., 2015; Vijay et al., 2015).

These findings have confirmed that E-cadherin ablation, in conjunction with *HK1.ras* and other factors like p53 or ß-catenin signalling, can lead to more aggressive tumour conversion and progression into pdSCC.

7.3 *HK1.fos-K14creP/Δ5PTEN$^{flx/flx}$/Δ6-10Ecad$^{flx/flx}$* cooperation drives malignant conversion to wdSCC, while E-cadherin heterozygosity in HK1.fos-*K14creP/Δ5PTEN$^{flx/flx}$/Δ6-10Ecad^{flxhet}* elicits KAs as in *HK1.fos-K14creP/Δ5PTEN$^{flx/flx}$*

The investigation into *HK1.fos-K14creP/Δ5PTEN$^{flx/flx}$* during KA development showed that the loss of PTEN and the subsequent activation of AKT signalling resulted in the inactivation of GSK3ß through AKT. This triggered a compensatory response involving the p53/p21 pathway, which redirected the excessive proliferation of keratinocytes toward extensive differentiation, leading to the typical keratosis observed in classic KA.

This study served as the foundation for investigating the role of E-cadherin loss in this project, based on the hypothesis that E-cadherin plays a crucial role in the underlying mechanisms of tumour progression. This hypothesis was supported, as endogenous E-cadherin expression was elevated in *HK1.fos-K14creP/Δ5PTEN$^{flx/flx}$* KAs, with pronounced membranous E-cadherin expression observed. As previously mentioned, in the context of *HK1.fos-K14creP/Δ5PTEN$^{flx/flx}$* KAs, no malignancy was detected due to GSK3ß inactivation, which triggered compensatory p53 expression, a pattern consistent with observations in heterozygous *HK1.fos-K14creP/Δ5PTEN$^{flx/flx}$/Δ6-10Ecad$^{flx/het}$* KAs models, which also do not progress to malignancy.

In *HK1.fos-K14creP/Δ5PTEN$^{flx/flx}$/Δ6-10Ecad$^{flx/het}$* models, the analysis of ß-catenin expression in KAs revealed predominantly cytoplasmic localisation rather than nuclear accumulation. This finding suggests a crucial role for E-cadherin in sequestering ß-catenin to its cytoplasmic tail, perhaps inhibiting its nuclear translocation. Such sequestration could be instrumental in maintaining cell adhesion and promoting differentiation,

rather than allowing ß-catenin to drive proliferation through nuclear signalling pathways, thus limiting its translocation to the nucleus and moderating Wnt/ß-catenin signalling. This suggests that the regulation of ß-catenin by E-cadherin may serve as a key mechanism in modulating the balance between keratinocyte proliferation and differentiation, particularly in the context of KA development (Gottardi et al., 2001). Additionally, the dominance of p53 expression, particularly in the early stage of KA development, supports the idea that the compensatory p53 expression is crucial for preventing malignancy. The pronounced K1 expression further reinforces the observation that these models favour differentiation over malignant progression. The interplay between E-cadherin/ß-catenin signalling, p53 expression, and the PI3K/AKT pathway signalling contributes to maintaining this benign phenotype in these models. Consequently, this interaction highlights the importance of E-cadherin in cooperation with fos activation and PTEN loss in stabilising tissue architecture and preventing unchecked cellular proliferation, reinforcing its role as a critical mediator in the pathogenesis of KAs.

In contrast to the findings from the heterozygous models, the expression of Δ6-10E-cadherin in RU486-treated *HK1.fos-K14creP/Δ5PTEN$^{flx/flx}$/Δ6-10Ecad$^{flx/flx}$* was different. Initially, the tumours formed in this model displayed characteristics similar to KAs-like lesions. However, these lesions eventually converted into wdSCC (at 12 weeks), reinforcing the idea that complete E-cadherin ablation might be directly linked to a more aggressive and invasive tumour behaviour, in conjunction with fos activation and PTEN loss.

The slow conversion to malignancy observed in the RU486-treated *HK1.fos-K14creP/Δ5PTEN$^{flx/flx}$/Δ6-10Ecad$^{flx/flx}$* genotypes is likely due to the absence of critical pathways that typically drive Wnt signalling and subsequent tumour formation. This lack of signalling may inhibit progression toward a more aggressive SCC in these models. The observed reduction in Δ6-10E-cadherin expression in RU486-treated *HK1.fos-K14creP/Δ5PTEN$^{flx/flx}$/Δ6-10Ecad$^{flx/flx}$* mice highlights the disruption in cell-cell adhesion, which is crucial for maintaining tissue integrity. This disturbance in adhesion suggests a failure to maintain E-cadherin-mediated signalling, particularly the stabilisation of ß-catenin, which may lead to

dysregulated localisation and altered transcriptional activity. Such changes ultimately facilitate tumour progression to wdSCC with occasional SCC-like invasion patches.

Additionally, ß-catenin was localised predominantly to the cell membrane in both basal and suprabasal layers, with occasional cytoplasmic signal and no nuclear accumulation. This pattern suggests that the canonical Wnt/ß-catenin signalling pathway is not activated through nuclear translocation in these lesions. Previous studies have reported that reduced membranous ß-catenin expression correlated with E-cadherin loss in colorectal tumours, suggesting that similar mechanisms may be at play in tumour progression (Isinger-Ekstrand et al., 2011). While these findings do not demonstrate nuclear accumulation, the observed membranous distribution suggests that ß-catenin may primarily fulfil its structural role in adherens junctions in wdSCC within this model. These findings suggest that the interplay between E-cadherin, ß-catenin dysregulation, along with fos activation, and PTEN ablation creates an environment conducive to tumour progression and invasion.

In comparison to the RU486-treated *HK1.ras.fos-K14creP/Δ5PTEN$^{flx/flx}$/Δ6-10Ecad$^{flx/flx}$* model, progression was limited to wdSCC with occasional patches of SCC-like invasion. However, in the *HK1.ras.fos-K14creP/Δ5PTEN$^{flx/flx}$/Δ6-10Ecad$^{flx/flx}$* model, tumour progression was more aggressive, invasive, and rapid. This suggests that the addition of ras plays a crucial role in accelerating tumour progression and promoting a more invasive phenotype. As ras is a well-established oncogene involved in early tumour formation, particularly benign tumours and papillomas (Vicent et al., 2010). Its presence likely enhances oncogenic pathways such as the MAPK/ERK and PI3K/AKT (Christofori, 2003; Delire & Stärkel, 2015; Endo et al., 2013). These pathways, when combined with fos activation, PTEN loss, and E-cadherin ablation, amplify cellular proliferation, inhibit apoptosis, and disrupt cell adhesion (Hu et al., 2016; Kim et al., 2011), leading to more rapid and invasive tumour behaviour. Thus, the absence of ras in this model may explain the slower progression and less aggressive nature of the tumours.

These observations underline the significant impact of ras and fos activation, PTEN, and E-cadherin loss on tumour behaviour, providing a basis

for further exploration of their interactions in driving invasion and progression in the following sections of this discussion.

7.4 *HK1.ras^{1276}.fos-K14creP/Δ5PTEN$^{flx/flx}$/Δ6-10Ecad$^{flx/flx}$* cooperation drives malignant conversion and progression to pdSCC

This study focuses on the critical role of E-cadherin loss in driving SCC progression within the RU486-treated *HK1.ras^{1276}.fos-K14creP/Δ5PTEN$^{flx/flx}$/Δ6-10Ecad$^{flx/flx}$* models. Its loss initiates a cascade of molecular events that promotes aggressiveness, and in these models, the absence of E-cadherin leads to the activation of multiple downstream signalling pathways, including the Wnt/ß-catenin pathway, the PI3K/AKT pathway, and the MAPK pathway, all of which are known to facilitate malignant transformation and enhance cellular invasiveness (Boelens et al., 2016; Lau et al., 2013; Sasaki et al., 2000).

Analysis of the RU486-treated *HK1.ras^{1276}.fos-K14creP/Δ5PTEN$^{flx/flx}$/Δ6-10Ecad$^{flx/flx}$* model (at 8-10 weeks) indicates features consistent with rapid malignant conversion and progression. The observed disorganisation in SCC suggests a complex interplay between E-cadherin loss, the activation of the PTEN signalling pathway, and other oncogenic signalling networks that facilitates rapid malignant conversion and contributes to the invasive phenotypes of these tumours (Phelps et al., 2009). The activation of the PI3K/AKT pathway can provide survival signals that contribute to the aggressive behaviour of these tumours, while also promoting processes such as angiogenesis and invasion (Reddy et al., 2020). In addition, the activation of the MAPK pathway in response to E-cadherin loss may enhance cell proliferation and survival while promoting the expression of matrix metalloproteinases (MMPs) that facilitate invasion (Schulz et al., 2021). The presence of bilateral tumours (TGE & NTGE) in these models highlights the systemic impact of these oncogenic alterations, suggesting that the tumorigenic process is not confined to localised lesions (TGE). This bilateral tumour formation may reflect the aggressive proliferation driven by the synergistic activation of ras and fos, coupled with E-cadherin loss, PTEN inactivation, and alterations in the cellular microenvironment. The

widespread tumour development indicates a more complex interplay of signalling pathways that not only facilitate local tumour growth but also promote progression, emphasising the need to consider both localised and systemic therapeutic strategies in managing SCC driven by these oncogenic factors.

In these models, the depletion of E-cadherin directly disrupts the structural integrity of AJs, triggering the destabilisation of ß-catenin (Behrens et al., 1996). This study revealed that the loss of E-cadherin was associated with the unusual loss of ß-catenin expression from both cytoplasmic and nuclear compartments. While the loss of E-cadherin is often linked to increased cell motility and invasiveness, the specific dynamics observed in RU486-treated *HK1.ras^{1276}.fos-K14creP/Δ5PTEN$^{flx/flx}$/Δ6-10Ecad$^{flx/flx}$* models suggest a unique regulatory mechanism is at play. Numerous studies have demonstrated that E-cadherin downregulation weakens cell adhesion, allowing cancer cells to become more regulatory and invasive (Syed et al., 2008). Specifically, the loss of E-cadherin initiates a cascade of molecular events that promote aggressiveness and may be linked to EMT, a process central to cancer invasion and metastasis (Bure et al., 2019), which warrants further investigation in this context. In classical EMT models, the downregulation of E-cadherin frees ß-catenin, enabling its translocation to the nucleus, where it interacts with TCF/LEF transcription factors to promote oncogenic gene expression, leading to a more invasive phenotype (Jiang et al., 2017).

However, in the RU486-treated *HK1.ras^{1276}.fos-K14creP/Δ5PTEN$^{flx/flx}$/Δ6-10Ecad$^{flx/flx}$* model, the apparent reduction of ß-catenin, particularly from both membrane and nucleus in SCC progression areas, presents an unusual observation. Typically, ß-catenin translocates to the nucleus to drive oncogenic transcription through the Wnt signalling pathway. The loss of E-cadherin in this model suggests that ß-catenin may undergo enhanced degradation or face upstream inhibition, which differs from other reports where nuclear ß-catenin accumulation promotes tumour growth (W. Zhang et al., 2015). Another potential explanation lies in the activity of ICAT (Inhibitor of ß-catenin and T-cell factor), a small protein known to inhibit Wnt/ß-catenin signalling by preventing ß-catenin from binding to TCF/LEF and promoting its degradation or sequestration (Jiang et

al., 2017). This deviation from classical models highlights the unique behaviour of ß-catenin in the context of E-cadherin loss in RU486-treated *HK1.ras^{1276}.fos-K14creP/Δ5PTEN$^{flx/flx}$/Δ6-10Ecad$^{flx/flx}$* SCC provides new insights into how the Wnt pathway might be dysregulated.

The loss of E-cadherin has been closely linked with dedifferentiation in epithelial tissue, a finding corroborated by the reduced K1 expression in this study. In pdSCC, K1 expression was diminished, suggesting that its downregulation is a direct consequence of E-cadherin loss. The loss of E-cadherin not only weakens cell adhesion but also contributes to the progression to poorly differentiated, more invasive SCC phenotype, characteristics typical of advanced and aggressive tumours (Hu et al., 2011). This decreased K1 expression aligns with reports showing that tumours lacking E-cadherin are generally poorly differentiated and more aggressive (Manjula & Meghana, 2023). Thus, the findings in this model highlight the importance of E-cadherin in maintaining epithelial characteristics and suggest that its loss may serve as a driving factor in the progression towards a more aggressive SCC phenotype.

The immediate loss of p53, further amplifies the consequences of E-cadherin loss in RU486-treated *HK1.ras^{1276}.fos-K14creP/Δ5PTEN$^{flx/flx}$/Δ6-10Ecad$^{flx/flx}$* SCC models. The rapid loss of p53 highlights the conversion and progression of SCC in this model. Without p53, tumour cells that have already lost E-cadherin expression can evade programmed cell death more easily, contributing to the increased invasiveness observed in this model (Derksen et al., 2011). This dual loss likely activates compensatory pathways such as PI3K/AKT and NF-KB, which sustain tumour progression independently of Wnt signalling (Gustin et al., 2001).

The loss of E-cadherin in RU486-treated *HK1.ras^{1276}.fos-K14creP/Δ5PTEN$^{flx/flx}$/Δ6-10Ecad$^{flx/flx}$* SCC models not only initiate the breakdown of cell adhesion but also trigger widespread signalling disruption, leading to a more aggressive tumour phenotype. This emphasises the central role of E-cadherin as a gatekeeper of epithelial integrity, whose loss induces a profound shift in tumour behaviour. While these models provide crucial insights, it is important to acknowledge that transgenic mouse models may not fully recapitulate the complexity of human SCC. Therefore, future studies should focus on validating these molecular pathways in human SCC

tissue and further explore whether targeting the compensatory pathways activated after E-cadherin loss, such as the Wnt/ß-catenin signalling, PI3K/AKT activation, or upregulation of alternative adhesion molecules like N-cadherin, could provide new therapeutic strategies.

7.5 Future directions

While some model-specific future experiments have been outlined in the relevant results chapters, several features are common across all the K14creP-Ecadherin expression models described. These include clear effects on the epidermis, with hyperplasia and changes in cellular architecture characterised by increased intercellular spacing and cell-cell adhesion failure, which have been linked to disrupted keratinocyte-dermal interactions (Yin et al., 2021). It is crucial to quantify these changes and investigate the underlying mechanisms, as this may reveal insights into the role of keratinocyte-released factors in tumour microenvironment dynamics. Additionally, future studies should explore the following areas to address key aspects highlighted by these findings:

- **Comparative expression analysis:** Given the importance of loricrin and filaggrin in maintaining skin barrier integrity and promoting terminal keratinocyte differentiation (Olson et al., 2019). Future experiments should include a comparative analysis of loricrin and filaggrin expression across various stages of SCC. Investigation of their expression may help determine whether alterations in these late differentiation markers correlate with tumour progression. Furthermore, understanding their roles in keratinocyte maturation could provide insights into how disrupted differentiation contributes to SCC biology and potentially informs diagnostic or prognostic strategies.

- **Investigating N-cadherin and P-cadherin:** Exploring the expression of N-cadherin and P-cadherin in SCC models may provide information regarding EMT processes, even in the absence of classic EMT markers. This could highlight alternative pathways of tumour invasion and metastasis that do not follow traditional EMT paradigms.

- **Hair follicle interactions:** Given the importance of hair follicles as reservoirs for stem cells and their role in epithelial homeostasis (Kang et al., 2017), future research should also focus on investigating the expression of E-cadherin/ß-catenin in hair follicles using IF and IHC techniques. Understanding how these proteins are expressed within hair follicle structures and their interactions with surrounding keratinocytes may elucidate their roles in tumour biology and skin homeostasis.

- **Correlation with tumour aggressiveness:** A key area for future research will be to establish any correlations between the expression levels of the cadherins and tumour characteristics, such as invasiveness and clinical outcomes. This will involve integrating histological analysis with molecular profiling to elucidate how these proteins influence tumour behaviour.

- **Therapeutic targeting:** Investigating potential therapeutic strategies that either target N-cadherin or aim to restore E-cadherin function could provide novel avenues for intervention in SCC. Future studies should assess the impact of these strategies on tumour progression in preclinical models.

- **Investigating the inducible E-cadherin ablation in conjunction with ß-catenin activation:** Based on the well-established role of ß-catenin signalling in driving tumorigenesis (W. Zhang et al., 2015). Further experiments should be conducted in conjunction with the *HK1.ras* model to assess how the epidermis responds to E-cadherin loss and ß-catenin activation, particularly in relation to cellular adhesion. This will help determine whether these changes promote tumorigenesis.

- **Cadherin switching dynamics:** Lastly, future research should delve into the phenomenon of cadherin switching in SCC, to examine how the loss of E-cadherin and upregulation of N-cadherin and P-cadherin may affect tumour microenvironment interactions and overall tumour biology.

By addressing these future directions, the understanding of the molecular mechanisms underlying SCC progression can be significantly advanced, potentially leading to improved prognostic markers and therapeutic strategies.

7.6 Conclusion

The epidermis, being highly susceptible to environmental carcinogens, employs various defence mechanisms to prevent benign tumours, which can become compromised in aggressive papillomas, leading to malignant conversion. This model underscores the importance of both the environmental context and the timing of oncogenic events in relation to tumour suppressor responses, which shape the resulting tumour phenotype. The strong reaction to E-cadherin loss, similar to observations in HK1.ras/fos/PTEN models, suggests that this mechanism may also play a role in internal epithelia, potentially blocking the early transition from benign papilloma/KAs. However, these defences can be overcome during the progression to malignancy. Going forward, these findings will be crucial for a comprehensive understanding of the processes involved.

References

Abe, K., & Takeichi, M. (2008). EPLIN mediates linkage of the cadherin-catenin complex to F-actin and stabilizes the circumferential actin belt. *Proceedings of the National Academy of Sciences - PNAS*, 105 (1), 13-19.

Aiello, N. M., Maddipati, R., Norgard, R. J., Balli, D., Li, J., Yuan, S., Yamazoe, T., Black, T., Sahmoud, A., Furth, E. E., Bar-Sagi, D., & Stanger, B. Z. (2018). EMT Subtype Influences Epithelial Plasticity and Mode of Cell Migration. *Developmental Cell*, 45 (6), 681-695.e684.

Alice, S. T. W., & Gumbiner, B. M. (2003). Adhesion-Independent Mechanism for Suppression of Tumor Cell Invasion by E-cadherin. *The Journal of Cell Biology*, 161 (6), 1191-1203.

Alonso, L., & Fuchs, E. (2003). Stem Cells of the Skin Epithelium. *Proceedings of the National Academy of Sciences - PNAS*, 100 (Suppl 1), 11830-11835.

Bajpai, S., Feng, Y., Krishnamurthy, R., Longmore, G. D., & Wirtz, D. (2009). Loss of α-Catenin Decreases the Strength of Single E-cadherin Bonds between Human Cancer Cells. *The Journal of Biological Chemistry*, 284 (27), 18252-18259.

Balmain, A. (2020). The critical roles of somatic mutations and environmental tumor-promoting agents in cancer risk. *Nature Genetics*, 52 (11), 1139-1143.

Balmain, A., Ramsden, M., Bowden, G. T., & Smith, J. (1984). Activation of the mouse cellular Harvey-ras gene in chemically induced benign skin papillomas. *Nature (London)*, 307 (5952), 658-660.

Bankfalvi, A., Terpe, H. J., Breukelmann, D., Bier, B., Rempe, D., Pschadka, G., Krech, R., Lelle, R. J., & Boecker, W. (1999). Immunophenotypic and prognostic analysis of E-cadherin and ß-catenin expression during breast carcinogenesis and tumour progression: a comparative study with CD44. *Histopathology*, 34 (1), 25-34.

Basset-Séguin, N., Escot, C., Blanchard, J. M., Kerai, C., Verrier, B., Mion, H., & Guilhou, J. J. (1990). High Levels of c-fos Proto-Oncogene Expression

in Normal Human Adult Skin. *The Journal of Investigative Dermatology*, 94 (4), 418-422.

Becker, K. F., Atkinson, M. J., Reich, U., Becker, Nekarda, H., Siewert, & Hofler, H. (1994). E-cadherin gene-mutations provide clues to diffuse-type gastric carcinomas. *Cancer research (Chicago, Ill.)*, 54 (14), 3845-3852.

Behrens, J., Jerchow, B.-A., Wurtele, M., Grimm, J., Asbrand, C., Wirtz, R., Kuhl, M., Wedlich, D., & Birchmeier, W. (1998). Functional Interaction of an Axin Homolog, Conductin, with ß-Catenin, APC, and GSK3ß. *Science (American Association for the Advancement of Science)*, 280 (5363), 596-599.

Behrens, J., von Kries, J. P., Kühl, M., Bruhn, L., Wedlich, D., Grosschedl, R., & Birchmeier, W. (1996). Functional interaction of ß-catenin with the transcription factor LEF-1. *Nature (London)*, 382 (6592), 638-642.

Bennett, S. L., Basko-Plluska, J. L., Shea, C. R., & Bolotin, D. (2021). Role of Wnt signaling in dermatofibroma induction phenomenon. *The Journal of cutaneous pathology*, 48 (2), 217-220.

Berton, T. R., Wang, X.-J., Zhou, Z., Kellendonk, C., Schütz, G., Tsai, S., & Roop, D. R. (2000). Characterization of an inducible, epidermal-specific knockout system: Differential expression of lacZ in different Cre reporter mouse strains. *Genesis (New York, N.Y. : 2000)*, 26 (2), 160-161.

Berx, G., Cleton-Jansen, A. M., Nollet, F., Leeuw, W. J., Vijver, M., Cornelisse, C., & Roy, F. (1995). E-cadherin is a tumour/invasion suppressor gene mutated in human lobular breast cancers. *The EMBO Journal*, 14 (24), 6107-6115.

Bodnar, L., Stanczak, A., Cierniak, S., Smoter, M., Cichowicz, M., Kozlowski, W., Szczylik, C., Wieczorek, M., & Lamparska-Przybysz, M. (2014). Wnt/ß-catenin pathway as a potential prognostic and predictive marker in patients with advanced ovarian cancer. *The Journal of Ovarian Research*, 7 (1), 16-16.

Boelens, Mirjam C., Nethe, M., Klarenbeek, S., de Ruiter, Julian R., Schut, E., Bonzanni, N., Zeeman, Amber L., Wientjens, E., van der Burg, E., Wessels, L., van Amerongen, R., & Jonkers, J. (2016). PTEN Loss in E-

Cadherin-Deficient Mouse Mammary Epithelial Cells Rescues Apoptosis and Results in Development of Classical Invasive Lobular Carcinoma. *Cell Reports (Cambridge)*, 16 (8), 2087-2101.

Boussadia, O., Kutsch, S., Hierholzer, A., Delmas, V., & Kemler, R. (2002). E-cadherin is a survival factor for the lactating mouse mammary gland. *Mechanisms of Development*, 115 (1), 53-62.

Bozdogan, O., Vargel, I., Cavusoglu, T., Karabulut, A. A., Karahan, G., Sayar, N., Atasoy, P., & Yulug, I. G. (2016). Metastasis suppressor proteins in cutaneous squamous cell carcinoma. *Pathology, Research and Practice*, 212 (7), 608-615.

Brash, D. E., Ziegler, A., Jonason, A. S., Simon, J. A., Kunala, S., & Leffell, D. J. (1996). Sunlight and sunburn in human skin cancer: p53, apoptosis, and tumor promotion. *The Journal of Investigative Dermatology Symposium Proceedings*, 1 (2), 136.

Brown, K., Strathdee, D., Bryson, S., Lambie, W., & Balmain, A. (1998). The malignant capacity of skin tumours induced by expression of a mutant H-ras transgene depends on the cell type targeted. *Current Biology*, 8 (9), 516-524.

Bure, I. V., Nemtsova, M. V., & Zaletaev, D. V. (2019). Roles of E-cadherin and Noncoding RNAs in the Epithelial-mesenchymal Transition and Progression in Gastric Cancer. *International Journal of Molecular Sciences*, 20 (12), 2870.

Calautti, E., Li, J., Saoncella, S., Brissette, J. L., & Goetinck, P. F. (2005). Phosphoinositide 3-Kinase Signaling to AKT Promotes Keratinocyte Differentiation Versus Death. *The Journal of Biological Chemistry*, 280 (38), 32856-32865.

Candi, E., Oddi, S., Paradisi, A., Terrinoni, A., Ranalli, M., Teofoli, P., Citro, G., Scarpato, S., Puddu, P., & Melino, G. (2002). Expression of Transglutaminase 5 in Normal and Pathologic Human Epidermis. *The Journal of Investigative Dermatology*, 119 (3), 670-677.

Canel, M., Serrels, A., Frame, M. C., & Brunton, V. G. (2013). E-cadherin-integrin crosstalk in cancer invasion and metastasis. *The Journal of Cell Science*, 126 (Pt 2), 393-401.

Chakraborty, P. K., Lee, W.-K., Molitor, M., Wolff, N. A., & Thévenod, F. (2010). Cadmium induces Wnt signaling to upregulate proliferation and survival genes in sub-confluent kidney proximal tubule cells. *Molecular Cancer*, 9 (1), 102-102.

Chen, M.-L., Xu, P.-Z., Peng, X., Chen, W. S., Guzman, G., Yang, X., Di Cristofano, A., Pandolfi, P. P., & Hay, N. (2006). The deficiency of AKT1 is sufficient to suppress tumor development in Pten super(+/-) mice. *Genes & Development*, 20 (12), 1569-1574.

Chen, Y., & Hu, Y. (2023). Wnt Signaling Activation in Gingival Epithelial Cells and Macrophages of Experimental Periodontitis. *Dentistry Journal*, 11 (5), 129.

Chen, Z., Dempsey, D. R., Thomas, S. N., Hayward, D., Bolduc, D. M., & Cole, P. A. (2016). Molecular Features of Phosphatase and Tensin Homolog (PTEN) Regulation by C-terminal Phosphorylation. *The Journal of Biological Chemistry*, 291 (27), 14160-14169.

Chiles, M. C., Ai, L., Zuo, C., Fan, C.-Y., & Smoller, B. R. (2003). E-Cadherin Promoter Hypermethylation in Preneoplastic and Neoplastic Skin Lesions. *Modern Pathology*, 16 (10), 1014-1018.

Christmann, M., Tomicic, M. T., Aasland, D., & Kaina, B. (2007). A role for UV-light-induced c-Fos: stimulation of nucleotide excision repair and protection against sustained JNK activation and apoptosis. *Carcinogenesis (New York)*, 28 (1), 183-190.

Christofori, G. (2003). Changing neighbours, changing behaviour: cell adhesion molecule-mediated signalling during tumour progression. *The EMBO Journal*, 22 (10), 2318-2323.

Christofori, G., Perl, A.-K., Wilgenbus, P., Dahl, U., & Semb, H. (1998). A causal role for E-cadherin in the transition from adenoma to carcinoma. *Nature (London)*, 392 (6672), 190-193.

Conacci-Sorrell, M., Zhurinsky, J., & Ben-Ze'ev, A. (2002). The cadherin-catenin adhesion system in signaling and cancer. *The Journal of Clinical Investigation*, 109 (8), 987-991.

Curran, T., & Teich, N. M. (1982). Candidate product of the FBJ murine osteosarcoma virus oncogene: characterization of a 55,000-dalton phosphoprotein. *The Journal of Virology*, 42 (1), 114-122.

Dalle Vedove, A., Falchi, F., Donini, S., Dobric, A., Germain, S., Di Martino, G. P., Prosdocimi, T., Vettraino, C., Torretta, A., Cavalli, A., Rigot, V., André, F., & Parisini, E. (2019). Structure-Based Virtual Screening Allows the Identification of Efficient Modulators of E-cadherin-Mediated Cell–Cell Adhesion. *International Journal of Molecular Sciences*, 20 (14), 3404.

Daulagala, A. C., Bridges, M. C., & Kourtidis, A. (2019). E-cadherin Beyond Structure: A Signaling Hub in Colon Homeostasis and Disease. *International Journal of Molecular Sciences*, 20 (11), 2756.

Davis, M. A., Ireton, R. C., & Reynolds, A. B. (2003). A Core Function for p120-Catenin in Cadherin Turnover. *The Journal of Cell Biology*, 163 (3), 525-534.

Delire, B., & Stärkel, P. (2015). The Ras/MAPK pathway and hepatocarcinoma: pathogenesis and therapeutic implications. *European Journal of Clinical Investigation*, 45 (6), 609-623.

Deng, T., & Karin, M. (1994). c-Fos transcriptional activity stimulated by H-Ras-activated protein kinase distinct from JNK and ERK. *Nature (London)*, 371 (6493), 171-175.

Der, C. J., Finkel, T., & Cooper, G. M. (1986). Biological and biochemical properties of human rasH genes mutated at codon 61. *Cell*, 44 (1), 167-176.

Derksen, P. W. B., Braumuller, T. M., van der Burg, E., Hornsveld, M., Mesman, E., Wesseling, J., Krimpenfort, P., & Jonkers, J. (2011). Mammary-specific inactivation of E-cadherin and p53 impairs functional gland development and leads to pleomorphic invasive lobular carcinoma in mice. *Disease Models & Mechanisms*, 4 (3), 347-358.

Derksen, P. W. B., Liu, X., Saridin, F., van der Gulden, H., Zevenhoven, J., Evers, B., van Beijnum, J. R., Griffioen, A. W., Vink, J., Krimpenfort, P., Peterse, J. L., Cardiff, R. D., Berns, A., & Jonkers, J. (2006). Somatic inactivation of E-cadherin and p53 in mice leads to metastatic lobular mammary carcinoma through induction of anoikis resistance and angiogenesis. *Cancer Cell*, 10 (5), 437-449.

Di Cunto, F., Topley, G., Calautti, E., Hsiao, J., Ong, L., Seth, P. K., & Dotto, G. P. (1998). Inhibitory Function of p21 {Cip1/WAF1} in Differentiation of Primary Mouse Keratinocytes Independent of Cell Cycle Control. *Science (American Association for the Advancement of Science)*, 280 (5366), 1069-1072.

DiGiovanni, J., Abel, E. L., Angel, J. M., & Kiguchi, K. (2009). Multi-stage chemical carcinogenesis in mouse skin: Fundamentals and applications. *Nature Protocols*, 4 (9), 1350-1362.

Djalilian, A. R. (2006). Connexin 26 regulates epidermal barrier and wound remodeling and promotes psoriasiform response. *The Journal of Clinical Investigation*, 116 (5), 1243-1253.

Doma, E., Rupp, C., & Baccarini, M. (2013). EGFR-ras-raf signaling in epidermal stem cells: roles in hair follicle development, regeneration, tissue remodeling and epidermal cancers. *International Journal of Molecular Sciences*, 14 (10), 19361-19384.

Drees, F., Pokutta, S., Yamada, S., Nelson, W. J., & Weis, W. I. (2005). α-catenin is a Molecular Switch that binds E-cadherin-ß-catenin and regulates actin filament Assembly. *Cell*, 123 (5), 903-915.

Endo, M., Yamamoto, H., Iwasaki, H., Dobashi, Y., Nishiyama, K., Iwamoto, Y., Oda, Y., Setsu, N., Kohashi, K., Takahashi, Y., Ishii, T., Lida, K.-I., Matsumoto, Y., Hakozaki, M., & Aoki, M. (2013). Prognostic Significance of AKT/mTOR and MAPK Pathways and Antitumor Effect of mTOR Inhibitor in NF1-Related and Sporadic Malignant Peripheral Nerve Sheath Tumors. *Clinical Cancer Research*, 19 (2), 450-461.

Fessler, M. B., Rudel, L. L., & Brown, J. M. (2009). Toll-like receptor signaling links dietary fatty acids to the metabolic syndrome. *Current Opinion In Lipidology*, 20 (5), 379-385.

Fisher, C., Byers, M. R., Iadarola, M. J., & Powers, E. A. (1991). Patterns of epithelial expression of Fos protein suggest important role in the transition from viable to cornified cell during keratinization. *Development (Cambridge)*, 111 (2), 253-258.

Fistarol, S. K., Anliker, M. D., & Itin, P. H. (2002). Cowden disease or multiple hamartoma syndrome--cutaneous clue to internal malignancy. *EJD. European Journal of Dermatology*, 12 (5), 411.

Fuchs, E. (2007). Scratching the surface of skin development. *Nature (London)*, 445 (7130), 834-842.

Fuchs, E., & Green, H. (1980). Changes in keratin gene expression during terminal differentiation of the keratinocyte. *Cell*, 19 (4), 1033-1042.

Fuchs, E., & Raghavan, S. (2002). Getting under the skin of epidermal morphogenesis. *Nature Reviews. Genetics*, 3 (3), 199-209.

Fujii, T., Duarte, S., Lee, E., Ke, B., Busuttil, R. W., & Coito, A. J. (2020). Tissue Inhibitor of Metalloproteinase 3 Deficiency Disrupts the Hepatocyte E-Cadherin/ß-Catenin Complex and Induces Cell Death in Liver Ischemia/Reperfusion Injury. *Liver Transplantation*, 26 (1), 113-126.

Fukunaga, Y., Liu, H. J., Shimizu, M., Komiya, S., Kawasuji, M., & Nagafuchi, A. (2005). Defining the roles of beta-catenin and plakoglobin in cell-cell adhesion: Isolation of beta-catenin/plakoglobin-deficient F9 cells. *Cell Structure and Function*, 30 (1-2), 25-34.

Gall, T. M. H., & Frampton, A. E. (2013). Gene of the month: E-cadherin (CDH1). *The Journal of Clinical Pathology*, 66 (11), 928-932.

Gao, Y., Yan, Y., Guo, J., Zhang, Q., Bi, D., Wang, F., Chang, Z., Lu, L., Yao, X., & Wei, Q. (2019). HNF-4α downregulation promotes tumor migration and invasion by regulating E-cadherin in renal cell carcinoma. *Oncology Reports*, 42 (3), 1066-1074.

Garinis, G. A., Menounos, P. G., Spanakis, N. E., Papadopoulos, K., Karavitis, G., Parassi, I., Christeli, E., Patrinos, G. P., Manolis, E. N., & Peros, G. (2002). Hypermethylation-associated transcriptional silencing of E-cadherin in primary sporadic colorectal carcinomas. *The Journal of Pathology*, 198 (4), 442-449.

Gavert, N., & Ben-Ze'ev, A. (2007). ß-Catenin signaling in biological control and cancer. *The Journal of Cellular Biochemistry*, 102 (4), 820-828.

Georgopoulos, N. T., Kirkwood, L. A., Walker, D. C., & Southgate, J. (2010). Differential regulation of growth-promoting signalling pathways by E-cadherin. *PloS One*, 5 (10), e13621.

Glick, A. B., Sporn, M. B., & Yuspa, S. H. (1991). Altered Regulation of TGF-ß1 and TGF-α in Primary Keratinocytes and Papillomas Expressing v-Ha-ras. *Molecular Carcinogenesis*, 4 (3), 210-219.

Goldenberg, G., & Harris, T. J. C. (2013). Adherens Junction Distribution Mechanisms during Cell-Cell Contact Elongation in Drosophila. *PloS One*, 8 (11), e79613.

Gonzalez, D. M., & Medici, D. (2014). Signaling mechanisms of the epithelial-mesenchymal transition. *Science Signaling*, 7 (344), re8-re8.

Gottardi, C. J., Wong, E., & Gumbiner, B. M. (2001). E-Cadherin Suppresses Cellular Transformation by Inhibiting ß-Catenin Signaling in an Adhesion-Independent Manner. *The Journal of Cell Biology*, 153 (5), 1049-1059.

Gravdal, K., Halvorsen, O. J., Haukaas, S. A., & Akslen, L. A. (2007). A Switch from E-Cadherin to N-Cadherin Expression Indicates Epithelial to Mesenchymal Transition and Is of Strong and Independent Importance for the Progress of Prostate Cancer. *Clinical Cancer Research*, 13 (23), 7003-7011.

Green, K. J., Geiger, B., Jonathan, C. R. J., Talian, J. C., & Goldman, R. D. (1987). The Relationship between Intermediate Filaments and Microfilaments before and during the Formation of Desmosomes and Adherens-Type Junctions in Mouse Epidermal Keratinocytes. *The Journal of Cell Biology*, 104 (5), 1389-1402.

Green, K. J., & Jones, J. C. R. (1996). Desmosomes and hemidesmosomes: structure and function of molecular components. *The FASEB Journal*, 10 (8), 871-881.

Green, K. J., Simpson, C. L., & Patel, D. M. (2011). Deconstructing the skin: cytoarchitectural determinants of epidermal morphogenesis. *Nature Reviews. Molecular Cell Biology*, 12 (9), 565-580.

Greenhalgh, D. A., Quintanilla, M. I., Orengo, C. C., Barber, J. L., Eckhardt, J. N., Rothnagel, J. A., & Roop, D. R. (1993c). Cooperation between v-fos and v-rasHA induces autonomous papillomas in transgenic epidermis but not malignant conversion. *Cancer Research (Chicago, Ill.)*, 53 (21), 5071-5075.

Greenhalgh, D. A., & Roop, D. R. (1994). Dissecting Molecular Carcinogenesis: Development Of Transgenic Mouse Models By Epidermal Gene Targeting. In *Advances in Cancer Research*. *Elsevier Science & Technology*, 64, 247-296.

Greenhalgh, D. A., Rothnagel, J. A., Quintanilla, M. I., Orengo, C. C., Gagne, T. A., Bundman, D. S., Longley, M. A., & Roop, D. R. (1993a). Induction of epidermal hyperplasia, hyperkeratosis, and papillomas in transgenic mice by a targeted v-Ha-ras oncogene. *Molecular Carcinogenesis*, 7 (2), 99-110.

Greenhalgh, D. A., Rothnagel, J. A., Wang, X. J., Quintanilla, M. I., Orengo, C. C., Gagne, T. A., Bundman, D. S., Longley, M. A., Fisher, C., & Roop, D. R. (1993b). Hyperplasia, hyperkeratosis and benign tumor production in transgenic mice by a targeted v-fos oncogene suggest a role for fos in epidermal differentiation and neoplasia. *Oncogene*, 8 (8), 2145.

Greenhalgh, D. A., Wang, X. J., Eckhardt, J. N., & Roop, D. R. (1995). 12-O-tetradecanoylphorbol-13-acetate promotion of transgenic mice expressing epidermal-targeted v-fos induces rasHA-activated papillomas and carcinomas without p53 mutation: association of v-fos expression with promotion and tumor autonomy. *Cell Growth & Differentiation*, 6 (5), 579.

Greenhalgh, D. A., Welty, D. J., Player, A., & Yuspa, S. H. (1990). Two Oncogenes, v-Fos and v-Ras, Cooperate to Convert Normal Keratinocytes to Squamous Cell Carcinoma. *Proceedings of the National Academy of Sciences - PNAS*, 87 (2), 643-647.

Greenhalgh, D. A., Welty, D. J., Strickland, J. E., & Yuspa, S. H. (1989). Spontaneous Ha-ras Gene Activation in Cultured Primary Murine Keratinocytes: Consequences of Ha-ras Gene Activation in Malignant Conversion and Malignant Progression. *Molecular Carcinogenesis*, 2 (4), 199-207.

Greenhalgh, D. A., & Yuspa, S. H. (1988). Malignant conversion of murine squamous papilloma cell lines by transfection with the fos oncogene. *Molecular Carcinogenesis*, 1 (2), 134-143.

Grigoryan, T., Wend, P., Klaus, A., & Birchmeier, W. (2008). Deciphering the function of canonical Wnt signals in development and disease: conditional loss- and gain-of-function mutations of beta-catenin in mice. *Genes & Development*, 22 (17), 2308-2341.

Guinea-Viniegra, J., Zenz, R., Scheuch, H., Jiménez, M., Bakiri, L., Petzelbauer, P., & Wagner, E. F. (2012). Differentiation-induced skin cancer suppression by Fos, p53, and TACE/ADAM17. *The Journal of Clinical Investigation*, 122 (8), 2898-2910.

Gustin, J. A., Maehama, T., Dixon, J. E., & Donner, D. B. (2001). The PTEN Tumor Suppressor Protein Inhibits Tumor Necrosis Factor-induced Nuclear Factor κB Activity. *The Journal of Biological Chemistry*, 276 (29), 27740-27744.

Hakim, S. G., Taubitz, C., Hoppe, S., Steller, D., Rades, D., Ribbat-Idel, J., Alsharif, U., & Falougy, M. (2023). Prognostic impact of the loss of E-cadherin and de novo expression of N-cadherin at the invasive front of primary and recurrent oral squamous cell carcinoma. *Frontiers In Oncology*, 13, 1151879-1151879.

Hanahan, D. (2022). Hallmarks of Cancer: New Dimensions. *Cancer Discovery*, 12 (1), 31-46.

Hanahan, D., & Weinberg, R. A. (2000). The Hallmarks of Cancer. *Cell*, 100 (1), 57-70.

Hanahan, D., & Weinberg, Robert A. (2011). Hallmarks of Cancer: The Next Generation. *Cell*, 144 (5), 646-674.

Hartsock, A., & Nelson, W. J. (2008). Adherens and tight junctions: Structure, function and connections to the actin cytoskeleton. *Biochimica et Biophysica Acta*, 1778 (3), 660-669.

Haslehurst, A. M., Koti, M., Dharsee, M., Nuin, P., Evans, K., Geraci, J., Childs, T., Chen, J., Li, J., Weberpals, J., Davey, S., Squire, J., Park, P. C., & Feilotter, H. (2012). EMT transcription factors snail and slug directly contribute to cisplatin resistance in ovarian cancer. *BMC Cancer*, 12 (1), 91-91.

Hennings, H., Glick, A. B., Greenhalgh, D. A., Morgan, D. L., Strickland, J. E., Tennenbaum, T., & Yuspa, S. H. (1993). Critical Aspects of Initiation, Promotion, and Progression in Multistage Epidermal Carcinogenesis. *Proceedings of the Society for Experimental Biology and Medicine*, 202 (1), 1-8.

Hesse, K., Satzger, I., Schacht, V., Köther, B., Hillen, U., Klode, J., Schaper, K., & Gutzmer, R. (2016). Characterisation of Prognosis and Invasion

of Cutaneous Squamous Cell Carcinoma by Podoplanin and E-cadherin Expression. *Dermatology (Basel)*, 232 (5), 558-565.

Hinck, L., Näthke, I. S., Papkoff, J., & Nelson, W. J. (1994). Dynamics of Cadherin/Catenin Complex Formation: Novel Protein Interactions and Pathways of Complex Assembly. *The Journal of Cell Biology*, 125 (6), 1327-1340.

Hobbs, G. A., Der, C. J., & Rossman, K. L. (2016). RAS isoforms and mutations in cancer at a glance. *The Journal of Cell Science*, 129 (7), 1287-1292.

Hollstein, M., Soussi, T., Thomas, G., von Brevern, M. C., & Bartsch. (1997). P53 gene alterations in human tumors: perspectives for cancer control. *Recent Results In Cancer Research*, 143, 369.

Hopkins, B. D., & Parsons, R. E. (2014). Molecular pathways: intercellular PTEN and the potential of PTEN restoration therapy. *Clinical Cancer Research*, 20 (21), 5379-5383.

Hu, Q. P., Kuang, J. Y., Yang, Q. K., Bian, X. W., & Yu, S. C. (2016). Beyond a tumor suppressor: Soluble E-cadherin promotes the progression of cancer. *International Journal Of Cancer*, 138 (12), 2804-2812.

Hu, X., Ruan, Y., Cheng, F., Yu, W., Zhang, X., & Larré, S. (2011). p130Cas, E-cadherin and ß-catenin in human transitional cell carcinoma of the bladder: Expression and clinicopathological significance. *International Journal Of Urology*, 18 (9), 630-637.

Huang, P. Y., & Balmain, A. (2014). Modeling cutaneous squamous carcinoma development in the mouse. *Cold Spring Harbor Perspectives In Medicine*, 4 (9), a013623-a013623.

Huang, T. S., Li, L., Moalim-Nour, L., Jia, D., Bai, J., Yao, Z., Bennett, S. A. L., Figeys, D., & Wang, L. (2015). A Regulatory Network Involving ß-Catenin, E-Cadherin, PI3k/Akt, and Slug Balances Self-Renewal and Differentiation of Human Pluripotent Stem Cells In Response to Wnt Signaling. *Stem cells (Dayton, Ohio)*, 33 (5), 1419-1433.

Huber, A. H., & Weis, W. I. (2001). The Structure of the ß-catenin/E-cadherin Complex and the Molecular Basis of Diverse Ligand Recognition by ß-catenin. *Cell*, 105 (3), 391-402.

Huelsken, J., Vogel, R., Erdmann, B., Cotsarelis, G., & Birchmeier, W. (2001). β-catenin Controls Hair Follicle Morphogenesis and Stem Cell Differentiation in the Skin. *Cell*, 105 (4), 533-545.

Hülsken, J., & Behrens, J. (2000). The Wnt signalling pathway. *The Journal of Cell Science*, 113 (20), 3545-3545.

Hülsken, J., Birchmeier, W., & Behrens, J. (1994). E-cadherin and APC Compete for the Interaction with β-catenin and the Cytoskeleton. *The Journal of Cell Biology*, 127 (6), 2061-2069.

Iijima, N., Sato, K., Kuranaga, E., & Umetsu, D. (2020). Differential cell adhesion implemented by Drosophila Toll corrects local distortions of the anterior-posterior compartment boundary. *Nature Communications*, 11 (1), 6320-6320.

Imamichi, Y., & Menke, A. (2007). Signaling Pathways Involved in Collagen-Induced Disruption of the E-cadherin Complex during Epithelial-Mesenchymal Transition. *Cells, Tissues, Organs*, 185 (1-3), 180-190.

Isinger-Ekstrand, A., Therkildsen, C., Bernstein, I., & Nilbert, M. (2011). Deranged Wnt signaling is frequent in hereditary nonpolyposis colorectal cancer. *Familial Cancer*, 10 (2), 239-243.

Jang, T. J. (2012). Epithelial to mesenchymal transition in cutaneous squamous cell carcinoma is correlated with COX-2 expression but not with the presence of stromal macrophages or CD10-expressing cells. *International Journal Of Pathology*, 460 (5), 481-487.

Janus, J. M., O'Shaughnessy, R. F. L., Harwood, C. A., & Maffucci, T. (2017). Phosphoinositide 3-Kinase-Dependent Signalling Pathways in Cutaneous Squamous Cell Carcinomas. *Cancers*, 9 (7), 86.

Jeanes, A., Gottardi, C. J., & Yap, A. S. (2008). Cadherins and cancer: how does cadherin dysfunction promote tumor progression? *Oncogene*, 27 (55), 6920-6929.

Jensen, K. B., Jones, J., & Watt, F. M. (2008). A stem cell gene expression profile of human squamous cell carcinomas. *Cancer Letters*, 272 (1), 23-31.

Jensen, P. J., & Wheelock, M. J. (1992). Regulation of urokinase plasminogen activator localization in keratinocytes by calcium ion and E-cadherin. *Experimental Cell Research*, 202 (1), 190-198.

Jiang, Y.-G., Luo, Y., He, D.-l., Li, X., Zhang, L.-l., Peng, T., Li, M.-C., & Lin, Y.-H. (2007). Role of Wnt/β-catenin signaling pathway in epithelial-mesenchymal transition of human prostate cancer induced by hypoxia-inducible factor-1α. *International Journal Of Urology*, 14 (11), 1034-1039.

Jiang, Y., Ren, W., Wang, W., Xia, J., Gou, L., Liu, M., Wan, Q., Zhou, L., Weng, Y., He, T., & Zhang, Y. (2017). Inhibitor of β-catenin and TCF (ICAT) promotes cervical cancer growth and metastasis by disrupting E-cadherin/β-catenin complex. *Oncology Reports*, 38 (5), 2597.

Jolly, M. K., Ware, K. E., Xu, S., Gilja, S., Shetler, S., Yang, Y., Wang, X., Austin, R. G., Runyambo, D., Hish, A. J., Bartholf DeWitt, S., George, J. T., Kreulen, R. T., Boss, M.-K., Lazarides, A. L., Kerr, D. L., Gerber, D. G., Sivaraj, D., Armstrong, A. J., & Somarelli, J. A. (2019). E-cadherin Represses Anchorage-Independent Growth in Sarcomas through Both Signaling and Mechanical Mechanisms. *Molecular Cancer Research*, 17 (6), 1391-1402.

Jones, J. C. R., Kam, C. Y., Harmon, R. M., Woychek, A. V., Hopkinson, S. B., & Green, K. J. (2017). Intermediate Filaments and the Plasma Membrane. *Cold Spring Harbor Perspectives In Biology*, 9 (1), a025866.

Joshi, S., De Angelis, P. M., Zucknick, M., Schjolberg, A. R., Andersen, S. N., & Clausen, O. P. F. (2020). Role of the Wnt signaling pathway in keratoacanthoma. *Cancer Reports*, 3 (2), e1219-n/a.

Kalluri, R., & Weinberg, R. A. (2009). The basics of epithelial-mesenchymal transition. *The Journal of Clinical Investigation*, 119 (6), 1420-1428.

Kang, J.-I., Kim, M.-K., Lee, J.-H., Jeon, Y.-J., Hwang, E.-K., Koh, Y.-S., Hyun, J.-W., Kwon, S.-Y., Yoo, E.-S., & Kang, H.-K. (2017). Undariopsis peterseniana Promotes Hair Growth by the Activation of Wnt/β-catenin and ERK Pathways. *Marine Drugs*, 15 (5), 130.

Kao, S. H., Wang, W. L., Chen, C. Y., Chang, Y. L., Wu, Y. Y., Wang, Y. T., Wang, S. P., Nesvizhskii, A. I., Chen, Y. J., Hong, T. M., & Yang, P. C. (2014). GSK3β controls epithelial–mesenchymal transition and tumor metastasis by CHIP-mediated degradation of Slug. *Oncogene*, 33 (24), 3172-3182.

Katsarou, S., Makris, M., Vakirlis, E., & Gregoriou, S. (2023). The Role of Tight Junctions in Atopic Dermatitis: A Systematic Review. *The Journal of Clinical Medicine*, 12 (4), 1538.

Kawahara, A., Harada, H., Abe, H., Yamaguchi, T., Taira, T., Nakashima, K., Mihashi, H., Akiba, J., & Kage, M. (2011). Nuclear ß-catenin expression in basal cell adenomas of salivary gland. *The Journal of Oral Pathology & Medicine*, 40 (6), 460-466.

Kellendonk, C., Tronche, F., Monaghan, A. P., Angrand, P.-O., Stewart, F., & Schütz, G. (1996). Regulation of Cre Recombinase Activity by the Synthetic Steroid RU 486. *Nucleic Acids Research*, 24 (8), 1404-1411.

Kern, F., Niault, T., & Baccarini, M. (2011). Ras and Raf pathways in epidermis development and carcinogenesis. *British Journal Of Cancer*, 104 (7), 1240-1240.

Khan, P., Manna, A., Saha, S., Mohanty, S., Mukherjee, S., Mazumdar, M., Guha, D., & Das, T. (2016). Aspirin inhibits epithelial-to-mesenchymal transition and migration of oncogenic K-ras-expressing non-small cell lung carcinoma cells by down-regulating E-cadherin repressor Slug. *BMC Cancer*, 16 (39), 39-39.

Khosravi-Far, R., White, M. A., Westwick, J. K., Solski, P. A., Chrzanowska-Wodnicka, M., Van Aelst, L., Wigler, M. H., & Der, C. J. (1996). Oncogenic Ras activation of Raf/mitogen-activated protein kinase-independent pathways is sufficient to cause tumorigenic transformation. *Molecular and Cellular Biology*, 16 (7), 3923-3933.

Kim, H. Y., Han, D., Kim, J., Yoo, M. S., Lee, J. S., Kim, H., Kim, H. M., & Jeong, H. J. (2021). An anti-cancer effect of Sambou bamboo saltTM in melanoma skin cancer both in vivo and in vitro models. *The Journal of Food Biochemistry*, 45 (9), n/a-n/a.

Kim, I., & He, Y.-Y. (2014). Ultraviolet radiation-induced non-melanoma skin cancer: Regulation of DNA damage repair and inflammation. *Genes & Diseases*, 1 (2), 188-198.

Kim, N.-G., Koh, E., Chen, X., & Gumbiner, B. M. (2011). E-cadherin mediates contact inhibition of proliferation through Hippo signaling-pathway components. *Proceedings of the National Academy of Sciences - PNAS*, 108 (29), 11930-11935.

Kim, N.-H., & Lee, A.-Y. (2010). Reduced Aquaporin3 Expression and Survival of Keratinocytes in the Depigmented Epidermis of Vitiligo. *The Journal of Investigative Dermatology*, 130 (9), 2231-2239.

Kim, T. H., Yoo, J.-Y., Kim, H. I., Gilbert, J., Ku, B. J., Li, J., Mills, G. B., Broaddus, R. R., Lydon, J. P., Lim, J. M., Yoon, H.-G., & Jeong, J.-W. (2014). Mig-6 suppresses endometrial cancer associated with Pten deficiency and ERK activation. *Cancer Research (Chicago, Ill.)*, 74 (24), 7371-7382.

Kim, W. K., Kwon, Y., Jang, M., Park, M., Kim, J., Cho, S., Jang, D. G., Lee, W.-B., Jung, S. H., Choi, H. J., Min, B. S., Il Kim, T., Hong, S. P., Paik, Y.-K., & Kim, H. (2019). β-catenin activation down-regulates cell-cell junction-related genes and induces epithelial-to-mesenchymal transition in colorectal cancers. *Scientific Reports*, 9 (1), 18440-18415.

Kourtidis, A., Ngok, S. P., Pulimeno, P., Feathers, R. W., Carpio, L. R., Baker, T. R., Carr, J. M., Yan, I. K., Borges, S., Perez, E. A., Storz, P., Copland, J. A., Patel, T., Thompson, E. A., Citi, S., & Anastasiadis, P. Z. (2015). Distinct E-cadherin-based complexes regulate cell behaviour through miRNA processing or Src and p120 catenin activity. *Nature Cell Biology*, 17 (9), 1145-1157.

Kowalski, P. J., Rubin, M. A., & Kleer, C. G. (2003). E-cadherin expression in primary carcinomas of the breast and its distant metastases. *Breast Cancer Research: BCR*, 5 (6), R217-R222.

Kühn, K., Cott, C., Bohler, S., Aigal, S., Zheng, S., Villringer, S., Imberty, A., Claudinon, J., & Römer, W. (2015). The interplay of autophagy and β-catenin signaling regulates differentiation in acute myeloid leukemia. *Cell Death Discovery*, 1 (1), 15031-15031.

Lau, M.-T., So, W.-K., & Leung, P. C. K. (2013). Fibroblast growth factor 2 induces E-cadherin down-regulation via PI3K/AKT/mTOR and MAPK/ERK signaling in ovarian cancer cells. *PloS One*, 8 (3), e59083.

Lau, M. T., Klausen, C., & Leung, P. (2011). E-cadherin inhibits tumor cell growth by suppressing PI3K AKT signaling via β-catenin-Egr1-mediated PTEN expression. *Oncogene*, 30 (24), 2753-2766.

Leiter, U. (2021). What is new in the 2020 British guidelines for cutaneous squamous cell carcinoma? *British Journal of Dermatology (1951)*, 184 (3), 384-385.

Li, B., Xu, W. W., Lam, A. K. Y., Wang, Y., Hu, H.-F., Guan, X. Y., Qin, Y. R., Saremi, N., Tsao, S. W., He, Q.-Y., & Cheung, A. L. M. (2017). Significance of PI3K/AKT signaling pathway in metastasis of esophageal squamous cell carcinoma and its potential as a target for anti-metastasis therapy. *Oncotarget*, 8 (24), 38755-38766.

Li, D., Lo, W., & Rudloff, U. (2018). Merging perspectives: genotype-directed molecular therapy for hereditary diffuse gastric cancer (HDGC) and E-cadherin–EGFR crosstalk. *Clinical and Translational Medicine*, 7 (1), 1-6.

Li, X., Deng, W., Nail, C. D., Bailey, S. K., Kraus, M. H., Ruppert, J. M., & Lobo-Ruppert, S. M. (2006). Snail induction is an early response to Gli1 that determines the efficiency of epithelial transformation. *Oncogene*, 25 (4), 609-621.

Li, X., Rokohl, A. C., Ju, X., Guo, Y., Hou, X., Fan, W., & Heindl, L. M. (2024). Global research trends in the treatment of squamous cell carcinoma over the past decade: A bibliometric analysis. *Advances In Ophthalmology Practice And Research*, 4 (4), 209-215.

Li, Y., Bharti, A., Chen, D., Gong, J., & Kufe, D. (1998). Interaction of Glycogen Synthase Kinase 3β with the DF3/MUC1 Carcinoma-Associated Antigen and β-Catenin. *Molecular and Cellular Biology*, 18 (12), 7216-7224.

Li, Z.-X., Zheng, Z.-Q., Wei, Z.-H., Zhang, L.-L., Li, F., Lin, L., Liu, R.-Q., Huang, X.-D., Lv, J.-W., Chen, F.-P., He, X.-J., Guan, J.-L., Kou, J., Ma, J., Zhou, G.-Q., & Sun, Y. (2019). Comprehensive characterization of the alternative splicing landscape in head and neck squamous cell carcinoma reveals novel events associated with tumorigenesis and the immune microenvironment. *Theranostics*, 9 (25), 7648-7665.

Liaw, D., Marsh, D. J., Li, J., Dahia, P. L. M., Wang, S. I., Zheng, Z., Bose, S., Call, K. M., Tsou, H. C., Peacoke, M., Eng, C., & Parsons, R. (1997). Germline mutations of the PTEN gene in Cowden disease, an inherited breast and thyroid cancer syndrome. *Nature Genetics*, 16 (1), 64-67.

Lilien, J., Balsamo, J., Arregui, C., & Xu, G. (2002). Turn-off, drop-out: Functional state switching of cadherins. *Developmental Dynamics*, 224 (1), 18-29.

Liu, C., Huang, H. U. I., Wang, C., Kong, Y., & Zhang, H. (2014). Involvement of ephrin receptor A4 in pancreatic cancer cell motility and invasion. *Oncology Letters*, 7 (6), 2165-2169.

Liu, R., Zhang, T., Zhu, G., & Xing, M. (2018). Regulation of mutant TERT by BRAF V600E/MAP kinase pathway through FOS/GABP in human cancer. *Nature Communications*, 9 (1), 579-513.

Liu, Y., Feng, X., Lai, J., Yi, W., Yang, J., Du, T., Long, X., Zhang, Y., & Xiao, Y. (2019). A novel role of kynureninase in the growth control of breast cancer cells and its relationships with breast cancer. *The Journal of Cellular And Molecular Medicine*, 23 (10), 6700-6707.

Lourenço, S. V., Kamibeppu, L., Fernandes, J. D., Sotto, M. N., & Nico, M. M. S. (2008). Relationship of adhesion molecules expression with epithelial differentiation markers during fetal skin development. *The Journal of Cutaneous Pathology*, 35 (8), 731-737.

Ma, Y., Yu, W.-D., Su, B., Seshadri, M., Luo, W., Trump, D. L., & Johnson, C. S. (2012). Regulation of Motility, Invasion and Metastatic Potential of Squamous Cell Carcinoma by 1,25D3. *Cancer*, 119 (3), 563-574.

MacDonald, B. T., Tamai, K., & He, X. (2009). Wnt/β-Catenin Signaling: Components, Mechanisms, and Diseases. *Developmental cell*, 17 (1), 9-26.

Macdonald, F. H., Yao, D., Quinn, J. A., & Greenhalgh, D. A. (2014). PTEN ablation in Ras(Ha)/Fos skin carcinogenesis invokes p53-dependent p21 to delay conversion while p53-independent p21 limits progression via cyclin D1/E2 inhibition. *Oncogene*, 33 (32), 4132-4143.

Mack, N. A., & Georgiou, M. (2014). The interdependence of the Rho GTPases and apicobasal cell polarity. *Small GTPases*, 5 (2), 10-10.

Malnou, C. E., Salem, T., Brockly, F., Wodrich, H., Piechaczyk, M., & Jariel-Encontre, I. (2007). Heterodimerization with Jun Family Members Regulates c-Fos Nucleocytoplasmic Traffic. *The Journal of Biological Chemistry*, 282 (42), 31046-31059.

Manjula, C., & Meghana, B. (2023). A study of E-cadherin expression in esophageal carcinoma. *Archives of Medicine and Health Sciences*, 11 (2), 229-233.

Margulis, A., Zhang, W., Alt-Holland, A., Crawford, H. C., Fusenig, N. E., & Garlick, J. A. (2005). E-cadherin suppression accelerates squamous cell carcinoma progression in three-dimensional, human tissue constructs. *Cancer Research (Chicago, Ill.)*, 65 (5), 1783-1791.

Martini, M., De Santis, M. C., Braccini, L., Gulluni, F., & Hirsch, E. (2014). PI3K/AKT signaling pathway and cancer: an updated review. *Annals of Medicine (Helsinki)*, 46 (6), 372.

Martins-Lima, C., Miranda-Gonçalves, V., Lobo, J., Constâncio, V., Leite-Silva, P., Guimarães-Teixeira, C., Monteiro-Reis, S., Sequeira, J. P., Cantante, M., Gonçalves, C. S., Costa, B. M., Henrique, R., & Jerónimo, C. (2022). Cadherin switches during epithelial-mesenchymal transition: CDH4/RCAD downregulation reduces bladder cancer progression. *Cellular Oncology (Dordrecht)*, 45 (1), 135-149.

Masre, S. F., Rath, N., Olson, M. F., & Greenhalgh, D. A. (2017). ROCK2/ras Ha co-operation induces malignant conversion via p53 loss, elevated NF-κB and tenascin C-associated rigidity, but p21 inhibits ROCK2/NF-κB-mediated progression. *Oncogene*, 36 (18), 2529.

Masre, S. F., Rath, N., Olson, M. F., & Greenhalgh, D. A. (2020). Epidermal ROCK2 induces AKT1/GSK3β/β-catenin, NFκB and dermal tenascin C; but enhanced differentiation and p53/p21 inhibit papilloma. *Carcinogenesis (New York)*, 41 (10), 1409-1420.

Mateus, A. R., Seruca, R., Machado, J. C., Keller, G., Oliveira, M. J., Suriano, G., & Luber, B. (2007). EGFR regulates RhoA-GTP dependent cell motility in E-cadherin mutant cells. *Human Molecular Genetics*, 16 (13), 1639-1647.

Mendonsa, A. M., Na, T.-Y., & Gumbiner, B. M. (2018). E-cadherin in contact inhibition and cancer. *Oncogene*, 37 (35), 4769-4780.

Migden, M. R., Chen, L., & Silapunt, S. (2020). *Basal cell carcinoma: advances in treatment and research*. Springer.

Ming, M., & He, Y.-Y. (2009). PTEN: New Insights into Its Regulation and Function in Skin Cancer. *The Journal of Investigative Dermatology*, 129 (9), 2109-2112.

Moch, M., Schwarz, N., Windoffer, R., & Leube, R. E. (2020). The keratin–desmosome scaffold: pivotal role of desmosomes for keratin network morphogenesis. *Cellular and Molecular Life Sciences: CMLS*, 77 (3), 543-558.

Mollereau, B., & Ma, D. (2014). The p53 control of apoptosis and proliferation: lessons from Drosophila. *Apoptosis (London)*, 19 (10), 1421-1429.

Morin, P. J. (1999). ß-catenin signaling and cancer. *BioEssays*, 21 (12), 1021-1030.

Muller, P. A. J., & Vousden, K. H. (2013). p53 mutations in cancer. *Nature Cell Biology*, 15 (1), 2-8.

Naoi, Y., Miyoshi, Y., Taguchi, T., Kim, S. J., Arai, T., Tamaki, Y., & Noguchi, S. (2007). Connexin26 expression is associated with lymphatic vessel invasion and poor prognosis in human breast cancer. *Breast Cancer Research And Treatment*, 106 (1), 11-17.

Nelson, W. J. (2008). Regulation of cell-cell adhesion by the cadherin-catenin complex. *Biochemical Society Transactions*, 36 (Pt 2), 149-155.

Nelson, W. J., & Nusse, R. (2004). Convergence of Wnt, ß-catenin, and cadherin Pathways. *Science (American Association for the Advancement of Science)*, 303 (5663), 1483-1487.

Nguyen, P. T., Kudo, Y., Yoshida, M., Iizuka, S., Ogawa, I., & Takata, T. (2011). N-cadherin expression is correlated with metastasis of spindle cell carcinoma of head and neck region. *The Journal of Oral Pathology & Medicine*, 40 (1), 77-82.

Nurismah, M. I., Noriah, O., Suryati, M. Y., & Sharifah, N. A. (2008). E-cadherin expression correlates with histologic type but not tumour grade in invasive breast cancer. *Asian Pacific Journal Of Cancer Prevention: APJCP*, 9 (4), 699.

Ogilvie, L. A., Kovachev, A., Wierling, C., Lange, B. M. H., & Lehrach, H. (2017). Models of Models: A Translational Route for Cancer Treatment and Drug Development. *Frontiers in Oncology*, 7, 219-219.

Olsen, C. M., & Green, A. C. (2012). More evidence of harms of sunbed use, particularly for young people. *BMJ (Online)*, 345 (oct02 3), e6101-e6101.

Olson, A., Le, V., Aldahl, J., Yu, E.-J., Hooker, E., He, Y., Lee, D.-H., Kim, W. K., Cardiff, R. D., Geradts, J., & Sun, Z. (2019). The comprehensive role of E-cadherin in maintaining prostatic epithelial integrity during oncogenic transformation and tumor progression. *PLoS Genetics*, 15 (10), e1008451.

Onder, T. T., Gupta, P. B., Mani, S. A., Yang, J., Lander, E. S., & Weinberg, R. A. (2008). Loss of E-cadherin promotes metastasis via multiple downstream transcriptional pathways. *Cancer Research (Chicago, Ill.)*, 68 (10), 3645-3654.

Ordóñez-Morán, P., Dafflon, C., Imajo, M., Nishida, E., & Huelsken, J. (2015). HOXA5 Counteracts Stem Cell Traits by Inhibiting Wnt Signaling in Colorectal Cancer. *Cancer Cell*, 28 (6), 815-829.

Padmanaban, V., Krol, I., Suhail, Y., Szczerba, B. M., Aceto, N., Bader, J. S., & Ewald, A. J. (2019). E-cadherin is required for metastasis in multiple models of breast cancer. *Nature (London)*, 573 (7774), 439-444.

Pećina-Slaus, N. (2003). Tumor suppressor gene E-cadherin and its role in normal and malignant cells. *Cancer Cell International*, 3 (1), 17-17.

Perez-Moreno, M., Jamora, C., & Fuchs, E. (2003). Sticky Business. *Cell*, 112 (4), 535-548.

Perrais, M., Chen, X., Perez-Moreno, M., & Gumbiner, B. M. (2007). E-cadherin homophilic ligation inhibits cell growth and epidermal growth factor receptor signaling independently of other cell interactions. *Molecular Biology Of The Cell*, 18 (6), 2013-2025.

Phelps, R. A., Chidester, S., Dehghanizadeh, S., Phelps, J., Sandoval, I. T., Rai, K., Broadbent, T., Sarkar, S., Burt, R. W., & Jones, D. A. (2009). A Two-Step Model for Colon Adenoma Initiation and Progression Caused by APC Loss. *Cell*, 137 (4), 623-634.

Pires, B. R. B., Mencalha, A. L., Ferreira, G. M., de Souza, W. F., Morgado-Díaz, J. A., Maia, A. M., Corrêa, S., & Abdelhay, E. S. F. W. (2017). NF-kappaB Is Involved in the Regulation of EMT Genes in Breast Cancer Cells. *PloS One*, 12 (1), e0169622-e0169622.

Prior, I. A., Lewis, P. D., & Mattos, C. (2012). A Comprehensive Survey of Ras Mutations in Cancer. *Cancer Research (Chicago, Ill.)*, 72 (10), 2457-2467.

Pugach, E. K., Richmond, P. A., Azofeifa, J. G., Dowell, R. D., & Leinwand, L. A. (2015). Prolonged Cre expression driven by the α-myosin heavy chain promoter can be cardiotoxic. *The Journal of Molecular And Cellular Cardiology*, 86, 54-61.

Pulford, C. S., Uppalapati, C. K., Montgomery, M. R., Averitte, R. L., Hull, E. E., & Leyva, K. J. (2022). A Hybrid Epithelial to Mesenchymal Transition in Ex Vivo Cutaneous Squamous Cell Carcinoma Tissues. *International Journal Of Molecular Sciences*, 23 (16), 9183.

Qi, L., Wang, Y., Su, S., Wang, M., Jablonska, E., Jia, Y., Wang, R., Hao, S., Feng, C., Li, G., Jiang, M., Du, L., Sun, H., Li, Q., & Wang, T. (2022). Sodium selenite inhibits cervical cancer growth via ROS mediated AMPK/FOXO3a /GADD45a axis. *Chemico-biological Interactions*, 367, 110171-110171.

Quail, D. F., & Joyce, J. A. (2013). Microenvironmental regulation of tumor progression and metastasis. *Nature Medicine*, 19 (11), 1423-1437.

Que, S. K. T., Zwald, F. O., & Schmults, C. D. (2018). Cutaneous squamous cell carcinoma: Incidence, risk factors, diagnosis, and staging. *The Journal of the American Academy of Dermatology*, 78 (2), 237-247.

Rangel-Huerta, E., & Maldonado, E. (2017). Transit-Amplifying Cells in the Fast Lane from Stem Cells towards Differentiation. *Stem Cells International*, 2017, 7602951-7602910.

Reddy, D., Kumavath, R., Tan, T. Z., Ampasala, D. R., & Kumar, A. P. (2020). Peruvoside targets apoptosis and autophagy through MAPK Wnt/β-catenin and PI3K/AKT/mTOR signaling pathways in human cancers. *Life Sciences* (1973), 241, 117147-117147.

Reddy, P. N., Javalgi, A. P., & Parmesh, P. (2024). Immunohistochemical Expression Status of HER2/neu and E-cadherin in Prostate

Adenocarcinoma: A Cross-sectional Study. *National Journal Of Laboratory Medicine*, 13 (1), 14-19.

Reed, J. C. (2000). Mechanisms of Apoptosis. *The American Journal Of Pathology*, 157 (5), 1415-1430.

Rischin, D., Harrington, K. J., Greil, R., Soulières, D., Tahara, M., de Castro Jr, G., Psyrri, A., Braña, I., Neupane, P., Bratland, Å., Fuereder, T., Hughes, B. G. M., Mesía, R., Ngamphaiboon, N., Rordorf, T., Ishak, W. Z. W., Hong, R.-L., Mendoza, R. G., Jia, F., & Burtness, B. (2022). Pembrolizumab alone or with chemotherapy for recurrent or metastatic head and neck squamous cell carcinoma: Health-related quality-of-life results from KEYNOTE-048. *Oral Oncology*, 128, 105815-105815.

Roberts, P. J., & Der, C. J. (2007). Targeting the Raf-MEK-ERK mitogen-activated protein kinase cascade for the treatment of cancer: MAPKs: Function, regulation, role in cancer and therapeutic targeting. *Oncogene*, 26 (22), 3291-3310.

Roop, D. R., Lowy, D. R., Tambourin, P. E., Strickland, J., Harper, J. R., Balaschak, M., Spangler, E. F., & Yuspa, S. H. (1986). An activated Harvey ras oncogene produces benign tumours on mouse epidermal tissue. *Nature (London)*, 323 (6091), 822-824.

Rossbach, P., Böhme, H.-J., Lange, S., & Voss-Böhme, A. (2021). Model-Based Prediction of an Effective Adhesion Parameter Guiding Multi-Type Cell Segregation. *Entropy (Basel, Switzerland)*, 23 (11), 1378.

Rothnagel, J. A., Seki, T., Ogo, M., Longley, M. A., Wojcik, S. M., Bundman, D. S., Bickenbach, J. R., & Roop, D. R. (1999). The mouse keratin 6 isoforms are differentially expressed in the hair follicle, footpad, tongue and activated epidermis. *Differentiation (London)*, 65 (2), 119-130.

Saadeddin, A., Babaei-Jadidi, R., Spencer-Dene, B., & Nateri, A. S. (2009). The Links between Transcription, ß-catenin/JNK Signaling, and Carcinogenesis. *Molecular Cancer Research*, 7 (8), 1189-1196.

Saez, E., Rutberg, S. E., Mueller, E., Oppenheim, H., Smoluk, J., Yuspa, S. H., & Spiegelman, B. M. (1995). c- fos is required for malignant progression of skin tumors. *Cell*, 82 (5), 721-732.

Salon, C., Moro, D., Lantuejoul, S., Brichon, P. Y., Drabkin, H., Brambilla, C., & Brambilla, E. (2004). E-cadherin-β-catenin adhesion complex in neuroendocrine tumors of the lung: a suggested role upon local invasion and metastasis. *Human Pathology*, 35 (9), 1148-1155.

Sasaki, C. Y., Lin, H., Morin, P. J., & Longo, D. L. (2000). Truncation of the extracellular region abrogrates cell contact but retains the growth-suppressive activity of E-cadherin. *Cancer Research (Chicago, Ill.)*, 60 (24), 7057-7065.

Saydam, O., Shen, Y., Würdinger, T., Senol, O., Boke, E., James, M. F., Tannous, B. A., Stemmer-Rachamimov, A. O., Yi, M., Stephens, R. M., Fraefel, C., Gusella, J. F., Krichevsky, A. M., & Breakefield, X. O. (2009). Downregulated MicroRNA-200a in Meningiomas Promotes Tumor Growth by Reducing E-Cadherin and Activating the Wnt/β-Catenin Signaling Pathway. *Molecular and Cellular Biology*, 29 (21), 5923-5940.

Schlingemann, J., Hess, J., Wrobel, G., Breitenbach, U., Gebhardt, C., Steinlein, P., Kramer, H., Fürstenberger, G., Hahn, M., Angel, P., & Lichter, P. (2003). Profile of gene expression induced by the tumour promotor TPA in murine epithelial cells. *International Journal Of Cancer*, 104 (6), 699-708.

Schulz, G. B., Elezkurtaj, S., Börding, T., Schmidt, E. M., Elmasry, M., Stief, C. G., Kirchner, T., Karl, A., & Horst, D. (2021). Therapeutic and prognostic implications of NOTCH and MAPK signaling in bladder cancer. *Cancer Science*, 112 (5), 1987-1996.

Schwartz, R. A. (2004). Keratoacanthoma: a clinico-pathologic enigma. *Dermatologic Surgery*, 30 (2 Pt 2), 326.

Seo, J. H., Lee, H. J., Sim, D. Y., Park, J. E., Ahn, C. H., Park, S. Y., Cho, A. R., Koo, J., Shim, B. S., Kim, B., & Kim, S. H. (2023). Honokiol inhibits epithelial–mesenchymal transition and hepatic fibrosis via activation of Ecadherin/ GSK3β / JNK and inhibition of AKT / ERK /p38/β-catenin/ TMPRSS4 signaling axis. *Phytotherapy Research*, 37 (9), 4092-4101.

Sharma, A., Birnie, A. J., Bordea, C., Cheung, S. T., Mann, J., Morton, C. A., Salim, A., Hasan, Z.-U., Hashme, M., Mansour Kiaee, Z., Mohd

Mustapa, M. F., & Exton, L. S. (2023). British Association of Dermatologists guidelines for the management of people with cutaneous squamous cell carcinoma in situ (Bowen disease) 2022. *British Journal Of Dermatology (1951)*, 188 (2), 186-194.

Shenoy, S. (2019). CDH1 (E-Cadherin) Mutation and Gastric Cancer: Genetics, Molecular Mechanisms and Guidelines for Management. *Cancer Management And Research*, 11, 10477-10486.

Sheth, P., Seth, A., Atkinson, K. J., Gheyi, T., Kale, G., Giorgianni, F., Desiderio, D. M., Li, C., Naren, A., & Rao, R. (2007). Acetaldehyde dissociates the PTP1B-E-cadherin-beta-catenin complex in Caco-2 cell monolayers by a phosphorylation-dependent mechanism. *Biochemical Journal*, 402 (2), 291-300.

Shu, H., Chen, H., Yang, B., Chang, Z., Xiong, M., & Chen, W. (2013). Aberrant expression of E-cadherin and integrin ß-1 in trophoblasts is associated with malignant gestational trophoblastic diseases. *International Journal Of Gynecological Cancer*, 23 (4), 749.

Silye, R., Karayiannakis, A. J., Syrigos, K. N., Poole, S., Van Noorden, S., Batchelor, W., Regele, H., Sega, W., Boesmueller, H., Krausz, T., & Pignatelli, M. (1998). E-cadherin/catenin complex in benign and malignant melanocytic lesions. *The Journal of Pathology*, 186 (4), 350-355.

Smeyne, R. J., Curran, T., & Morgan, J. I. (1992). Temporal and spatial expression of a fos-lacZ transgene in the developing nervous system. *Brain research. Molecular Brain Research*, 16 (1), 158-162.

South, A. P., Purdie, K. J., Watt, S. A., Haldenby, S., den Breems, N. Y., Dimon, M., Arron, S. T., Kluk, M. J., Aster, J. C., McHugh, A., Xue, D. J., Dayal, J. H. S., Robinson, K. S., Hasan Rizvi, S. M., Proby, C. M., Harwood, C. A., & Leigh, I. M. (2014). NOTCH1 Mutations Occur Early during Cutaneous Squamous Cell Carcinogenesis. *The Journal of Investigative Dermatology*, 134 (10), 2630-2638.

Stappenbeck, T. S., Bornslaeger, E. A., Corcoran, C. M., Luu, H. H., Maria Luisa, A. V., & Green, K. J. (1993). Functional Analysis of Desmoplakin Domains: Specification of the Interaction with Keratin versus Vimentin

Intermediate Filament Networks. *The Journal of Cell Biology*, 123 (3), 691-705.

Strickland, J. E., Greenhalgh, D. A., Koceva-Chyla, A., Hennings, H., Restrepo, C., Balaschak, M., & Yuspa, S. H. (1988). Development of murine epidermal cell lines which contain an activated rasHa oncogene and form papillomas in skin grafts on athymic nude mouse hosts. *Cancer Research (Chicago, Ill.)*, 48 (1), 165-169.

Strumane, K., Bonnomet, A., Stove, C., Vandenbroucke, R., Nawrocki-Raby, B., Bruyneel, E., Mareel, M., Birembaut, P., Berx, G., & van Roy, F. (2006). E-Cadherin Regulates Human Nanos1, which Interacts with p120ctn and Induces Tumor Cell Migration and Invasion. *Cancer Research (Chicago, Ill.)*, 66 (20), 10007-10015.

Su, F., Viros, A., Milagre, C., Trunzer, K., Bollag, G., Spleiss, O., Reis-Filho, J. S., Kong, X., Koya, R. C., Flaherty, K. T., Chapman, P. B., Kim, M. J., Hayward, R., Martin, M., Yang, H., Wang, Q., Hilton, H., Hang, J. S., Noe, J., & Marais, R. (2012). RAS Mutations in Cutaneous Squamous-Cell Carcinomas in Patients Treated with BRAF Inhibitors. *The New England Journal Of Medicine*, 366 (3), 207-215.

Sun, M., Li, Y., Qian, J., Ding, S., Sun, M., Tan, B., & Zhao, Y. (2021). Connexin26 Modulates the Radiosensitivity of Cutaneous Squamous Cell Carcinoma by Regulating the Activation of the MAPK/NF-κB Signaling Pathway. *Frontiers In Cell And Developmental Biology*, 9, 672571.

Sunkara, R. R., Sarate, R. M., Setia, P., Shah, S., Gupta, S., Chaturvedi, P., Gera, P., & Waghmare, S. K. (2020). SFRP1 in Skin Tumor Initiation and Cancer Stem Cell Regulation with Potential Implications in Epithelial Cancers. *Stem Cell Reports*, 14 (2), 271-284.

Sutter, C., Greenhalgh, D. A., Ueda, M., Abhyankar, S., Ngai, P., Hennings, H., Schweizer, J., Yuspa, S. H., & Strickland, J. E. (1994). SENCAR mouse skin tumors produced by promotion alone have A to G mutations in codon 61 of the c-rasHa gene. *Carcinogenesis (New York)*, 15 (9), 1975-1978.

Suzuki, A., de la Pompa, J. L., Stambolic, V., Elia, A. J., Sasaki, T., Barrantes, I. d. B., Ho, A., Wakeham, A., ltie, A., Khoo, W.,

Fukumoto, M., & Mak, T. W. (1998). High cancer susceptibility and embryonic lethality associated with mutation of the PTEN tumor suppressor gene in mice. *Current Biology*, 8 (21), 1169-1178.

Suzuki, A., Itami, S., Mak, T. W., Nakano, T., Ohishi, M., Hamada, K., Inoue, T., Komazawa, N., Senoo, H., Sasaki, T., Takeda, J., & Manabe, M. (2003). Keratinocyte-specific Pten deficiency results in epidermal hyperplasia, accelerated hair follicle morphogenesis and tumor formation. *Cancer Research (Chicago, Ill.)*, 63 (3), 674-681.

Syed, V., Mak, P., Du, C., & Balaji, K. C. (2008). ß-catenin mediates alteration in cell proliferation, motility and invasion of prostate cancer cells by differential expression of E-cadherin and protein kinase D1. *The Journal of Cellular Biochemistry*, 104 (1), 82-95.

Tan, M.-H., Mester, J. L., Ngeow, J., Rybicki, L. A., Orloff, M. S., & Eng, C. (2012). Lifetime Cancer Risks in Individuals with Germline PTEN Mutations. *Clinical Cancer Research*, 18 (2), 400-407.

Thiery, J. P., & Sleeman, J. P. (2006). Complex networks orchestrate epithelial-mesenchymal transitions. *Nature Reviews. Molecular Cell Biology*, 7 (2), 131-142.

Tian, X., Liu, Z., Niu, B., Zhang, J., Tan, T. K., Lee, S. R., Zhao, Y., Harris, D. C. H., & Zheng, G. (2011). E-cadherin/ß-catenin Complex and the Epithelial Barrier. *The Journal of Biomedicine & Biotechnology*, 2011, 567305-567306.

Tinkle, C. L., Lechler, T., Pasolli, H. A., & Fuchs, E. (2004). Conditional Targeting of E-Cadherin in Skin: Insights into Hyperproliferative and Degenerative Responses. *Proceedings of the National Academy of Sciences - PNAS*, 101 (2), 552-557.

Tinkle, C. L., Pasolli, H. A., Stokes, N., & Fuchs, E. (2008). New insights into cadherin function in epidermal sheet formation and maintenance of tissue integrity. *Proceedings of the National Academy of Sciences - PNAS*, 105 (40), 15405-15410.

Tittarelli, A., Guerrero, I., Tempio, F., Gleisner, M. A., Avalos, I., Sabanegh, S., Ortíz, C., Michea, L., López, M. N., Mendoza-Naranjo, A., & Salazar-Onfray, F. (2015). Overexpression of connexin 43 reduces

melanoma proliferative and metastatic capacity. *British Journal Of Cancer*, 113 (2), 259-267.

Topley, G. I., Okuyama, R., Gonzales, J. G., Conti, C., & Dotto, G. P. (1999). p21WAF1/Cip1 Functions as a Suppressor of Malignant Skin Tumor Formation and a Determinant of Keratinocyte Stem-Cell Potential. *Proceedings of the National Academy of Sciences - PNAS*, 96 (16), 9089-9094.

Toualbi, K., Güller, M. C., Mauriz, J. L., Labalette, C., Buendia, M. A., Mauviel, A., & Bernuau, D. (2007). Physical and functional cooperation between AP-1 and ß-catenin for the regulation of TCF-dependent genes. *Oncogene*, 26 (24), 3492-3502.

Tremmel, L., Rho, O., Slaga, T. J., & DiGiovanni, J. (2019). Inhibition of skin tumor promotion by TPA using a combination of topically applied ursolic acid and curcumin. *Molecular Carcinogenesis*, 58 (2), 185-195.

Tuveson, D. A. (2021). Fighting the Sixth Decade of the Cancer War with Better Cancer Models. *Cancer Discovery*, 11 (4), 801-804.

Vaseva, A. V., Marchenko, N. D., & Moll, U. (2009). The transcription-independent mitochondrial p53 program is a major contributor to Nutlin-induced apoptosis in tumor cells. *Cell Cycle (Georgetown, Tex.)*, 8 (11), 1711-1719.

Venables, Z. C., Nijsten, T., Wong, K. F., Autier, P., Broggio, J., Deas, A., Harwood, C. A., Hollestein, L. M., Langan, S. M., Morgan, E., Proby, C. M., Rashbass, J., & Leigh, I. M. (2019). Epidemiology of basal and cutaneous squamous cell carcinoma in the U.K. 2013-15: a cohort study. *British Journal Of Dermatology (1951)*, 181 (3), 474.

Vicent, S., Chen, R., Sayles, L. C., Lin, C., Walker, R. G., Gillespie, A. K., Subramanian, A., Hinkle, G., Yang, X., Saif, S., Root, D. E., Huff, V., Hahn, W. C., & Sweet-Cordero, E. A. (2010). Wilms tumor 1 (WT1) regulates KRAS-driven oncogenesis and senescence in mouse and human models. *The Journal of Clinical Investigation*, 120 (11), 3940-3952.

Vijay, A., Ram, L., Mathew, R. K., & Chawdhery, M. Z. (2015). Solid pseudopapillary tumor of the pancreas in a patient with cervical

cancer: relation of E-cadherin/β-catenin adhesion complex in their carcinogenesis. *The Journal of Surgical Case Reports*, 2015 (4).

Vleminckx, K., Vakaet, L., Mareel, M., Fiers, W., & Van Roy, F. (1991). Genetic manipulation of E-cadherin expression by epithelial tumor cells reveals an invasion suppressor role. *Cell*, 66 (1), 107-119.

Volpini, X., Ambrosio, L. F., Fozzatti, L., Insfran, C., Stempin, C. C., Cervi, L., & Motran, C. C. (2018). Trypanosoma cruzi Exploits Wnt Signaling Pathway to Promote Its Intracellular Replication in Macrophages. *Frontiers in Immunology*, 9, 859-859.

Vousden, K. H., & Prives, C. (2009). Blinded by the Light: The Growing Complexity of p53. *Cell*, 137 (3), 413-431.

Wang, H., Xu, L., Zhu, X., Wang, P., Chi, H., & Meng, Z. (2014). Activation of phosphatidylinositol 3-kinase/Akt signaling mediates sorafenib-induced invasion and metastasis in hepatocellular carcinoma. *Oncology Reports*, 32 (4), 1465-1472.

Wang, X.-J., Greenhalgh, D. A., Donehower, L. A., & Roop, D. R. (2000). Cooperation between Ha-ras and fos or transforming growth factor α overcomes a paradoxic tumor-inhibitory effect of p53 loss in transgenic mouse epidermis. *Molecular Carcinogenesis*, 29 (2), 67-75.

Wang, X., Ramirez, A., & Budunova, I. (2010). Overexpression of connexin26 in the basal keratinocytes reduces sensitivity to tumor promoter TPA. *Experimental Dermatology*, 19 (7), 633-640.

Wang, X. J., Greenhalgh, D. A., Lu, X. R., Bickenbach, J. R., & Roop, D. R. (1995). TGF alpha and v-fos cooperation in transgenic mouse epidermis induces aberrant keratinocyte differentiation and stable, autonomous papillomas. *Oncogene*, 10 (2), 279.

Watt, F. M., & Collins, C. A. (2008). Role of beta-catenin in epidermal stem cell expansion, lineage selection, and cancer. *Cold Spring Harbor Symposia on Quantitative Biology*, 73, 503.

Watt, F. M., & Jensen, K. B. (2009). Epidermal stem cell diversity and quiescence. *EMBO Molecular Medicine*, 1 (5), 260-267.

Wei, G., Wang, L., Dong, D., Teng, Z., Shi, Z., Wang, K., An, G., Guan, Y., Han, B., Yao, M., & Xian, C. J. (2018). Promotion of cell growth and

adhesion of a peptide hydrogel scaffold via mTOR/cadherin signaling. *The Journal of Cellular Physiology*, 233 (2), 822-829.

Weinberg, R. A. (2007). *The biology of cancer*. Garland Science.

Wen, L., Ding, Y., Chen, X., Tian, K., Li, D., Liang, K., & Yue, B. (2021). Influences of S100A8 and S100A9 on Proliferation of Nasopharyngeal Carcinoma Cells through PI3K/Akt Signaling Pathway. *BioMed Research International*, 2021, 9917365-9917367.

Wend, P., Runke, S., Wend, K., Anchondo, B., Yesayan, M., Jardon, M., Hardie, N., Loddenkemper, C., Ulasov, I., Lesniak, M. S., Wolsky, R., Bentolila, L. A., Grant, S. G., Elashoff, D., Lehr, S., Latimer, J. J., Bose, S., Sattar, H., Krum, S. A., & Miranda-Carboni, G. A. (2013). WNT10B/β-catenin signalling induces HMGA2 and proliferation in metastatic triple-negative breast cancer. *EMBO Molecular Medicine*, 5 (2), 264-279.

Werling, A. M., Doerflinger, Y., Brandner, J. M., Fuchs, F., Becker, J. C., Schrama, D., Kurzen, H., Goerdt, S., & Peitsch, W. K. (2011). Homo- and heterotypic cell-cell contacts in Merkel cells and Merkel cell carcinomas: heterogeneity and indications for cadherin switching. *Histopathology*, 58 (2), 286-303.

Wheelock, M. J., & Jensen, P. J. (1992). Regulation of Keratinocyte Intercellular Junction Organization and Epidermal Morphogenesis by E-cadherin. *The Journal of Cell Biology*, 117 (2), 415-425.

Wijshake, T., Zou, Z., Chen, B., Zhong, L., Xiao, G., Xie, Y., Doench, J. G., Bennett, L., & Levine, B. (2021). Tumor-suppressor function of Beclin 1 in breast cancer cells requires E-cadherin. *Proceedings of the National Academy of Sciences - PNAS*, 118 (5).

Winter, J. M., Ting, A. H., Vilardell, F., Gallmeier, E., Baylin, S. B., Hruban, R. H., Kern, S. E., & Iacobuzio-Donahue, C. A. (2008). Absence of E-cadherin Expression Distinguishes Noncohesive from Cohesive Pancreatic Cancer. *Clinical Cancer Research*, 14 (2), 412-418.

Wu, H., Goel, V., & Haluska, F. G. (2003). PTEN signaling pathways in melanoma. *Oncogene*, 22 (20), 3113-3122.

Xu, M., Deng, X., Xiang, N., Zhang, Z., Yang, M., & Liu, Q. (2024). PlK3 Enhances Cisplatin Sensitivity of Nonsmall-Cell Lung Cancer Cells

through Inhibition of the PI3K/AKT Pathway via Stabilizing PTEN. *ACS Omega*, 9 (8), 8995-9002.

Yao, D., Alexander, C. L., Quinn, J. A., Chan, W.-C., Wu, H., & Greenhalgh, D. A. (2008). Fos cooperation with PTEN loss elicits keratoacanthoma not carcinoma, owing to p53/p21 WAF-induced differentiation triggered by GSK3beta inactivation and reduced AKT activity. *The Journal of Cell Science*, 121 (Pt 10), 1758.

Yao, D., Alexander, C. L., Quinn, J. A., Porter, M. J., Wu, H., & Greenhalgh, D. A. (2006). PTEN loss promotes rasHa-mediated papillomatogenesis via dual up-regulation of AKT activity and cell cycle deregulation but malignant conversion proceeds via PTEN-associated pathways. *Cancer Research (Chicago, Ill.)*, 66 (3), 1302-1312.

Yasarbas, S. S., Inal, E., Yildirim, M. A., Dubrac, S., Lamartine, J., & Mese, G. (2024). Connexins in epidermal health and diseases: insights into their mutations, implications, and therapeutic solutions. *Frontiers in Physiology*, 15, 1346971.

Yeruva, S., & Waschke, J. (2023). Structure and regulation of desmosomes in intercalated discs: Lessons from epithelia. *The Journal of Anatomy*, 242 (1), 81-90.

Yin, C., Peterman, E., Rasmussen, J. P., & Parrish, J. Z. (2021). Transparent Touch: Insights From Model Systems on Epidermal Control of Somatosensory Innervation. *Frontiers in Cellular Neuroscience*, 15, 680345.

Yotsumoto, Y., Harada, A., Tsugawa, J., Ikura, Y., Utsunomiya, H., Miyatake, S., Matsumoto, N., Kanemura, Y., & Hashimoto-Tamaoki, T. (2020). Infantile macrocephaly and multiple subcutaneous lipomas diagnosed with PTEN hamartoma tumor syndrome: A Case Report. *Molecular And Clinical Oncology*, 12 (4), 329-335.

Young, P., Boussadia, O., Halfter, H., Grose, R., Berger, P., Leone, D. P., Robenek, H., Charnay, P., Kemler, R., & Suter, U. (2003). E-cadherin controls adherens junctions in the epidermis and the renewal of hair follicles. *The EMBO Journal*, 22 (21), 5723-5733.

Yuspa, S. H. (1994). The pathogenesis of squamous cell cancer: lessons learned from studies of skin carcinogenesis--thirty-third G. H. A.

Clowes Memorial Award Lecture. *Cancer Research (Chicago, Ill.)*, 54 (5), 1178.

Yuspa, S. H. (2000). Overview of carcinogenesis: past, present and future. *Carcinogenesis (New York)*, 21 (3), 341-344.

Yuspa, S. H., Kilkenny, A. E., Steinert, P. M., & Roop, D. R. (1989). Expression of Murine Epidermal Differentiation Markers Is Tightly Regulated by Restricted Extracellular Calcium Concentrations in vitro. *The Journal of Cell Biology*, 109 (3), 1207-1217.

Zanconato, F., Forcato, M., Battilana, G., Azzolin, L., Quaranta, E., Bodega, B., Rosato, A., Bicciato, S., Cordenonsi, M., & Piccolo, S. (2015). Genome-wide association between YAP/TAZ/TEAD and AP-1 at enhancers drives oncogenic growth. *Nature Cell Biology*, 17 (9), 1218-1227.

Zhang, Zhou, D.-l., Lei, Y., Zheng, L., Chen, S.-X., Gou, H.-J., Gu, Q.-L., He, X.-D., Lan, T., Qi, C.-L., Li, J.-C., Ding, Y.-Q., Qiao, L., & Wang, L.-J. (2015). Slit2/Robo1 signaling promotes intestinal tumorigenesis through Src-mediated activation of the Wnt/β-catenin pathway. *Oncotarget*, 6 (5), 3123-3135.

Zhang, W., Chen, J., Ji, L., Li, J., & Ye, Z. (2015). Wnt/β-Catenin Signaling Pathway in Skin Carcinogenesis and Therapy. *BioMed Research International*, 2015 (2015), 1-8.

Zhang, Y., Li, H., Nishiyama, T., McAnally, J. R., Sanchez-Ortiz, E., Huang, J., Mammen, P. P. A., Bassel-Duby, R., & Olson, E. N. (2022). A humanized knockin mouse model of Duchenne muscular dystrophy and its correction by CRISPR-Cas9 therapeutic gene editing. *Molecular therapy. Nucleic Acids*, 29, 525-537.

Zhang, Y., Sivasankar, S., Nelson, W. J., & Chu, S. (2009). Resolving cadherin interactions and binding cooperativity at the single-molecule level. *Proceedings of the National Academy of Sciences - PNAS*, 106 (1), 109-114.

Zhang, Z., Ren, J.-H., Li, Z.-Y., Nong, L., & Wu, G. (2012). Fasudil inhibits lung carcinoma-conditioned endothelial cell viability and migration. *Oncology Reports*, 27 (5), 1561.

Zhao, H., Liang, Y., Xu, Z., Wang, L., Zhou, F., Li, Z., Jin, J., Yang, Y., Fang, Z., Hu, Y., Zhang, L., Su, J., & Zha, X. (2008). N-Glycosylation affects the adhesive function of E-cadherin through modifying the composition of adherens junctions (AJs) in human breast carcinoma cell line MDA-MB-435. *The Journal of Cellular Biochemistry*, 104 (1), 162-175.

Zhitnyak, I. Y., Rubtsova, S. N., Litovka, N. I., & Gloushankova, N. A. (2020). Early Events in Actin Cytoskeleton Dynamics and E-cadherin-Mediated Cell-Cell Adhesion during Epithelial-Mesenchymal Transition. *Cells (Basel, Switzerland)*, 9 (3), 578.

Zhu, W., Leber, B., & Andrews, D. W. (2001). Cytoplasmic O-glycosylation prevents cell surface transport of E-cadherin during apoptosis. *The EMBO Journal*, 20 (21), 5999-6007.

Ziegler, A., Jonason, A. S., Leffellt, D. J., Simon, J. A., Sharma, H. W., Kimmelman, J., Remington, L., Jacks, T., & Brash, D. E. (1994). Sunburn and p53 in the onset of skin cancer. *Nature (London)*, 372 (6508), 773-776.